UNIVERSIDADE FEDERAL DO PARANA

ROBINSON PLOSZAI

CLIMATE CHANGE SCENARIOS IN THE PARANA STATE: A NON-STATIONARY ANALYSIS USING DROUGHT INDICES

CURITIBA

2020

ROBINSON PLOSZAI

CLIMATE CHANGE SCENARIOS IN THE PARANA STATE: A NON-STATIONARY ANALYSIS USING DROUGHT INDICES

Tese de doutorado apresentada ao Programa de Pós-Graduação em Engenharia de Recursos Hídricos e Ambiental (PPGERHA), área de engenharia de recursos hídricos, Departamento de Hidráulica e Saneamento, Setor de Tecnologia, Universidade Federal do Paraná, como requisito parcial para obtenção do título de Doutor.

Orientador: Dra. Miriam R. M. Mine.

Co-Orientador: Dr. Daniel H. M. Detzel.

CURITIBA

2020

CATALOGAÇÃO NA FONTE – SIBI/UFPR

P729c Ploszai, Robinson

Climate change scenarios in the parana state: a nonstationary analysis using drought indices [recurso eletrônico]/ Robinson Ploszai, 2020.

Tese (Doutorado) - Programa de Pós-Graduação em Engenharia de Recursos Hídricos e Ambiental (PPGERHA), Setor de Tecnologia, Universidade Federal do Paraná, como requisito parcial para obtenção do título de Doutor.
Orientador: Dra. Miriam R. M. Mine.
Co-Orientador: Dr. Daniel H. M. Detzel.

1. Mudança climática. 2. Engenharia de Recursos Hídricos e Ambiental. I. Mine, Miriam R. M. II. Detzel, Daniel H. M. III. Universidade Federal do Paraná. IV. Título.

CDD 304.25

Bibliotecária: Vilma Machado CRB9/1563

ATA Nº53

ATA DE SESSÃO PÚBLICA DE DEFESA DE DOUTORADO PARA A OBTENÇÃO DO GRAU DE DOUTOR EM ENGENHARIA DE RECURSOS HÍDRICOS E AMBIENTAL

No dia nove de junho de dois mil e vinte às 09:00 horas, na sala Jitsi, Remoto, foram instaladas as atividades pertinentes ao rito de defesa de tese do doutorando **ROBINSON PLOSZAI**, intitulada**: Climate Change Scenarios in the Parana State: A Non-Stationary Analysis Using Drought Indices.**. A Banca Examinadora, designada pelo Colegiado do Programa de Pós-Graduação em ENGENHARIA DE RECURSOS HÍDRICOS E AMBIENTAL da Universidade Federal do Paraná, foi constituída pelos seguintes Membros: MIRIAM RITA MORO MINE (UNIVERSIDADE FEDERAL DO PARANÁ), HEINZ DIETER OSKAR AUGUST FILL (UNIVERSIDADE FEDERAL DO PARANÁ), ANSELMO CHAVES NETO (UNIVERSIDADE FEDERAL DO PARANÁ), EBER JOSE DE ANDRADE PINTO (null), MARCELO RODRIGUES BESSA (UNIVERSIDADE FEDERAL DO PARANÁ), DANIEL HENRIQUE MARCO DETZEL (UNIVERSIDADE FEDERAL DO PARANÁ). A presidência iniciou os ritos definidos pelo Colegiado do Programa e, após exarados os pareceres dos membros do comitê examinador e da respectiva contra argumentação, ocorreu a leitura do parecer final da banca examinadora, que decidiu pela APROVAÇÃO. Este resultado deverá ser homologado pelo Colegiado do programa, mediante o atendimento de todas as indicações e correções solicitadas pela banca dentro dos prazos regimentais definidos pelo programa. A outorga de título de doutor está condicionada ao atendimento de todos os requisitos e prazos determinados no regimento do Programa de Pós-Graduação. Nada mais havendo a tratar a presidência deu por encerrada a sessão, da qual eu, MIRIAM RITA MORO MINE, lavrei a presente ata, que vai assinada por mim e pelos demais membros da Comissão Examinadora.

CURITIBA, 09 de Junho de 2020.

Assinatura Eletrônica
09/06/2020 17:35:35.0
MIRIAM RITA MORO MINE
Presidente da Banca Examinadora

Assinatura Eletrônica
15/06/2020 09:34:21.0
HEINZ DIETER OSKAR AUGUST FILL
Avaliador Interno (UNIVERSIDADE FEDERAL DO PARANÁ)

Assinatura Eletrônica
10/06/2020 12:19:19.0
ANSELMO CHAVES NETO
Avaliador Externo (UNIVERSIDADE FEDERAL DO PARANÁ)

Assinatura Eletrônica
16/06/2020 11:37:15.0
EBER JOSE DE ANDRADE PINTO
Avaliador Externo (null)

Assinatura Eletrônica
09/06/2020 15:30:23.0
MARCELO RODRIGUES BESSA
Avaliador Interno (UNIVERSIDADE FEDERAL DO PARANÁ)

Assinatura Eletrônica
10/06/2020 14:36:50.0
DANIEL HENRIQUE MARCO DETZEL
Avaliador Interno (UNIVERSIDADE FEDERAL DO PARANÁ)

Documento assinado eletronicamente de acordo com o disposto na legislação federal Decreto 8539 de 08 de outubro de 2015.
Gerado e autenticado pelo SIGA-UFPR, com a seguinte identificação única: 43152
Para autenticar este documento/assinatura, acesse https://www.prppg.ufpr.br/siga/visitante/autenticacaoassinaturas.jsp e insira o codigo 43152

TERMO DE APROVAÇÃO

Os membros da Banca Examinadora designada pelo Colegiado do Programa de Pós-Graduação em ENGENHARIA DE RECURSOS HÍDRICOS E AMBIENTAL da Universidade Federal do Paraná foram convocados para realizar a arguição da tese de Doutorado de **ROBINSON PLOSZAI** intitulada: **Climate Change Scenarios in the Parana State: A Non-Stationary Analysis Using Drought Indices.**, que após terem inquirido o aluno e realizada a avaliação do trabalho, são de parecer pela sua APROVAÇÃO no rito de defesa.

A outorga do título de doutor está sujeita à homologação pelo colegiado, ao atendimento de todas as indicações e correções solicitadas pela banca e ao pleno atendimento das demandas regimentais do Programa de Pós-Graduação.

CURITIBA, 09 de Junho de 2020.

Assinatura Eletrônica
09/06/2020 17:35:35.0
MIRIAM RITA MORO MINE
Presidente da Banca Examinadora

Assinatura Eletrônica
15/06/2020 09:34:21.0
HEINZ DIETER OSKAR AUGUST FILL
Avaliador Interno (UNIVERSIDADE FEDERAL DO PARANÁ)

Assinatura Eletrônica
10/06/2020 12:19:19.0
ANSELMO CHAVES NETO
Avaliador Externo (UNIVERSIDADE FEDERAL DO PARANÁ)

Assinatura Eletrônica
16/06/2020 11:37:15.0
EBER JOSE DE ANDRADE PINTO
Avaliador Externo (null)

Assinatura Eletrônica
09/06/2020 15:30:23.0
MARCELO RODRIGUES BESSA
Avaliador Interno (UNIVERSIDADE FEDERAL DO PARANÁ)

Assinatura Eletrônica
10/06/2020 14:36:50.0
DANIEL HENRIQUE MARCO DETZEL
Avaliador Interno (UNIVERSIDADE FEDERAL DO PARANÁ)

I dedicate this dissertation to Alfonso and Irmgard.

They turned everything possible.

“Jedi’s don’t rest to watch the world burn”

R.I.P.

AGRADECIMENTOS

Primeiramente eu quero agradecer à Força, Poder Superior Universal, Deus, enfim todos os nomes que significam a mesma coisa. Existe sim algo superior e eu comecei a viver isso durante o doutorado.

Agradeço profundamente por eu estar vivo! É um milagre! Após anos vivendo nas trevas e escuridão eu consegui chegar até a luz na estrada do autoconhecimento.

Os meus maiores agradecimentos às pessoas, é claro, vão para os meus pais Alfonso e Irmgard! Sempre se dedicaram para me dar o melhor que estivera ao seu alcance, passando muitas vezes por dificuldades para me ajudar. Obrigado Pai e Mãe pelo amor, pelo carinho, pela preocupação excessiva e pelos mimos que obtive em toda a minha vida! Obrigado Pai e Mãe pelo auxílio financeiro que vocês nunca negaram, pelas escolas particulares, pelos presentes, pelos cursos, por me ajudar na faculdade e após a faculdade, pela Casa Vida, enfim, por tudo! Sem vocês, eu jamais seria engenheiro civil, muito menos mestre e doutor. Aliás, sem vocês eu jamais seria o grande homem que sou hoje, feliz, em paz, buscando incessantemente por autoconhecimento e buscando evolução diariamente no caminho do amor e da paz. Obrigado por simplesmente existirem, meus dois velhinhos!

Impossível escrever os agradecimentos e não chorar né?

Agradeço também e muito aos meus orientadores Miriam e Detzel. Miriam, essa tese jamais teria sido escrita se não fosse seus puxões de orelha e seus comentários escritos que eu sentia a sua emoção de alegria ou ira. Além disso, obrigado por ter confiado em mim no momento em que mais precisei de ajuda para sair da depressão. Eu consegui, eu venci, e aqui estou eu! Daniel, obrigado por tudo também, desde suas correções supercuidadosas, suas valiosas sugestões na tese, como também as dicas, conselhos e conversas no estacionamento do bloco 5 após o horário. O seu comentário em uma reunião nossa foi essencial para o desenvolvimento dessa tese, obrigado!

Agradeço aos meus grandes amigos Clecio, Fabio, Ricardo e Vanderlei. Vocês me conhecem mais que minha família de sangue e são vocês a família que eu escolhi para a minha vida. Sempre estiveram presentes nos momentos de tristeza e alegria. Com vocês eu descobri o verdadeiro significado da palavra irmão!

Falando em irmão, agradeço muito à minha irmã Etiane, pelo carinho, pelo amor e por sempre acreditar em mim. Obrigado por simplesmente existir! Te amo!

Agradeço também imensamente ao meu primo Bruno e ao meu cunhado Maicon. Vocês são incríveis e parte do meu desenvolvimento pessoal se deve a vocês. Obrigado pela força e dicas, sempre.

Agradeço ao Programa de Pós-Graduação em Engenharia de Recursos Hídricos e Ambiental (PPGERHA), Departamento de Hidráulica e Saneamento (DHS) e a Universidade Federal do Paraná (UFPR), pela oportunidade de realizar meu doutorado com vocês.

Agradeço aos órgãos Agência Nacional das Águas (ANA), Instituto de Meteorologia (INMET), Instituto Agronômico do Paraná (IAPAR) e Instituto Nacional de Pesquisas Espaciais (INPE) pelos dados fornecidos para a realização da tese.

Agradeço aos professores membros da banca pelas valiosas sugestões para o enriquecimento da tese. Obrigado Professores Fill, Bessa, Eber e Anselmo. Agradeço também aos funcionários do PPGERHA, e principalmente ao Cristóvão por seu amor incondicional, e por dar seu sangue ao PPGERHA.

Agradeço também ao Arthur, João, Natel e Avila com as inúmeras ajudas com a programação do método e elaboração de mapas. Jean Bambini, Maurício Romero, Márcia, Marcella, Drevek e Natel agradeço muito a vocês pela amizade sincera e por todos os momentos bons e não tão bons que passamos juntos durante o doutorado. De colegas se tornaram amigos!

Agradeço também aos meus amigos do PPGERHA e os papos incríveis que tínhamos sempre que pudéssemos: Arthur, Adelino, Buchir, Richter, Kozak, Kubas, Mora, Elaine, Teffy, Dudu Figueiredo, Ju Prima, Lu Laboratório, Kenedy, Avila, Maria Jose Escobar, Michel, Jaque, Nanubia, Lari, Gabi, Aninha, Cézar, Macambaco, Félix, Joao, Degraf, Coelho, Jéssica Albizu e tantos outros que eu possa ter esquecido o nome, mas foram igualmente importantes para o bom andamento da tese e da saúde mental durante o doutorado.

Agradeço também aos meus amigos do Restaurante Universitário: Severiano, Tony, Davi, Renan, Alana e Cintia. Obrigado aos amigos e colegas dos departamentos de Geografia, Estatística, Métodos Numéricos, Construção Civil, Física e Química.

Obrigado às meninas da limpeza pelas conversas de corredor e conselhos e também à equipe do Restaurante Universitário pelos incríveis cafés da manhã, almoços e jantas. Obrigado

aos seguranças do campus que sempre abriram os portões para eu trabalhar em qualquer horário que precisasse.

Agradeço também à equipe do CAPA UFPR pelas dicas de aperfeiçoamento da escrita em inglês. Principalmente ao João, Maria e Bruna.

Agradeço também a todas as pessoas que passaram pela minha vida e por alguma razão do destino, nos distanciamos. Porém todas contribuíram de alguma forma para o meu amadurecimento e finalização do doutorado.

Agradeço à Regina e ao TAO que me ajudaram a acordar para uma nova filosofia de vida. Enfim, agradeço ao meu esforço, dedicação, persistência e resiliência para finalizar o doutorado e contribuir com a sociedade com uma boa pesquisa. Obrigado pela vida e pela nova maneira de viver! Estou certo do que quero para mim e para o mundo: paz, felicidade, força, esperança e amor!

AKNOWLEDGEMENTS

First, I want to thank to the Force, Universal Supreme Power, God, whatever all names that means the same thing. There is some superior force and I started living this during my doctorate.

I thank profoundly for being alive! It is a miracle! After years living in the shadows and darkness, I managed to reach the light on the road of self-knowledge.

My greatest thanks to people, of course, go to my parents Alfonso and Irmgard! They always dedicated themselves to provide me the best they could, passing sometimes for difficulties to help me. Thank you Dad and Mom for the love, care, excessive worries and pampers that I had in my entire life! Thank you Dad and Mom for all financial support that you never neglected, schools, gifts, courses, college and after college, for Casa Vida, whatever, for everything! Without you, I could not turn myself the man I am today, happy, in peace, looking incessantly for self-knowledge and seeking for daily improvement in the road of love and peace. Thank you for simply exist, my two little old!

Impossible write the acknowledgments and not cry, right?

I also thank a lot to my supervisors Miriam and Detzel. Miriam, this dissertation could not happen without your “ear tugs” and written comments that I felt your joy or anger emotions. Besides that, thank you for trusting me in the moment I most needed help to leave depression. I got it, I won and here I am! Daniel, thank you for everything too, from your super-careful corrections, your valuable dissertation suggestions, as well as the tips, advices and conversations in the block 5 parking after hour. Your comment in our meeting was essential for this dissertation development, thank you!

I thank to my greatest friends Clecio, Fabio, Ricardo and Vanderlei. You know me more than my blood family and you are the family that I choose for my life. You have always been present in sadness and happiness moments. I discovered the real meaning of the word brother with you!

Talking in brother, I thank a lot to my sister Etiane, for the care, love and for always believing in me. Thank you for simply exist! Love you!

Thank you immensely to my cousin Bruno and my brother-in-law Maicon. You are incredible and part of my personal development I dedicate to you. Thank you for the force and tips, always.

I thank to the Postgraduate Program in Water Resources and Environmental Engineering (PPGERHA, acronym in Portuguese), Department of Hydraulics and Sanitation (DHS, acronym in Portuguese) and the Universidade Federal do Parana (UFPR), for the opportunity in performing my doctorate.

I also thank to the National Water Agency (ANA, acronym in Portuguese), Institute of Meteorology (INMET, acronym in Portuguese), the Weather Database for Teaching and Research (BDMEP, acronym in Portuguese) held by the National Institute of Meteorology (INMET, acronym in Portuguese) and the Parana Agronomic Institute (IAPAR, acronym in Portuguese). All these institutes provided me the data to perform this dissertation.

I thank to the Professor members of the board for the valuable suggestions for this dissertation improvement. Thank you Professors Fill, Bessa, Eber and Anselmo. I also thank to all PPGERHA employees, and mainly to Cristovao by your unconditional love, and to “give his blood” for the PPGERHA.

I also thank to Arthur, Joao, Natel and Avila for your unmeasurable help with the method programming and map making. Jean Bambini, Mauricio Romero, Marcia, Marcella, Drevek and Natel, I thank you a lot for the sincere friendship and for all god and not so good moments, we passed together during the doctorate. From colleagues you turned friends!

I also thank for my PPGERHA friends and for the amazing chats, we always had when it was possible. Thank you Arthur, Adelino, Buchir, Richter, Kozak, Kubas, Mora, Elaine, Teffy, Dudu Figueiredo, Ju Prima, Lu Lab, Kenedy, Avila, Maria Jose Escobar, Michel, Jaque, Nanubia, Lari, Gabi, Aninha, Cezar, Macambaco, Felix, Degraf, Coelho and Jessica Albizu, and so many other that I could forget the name. Even I forgot someone, you were equally important for the good progress of this dissertation and mental health during the doctorate.

I also thank to my friends of the University Restaurant: Severiano, Tony, Davi, Renan, Alana and Cintia. Thank you to my friends and colleagues of the Geography, Statistics, Numerical Methods, Civil Construction, Physics and Chemistry departments.

Thank you for the cleanness girls for our corridor chats and advices. Thank you for the University Restaurant team for the tasteful breakfast, lunch and dinner times. Thank you to the security guards that always opened the campus gates for me to work in any schedule I need.

I also thank to the CAPA UFPR team for the tips to improve my English written. Mainly to Joao, Maria and Bruna.

I also thank to all people that passed during my entire life, and for some destiny reason, we walked in different ways. However, everyone contributed in any way for my personal and professional improvement to end this doctorate.

I thank to Regina and TAO that helped me to wake up for a new life philosophy. Finally, I thank to my effort, dedication, persistence and resilience to end the doctorate, contributing with a good research for the society. Thanks life and for a new way of living! I am right of what I want for me and to the world: peace, happiness, force, hope and love!

RESUMO

Mudanças climáticas afetam o ciclo hidrológico e influenciam significativamente o uso dos recursos hídricos. O grande número de eventos extremos e a prolongada extensão destes são indicativos de que as mudanças climáticas estão se intensificando nas últimas décadas. Uma forma de avaliar os extremos de seca consiste em utilizar os índices de seca acumulados em diversos períodos e ajustar modelos estatísticos. Há vários índices de seca na literatura e os mais utilizados mundialmente são o Índice Padronizado de Precipitação (SPI, acrônimo em inglês), Índice de Reconhecimento de Seca (RDI, acrônimo em inglês) e o Índice Padronizado de Evapotranspiração e Precipitação (SPEI, acrônimo em inglês). O cálculo da evapotranspiração potencial, quando necessário foi realizado utilizando o método de Thornthwaite e foi usada a distribuição de probabilidade gama ajustada aos índices de seca. Estes índices se baseiam na premissa de modelos estacionários, onde os parâmetros (média, desvio-padrão, etc.) e a distribuição das variáveis meteorológicas não variam com o tempo. Nas projeções de mudanças climáticas para o sul do Brasil, os parâmetros estatísticos das séries meteorológicas (média, variância, entre outras) variam no tempo e tal fato torna a análise de seca pobre utilizando as atuais abordagens estacionárias. Portanto, esta tese propõe uma análise não-estacionária no RDI, ajustando os tradicionais modelos estacionários nas séries históricas observadas e futuras simuladas (usando cenários de Modelos Climáticos Regionais), comparando os resultados com as séries de seca não-estacionárias acumuladas em diferentes períodos, em termos de tendência e ponto de quebra. Quando ambos (série histórica mensal de precipitação e/ou temperatura e a série acumulada do RDI) apresentaram não-estacionariedade, o método divide as séries de seca no ponto de quebra e ajusta modelos estatísticos separados em ambas as partes, comparando as diferenças entre o método estacionário (único ajuste na análise de secas) e o método não-estacionário (dois ajustes na análise de secas). A análise das principais estatísticas de secas avaliou o desempenho de ambos os métodos, e a aplicação da análise adicional com uma janela móvel de 30 períodos verifica a evolução temporal dos parâmetros. Comparando as análises estacionária e não-estacionária, os resultados mostraram em geral uma subestimação na severidade das secas quando o modelo estacionário é adotado. A análise das principais estatísticas de seca, como magnitude máxima, duração, número de eventos, frequência de ocorrência e intensidade mostrou subestimação dos eventos de seca, quando utilizada a abordagem estacionária em comparação à abordagem não-estacionária. Os resultados da análise complementar de janela móvel de 30 períodos apresentaram uma tendência decrescente no parâmetro de forma da distribuição, enquanto que os parâmetros de localização e escala, assim como os valores mínimos apresentaram uma tendência crescente, indicando uma seca mais severa ao final do período histórico. A análise de seca no Estado do Paraná mostrou uma intensificação de secas para o futuro quanto às principais estatísticas de seca, independentemente do cenário climático adotado (RCP 4.5 e RCP 8.5). Os resultados na maioria mostram a importância de aplicar modelos não-estacionários para análise de secas e apontam que as secas podem se intensificar até 2100 em severidade, magnitude e duração.

Palavras-chave: mudanças climáticas, Índice de Reconhecimento de Seca, análise estacionária, análise não-estacionária, Modelos Climáticos Regionais.

ABSTRACT

Climate changes affect the hydrological cycle and influence significantly the use of water resources. The great number and prolonged extension of drought events are indicative that climate changes are intensifying in the last decades. A way to evaluate the drought extremes is using the drought indices accumulated in several periods and fitting statistical distribution models. There are several drought indices in the literature and the most used worldwide are the Standardized Precipitation Index (SPI), Reconnaissance Drought Index (RDI), and the Standardized Precipitation Evapotranspiration Index (SPEI). The computation of potential evapotranspiration, when necessary was performed using the Thornthwaite method and the gamma probability distribution was used and fitted to the drought indices. These indices are based on the assumption of stationary models, where both meteorological variable distribution and parameters (mean, variance, among others) do not vary in time. In climate change projections for Southern Brazil, the meteorological series statistical parameters (mean, variance, among others) vary in time and this fact makes the drought analysis poor using the current stationary approaches. For this reason, this dissertation proposes a non-stationary analysis in the RDI, fitting the traditional stationary models in both observed historical and future simulated series (using Regional Climate Model scenarios), and comparing results with the non-stationary drought series accumulated in different periods, in terms of trend and changing point. When both (historical observed monthly precipitation and/or temperature series and accumulated RDI series) present non-stationarity, the method splits the drought series at the changing point and fits separated statistical distribution models in both parts, comparing the differences between the stationary (one fit for drought analysis) and the non-stationary (two fit for drought analysis). The drought statistics analysis evaluated the performance of both methods, and the application of an additional 30-period moving window analysis verified the parameter temporal evolution. Comparing the stationary and non-stationary analyses, results showed a general underestimation in the drought severity when the stationary model is adopted. The main drought statistics, such as maximum magnitude, duration, number of events, occurrence frequency and intensity showed drought events underestimation when used the stationary approach, in comparison with the non-stationary approach. Results of the complementary 30-period moving window analysis presented a decreasing trend in the shape parameter of the distribution, while both location and scale parameters and, the minimum values presented a slight increase trend, meaning more severe droughts at the end of the historical period. The drought analysis in Parana State showed a drought intensification in the future in relation to the main drought statistics, independently of the climatic scenario adopted (RCP 4.5 and RCP 8.5). General results show the importance in applying the non-stationary models for drought analysis and point that droughts may intensify up to 2100 in severity, magnitude and duration.

Keywords: climate change, Reconnaissance Drought Index, stationary analysis, non-stationary analysis, Regional Climate Models.

SUMMARY

LIST OF FIGURES

LIST OF TABLES

LIST OF SYMBOLS

A: Non-dimensional parameter obtained from Maximum Likelihood Estimator (MLE)

$argmax$: Maximum values along an axis of the Pettitt test

b_0: Linear coefficient (intercept) of the SLR

b_1: Angular coefficient of the SLR

b_m: M-month of the Power Transformation (PT) method

$COV[x(t_i),\ x(t_j)]$: Covariance of $x(t_i)$ and $x(t_j)$ in stationarity definition

D: Drought duration (months)

$eCDF_{obs,m}^{-1}$: Inverse of the empirical CDF of observed series of the EQM method

$eCDF_{sim,m}$: Empirical Cumulative Density Function (CDF) of simulated series of the Empirical Quantile Mapping (EQM) method

$E(S_{MK})$: Expected value of the MK test statistics

exp: Exponential function

$E[x(t)]$: Variable mean in stationarity definition

$E(\tau)$: Expected value in return period

$g(x)$: Probability Density Function (PDF) of the gamma function

$G(x)$: Cumulative Density Function (CDF) of the gamma function

H_0: Null hypothesis

$H(x)$: Cumulative probability without zeros in the series of the gamma probability distribution

i: The R_i position at the previous time in the MK and Pettitt tests

I: Heat index of the Thornthwaite method

Int: Drought intensity in the Run Theory

$I(x)$: Incomplete cumulative gamma function

j: The R_j position at the remaining time in the MK test and Pettitt tests

L: Average day length (hours) of the Thornthwaite method

ln: Natural logarithm

m: Number of zeros in the series of the gamma probability distribution

M: Drought magnitude (deficit volume and dimensionless)

MAE: Mean absolute error

max: Maximum value of the Pettitt test

n: Number of observations and/or simulations (months)

N: Number of days in a month of the Thornthwaite method

P: Probability of fail in the considered period in return period

P_i: Monthly precipitation accumulated in i months

P_{ij}: Monthly precipitation of month j and year i

$P_{lim,m}$: M-month precipitation limit for raw (observed) series of the PT method

$P_{LOCI,m}$: Corrected variable of the m-month by LOCI method in the PT method

$P_{obs,m}$: M-month observed precipitation of the PT method

$P_{PT,m}$: Bias corrected series using the PT method

$P_{sim,m}$: M-month simulated precipitation of the PT method

$P(s_t|s_{t-1})$: Probability of dependent variable in time t given time $t-1$

PET: Potential evapotranspiration in mm/month of the Thornthwaite method

PET_{ij}: Monthly potential evapotranspiration of month j and year i

R_i: Previous observation in the MK test

R_j: Remaining observation in the MK test

$RDI_{st(k)}^{(i)}$: Standardized RDI accumulated in i months

S: Drought severity (dimensionless)

sgn: Signal (positive or negative)

S_{MK}: Statistics of the Mann-Kendall (MK) test

$SPEI_{st(k)}^{(i)}$: Standardized SPEI accumulated in i months

$SPI_{st(k)}^{(i)}$: Standardized SPI accumulated in i months

T: Return period in years

$T^*_{contr}(d)$: Third step of mean-corrected control run (simulated) of the VARI method

$T^{*1}_{contr}(d)$: First step of mean-corrected control run (simulated) of the VARI method

$T^{*2}_{contr}(d)$: Second step of mean-corrected control run (simulated) of the VARI method

T_m: Average temperature in monthly scale of the Thornthwaite method

$T_{obs}(d)$: Observed variable of the VARI method

$T^*_{scen}(d)$: Third step of scenario runs of the Variance Scaling (VARI) method

$T^{*1}_{scen}(d)$: First step of scenario runs of the Variance Scaling (VARI) method

$T^{*2}_{scen}(d)$: Second step of scenario runs of the Variance Scaling (VARI) method

$V_{cor}(n)$: Simulated variable with corrected bias at time n of the LS method

$V_{EQM,m}$: Bias corrected variable through the EQM method

$V_{sim,m}$: Simulated variable at m-month of the EQM method

$V_{sim}(n)$: Simulated RCM variable at time n of the Linear Scaling (LS) method

$VAR(S_{MK})$: Variance of the MK test statistics

x: Precipitation or temperature of the gamma probability distribution

X: Random variable in return period

$\bar{x}$: mean of observed values (precipitation or temperature) of the gamma probability distribution

x_i: Previous observation of the Pettitt test

x_j: Remaining observation of the Pettitt test

x_{SLR}: Variable of the neighbouring station used to fill the gaps using SLR

x_t: Observed data at time t of the MAE method

x_T: Specified level in return period

$x(t_i)$: Joint density function variable in stationarity definition

$\overline{\gamma_k}$: Arithmetic mean of SPEI accumulated in i months

$\gamma_k^{(i)}$: Standardized Precipitation Evapotranspiration Index (SPEI) accumulated in i months

y_t: Modelled data at time t of the MAE method

y_{t_SLR}: Variable (precipitation or temperature) in monthly scale to fill $f(x)$ using Simple Linear Regression (SLR)

Z: Mann-Kendall test statistic

α: Significance level

ak: Reconnaissance Drought Index (RDI) series

$\overline{\alpha_k}$: Arithmetic mean of RDI accumulated in i months

$\alpha_k^{(i)}$: RDI series accumulated in i months

$a(t)$: Shape factor of the gamma probability distribution

$\overline{\beta_k}$: Arithmetic mean of SPI accumulated in i months

$\beta_k^{(i)}$: SPI accumulated in i months

$\beta(t)$: Scale factor of the gamma probability distribution

Γ: Gamma function

ϵ: SLR Error

$k(\tau)$: Pettitt test statistics

μ: mean of values

μ_m: mean of the RCM-simulated series

$\mu(V_{obs})$: Mean of the observed variables of the LS method

$\mu(V_{sim})$: Mean of the simulated variables of the LS method

ρ: Correlation coefficient

σ: Standard deviation of the PT method

Σ: Sum operator

σ_m: Standard deviation of the corrected time series

$\widehat{\sigma_{\alpha k}}$: Standard deviation of RDI accumulated in i months

$\widehat{\sigma_{\beta k}}$: Standard deviation of SPI accumulated in i months

$\widehat{\sigma_{\gamma k}}$: Standard deviation of SPEI accumulated in i months

τ: Ranking coefficient of the Pettitt test

∞: Infinite

$\int$: Integer operator

LIST OF ACRONYMS

AICc	Corrected Akaike Information Criterion
AMO	Atlantic Multidecadal Oscillation
ANA	National Water Agency (in Portuguese)
AR5	Assessment Report number 5
ARCH	Autoregressive Conditional Heteroscedasticity
BDMEP	Weather Database for Teaching and Research (in Portuguese)
CAFEC	Climatically Appropriate For Existing Conditions
CDF	Cumulative Distribution Function
CMIP5	Coupled Model Intercomparison Project Phase 5
CMR	Curitiba Metropolitan Region
CP	Changing point
CPTEC	Weather Forecast and Climatic Studies Centre (in Portuguese)
DM	Distribution Mapping
DT	Delta Change
EDII	European Drought Impact report Inventory
ENSO	El-Niño Southern Oscillation
EQM	Empirical Quantile Mapping
ETA	Estimated Time of Arrival
GAMLSS	Generalized Addictive Models for Location, Scale and Shape
GARCH	Generalized Autoregressive Conditional Heteroscedasticity
GCM	Global Circulation Model
GDP	Gross Domestic Product
GEV	Generalized Extreme Value
GHG	Greenhouse Gas
GLD	Generalized Logistic Distribution
GPD	Generalized Pareto Distribution
IDF	Intensity-Duration-Frequency
IDW	Inverse Distance Weighting
IAPAR	Parana Agronomic Institute
INMET	National Meteorology Institute (in Portuguese)
INPE	National Institute for Spatial Research (in Portuguese)
IPCC	Intergovernmental Panel on Climate Change
KS	Kolmogorov-Smirnov
LN2	2-parameter Lognormal
LN3	3-parameter Lognormal
LOCI	Local Intensity Scale
LPB	La Plata Basin
SLR	Simple Linear Regression
LS	Linear Scaling
MAE	Mean Absolute Error
MK	Mann-Kendall

MLR	Multiple Linear Regression
MPDSI	Modified Palmer Drought Severity Index
MPT	Modified Power Transformation
MSDI	Multivariate Standardized Drought Index
MW	Megawatt
NAO	North Atlantic Oscillation
NEB	Northeast Brazil
NFA	Non-stationary Frequency Analysis
NS	Nash-Sutcliffe
NSPI	Non-stationary Standardized Precipitation Index
PDF	Probability Density Function
PDI	Palmer Drought Index
PDO	Pacific Decadal Oscillation
PDSI	Palmer Drought Severity Index
PET	Potential Evapotranspiration
POT	Peaks over Threshold
PP	Percentile-percentile
PROJETA	ETA Project (in Portuguese)
PROMES	Prognostic Mesoscale
PT	Pettitt
PT	Power Transformation
PWM	Probability Weighted Moments
PWT	Pre-Whitening Trend
QM	Quantile Mapping
QQ	Quantile-Quantile
RCA1	Rossby Centre Regional Atmospheric Climate Model
RCM	Regional Circulation Model
RCP	Representative Concentration Pathway
RDI	Reconnaissance Drought Index
sc-PDSI	Self-calibrated Palmer Drought Severity Index
SDDI	Supply-Demand Drought Index
SDI	Streamflow Drought Index
SDVI	Standardized Difference Vegetation Index
SIN	National Interconnected System (in Portuguese)
SPEI	Standardized Precipitation Evapotranspiration Index
SPERI	Standardized Precipitation Evapotranspiration Runoff Index
SPI	Standardized Precipitation Index
SRI	Standardized Runoff Index
SSI	Standardized Soil moisture Index
SSI	Standardized Streamflow Index
SSS	Strict Sense Stationarity
STD	Standard Deviation
UK	United Kingdom
US	United States

USDM	United States Domestic Market
VARI	Variance Scaling
WMO	World Meteorological Organization
WSS	Wide Sense Stationarity

INTRODUCTION

Climate change and its related impacts in the environment are a common debate in several countries, organizations, universities, non-governmental institutes and researchers from all over the world, mainly in the last decades.

The high levels of Greenhouse Gases (GHG) emission rates combined with the intense deforestation and substitution of the forests by agriculture, pasture and urban areas change the hydrological cycle. The land changes in cover/use affect the evapotranspiration levels regionally and consequently the formation of clouds. More clouds in the troposphere as well as GHG emissions change the temperature, and alter the rainfall patterns, affecting the climate significantly.

Impermeability is another indicator of the anthropic influence in the Earth. The main problem arises because the water that should infiltrate in some region will flow and infiltrate in another region. In this scenario, the occurrence of extreme events becomes frequent, like floods and droughts. Both affect the planet and population in general.

Hydropower generation systems are some of the most affected due to climate change impacts. The concentration of GHG in the atmosphere increases due to the industrialization and combustion engines, as well as thermal power plants.

Among the climate change impacts, drought events are very harmful for the affected populations. Some droughts can last months or decades (e.g. Federation Drought, Australia). Some researchers consider the drought events as the most hazardous natural events of the globe. They cause starvation, flora and fauna unbalance, affecting socioeconomically the countries.

It is important to study droughts in order to take mitigation measures for governments and populations. To study drought events, drought indices are used. These indices reveal the intensity, duration and persistence of the drought events. Researchers have been applying them worldwide since the second half of the twentieth century.

The most applied drought indices in the world are based on precipitation. Some of them combine other variables like potential evapotranspiration i.e., include the temperature effects. These indices provide drought scenarios. Climate scientists accumulate drought series in periods (3, 6, 12, 24, 36, 48 and 60 months).

In the last years, researchers published several studies relating the drought phenomena to climate change impacts as the consequence of the anthropic influence. These publications worldwide performed, evidenced the importance of extreme event prediction in the future. Few of them, take into account the non-stationarity issue.

Non-stationarity is present in most hydro-meteorological variables series in subtropical regions. In other words, it may indicate the presence of trends or changes in the statistical parameters of the series. There are few studies worldwide considering the non-stationarity in drought series.

Therefore, **one of the innovations of this dissertation is the non-stationary approach for analysing droughts.** It is based on results of the trend and changing point tests to verify the point where the meteorological series changed. Then, the series at this changing point are split, and separate probability distributions are fitted in each segment. The traditional drought analysis performed fits only one distribution in the drought series.

The hypothesis is that drought statistics vary under a non-stationary approach. To perform the drought analysis it is necessary to compare the stationary and non-stationary methods first. This research verifies the consequences of adopting the stationary approach to model non-stationary drought series.

Droughts occur in many regions of the planet, including regions with well-defined pluviometry. It is important to analyse both dry and wet regions. In the future both dry and wet regions may suffer from some type of drought unbalance. Thus, it is necessary to study these characteristics for a better socioeconomic planning.

Droughts may be a consequence of the climate change impacts due to anthropic action on the Earth surface. It is important to study droughts because some regions of the planet are becoming drier, affecting populations and economy.

Some authors state that changes in the rainfall and temperature patterns occur due to the natural climate variability. Despite that, changes in the soil cover/use and the GHG increased significantly since the nineteenth century due to the second industry revolution. These changes may affect the modern human civilization in the future.

The evaluation of these changes consists in analysing the drought indices applied to future projections, i.e., using the downscaled outputs of the Global Climate Models (GCM) to the Regional Climate Models (RCM). Thus, despite presenting some errors in the simulations

of these models due to difficulty in representing the complex processes within the troposphere, these scenarios are useful tools to predict and forecast the Earth's climate.

For this reason, **this dissertation has the main objective of performing a non-stationary drought analysis in climate change scenarios**. The specific objectives of this dissertation are:

1. Evaluate the potential key stations in Parana State to evaluate the historical scenarios.
2. Evaluate the RCM simulations for drought analysis and compare their statistics with the historical series.
3. Apply the non-stationary analysis in the historical series and compare with the stationary analysis.
4. Apply the non-stationary analysis in the simulated future scenarios and compare with the stationary analysis.
5. Evaluate the parameters of the gamma probability distribution in the 30-period moving window analysis in both historical and future series.
6. Develop the drought analysis using the non-stationary approach in the past and future series.

A non-stationary drought analysis can improve drought analysis in Brazil and in the world. It can evaluate the potential impacts on the climate change in drought analysis. Despite it is not possible to avoid these hazardous events, researchers and policy makers can take mitigation measures in water resources planning and management, as well as in hydropower generation.

This dissertation is organized as follows: the first chapter is the literature review presenting a general overview about the climate change impacts. It also presents the evaluation methods using RCM simulations, as well as the drought phenomenon and manners of evaluating them. The trend tests and the non-stationary analysis approach with studies performed worldwide are presented in the last subchapters of the first chapter. The second chapter presents the flowchart of this dissertation and the description of all methods applied. The third chapter provides a general overview of the study area and data used. The fourth

chapter presents the results achieved with the proposed method. The fifth chapter presents the drought analysis considering the non-stationary approach, followed by conclusions and recommendations.

1. LITERATURE REVIEW

In a climate change scenario affecting the hydrological cycle, researchers believe these changes are the main drivers of the drought phenomena. The literature review aims at understanding the climate change impacts and gives a brief overview of the techniques currently applied and possible scenarios to analyse the future climate on Earth.

It also presents a general overview of the past drought events and the most applied indices around the world, as well as a summary of methods to detect non-stationarity in the hydro-meteorological series and the non-stationary analysis studies performed. Through these concepts presented in the following subsections, it is possible to evaluate the climate change impacts in droughts.

1.1. Climate change impacts

A great number of researches aims at investigating the effects of the global warming and/or climate change in the planet. Researchers highlight that changes in the precipitation and temperature patterns relate to the anthropic influence in the globe (IPCC, 2013; NAM et al., 2015). Changes in the atmosphere alter the temperature, precipitation and other water balance variables. This cause to some areas the extreme event occurrence, such as hurricanes, twisters, typhoons, extreme rainfall or droughts.

In one hand, there is a natural disasters intensification. In another hand, other variables may relate to anthropic influence. They are: population growth, high deforestation rates, land-use cover change, waterproofing, pasture, agriculture, human needs of drinking water and other uses, increasing urbanization and industrialization, and high Greenhouse Gases (GHG) emission rates (SALAS et al., 2012; NAM et al., 2015). These changes alter significantly the Earth's climate, changing the flora, fauna and all living beings consequently (TUCCI, 2002). AZEVEDO et al. (2006a) explain how waterproofing and deforestation increase the flooding risks causing socioeconomic damages.

Researchers from all around the world discuss the climate change impacts on Earth. They relate them to the variation of precipitation patterns and the increase in temperature rates. According to TRENBERTH et al. (2007), global temperature increased around 0.8°C in the last

century and they believe most of this change relates to the anthropic cause. In an assessment, IPCC (2013) found increases in temperature rates of approximately 0.3°C in the Mediterranean region in one decade. In the same report, researchers point to the last half of the twentieth century as the warmest period in the entire history of the European continent. VICENTE-SERRANO et al. (2010) studied meteorological variables (precipitation and temperature) and found increases in monthly mean temperature from 2°C to 4°C in the period 1910 to 2007 in the Albuquerque weather station, US.

Increases in temperature can generate heatwaves. CHATTOPADHYAY et al. (2017) and DIFFENBAUGH & ASHFAQ (2010) state that heatwaves will be common in a close future in the continental US in the period 2010 to 2039. MISHRA & SINGH (2010) highlight the warmest period of the twentieth century started in 1970s with an increase in temperature of approximately 0.6°C. They found that the temperature increase between 1910s and 1940s was milder with an increase of around 0.4°C, when compared to the warmest period (after 1970).

According to CLARK et al. (1999) and MISHRA & SINGH (2010), the temperature on Earth increased in 21,000 years after the last glacial period, leading to changes in runoff, evapotranspiration and precipitation patterns. In several localities of the planet, like Western Australia, central Africa and parts of Russia, HAO & AGHAKOUCHAK (2013) and HAO et al. (2018) highlight the dry extremes allied to warm temperatures increased relatively since 1978 until 2004.

Increases in dry and warm seasons were found in Indonesian and Amazonian regions comparing the baseline period (using the Coupled Model Intercomparison Project Phase 5 (CMIP5) climate scenarios) with the historical records (HAO et al., 2018; ZSCHEISCHLER & SENEVIRATNE, 2017). AMENGUAL et al. (2012) concluded that daily temperature might increase, while other variables (relative humidity, precipitation, and wind speed) might decrease until 2100. They also found precipitation and temperature extremes during the twenty-first century in Mallorca Island, Spain.

Although there is an increase in the temperature rates, climate scientists also studied changes in the precipitation patterns worldwide in the last century. CISLAGHI et al. (2005) assessed daily precipitation series in Italy and found changes in the rainfall intensity. Their results showed that the South suffered a decrease in the rainfall rates, while the North presented an increase in the rainfall rates. The most industrialized part of the country situates in the North, making the authors believe these changes in the precipitation rates relate to the industrialization.

Still in Italy and years later, COSCARELLI & CALOIERO (2012) concluded that daily and monthly precipitation series in the Calabria region were more intense in the last century. They found differences between the West (more intense) and East (milder events). These events lead to soils instability and high flood rates. In another study, changes in precipitation patterns (decreasing trends) occurred in Mediterranean, North and Northeast Brazil, Southwest US and Southwest Australia and in some locations in Africa (JONG et al., 2019).

FU et al. (2013) studied the inter-annual and interdecadal variations aiming at detecting changes in the rainfall patterns. They related these changes to global warming effects, monsoons and wind circulations. BARROS et al. (2000) noticed more abundant rainfall events in the Southern Brazilian region in the summer season. MARENGO (2001) observed perturbations in the ocean currents, relating these events to alterations in the rainfall extreme events.

Still in Brazil, AZEVEDO et al. (2006a) examined the rainfall patterns concluding that there is more intense rainfall in the South, when compared to the Southeast. In Southeast, the driest months comprise the winter (June to September), while the wettest months the summer (December to March). They concluded that there might be more intense rainfall rates in the winter under the El-Niño Southern Oscillation (ENSO) phenomena, leading to hazardous floods.

The IPCC (2013) stated that the extreme rainfall rates would intensify in the wet regions, while the dry regions tend to become drier in the close future. AHMADALIPOUR et al. (2017) highlight the Northeast Pacific, US, will suffer from increases in the annual precipitation rates due to the climate change impacts.

According to VICENTE-SERRANO et al. (2010), precipitation rates reduce in some regions of the planet as consequence of the climate change impacts. This reduction generates more effects in the North Hemisphere, increasing the temperature and evapotranspiration rates and intensifying the lack of precipitation and consequently, the drought phenomena. For example, in the Mediterranean, AMENGUAL et al. (2012) found rainfall decrease from 5% to 20% between 1901 and 2005.

The global climate change relates to an ensemble of variations in the Earth surface. These changes increased when fossil fuels started being used, since the industrial revolution. Consequently, it started the high GHG emission rates in the atmosphere, changing the climate

because they interfere on temperature and clouds formation nuclei. LUCENA et al. (2018) highlights: *"the magnitude of climate change depends on the carbon intensity of global development pathways. On the other hand, the systems affected by climate change are influenced by the same development pathway"*. MISHRA & SINGH (2010) highlight the climate change is *"one of the major threats"* of the current century.

According to MOHOR et al. (2015), the GHG emission rates and land-use changes are higher in the last decades. These events attributed to anthropic origin alter the regional level of evapotranspiration. The substitution of forests by agricultural and pasture areas change the evapotranspiration rates and consequently, alter the hydrological cycle. The waterproofing (present mainly in urban areas) also changes the water cycle, because the precipitation that should infiltrate in the soil is deviated to another region. Only these two changes (in evapotranspiration and waterproofing) in the Earth surface can generate flood hazards in some regions, while others tend to desertification.

Some changes can be irreversible in the global climate as pointed by LIANG et al. (2011). They highlight the changes in the water levels; snow melting, rainfall regimes and evapotranspiration affect the globe dramatically.

NAM et al. (2015) highlight the extreme events (e.g. droughts) which tend to increase in the future due to the global warming. According to MISHRA & SINGH (2010), the increase of extreme events relates to global warming. More rainfall occurs when there are increasing temperature rates, which increase the evapotranspiration rates, altering the hydrological balance. The impacts of the climate change are unavoidable, but forecasting their magnitude turn possible to mitigate them (CHATTOPADHYAY et al., 2017).

Climate change impacts intensify the drought events leading to desertification of some areas. Drought impacts become more intense under a climate change scenario, such as extreme low precipitation and high temperature. These impacts affect the environment, societies and their economies. It is important to forecast droughts related to climate change impacts in order to establish innovative strategies and propose appropriate preparedness and mitigation measures, reducing the vulnerability to drought events (NAM et al., 2015).

Under this premise, MISHRA & SINGH (2009) studied the Kansabati River basin in India and compared the historical droughts with the climate change scenarios. They noticed changes in droughts in terms of frequency, severity, and affected area. They point that droughts

will cause severe impacts on the crop production in the future. TODD et al. (2013) found low rainfall rates and high temperature in the UK droughts, during the periods 2004 to 2006 and 2010 to 2012. In the other side of the world, Southern Korea experienced a historical huge drought in the recent years (NAM et al., 2015).

Researchers generally analyse the climate on Earth considering the hydro-meteorological series stationary. If their statistics (mean, variance, among others) vary on time, they are non-stationary and it may be a change in the series. This can relate to the anthropic influence.

Planners and system operators commonly assume that the climatic variables are stationary. Climate change and climate variability could affect seriously the energy consumption and production. Renewable energy systems are more sensitive to climate variations, than that based on fossil fuels. Great amounts of GHG emissions are related to human activities (LUCENA et al., 2018). The development of new technologies depend on human decisions aiming at the sustainable human progress (there is no progress under a scenario of environment degradation).

PEEL & BLÖSCHL (2011) discuss the climate change representation in modelling. They defend the incorporation of the non-stationarity of the hydro-meteorological series for a better representation of the extreme indices.

The presence of monotonic trends along the series indicate the non-stationary pattern of the hydro-meteorological series. Most of the hydrological variables present the non-stationary pattern (MATALAS, 1997). ALEXANDRE et al. (2010) discuss that most projections of the water resource systems are based on the assumption that hydrological variables follow the stationary pattern. In other words, the water resources operational management relies in a stationary scenario.

1.2. Climate models and scenarios

Despite some authors not agreeing about the climate change impacts or the natural climate variability on Earth, there are several methods and data to study whether there are changes or not. A way of analysing the Earth's climate consists in using the Global Climate Models (GCM) outputs.

The GCM produce outputs of precipitation, temperature, air pressure, wind speed, solar radiation and other important variables to study the climate at a grid size of about 200 km. To represent the climate change impacts at lower scales (20 to 50 km), it is necessary to downscale the GCM outputs into the Regional Climate Models (RCM). The GCM provide estimates of the climate at large scales of the future climate (KIRONO et al., 2011; IPCC, 2013), despite of significant differences among particular models.

CHATTOPADHYAY et al. (2017) highlight the difficulty in determining the climate with precision due to the large spatial resolution of the GCM grids (2° latitude and 2° longitude) and the representation of atmospheric variables. The GCM are a way to determine the long-term temperature and precipitation under different GHG emission scenarios (NAM et al., 2015). According to both KIRONO et al. (2011) and IPCC (2013) studies, at a continental scale, the GCM can provide significant estimates for drought projections.

The RCM scenarios perform a preliminary analysis of the regional climate at grid scales of 20 to 50 km. They allow governments to take strategies and prevent society from the climate change effects and their consequences to water resources (CHATTOPADHYAY et al., 2017). The RCM provide a better assessment to perform climate change studies in a regional scale. A way of analysing the climate change impacts using the RCM is the evaluation of the climate change projections, the Representative Concentration Pathways (RPC).

The RCP are the representation of the GHG in the atmosphere adopted in 2014 on the fifth Assessment Report (AR5) of the Intergovernmental Panel on Climate Change (IPCC) held by the World Meteorological Organization (WMO). The future scenarios (labelled RCP 2.6, RCP 4.5, RCP 6.0 and RCP 8.5) represent the radiative forcing values (W/m^2) possible to occur until 2100. In the RCP 2.6, there is a peak in the global GHG emissions between 2010 and 2020, while in the RCP 4.5 and RCP 6.0 the peak is around 2040 and 2080, respectively. Thus, the GHG concentration of the three RCP scenarios will decline until 2100. The RCP 8.5 differs because it considers the GHG emissions will continue rising in the twenty-first century. The scenarios RCP 4.5 and RCP 8.5 are available in the PROJETA CPTEC platform. In general, climate change studies consider mostly the RCP 4.5 and RCP 8.5 in their projections (NAM et al., 2015; CHATTOPADHYAY et al., 2017; PARK et al., 2018; LUCENA et al., 2018). The RCP 4.5 scenario is a scenario with a CO2 reduction in the middle of the twenty-first century and the RCP 8.5 considers the CO2 rates constantly increasing until 2100.

There are several studies applying the GCM and RCM aiming at evaluating the climate change impacts on Earth. LUCENA et al. (2018) used 16 GCM data and concluded that the high GHG scenario (RCP 8.5) affects severely the hydropower generation, when compared to the RCP 4.5 scenario. They analysed the impact of implementation of alternative energy generation and concluded these are cheaper than using coal as an alternative for Brazil.

In the work of PARK et al. (2018), they analysed the RCP 8.5 scenario and found an increase of 2°C in the global mean temperature. MEINSHAUSEN et al. (2011) evaluated the four RCP scenarios and concluded that temperature will increase of around 4.5°C in the worst scenario (RCP 8.5) and considering the RCP 2.6 scenario (less probable), temperature will increase approximately 1.5°C.

Analysis of the climate change impacts were performed by CHATTOPADHYAY et al. (2017) across the Kentucky River Basin, US. They compared the baseline period with the observed series and found increases in both precipitation and temperature series. They also found a decrease in the evapotranspiration series in the summer, while found an increase in the winter in the future series, as pointed by the RCP 4.5 and RCP 8.5 scenarios.

Researchers apply the RCM ETA in Brazilian projections of climate change impacts. DERECZYNSKI et al. (2010) applied it in seven hydro-meteorological stations located in Serra do Mar, Sao Paulo State. They found overestimation in the frequency of precipitation events and in the 10-m wind speed. They also found a good estimation in the 2-m temperature. Compared to other models, the HADGEM2-ES/ETA preserved the series median (JONG et al., 2019). Generally, there are some inconsistencies in the downscaling process that turns necessary to apply bias correction methods to minimize these errors. The GCM scales cover big areas (ROCHA, 2015).

Researchers recommend the application of bias correction methods in the RCM data in order to minimize the downscaling errors. JOHNSON & SHARMA (2015) evaluated the performance between two bias correction methods: Nested Bias Correction and Quantile Mapping (QM). Results showed differences between both bias correction methods and the raw GCM data.

Some authors prefer using the Quantile-Quantile (QQ) bias correction method, as performed SAURRAL & BARROS (2010) and AMENGUAL et al. (2012). In both studies, they observed a good agreement between the observed series and the baseline period (control

run), except for the extreme rainfalls. The QQ corrects the RCM data classifying and splitting them in frequency intervals, computing the difference (bias) for each interval.

FILL et al. (2013) used RCM PROMES and RCA1 simulations. They applied them for the major hydropower plants located in the Brazilian part of the La Plata River Basin. They aimed at evaluating the climate change impacts during the twenty-first century. They applied the Quantile-Quantile (QQ) method and found a dependable energy decrease of the hydropower plants during the twenty-first century.

Some studies performed in different localities like China, Spain, India, Germany and others used other bias correction methods. FANG et al. (2015) compared the Linear Scaling (LS) and the Distribution Mapping (DM) for temperature and precipitation series in China. They also applied only for precipitation the Quantile Mapping (QM), Power Transformation (PT) and the Local Intensity Scaling (LOCI); and only for temperature, the Variance Scaling (VARI). The LOCI method improved the correlation of Nash-Sutcliffe (NS) coefficients and the QM and PT methods performed well to correct the percentile values and the standard deviation of the precipitation series.

RAJCZAK et al. (2016) compared the Quantile Mapping (QM) bias correction method to the simulated raw RCM series. Results presented a good performance of the QM method for the precipitation series. SMITHA et al. (2018) observe that generally the bias correction methods apply on monthly scale, generating errors when the application occurs on daily scale.

SMITHA et al. (2018) applied the LS, LOCI, PT, Modified Power Transformation (MPT) and DM bias correction methods for the Indian rainfall. Results showed the DM, LS and PT performed better than LOCI and MPT in terms of adjusting the wet daily frequencies.

In a different work, TEUTSCHBEIN & SEIBERT (2012) applied the LS, DM and the Delta Change (DT) for temperature and precipitation series. They applied the LOCI and PT only for precipitation, and the VARI only for temperature. Results also showed the DM and PT reproduced well the percentiles and the standard deviation of the baseline period. They highlight the DM is the most appropriate method in terms of representing the means.

WILLKOFER et al. (2018) applied the LOCI, QM and LS bias correction methods in the Mindel River catchment, Germany. Results showed the QM method is the most representative to perform climate change impacts. All methods failed in representing the flow extremes.

Another approach in the bias correction scene was applied by GU et al. (2019). They applied the Empirical Quantile Mapping (EQM) for both precipitation and temperature in the RCM simulations across China. Results pointed that the bias correction method reduce both standard deviation and mean errors in about 5%.

Analysing this briefly presentation of the climate change scenarios and bias correction methods, the most used among these are the Linear Scaling (LS), Power Transformation (PT), Variance Scaling (VARI) and the Empirical Quantile Mapping (EQM). For climate change studies, both future scenarios RCP 4.5 and RCP 8.5 are most used in order to forecast the future behaviour of the hydro-meteorological variables.

Bias correction methods may not being based on applying the stationary or non-stationary features in the future series, i.e., they do not correct the non-stationarity in the historical series and consequently, do not correct in the future series. The same process occurs with the stationarity feature in a time series. In this sense, it is important to apply bias correction in order to minimize the downscaling inherent errors of climate model data.

1.3. Droughts

Droughts are a complex phenomenon that originate from the lack of precipitation over a prolonged period and rely in an extended area (WILHITE, 2000; TSAKIRIS & VANGELIS, 2005; ZARCH et al., 2015; TU et al., 2018). The rise of temperature combined with lack of precipitation can generate the drought phenomenon. The land use/cover leads to changes in the regional and global hydrological cycle and consequently, can increase the occurrence of extreme events (HAO & SINGH, 2015).

Some authors state that this natural hazard (drought phenomenon) leads to difficulties for agriculture, drinking water, environmental and ecological imbalance, socioeconomic and livestock damages (TU et al., 2018). According to PAULO & PEREIRA (2006) and MOREIRA et al. (2013), drought is a persistent event with a temporary water shortage, and it is difficult to predict its duration, severity and frequency. Droughts can be treated as stochastic events since their main variables may present random behaviour (SANTOS, 1983; CEBRIÁN & ABAURREA, 2012).

Researchers from all around the world study the impacts of climate changes and their contributions to the drought events. Researchers believe that the rainfall pattern changes together with other human interventions (e.g. increasing GHG emission rates, deforestation and substitution to agriculture areas) reflect in the droughts increase. SHEFFIELD & WOOD (2008), DAI (2011) and HAO & SINGH (2015) suggest a drought intensification under a climate change scenario, causing several economic, environmental and agricultural damages.

Several damages related to droughts occurred worldwide. According to COMEC (2007), TIGKAS et al. (2012) and VANGELIS et al. (2013), 100 billion euros is the estimated cost of droughts in the last 30 years in Europe. In East Hungary, the soil moisture was drier in the last century when compared to the North Hemisphere changes (SZÉP et al., 2005; MISHRA & SINGH, 2010).

Economic losses related to droughts in the US costed annually 6 to 8 billion dollars between 1980 and 2014 (WILHITE, 2000; HAO & AGHAKOUCHAK, 2013; RAJSEKHAR et al., 2015; YANG et al., 2018). The central part of the country suffered an extreme drought in 2012 and the Texas, in 2011. Both drought events affected ecosystems, agriculture, energy production and recreation (HAO et al., 2016b).

According to RAJSEKHAR et al. (2015), droughts impact severily more people when compared to any other natural disaster. This turns necessary to study them as well as improve the prediction methods (MISHRA & SINGH, 2011). YANG et al. (2018) affirm that meteorological disasters provoke fewer losses when compared to droughts. In general, there are several studies predicting droughts in short-term scale, as well as focused in drought frequency analysis and monitoring, using several types of variables and different drought indices (NAM et al., 2015).

MISHRA & SINGH (2010) pointed that the Southeast and central Asia suffered a severe drought between 1998 and 2001 affecting more than 60 million people. According to GUPTA & JAIN (2018), since 1974 droughts affected more than one million people globally. Around 33% of damages to people and 22% of the economic losses, relate to droughts in the world. These events persist from months, years and in some extreme cases, until decades (WILHITE, 2000; KHADR, 2016).

Some researchers consider droughts in Australia as a “normal” feature of the national climate (MCKERNAN, 2005). The most extended droughts occurred: between (1) 1895 and

1902 (known as the Federation drought), (2) between 1937 and 1945 (known as the World War Second drought) and (3) the post-1995 drought. The (3) event shrank in 3% the agricultural Gross Domestic Product (GDP), while the (2) event killed 30 million sheep's (ABARE, 2008; KIRONO et al., 2011).

Drought risk and drought quantification evaluate the: (1) impacted area, (2) frequency, (3) duration and (4) intensity (NAM et al., 2012; SPINONI et al., 2014; NAM et al., 2015; HAO & SINGH, 2015). It is difficult to determine the onset and end of a drought period. Generally, researchers evaluate droughts using single or bivariate indices due to the lack of hydro-meteorological data (HAO et al., 2016). Indices are series of variables such as temperature, precipitation and streamflow, while indicators are single numbers (HAO & SINGH, 2015).

There is a difference between aridity and water scarcity. The first consists in a low ratio between precipitation and evapotranspiration and is a climatic feature of a region. The second means that demand of water is higher than water availability and represents the water bodies overexploitation (TSAKIRIS & VANGELIS, 2005; VAN LOON & VAN LANEN, 2013; PEDRO-MONZONÍS et al., 2015).

There is a drought classification according to the percentiles of the run theory in the work of SVOBODA (2002) and HAO et al. (2016), based on USDM (United States Domestic Market). There are five drought types: (1) abnormally dry (D0) (20 to 30^{th} percentiles), (2) moderate (D1) (10^{th} to 20^{th} percentiles), (3) severe (D2) (5 to 10^{th} percentiles), (4) extreme (D3) (2 to 5^{th} percentiles), and (5) exceptional (D4) (less or equal to the second percentile). A way of analysing the drought percentiles consists in plotting the variables and applying the run theory (see section 2.10).

The Run Theory evaluates droughts as runs of deficits (below an established threshold) (MARCOS-GARCIA et al., 2017). Drought is an extended period in which an index is below a predefined threshold, like the drought percentiles (truncation level) according to the run theory (YEVJEVICH, 1967). Drought duration is a period between the onset and end, while the magnitude is the accumulated standardized index, i.e., the area duration versus intensity (WU et al., 2018).

Determining the threshold is the challenge for drought researchers; since it depends on the study area, (e.g. a severe drought in Sao Paulo is equivalent to a moderate drought in Iran in terms of drought severity thresholds). It is important to determine the number of drought

events as well as their duration and magnitude. The drought analysis is based on the cumulative probability of droughts under a pre-specified threshold.

NAM et al. (2015) and GU et al. (2019) used the run theory and drought indices. Both works evaluated droughts under a specified threshold of a significant drought (below -1.0). This threshold change from region to region, being less significant for arid and semiarid regions, while more significant in normal conditions for humid regions.

1.4. Types of droughts

Independent on the threshold adopted in the run theory, droughts can be classified in different types: meteorological, agricultural, hydrological, and socioeconomic (KOGAN, 1997; WILHITE, 2000; HEIM, 2002; SIVAKUMAR et al., 2005; MISHRA & SINGH, 2010; HAO & SINGH, 2015; RAJSEKHAR et al., 2015; MAITY et al., 2016; LI et al., 2016; GUO et al., 2019). PEDRO-MONZONÍS et al. (2015) include the operational drought in this classification.

Meteorological droughts characterize by a prolonged deficit of precipitation (below an average threshold) and is the 1st type of drought, that develops quickly (HEIM, 2002; HAO & SINGH, 2015; RAJSEKHAR et al., 2015; WU et al., 2018; GUO et al. (2019). Meteorological drought can generate the other types of droughts, due to the hydrological balance on Earth and in the atmosphere (MAITY et al., 2016).

The agricultural droughts are the lag of the meteorological droughts and characterize by a deficit of the soil moisture leading to insufficient water to agriculture (HEIM, 2002; HAO & SINGH, 2015; WU et al., 2018; GUO et al., 2019). High evaporation loss and extended meteorological droughts cause agricultural droughts (MAITY et al., 2016).

Hydrological droughts characterize by a deficit in groundwater as well as the reduction of streamflow and reservoirs level. This type of drought occurs after a prolonged period without rainfall (HAO & SINGH, 2015; WU et al., 2018; GUO et al., 2019). Society and economy depend on catchment stores (e.g. aquifers, rivers, and lakes). Hydrological droughts occur due to the direct impact of other droughts (meteorological and agricultural) that lead to a deficit in drinking water as well as consequences for industry and energy generation (VAN LOON & LAAHA, 2015; HAO et al., 2016; MAITY et al., 2016; WU et al., 2018).

According to WU et al. (2018), reservoir and dams construction, land-cover/use, irrigation and other acceleration actions due to the anthropic scene may cause hydrological droughts worldwide. Geographical, climatological and topographical features affect the correlation of the droughts transition (the passage from one state to another, i.e., from agricultural to hydrological droughts).

In a water exploitation system, PEDRO-MONZONÍS et al. (2015) define the period under an extreme supply failure of the water demand as the operational drought. This happens due to an inadequate design of the operating and water exploitation systems, and the demand excess. It is an extension of the hydrological droughts and water scarcity, generating environmental and posterior socioeconomic impacts.

The combination of the other three types of drought characterize socioeconomic droughts, for instance when the water supply is insufficient for the demand (MISHRA & SINGH, 2010; HAO & SINGH, 2015; GUO et al., 2019) or affects other sectors of the economy such as livestock. According to GUO et al. (2019), this type of drought tend to intensify (become more frequent) in the future. In order to analyse them, some authors (HUANG et al., 2016a; GUO et al., 2019) proposed several multivariate approaches that consider the outflow of a reservoir as the water demand to compute the socioeconomic droughts.

Analysing droughts in different accumulation periods turns possible the identification of distinct types of droughts. In a general overview, researchers point the short accumulation periods as ideal to analyse the meteorological and agricultural droughts, while the long-term accumulation periods as ideal to analyse the hydrological, operational and socioeconomic droughts.

It is important to evaluate and identify different types of drought for a better water resources management, because the type of drought gives the information of the respective phenomenon occurring in a region and its duration (given by the timescale).

According to SIMS et al. (2002) and VICENTE-SERRANO (2006), the short timescales represent the water availability for agriculture and vegetation, since they represent the soil moisture variations. The authors applied a drought index accumulated in short periods (3 and 6 months) to evaluate the agricultural droughts. AHMADALIPOUR et al. (2017) highlight that distinct timelags allow the analysis of different types of droughts.

VICENTE-SERRANO (2006) applied different accumulation periods (1 to 48 months) to identify the response of different types of drought. The author highlights the importance of the timescale to characterize a hydrological drought. The annual scale (12-month accumulation period) is ideal for hydrological drought studies (CHANGNON AND EASTERLING, 1989). The longer timescales (24 months or longer) can evaluate the operational droughts.

The operational and socioeconomic droughts happen after the occurrence of the three types of drought presented previously. They are difficult to analyse since they depend on operational and/or socioeconomic factors.

It is important to study all drought types, since they are dependent on each other, i.e., the hydrological drought happens after the development of the meteorological drought and consequently the agricultural drought. The water deficit in the atmosphere (meteorological) and in the upper soil layer (agricultural) leads, after a time, to streamflow and groundwater deficits (hydrological drought). Altogether, the hydrological drought affects aquifers and reservoir levels, which leads to operational droughts and after some time, they affect both society and economy (socioeconomic droughts).

1.5. Drought indices

Climate scientists developed several drought indices all over the recent history (post 1950s). They are univariate and bivariate indices, and combine hydro-meteorological variables, as occur in the water balance and latent (hidden) variable drought indices, respectively.

Some authors developed multiple drought indices based on the water balance model, like the Palmer Drought Severity Index (PDSI) (PALMER, 1965). The PDSI uses precipitation, temperature, as well as water content in the upper soil layers.

The latent variable indices consist in a mathematical transformation (e.g. ratio or difference) of some meteorological variables that relate to each other physically. The difference between evapotranspiration and precipitation is the water deficit and is a hidden or latent variable.

The computation of these indices consist in fitting a probability distribution to the series, followed by standardization. It is important to fit a probability distribution to compute and evaluate the *"magnitude, occurrence and/or frequency of the phenomenon in a certain*

interval". GUTTMAN (1998) discuss several probability distributions to fit the hydro-meteorological data and to compute quantiles of the drought indices, like the Generalized Extreme Value (GEV), beta distribution and Generalized Logistic Distribution (GLD) (MCKEE et al., 1993; SHEFFIELD & WOOD, 2008; VICENTE-SERRANO et al., 2010; STAGGE et al., 2015).

TSAKIRIS & VANGELIS (2005), VANGELIS et al. (2013), HAO & SINGH (2015) and AMIN et al. (2015) propose the Gamma distribution as the most suitable for drought analysis, followed by the 2-parameter Lognormal (LN2) distribution. They suggest that both distributions are suitable for small timescales (monthly to quarter) and suggest the application of a procedure in the gamma distribution (described in chapter 2 – Methods) to overcome the "zeros issue". Other authors like STAGGE et al. (2015) fitted the Gamma, Gumbel, Logistic, Log-Logistic, Lognormal, Normal and Weibull probability distributions. Results showed the 2-parameter Gamma and the Generalized Extreme Value (GEV) as the most suitable for drought analysis in Europe.

Despite the probability distribution adopted, there are several drought indices applied around the world in the univariate and bivariate approaches. The most applied drought indices description and application are presented in the next subsections. They are the Palmer Drought Severity Index (PDSI), the Standardized Precipitation Index (SPI), the Reconnaissance Drought Index (RDI) and the Standardized Precipitation Evapotranspiration Index (SPEI).

1.5.1. Palmer Drought Severity Index (PDSI)

The Palmer Drought Severity Index (PDSI) was the first and most used drought index in the second half of the twentieth century. It is a pioneer in drought analysis (GUTTMAN, 1998; DUBROVSKY et al., 2009; DAI, 2011; HOERLING, 2012; NAM et al., 2015).

PALMER (1965) created the PDSI and applied it across US. The computation of the PDSI involves the water balance equation and it is necessary to determine the Climatically Appropriate Factor for Existing Conditions (CAFEC) coefficient, to obtain the moisture anomaly index (referred as Z index). The CAFEC is an empirical weighting factor (parameter) determined for each location in the US and it consists in the moisture amount during "normal" weather.

The combination of evapotranspiration, precipitation, runoff, and temperature is one of the main advantages of using the PDSI (WELLS et al., 2004), since it can represent the processes of the Earth' surface related to drought events.

One of the disadvantages is the non-representativeness of groundwater in its formulation (HAO & SINGH, 2015). ZHAO et al. (2017) point that the PDSI is more suitable to assess long time scale droughts but it has shortcomings like complex computation and high input data requirements (LLOYD-HUGHES & SAUNDERS, 2002; MISHRA & SINGH, 2010; WU et al., 2018).

Another disadvantage of the PDSI is the necessity to compute the CAFEC coefficient, since in developing countries there are not sufficient data to determine it. ALLEY (1984) criticizes the use of the PDSI because of the CAFEC limitation that generates extensive number of water balance equations to perform a drought analysis for each region. The author highlights the PDSI is a useful tool for analysing droughts when comparing to the observed time series and is largely applicable for drought analysis in a country with a large amount of hydro-meteorological data. It is a robust method to perform drought analysis in a region, when compared to other methods.

In order to overcome the CAFEC issue, WELLS et al. (2004) proposed the self-calibrated Palmer Drought Severity Index (sc-PDSI) using the data for each location, *"replacing empirical constants with dynamically calculated values"* (VAN DER SCHRIER et al., 2013; NAM et al., 2015). TODD et al. (2013) applied the sc-PDSI to generate drought series in three locations in Southeast UK and observed differences in duration among the analysed sites.

1.5.2. Standardized Precipitation Index (SPI)

The Standardized Precipitation Index (SPI) is the standardization of the precipitation widely applied to determine meteorological droughts. The SPI relies on the premise that a deficit in precipitation is the sufficient variable to determine droughts (MCKEE et al., 1993). According to SOBRAL et al. (2019), the SPI is the most applied drought index worldwide and the World Meteorological Organization (WMO) recommends its application in drought studies.

Topographical or geographical differences do not affect the SPI and researchers compare it in space and time (LANA et al., 2001; VICENTE-SERRANO, 2006).

There are several studies applying the SPI throughout the world due to its simplicity in application and evaluation, generating significant results. SPINONI et al. (2014) applied the SPI and results showed a global increase in severity, duration and intensity of droughts. They found an exception in the Northern Hemisphere, where the frequency decreased in the baseline period of observed series. JOHNSON & SHARMA (2015) evaluated the impact of bias correction methods in drought assessment using a multi-year scale and the SPI. They found significant differences in all SPI computed statistics.

1.5.3. Reconnaissance Drought Index (RDI)

The authors TSAKIRIS & VANGELIS (2005) state that the SPI is not sufficient to evaluate droughts, since it uses only precipitation in its formulation. For this reason, TSAKIRIS & VANGELIS (2005) developed the Reconnaissance Drought Index (RDI) computed as the ratio between precipitation and potential evapotranspiration, both accumulated in predefined periods. According to HAO & SINGH (2015), the potential evapotranspiration is the key variable, because it represents the water return to the atmosphere.

TSAKIRIS & VANGELIS (2005) and TSAKIRIS et al. (2007) point some advantages in applying the RDI: (1) calculus of aggregated deficit between input variables (evapotranspiration and precipitation) in the atmosphere, (2) similar way of calculation as in SPI and (3) it is associated to agricultural drought, due to the temperature consideration (HAO & SINGH, 2015). VICENTE-SERRANO et al. (2010) point some disadvantages of using RDI, such as: (1) unknown definition when the variable ratio is zero (no rainfall) and (2) the same ratio reduces the variability range.

To determine the Potential Evapotranspiration (PET), VANGELIS et al. (2013) suggest applying several methods such: Penman-Monteith, Thornthwaite, Blaney-Criddle, and Hargreaves. MOHAMMED & SCHOLZ (2017) applied these four methods to compute the PET and results showed differences among them in drought severity, presenting the Hargreaves as the best model. They pointed the Hargreaves as the best method to compute PET for climate change studies. It has the advantage of considering the solar radiation in its formulation,

improving the accuracy of results in arid and semiarid regions. However, the authors TSAKIRIS et al. (2007) and VANGELIS et al. (2013) suggest applying the Thornthwaite or Blaney-Criddle methods to compute PET in order to minimize the data requirements.

KOPSIAFTIS et al. (2017) evaluated the drought severity in a coastal aquifer flow and applied the RDI, since the potential evapotranspiration affects the recharge processes. They also evaluated the effect of the multi-year drought and results showed that the RDI is a good index to achieve their goals. MOHAMMED & SCHOLZ (2017b) applied the RDI in different time scales and compared to original precipitation and temperature data. Results showed that the RDI normalized form better represents drought events in the region, instead of using only original precipitation series.

1.5.4. Standardized Precipitation Evapotranspiration Index (SPEI)

The authors VICENTE-SERRANO et al. (2010) created the Standardized Precipitation Evapotranspiration Index (SPEI) to include the potential evapotranspiration in climate change studies, turning it a suitable tool to study global warming effects (NAM et al., 2015). The SPEI and RDI differ because the SPEI is the difference between precipitation and potential evapotranspiration, while the RDI is the ratio between both variables. The SPEI is a good index to represent the dynamical balance between water and energy (LIU et al., 2019).

Due to its multi-scalar nature, it assesses different types of droughts (VICENTE-SERRANO et al., 2012). VICENTE-SERRANO et al. (2010) fitted a log-logistic distribution and accumulated the deficits in several SPEI timescales. They applied the SPEI worldwide under different climate conditions and observed a general increase of severe droughts related to higher water demand, result of evapotranspiration.

TONG et al. (2018) applied the SPEI to evaluate drought events in the Mongolian Plateau, China. Results showed an annual decreasing trend rate of drought and found changes of drought into wet periods and vice-versa. WANG et al. (2019) applied the SPEI to evaluate the drought intensity variation in distinct time intervals. They performed the non-stationary analysis in Inner Mongolia and results showed drought trend from 1945 onwards. They also found an increasing drought trend in the Northeast Inner Mongolia, where the most intense drought occurred between 1960 and 1970.

LU et al. (2019) applied the SPEI globally and results showed significant trends of drought severity in America, Africa and Oceania in all future scenarios. The African continent presented severe droughts in both South and North in all scenarios and three decades, also pointing to the Southern American continent as another most affected region by droughts. The most affected countries due to the increase of PET are Canada, Turkey, Russia and Ukraine.

1.5.5. Other indices and combined application

Around the world, researchers compared drought indices and analysed their performances under different climatic conditions and timescales. ZHAO et al. (2017) compared the performance of the self-calibrated Palmer Drought Severity Index (sc-PDSI) and the SPEI. Results in the Chinese stations showed the SPEI underestimates the dry periods in shorter time scales (3 and 6 months), while in longer time scales (12 to 48 months) dry periods of both indices remained the same. General results showed the SPEI performing better for short-term droughts, while the sc-PDSI for long-term droughts.

A modified version of the PDSI (MPDSI) proposed by KANG & SRIDHAR (2017) was applied in Virginia State, US. They compared the MPDSI performance with the Standardized Soil moisture Index (SSI) and the Multivariate Standardized Drought Index (MSDI). Results showed increase in agricultural droughts due to high evapotranspiration rates, groundwater and surface flow.

A comparison between the SPI and PDI (a modified version of the PDSI to apply in water supply monitoring) was made by GUTTMAN (1998). Results of the spectral analysis showed the PDI lags behind the SPI in shorter time scales (less than 1 year), while in longer time scales both present the same drought behaviour. Results also showed a spatial variation between both indices and the author arguments that this happens due to the variation in both potential evapotranspiration and groundwater flow, since both depend on the soil use of each region.

The temperature influences the evapotranspiration rates and TOUMA et al. (2015) applied the SPEI, SPI, SRI, and the Supply-Demand Drought Index (SDDI) worldwide to evaluate the drought magnitude due to changes in precipitation, temperature and soil moisture. Results showed increasing exceptional droughts in terms of duration, spatial extent and

occurrence in tropical and subtropical regions. They found higher changes in the SPEI and SDDI, concluding that temperature influences the results, when compared to changes in the SPI and SRI.

Other authors performed a study concentrating their research area in the countries United Kingdom (UK), Germany, Slovenia, Bulgaria and Norway (STAGGE et al., 2015). They combined the SPEI and SPI aiming at establishing a link between drought and its impact on society (energy, livestock, freshwater, public water supply, industry and agriculture). They compared the drought indices analysis with drought impact reports of the European Drought Impact Inventory (EDII). In each report category, there is a typical drought period (accumulated months). Two to 12 months anomalies explain the agricultural impacts, while the 6 to 12 months explain the energy and hydropower deficits. One to 3 months anomalies relate to freshwater and public water supply. They observed anomalies between the report predictions and observed series, as well as the feasibility in applying these reports (models) combined to meteorological drought indices.

WANG et al. (2019) proposed a modification in the SPEI, combining it with the runoff series and used a two-dimensional copula function. The Standardized Precipitation Evapotranspiration Runoff Index (SPERI) used the Penman-Monteith to compute the PET. Results showed similar relationships between SPEI and SPI applications and presented a good performance for the 3-month SPERI, when compared to the SPEI and SPI.

MARCOS-GARCIA et al. (2017) made a comparison between the SPI and SPEI and applied the Thornthwaite method for a better intra-annual representation of the PET in the Spanish Jucar River basin. Results showed an increase in magnitude and intensity of drought events in climate change scenarios, in both meteorological and hydrological droughts. They suggest these increases occurred due to both increasing evapotranspiration rates and rainfall reduction. The SPI may underestimate drought severity since it neglects the temperature in its formulation.

In the work of SPINONI et al. (2017), the Hargreaves-Samani method was applied in the SPEI. The authors compared the SPEI results with the SPI and studied the short-term droughts (3-months) in the European continent. General results showed more severe and frequent dry events since 1980s in Mediterranean, Central Europe and Eastern Europe in the summer, spring and autumn, respectively. BYAKATONDA et al. (2018) concluded the SPI overestimates the winter season and the SPEI better represents the drought spatial coverage.

Other researchers compared the SPI with other indices, like the Standardized Streamflow Index (SSI). WU et al. (2018) compared both indices aiming at evaluating the operational rules impacts in reservoirs in different timescales (e.g. 1, 3, 6, 12, and 24 months). They correlated the pre- and post-reservoir levels with both indices results. They found changes in linear correlation between meteorological and hydrological droughts, comparing the post- and pre-reservoir levels. For 1 to 3-month (short-term) droughts, both indices alleviated the drought magnitude and duration.

Some researchers compared the SPI with other indices, like the RDI. TSAKIRIS et al. (2007) compared both indices with the deciles method to evaluate drought events in the Greek Nestos and Mornos River basins. They concluded the RDI performs better when compared to both SPI and deciles method to represent drought severities.

ZARCH et al. (2011) applied the SPI and RDI across Iran and found slight differences between them. They relate these differences to potential evapotranspiration, which was computed using the Penman-Monteith method. They also found significant correlations between both indices in short-term accumulation periods (3, 6, and 9 months).

In another study, ZARCH et al. (2015) evaluated the effect of considering the potential evapotranspiration in drought analysis. They applied both SPI and RDI worldwide and concluded that there is no significant trend across meteorological stations in the world, except in arid regions, which presented upward and downward trends. They highlight the importance of considering the potential evapotranspiration to compute these indices in climate change studies. They showed differences in both indices results in different climate types, i.e., hyper-arid to humid zones (RDI tends to become drier in humid zones).

In Kentucky River Basin, US, CHATTOPADHYAY et al. (2017) evaluated climate change impacts applying the RDI. According to them, meteorological droughts show a slight decrease in intensity but duration may remain the same, when comparing the baseline period with the projected future of RCMs. The hydrological drought durations may increase in the future, while the intensity may decrease. They also applied the Streamflow Drought Index (SDI) to evaluate hydrological droughts.

HUANG et al. (2017) applied both Standardized Streamflow Index (SSI) and SPI to evaluate streamflow series. They aimed at analysing the change of meteorological to hydrological droughts using also, the cross-wavelet analysis to compare correlations between

these two types of droughts. Results showed that both winter and autumn presented long duration, while summer and spring presented short duration, as well as positive statistical linkages were found in short and long-time scales.

1.6. Drought analysis in Brazil and Southern America

Usually, researchers perform drought analysis studies in regions where there is a constant lack of precipitation, like in deserts, arid and semiarid areas. The Northeast Brazil (NEB) is a semiarid region. MARENGO et al. (2017) show rising temperature trends and precipitation reduction in NEB along the future. According to them, between 2012 and 2015, NEB suffered severe drought impacts that affected farming and pasture, and consequently, both society and economy.

SILVA et al. (2016) evaluated the space-time variability in NEB of both streamflow and precipitation applying the Shannon entropy principle, which evaluates the random process uncertainty. Spatial patterns generated by Shannon entropy led the authors to understand the NEB streamflow and rainfall characteristics. They also found that rainy season and annual features affected the total relative entropy of both series. VAN OEL et al. (2018) evaluated droughts due to the reservoir network impacts, applying both SPI and Standardized Streamflow Index (SSI). They showed the reservoir stored water volume during a drought period.

One of drought impacts in water resources relies in hydropower generation, and Brazil is a largely affected country (LIMA, 2014). In a country highly dependent on hydropower generation, it is necessary to evaluate and forecast drought events in order to reduce their socioeconomic impacts. According to JONG et al. (2019), more than 80% of the Brazilian electricity comes from renewable sources and the hydropower plants generate around 64% of the national electricity demand (ANEEL, 2018). In Brazil, low-level reservoirs imply thermal power generation and thus increase electricity cost.

According to JONG et al. (2019), high temperatures and reduced precipitation patterns occurred over the end of the last century in NEB. They observed this behaviour in the Sao Francisco River basin and they believe these effects occur in response of the climate change impacts. They also found the 3.6% radiation increase in NEB might be a consequence of climate changes. They compared the past (1970s) to the future (2080s) scenarios. BARBOSA &

KUMAR (2016) identified patterns between rainfall and vegetation dynamics in a spatiotemporal analysis in Brazil. Results showed a higher correlation between SPI and Standardized Difference Vegetation Index (SDVI) in the 3-month analysis.

Droughts also occur in regions where there are high rainfall rates during the year, like the Southern Brazil. CARVALHO et al. (2013) studied the drought phenomena in the South, Southeast and Midwest of Brazil and determined the return period as well as dry spell occurrence. Results showed that increasing drought trends occur due to the irregular rainfall distribution in the Midwest region. In South and Southeast, results pointed rainfall decrease leading to dry spell reduction. In Midwest, a damage to agriculture leads to losses in grain filling and flowering phases. Results also showed the South region is the most vulnerable in terms of dry spell intensity.

The city of Sao Paulo suffered an intense drought between 2014 and 2015. This drought is the worst in 100 years, where the Cantareira storage (main water supply of the city) was around 6% of its capacity in February of 2015. SORIANO et al. (2016) attribute the Sao Paulo longest drought to irregular occupation of the banks allied to a poor planning in distribution and supply. The Sao Paulo government declared this drought as a public calamity and applied bonus payments for water consumption decreases.

SOBRAL et al. (2019) evaluated the relationship between the annual SPI and ENSO as well as drought trends. They applied the SPI in hydrological stations located across Rio de Janeiro State, Brazil. They found decreasing trends in the Centre and South regions, while found increasing trends in the North region.

In the Upper Sao Francisco River catchment, SANTOS et al. (2019) applied the SPI and wavelet analysis to characterize drought events. They applied the continuous wavelet transform to investigate the teleconnections with the ENSO and Pacific Decadal Oscillation (PDO), in terms of time frequency information. When both PDO and ENSO cold phase coincides, the climate indices result in severe droughts in the wavelet analysis. For large-scale anomalies, researchers must investigate climate variations.

VICENTE-SERRANO et al. (2015) found average decadal variations in Bolivian stations and differences in terms of spatiotemporal variability in the Amazonian region. They believe these differences relate to high atmospheric water content due to intense evapotranspiration rates of the forest. They applied both SPEI and SPI, and found drought

trends in the Bolivian Altiplano. They showed the temperature effect intensified drought severity and increased both duration and magnitude of drought events.

Finally, MARENGO et al. (1998) applied the Mann-Kendall coupled with t-test and linear regression. They found negative and positive trends in the summer, with the first applying to the Sao Francisco River and to the Peruvian territory, while the last applies to the Parnaiba River basin.

1.7. Tests and trend analysis

It is important to analyse drought impacts and intensities in the future, as well as evaluate their relations with climate changes, analysing the simulated scenarios of temperature, precipitation and other variables, and identify possible trends of the drought events (KANG & SRIDHAR, 2017).

According to ROUGÉ et al. (2013), the hydrological series (precipitation and streamflow) presented more trends due to anthropic and/or natural changes. It is important to detect these changes and eventual shifts in the series (gradual or abrupt) for a better water resources management and planning.

A way to evaluate the extreme events consists in applying trend and changing point tests like Mann-Kendall (MK) and Pettitt (PT), respectively. The MK is a worldwide applied test to detect trends in the series and the World Meteorological Organization (WMO) recommends it for climate change studies (BACK, 2001; BARROS et al., 2011). According to COSCARELLI & CALOIERO (2012), the MK presented increasing trends in Italian rainfall patterns.

In the work of WANG et al. (2008), they found changes in both rainfall and runoff in the Dongjiang River basin, China. They applied the MK, Kolmogorov-Smirnov (KS) and the quantiles test to verify changes in the probability distributions. A small variation in the annual extreme rainfall let them establish a relationship with climate changes.

ROMANO et al. (2011) and SAYEMUZZAMAN & JHA (2014) applied the MK in precipitation and runoff series. The first authors found a decrease in the winter rainfalls and in the annual flows, concluding that the annual precipitation decrease relates to runoff decrease. SAYEMUZZAMAN & JHA (2014) analysed the historical period (last 50 years) of North

Carolina stations, US, and observed increasing trends in the winter at the same time they observed decreasing trends in the summer.

GOCIC & TRAJKOVIC (2013) applied the MK combined with Spearman's Rho test, and linear regression in Serbian stations. They found between October and January an increasing trend, while in February to September a decreasing trend in the monthly analysis. Results also showed no significant trends in the seasonal analysis, except in the winter and autumn. They also applied the SPI, where two stations presented decreasing trend in the SPI annual analysis, while the other ten presented increasing trends.

GÜÇLÜ (2018) applied the Linear Regression (LR), Spearman's Rho, partial Mann-Kendall, and the Sen's slope to identify possible trends in temperature, runoff and precipitation series. They applied all methods in different stations located sparsely in Turkey and results showed improvement in trend analysis, when comparing all methods.

It is possible to combine the Mann-Kendall (MK) and Sen's slope estimator, as performed SHIRU et al. (2019) across Nigeria. They applied the Sen's slope to quantify droughts combined with the MK to evaluate trends. They evaluated temperature and precipitation trends using a 10-year time step and a 50-year moving window to evaluate temporal drought variations. Results showed increasing drought severity in all cropping of Nigerian seasons. They found the precipitation in tropical savannah and monsoon areas, and the temperature in semiarid areas, were the main drivers of the increasing trends. They suggest the global warming alters the temperature rates, increasing both frequency and severity of droughts.

AHMED et al. (2018) applied both 10-year time step and 50-year moving window as evaluation methods for analysing drought temporal variations. They analysed climate change impacts and climate variability across Pakistan. They found increasing drought frequencies due to the increasing temperature in crop seasons. Results indicate increasing drought frequency and severity related to global warming mainly in arid areas.

The Mann-Kendall test and Pre-Whitening Trend (PWT) method were applied by MODARRES et al. (2016). They aimed at verifying trends and serial correlation in the magnitude of droughts and floods in Iran. They found significant increasing trends after the PWT application, and found decreasing trends in flood magnitude and increasing trends in

drought severity. They relate both decreasing and increasing trends with the land use changes, and the increasing trends with the annual precipitation.

In the works performed by GROPPO et al. (2001), MESCHIATTI et al. (2012) and ROUGÉ et al. (2013), they applied both MK and Pettitt tests and found increasing trends in the precipitation series. The temperature series presented increasing trends in the works of MESCHIATTI et al. (2012) and ROUGÉ et al. (2013). MESCHIATTI et al. (2012) also analysed the streamflow series that presented positive trends in the major studied rivers, and just one presented a negative trend.

The Pettitt test is widely applied to detect changing point in the series. ROUGÉ et al. (2013) combined both MK and Pettitt tests to evaluate abrupt or gradual shifts in the series across US. Results showed a decrease in temperature in Southeast US, while in other areas a linear increase. According to ENGSTRÖM & WAYLEN (2017), there is a limited long-term information in the water resources series.

In the same work, ENGSTRÖM & WAYLEN (2017) analysed long-term changes using streamflow and precipitation data and applied the Pettitt test to detect the changing point in the series of the Southeast US. Results showed a strong relationship between the Atlantic Multidecadal Oscillation (AMO) and hurricanes precipitation with long-term and seasonal changes in the precipitation-runoff after 1990.

General studies applied the MK test combined with many other methods, as did ZHANG et al. (2018) using the Kling-Gupta efficiency method. Results showed precipitation occurrence increase, and that potential evapotranspiration increases the drought peak value. They suggest the increases in duration, peak value and severity of hydrological droughts may relate to human activities in the middle Yangtze River, China. According to them, human activities and climate variation are the main drivers to alter the drought severity.

CARVALHO et al. (2013) evaluated the non-stationarity by Dickey-Fuller test and applied the MK test to verify the significance of the positive drought trend. They applied the percentile-percentile (PP) plots and the Kolmogorov-Smirnov (KS) test to verify the goodness-of-fit of the Generalized Extreme Value (GEV) probability distribution. They used the maximum likelihood method for parameters estimation.

Given the application of both trend and changing point tests around the world, it is useful to perform drought analysis using these tests. The traditional drought indices are based

on fitting a stationary probability distribution, at the same time several meteorological stations present non-stationarity. For this reason, it is recommendable to apply the non-stationary drought analysis in drought series, using trend and changing point tests for non-stationarity detection.

It is important to highlight that both MK and Pettitt tests results may have impacts due to the series length in each study, i.e., both tests results may change under the time period considered. In this sense, KOUTSOYIANNIS (2006) states *"the longer is the observation period, the more truthful is the picture of the runoff variation through time"*. In the same paper, KOUTSOYIANNIS (2006) discussed about the scaling approach and according to the author, a time series piece can result non-stationary behaviour after the non-stationary tests application. However, considering the entire series, this non-stationarity does not exist and the series is stationary, according to MK and Pettitt tests results. This is the main advantage in using non-stationary tests detection to evaluate the time series non-stationarity, since it can change depending on the time series length.

1.8. Non-stationary Frequency Analysis (NFA)

The Non-stationary Frequency Analysis (NFA) is a possible solution to deal with fluctuations, trends and changing points in the meteorological series statistics. Before applying the NFA, it is useful the application of specific tests to verify the stationarity in the series. Under a non-stationarity verification, some researchers perform the NFA fitting probability distributions varying in time. They perform it varying one or more parameters of the probability distributions and verifying possible trends in the estimated parameters.

Researchers that analyse droughts first establish a relationship between variables (drought indices formulation) and then fit a probability distribution to them in order to obtain information about duration, intensity and magnitude. A probability distribution fitting relies on a stationarity premise, and most of hydrological variables are non-stationary. In this way, there is a conceptual inconsistency in fitting stationary distributions to non-stationary series.

Stationarity is the statistical balance of a stochastic process (DETZEL, 2015), in other words, when the mean of the time series remains constant over time. This behaviour does not happen in mostly of the time and the non-stationary pattern expects to become more frequent

in hydro-climatological variables due to climate change impacts. Signs of non-stationary pattern in time series are the presence of random walks, cycles, trends, changing points, or the combination of two or more. However, the stationary pattern in time series indicate that there are not variations in variance, covariance and/or mean. A stochastic process balance when their statistical properties does not depend on time means a stationary pattern. Changes in hydro-meteorological stations like relocation, as well as changes in hydro-meteorological variables and soil use can reflect in non-stationarity (NAGHETTINI & PINTO, 2007).

There are two stationarity types: (1) Strict Sense Stationarity (SSS) and (2) Wide Sense Stationarity (WSS). The first is defined by $f[x(t_1),\ x(t_2), \dots] = f[x(t_1 + \zeta),\ x(t_2 + \zeta), \dots]$ where the term $f[x(t_1),\ x(t_2), \dots]$ is the variable $x(t_i)$ joint density function. The second relies in the weak or wide sense, where $E[x(t)] = constant$ and $COV\left[x(t_i),\ x\left(t_j\right)\right] = f\left(t_i - t_j\right) = f(\tau)$, being $E[x(t)]$ the $x(t_i)$ variables mean and $COV\left[x(t_i),\ x\left(t_j\right)\right]$ the covariance of $x(t_i)$ and $x\left(t_j\right)$ (PAPOULIS, 1965; PEDROZO, 2017). In the work of CHENG & AGHAKOUCHAK (2014), results showed low differences between stationary and non-stationary modelling.

There are many works in the literature using the non-stationary frequency analysis to analyse rainfall extremes, as well as drought series fitting a stationary probability distribution. Recently, few researchers have studied the non-stationary approach for droughts and this is the main contribution of this dissertation.

Some authors attribute the non-stationarity within hydrological series (mainly precipitation) to climate change and/or climate variability (ZHANG et al., 2010). Some researchers performed the NFA in extreme rainfall series in different countries around the world. YILMAZ & PERERA (2014) fitted the Generalized Extreme Value (GEV) and identified the changing point year (1967), and split the series in 1925 to 1966 and 1967 to 2010. They did not find significant difference in extreme rainfall trends, comparing the stationary and non-stationary GEV models.

The authors VU & MISHRA (2019) also evaluated the rainfall extremes and applied the non-stationary GEV, where they varied both location and scale parameter over time. They used the time-covariate as well as other time-varying covariates, such as mean and maximum temperature, and the ENSO cycle. Results showed that different combinations and type of

covariates could result in increased precipitation events. Results also showed the return periods of the stationary method are higher, when compared to the non-stationary method.

Other researchers apply different methods to evaluate rainfall extremes, such did SUGAHARA et al. (2009) applying the Peaks over Threshold (POT) method and the Generalized Pareto Distribution (GPD) in Sao Paulo, Brazil. They maintained the shape parameter constant and varied the scale parameter. In the fitted models, results showed the scale parameter presented positive trend.

CHENG & AGHAKOUCHAK (2014) evaluated trends in the hydro-meteorological variables applying the NFA. They used the non-stationary Intensity-Duration-Frequency (IDF) curves, occurrence of extremes and uncertainties using the Generalized Extreme Value (GEV) distribution and the Bayesian inference (for uncertainty analysis). They concluded after applying the Mann-Kendall (MK) test that there are underestimation of extreme rainfall in the IDF curves of around 60%.

AGILAN & UMAMAHESH (2017) fitted the non-stationary GEV distribution using time as covariate in the analysis in the Hyderabad city, India. They applied the corrected Akaike Information Criterion (AICc) value to evaluate the duration of rainfall series and modelled the physical covariates in two sections: (1) the location parameter is non-stationary and (2) the location and scale parameter are non-stationary. They found underestimation in the extreme events, comparing the stationary and the non-stationary models.

Some authors applied the variation of parameters on time, as did LI et al. (2019), who developed a non-stationary model to analyse the frequency of the intensity and rainfall volume of daily precipitation. They applied a 30-period moving window to investigate the temporal and dependence evolution of the linear regression analysis in the parameters series. They fitted the GEV distribution to model the marginal distribution and results showed an increase in both rainfall intensity and volume for the study region. They highlight the importance of developing non-stationary analysis in rainfall series.

The Generalized Addictive Models for Location, Scale and Shape (GAMLSS) are another tool to perform the NFA. OSORIO & GALIANO (2012) applied them combined with a bootstrap technique. They aimed at fitting Probability Density Functions (PDF) to the maximum dry spells in annual monsoon series in the Senegal River Basin. Results showed an

increase in both variance and mean of the annual drought spells, along with an increase of dry spell lengths.

Another application of the GAMLSS occurred in the work of GU et al. (2016). They modelled the flood occurrences and frequencies using the Peak over Threshold (POT) and GAMLSS methods, respectively. They found non-stationarity in the floods and observed an increase in the flood magnitude and frequency in the 1990s. They found two periods of increasing floods occurrence and some fluctuations. The non-stationary models represented well the floods occurrence and its fluctuations.

SUN et al. (2018) applied the GAMLSS combined with the Pettitt method to evaluate the monthly flood frequency across Huai River basin, China. Results showed six stationary and three non-stationary flow series. They fitted both 2-parameter Lognormal (LN2) and Weibull distributions to the flow series, suggesting the Weibull as the most appropriate. This analysis let them conclude that fitting the Pearson Type III and considering the stationary premise when it is non-stationary, produced biased flood frequencies.

Finally, RASHID & BEECHAM (2019) applied the GAMLSS in the Southern Australia. They developed the Non-stationary Standardized Precipitation Index (NSPI) and incorporated climate indices as external covariates. They showed that a non-stationary model better reproduces droughts. Results showed that drought duration and severity are significantly different, when comparing the NSPI to the stationary SPI.

1.9. Chapter summary

A general overview about research of climate change impacts in hydro-meteorological series and correlated studies performed around the world was presented. Researchers believe these impacts alter significantly the drought event occurrences and consequently affect the world climate.

The climate model scenarios as well as the bias correction methods, in order to perform the drought analysis of the future drought series were also briefly presented. According to the subsection 1.2, the most used bias correction methods are: Linear Scaling (LS), Power Transformation (PT), Variance Scaling (VARI) and Empirical Quantile Mapping (EQM).

Subsections 1.3 until 1.6 provided a general overview of the drought phenomena, including the worldwide division of the drought types in meteorological, hydrological, agricultural, operational and socioeconomic. In this dissertation, the focus is on meteorological droughts only.

The following subsections provided the most applied drought indices all over the world to assess meteorological droughts, and the Reconnaissance Drought Index (RDI) is the chosen model to apply in this research.

Hence, the drought analysis in Brazil was presented, showing the need in study droughts not only in semiarid regions, but also in humid areas with a non-stationary pattern, like the Southern Brazil. These regions usually present drought events and it is important to evaluate them for water resources management and planning, in both domestic and industrial water supply, as well as in the hydropower generation sector.

Finally, it was briefly presented the application in literature of both trend and changing point tests to verify the hydro-meteorological series stationarity or non-stationarity. These recent studies in rainfall and floods provide the premise to perform the NFA in droughts. Hence, the general NFA performed around the world was presented, indicating that it is feasible to apply simple probabilistic models for a local drought analysis.

2. METHODS

This chapter describes the methods applied to investigate the hypothesis of this dissertation that drought statistics vary under a non-stationary approach. The literature review presented some aspects of the drought analysis analysing both past and future series of meteorological variables. The present work used both monthly mean precipitation and temperature series to perform the drought analysis. The implementation of all methods occurred in Python environment. The first subsection of this chapter is the flowchart, which introduces the steps of the analysis. The detail of all applied methods is described in the next subsections to achieve this dissertation main goal of performing a non-stationary drought analysis in climate change scenarios.

2.1. Dissertation's flowchart

The dissertation follows the flowchart presented in the Figure 1. Step 1 is the acquisition of historical monthly mean precipitation and temperature data from governmental institutions, as explained in the subsection 3.2. Step 2 is the application of the simple linear regression filling in missing observations in the series, using the closest (neighbour) meteorological stations. If data are missing in some of the closest stations, the arithmetic mean between the four closest values was computed for the respective month (e.g. four months above in the end of the series, four months below in the beginning of the series or two months "previous and after" in the middle of the series).

Step 3 is the acquisition of the baseline series (for comparison with the historical series) and the future series. Step 4 is the application of bias correction methods to regionalize the data, according to the observed series. The bias correction methods applied are Linear Scaling (LS), Empirical Quantile Mapping (EQM) for precipitation and temperature and the Power Transformation (PT) for precipitation only and the Variance scaling (VARI) for temperature only. Analysing the descriptive statistics (mean, standard deviation, minimum, maximum, kurtosis, skewness, and percentiles at 5%, 10%, 25%, 50%, 75%, 90% and 95%), the best regionalization performance among the bias correction methods was applied. The Mean Absolute Error (MAE) coefficient was also computed to evaluate the bias correction methods.

Step 5 is the computation of potential evapotranspiration using the Thornthwaite method in both historical and future series. Along with the temperature, in order to perform the computation, it is necessary to include the daylight length as an input data, downloaded via a public domain website, as explained in detail in the chapter Study Area and Data.

Figure 1 – Dissertations' flowchart.

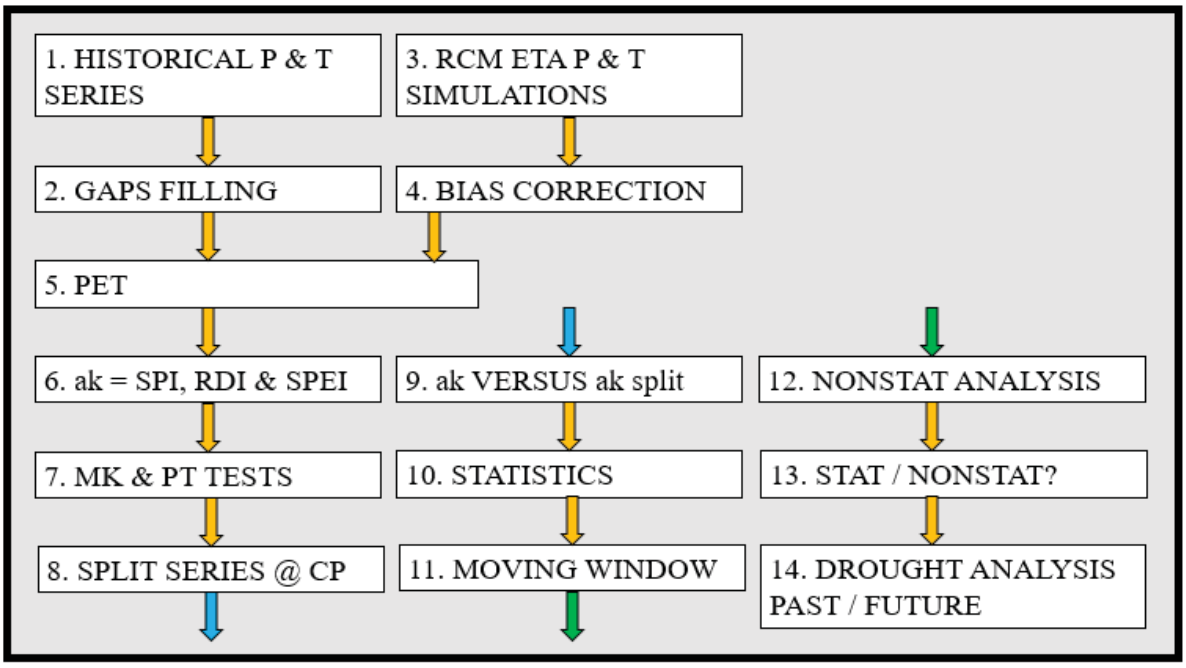

Font: Author.[1]

Step 6 is the computation of the Reconnaissance Drought Index (RDI), considering precipitation and potential evapotranspiration series. The ak values correspond to the respective drought index. This step also contemplates the computation of the drought indices in different accumulation periods (3, 6, 12, 24, 36, 48 and 60 months), which is proposed worldwide by drought researchers. The Palmer Drought Severity Index (PDSI) was not used in this dissertation due to the large amount of data required for computation. Both Standardized Precipitation Index (SPI) and Standardized Precipitation Evapotranspiration Index (SPEI) applications occurred, being discarded due to the great amount of computed data.

[1] Note: P is the precipitation monthly series; T is the temperature monthly series, PET is the potential evapotranspiration and ak are the indices series (SPI, RDI and SPEI). MK is the Mann-Kendall test application, PT is the Pettitt test application and CP relates to the changing point. STAT refers to stationary approach, while NONSTAT refers to the non-stationary approach.

There are few studies in the literature review incorporating the non-stationary analysis in drought indices, as presented in the previous chapter. This dissertation proposes the development of a different approach for drought analysis, splitting the original series in the point where the change occurs and then fitting a probability distribution in the split series. In order to test the hypothesis of this research, it is necessary to apply tests for trend and changing point. This research used the Mann Kendall (MK) and Pettitt (PT) tests to verify trend and changing point, respectively. The application occurs in both original (monthly precipitation and temperature series) and accumulated (3- to 60-month accumulation series) to verify differences (in terms of trend and changing point) between them.

If some series presented trend and/or changing point in both monthly and accumulated series, these series were split in the changing point. Thus, a probability distribution was fitted from the beginning to the changing point, and from the changing point to the end of the series; resulting in two gamma fits. Then, the original and split series comparison using drought statistics such as magnitude, frequency, duration, minimum values (intensity), provide the best performance among the fitted models. The maximum values analysis are unnecessary since the focus is the drought analysis, i.e., minimum values only. The maximum likelihood estimator was used to estimate the parameters of the gamma probability distribution.

In the work of PLOSZAI et al. (2019), the authors evaluated four probability distributions applied in the Reconnaissance Drought Index (RDI) in the Parana State. They fitted the 2-parameter Gamma, 2-parameter Lognormal, Generalized Extreme Value type I and Weibull. They evaluated the distributions performance using both Kolmogorov-Smirnov and Anderson Darling adherence tests. They found that gamma distribution presented the best fit, among them. For this reason, the gamma distribution was chosen in this work.

Since droughts are persistent events, different of floods that are determined by a specific event, the drought analysis generally are based on drought indices computation, instead of the return period computation, that occurs for flood analysis. The gamma probability distribution fitting is an auxiliary method to the drought indices computation.

Step 7 is the computation of both Mann-Kendall and Pettitt tests in the drought indices and monthly series for a later comparison. Step 8 is the non-stationary analysis application (fitting gamma distributions to the split series). Step 9 is the comparison of the original ak series (before split or stationary approach) and the ak split series (split in the changing point or non-stationary approach).

Step 10 is the application of typical drought statistics, like the drought magnitude (run theory), frequency, intensity and duration. The number of differences under a given threshold (e.g., -1.0 and -1.5) compares the performance of both stationary and non-stationary approaches. The drought magnitude analysis provided the mean, median and maximum magnitudes that were used in order to choose between the stationary and non-stationary approaches.

Step 11 is the application of the 30-period moving window analysis to verify the evolution of the gamma fit parameters (shape, location and scale) and the minimum values in all split meteorological stations. It was necessary to fit a linear regression line in the parameters series to analyse their temporal evolution. This step helps analysing the parameters temporal variation in a non-stationary approach. See sections 2.2 Non-stationary Frequency Analysis (NFA) and 4.7 Moving window for more details.

Steps 12 and 13 are the non-stationary analysis to choose which approach is the most suitable to perform the drought analysis, when comparing drought statistics and visual graphs (run theory and moving window analysis). Both steps 12 and 13 are the application of this dissertation hypothesis that drought statistics vary under a non-stationary approach, achieving the main goal of performing a non-stationary drought analysis in climate change scenarios. Step 14 is the drought analysis in both past and future series for the study region.

According to FILL et al. (2013) in the CLARIS LPB project, the most suitable models for Southern America are the RCA1, PROMES and ETA (LPB, 2012). PLOSZAI & MINE (2016) pointed the most suitable for the study region is the RCM ETA and it was used in this dissertation.

2.2. Non-stationary Frequency Analysis (NFA)

In the Non-stationary Frequency Analysis (NFA), YILMAZ & PERERA (2014) and BEGUERIA et al. (2011) point that samples with lower sizes (e.g. short data record) affect the GEV parameters estimation. They fitted the GEV distribution to the rainfall series, as presented in the literature review. KOUTSOYIANNIS (2006) defends the 30-year window is the minimum length of series to perform any statistical analysis. According to him, in climatology this time window is *"sufficient to smooth out transient characteristics of a time series and yield*

a value representative of the climate". VAN LOON (2015) applied a moving window of 30 days to characterize drought events.

Although some authors state that both Generalized Pareto Distribution (GPD) and GEV distributions are the best to perform non-stationary frequency analysis (YILMAZ & PERERA, 2014; COOLEY 2009; BEGUEIRA ET AL. 2011), this dissertation considers the application of the gamma distribution for the drought series, because the gamma distribution is the most used for drought analysis (TSAKIRIS, 2005; KOUSARI et al., 2014). The gamma distribution presented the best fit in application of the RDI in the Parana State (PLOSZAI et al., 2019). The application of the non-stationary approach for drought analysis is the main innovation of this dissertation.

The non-stationary analysis applied to the drought indices came up looking at the behaviour of meteorological variables in the referred region (Parana State). Since there is non-stationarity in the Parana series, applying the proposed method helps in identifying which of them present non-stationarity and fit a gamma distribution in the first and second parts separately. Hence, it is necessary to split the RDI series. In case of non-exact split when accumulating the RDI series, they were split in the closest position that returned an integer number for posterior RDI accumulation.

The moving window is a correlated analysis, characterized by the selection of a time window (30 accumulation periods), fitting the gamma probability distribution in every time step, and moving the time window until the end of the series, obtaining a set of parameters of the gamma distribution. Through parameters graphs, it is possible to evaluate trend in each one of these sets of parameters. The algorithm applied the 30-period moving window analysis in this dissertation.

2.3. Linear regression for gaps filling in

The Simple Linear Regression (SLR) method is used for filling in the gaps in both precipitation and temperature series. The minimum correlation coefficient ($\rho = 0.8$) may be considered a SLR good performance (VITART et al., 2001; PEÑA-GALLARDO et al., 2019) between pairs of meteorological stations. The Equation (1) represents the SLR method.

$$y_{t\_SLR} = b_1 x_{SLR} + b_0 + \epsilon_t \quad (1)$$

where y_{t_SLR} is the variable (precipitation or temperature) to fill in $f(x)$; x_{SLR} is the variable of the neighbouring station used to fill in the gaps; b_1 is the angular coefficient; b_0 is the linear coefficient (intercept) and ϵ is the SLR error (SHARMA et al., 2000).

2.4. Bias correction methods

Precipitation and temperature data generated from Global Climate Models (GCM) simulations are downscaled to the Regional Climate Models (RCM), producing bias in the series. There are several bias correction methods to remove these inconsistencies before applying the RCM outputs in any study. According to the literature review, the most applied bias correction methods are the Linear Scaling (LS), Empirical Quantile Mapping (EQM) for both precipitation and temperature, and the Power Transformation (PT) for precipitation only and the Variance scaling (VARI) for temperature only.

2.4.1. Linear scaling

The Linear Scaling (LS) method corrects the bias of meteorological variables in monthly scale, as presented by Equation (2).

$$V_{cor}(n) = V_{sim}(n) \times \frac{\mu(V_{obs})}{\mu(V_{sim})} \quad (2)$$

where $V_{sim}(n)$ is the simulated RCM variable at time n; $V_{cor}(n)$ is the simulated variable with corrected bias at time n; $\mu(V_{obs})$ is the mean of the observed variables and $\mu(V_{sim})$ is the mean of the simulated variables (LENDERINK *et al.*, 2007; TEUTSCHBEIN e SEIBERT, 2012).

2.4.2. Power transformation

The Power Transformation (PT) method corrects only the precipitation bias and before applying it, according to FANG et al. (2015) and TEUTSCHBEIN & SEIBERT (2012), it is necessary to apply the Local Intensity Scale (LOCI) method, as presented by Equations (3) and (4).

$$s_m = \frac{\mu\left(P_{obs,m} \middle| P_{obs,m} > 0\right)}{\mu\left(P_{sim,m} \middle| P_{sim,m} > P_{lim,m}\right)} \tag{3}$$

$$P_{LOCI,m}^{b_m} = \begin{cases} 0 \; se \; P_{sim,m} < P_{lim,m} \\ P_{sim,m} \times s_m \; se \; P_{sim,m} > P_{lim,m} \end{cases} \tag{4}$$

Before applying the PT method, we estimate the b_m as presented by Equation (5).

$$b_m = \frac{\sigma\left(P_{obs,m}\right)}{\mu\left(P_{obs,m}\right)} - \frac{\sigma\left(P_{LOCI,m}^{b_m}\right)}{\mu\left(P_{LOCI,m}^{b_m}\right)} \tag{5}$$

where b_m is the m-month, σ is the standard deviation, μ is the mean and $P_{LOCI,m}$ is the corrected variable of the m-month by the LOCI method. The $P_{lim,m}$ is the exceedance threshold for wet-day observation frequency for the m-month. The series construction occurs after determining the b_m, as presented by Equation (6) (FANG et al., 2015).

$$P_{PT,m} = b_m \times P_{LOCI,m}^{b_m} \tag{6}$$

where $V_{sim}(n)$ is the simulated RCM variable at time n; $V_{cor}(n)$ is the simulated variable with corrected bias at time n: $\mu(V_{obs})$ is the mean of the observed variables; $\mu(V_{sim})$ is the mean of the simulated variables; μ is the mean of values. The variable b_m is the difference between observed and LOCI variation coefficients in the m-month; σ is the standard deviation; $P_{LOCI,m}$ is the corrected variable of the m-month by the LOCI method; $P_{PT,m}$ is the bias corrected series;

$P_{sim,m}$ is the m-month simulated precipitation; $P_{lim,m}$ is the m-month precipitation limit for raw (observed) series and $P_{obs,m}$ is the m-month observed precipitation.

2.4.3. Variance Scaling

The Variance Scaling (VARI) method is a good tool to correct the bias of the temperature series, correcting both variance and mean of the simulated series (CHEN et al., 2011). According to TEUTSCHBEIN & SEIBERT (2012), the first step is the adjust of RCM variables, using the LS equation and then using both scenario runs $\left(T^{*1}_{scen}(d)\right)$ and mean-corrected control $\left(T^{*1}_{contr}(d)\right)$, shifting to a monthly zero mean basis, as presented by Equations (7) and (8).

$$T^{*2}_{contr}(d) = T^{*1}_{contr}(d) - \mu_m(T^{*1}_{contr}(d)) \quad (7)$$

$$T^{*2}_{scen}(d) = T^{*1}_{scen}(d) - \mu_m(T^{*1}_{scen}(d)) \quad (8)$$

Hence, the standard deviation scaling bases on the ratio below, as presented by Equations (9) and (10).

$$T^{*3}_{contr}(d) = T^{*2}_{contr}(d)\left[\frac{\sigma_m(T_{obs}(d))}{\sigma_m\left(T^{*2}_{contr}(d)\right)}\right] \quad (9)$$

$$T^{*3}_{scen}(d) = T^{*2}_{scen}(d)\left[\frac{\sigma_m(T_{obs}(d))}{\sigma_m\left(T^{*2}_{contr}(d)\right)}\right] \quad (10)$$

Follow the computation of the sigma-corrected series and shift back using the corrected mean, as presented by Equations (11) and (12) (TEUTSCHBEIN & SEIBERT, 2012).

$$T^{*}_{contr}(d) = T^{*3}_{contr}(d) + \mu_m(T^{*1}_{contr}(d)) \quad (11)$$

$$T^{*}_{scen}(d) = T^{*3}_{scen}(d) + \mu_m(T^{*1}_{scen}(d)) \quad (12)$$

where ${T^*}^1_{scen}(d)$ is the first step of scenario runs; ${T^*}^1_{contr}(d)$ is the first step of mean-corrected control run (simulated); ${T^*}^2_{contr}(d)$ is the second step of mean-corrected control run (simulated); μ_m is the mean of the RCM-simulated series; ${T^*}^2_{scen}(d)$ is the second step of scenario runs and σ_m is the standard deviation of the corrected time series. The variable $T_{obs}(d)$ is the observed variable; ${T^*}_{contr}(d)$ is the third step of mean-corrected control run (simulated) and ${T^*}_{scen}(d)$ is the third step of scenario runs. The authors TEUTSCHBEIN & SEIBERT (2012) affirm that this method guarantees the same variance between control run (baseline) period and observed values (historical).

2.4.4. Empirical Quantile Mapping

The Empirical Quantile Mapping (EQM) corrects the bias simulation of both temperature and precipitation series at monthly scale using the Equation (13). According to FANG et al. (2015), the EQM application is expressed by both empirical CDF ($eCDF_{sim,m}$) and its inverse $\left(eCDF^{-1}_{obs,m}\right)$ for all distributions fitted, as presented by Equation (13). The variable $V_{EQM,m}$ represents the bias corrected variable through the EQM method and the $V_{sim,m}$ represents the simulated variable at m-month.

$$V_{EQM,m} = eCDF^{-1}_{obs,m}(eCDF_{sim,m}(V_{sim,m})) \tag{13}$$

2.4.5. Mean Absolute Error

The Mean Absolute Error (MAE) computes the difference between observed and modelled data. It consists in the average of the absolute errors (LI et al., 2017). Equation (14) represents the MAE.

$$MAE = \frac{\sum_{t=1}^{n}|y_t - x_t|}{n} \tag{14}$$

where n is the number of observations or simulations in monthly scale, y_t is the modelled data at time t, and x_t is the observed or simulated data at time t. The MAE uses the same scale as the values (observed and simulated) and it is a useful measure for time series analysis and as a forecasting measure.

2.5. Drought indices

Researchers from all over the world evaluate droughts using drought indices. In general, under different approaches of drought analysis, there is an agreement between indices and accumulation periods in terms of drought intervals. The Drought Interval (DI) is the measure of the standardized drought indices, such the Reconnaissance Drought Index (RDI).

Table 1 – Drought classification and the respective intervals.

Indices classification	**Drought Interval (DI)**
Extreme drought	DI ≥ -2
Severe drought	-1,99 ≤ DI ≤ -1,50
Moderate drought	-1,49 ≤ DI ≤ -1,00
Normal	-0,99 ≤ DI ≤ 0,99
Moderate wet	1,00 ≤ DI ≤ 1,49
Severe wet	1,50 ≤ DI ≤ 1,90
Extreme wet	DI ≥ 2

Font: adapted from Mohammed & Scholz (2017).

In the indices, positive values indicate the wet season, while the negative values indicate the drought season. The negative values indicate the drought intensity and the Table 1 presents the drought intervals. Following the literature review, a drought below the (-1.0) threshold is a moderate drought and below the (-1.5) threshold is a severe drought.

2.5.1. Standardized Precipitation Index

The Standardized Precipitation Index (SPI) consists in the standardized form of the precipitation, as proposed by Equations (15) and (16). The SPI computation occurs in different timescales, accumulating (summing) the standardized precipitation (MCKEE et al., 1993).

$$\beta_k^{(i)} = \sum_{j=1}^{k} P_i\,, \qquad with\ i = 1, 2, 3, \dots, n \tag{15}$$

$$SPI_{st(k)}^{(i)} = \frac{\beta_k^{(i)} - \overline{\beta_k}}{\widehat{\sigma_{\beta k}}} \tag{16}$$

where P_i is the monthly precipitation accumulated in i months; n is the total number of observations or simulations, $SPI_{st(k)}^{(i)}$ is the standardized SPI accumulated in i months; $\beta_k^{(i)}$ is the SPI accumulated in i months; $\overline{\beta_k}$ is the mean of SPI accumulated in i months and $\widehat{\sigma_{\beta k}}$ is the standard deviation of SPI accumulated in i months.

2.5.2. Reconnaissance Drought Index

The Reconnaissance Drought Index (RDI) initially proposed by TSAKIRIS & VANGELIS (2005) is the ratio between precipitation and potential evapotranspiration, represented by α_k in the Equation (17).

$$\alpha_k^{(i)} = \frac{\sum_{j=1}^{k} P_{ij}}{\sum_{j=1}^{k} PET_{ij}}, \qquad with\ i = 1, 2, 3, \dots, n \tag{17}$$

where P_{ij} is the monthly precipitation of month j and year i and PET_{ij} is the monthly potential evapotranspiration of month j and year i and n is the total number of observations or simulations. Both P_{ij} and PET_{ij} computations occur at 3, 6, 12, 24, 36, 48 and 60 months accumulation periods.

TSAKIRIS et al. (2008) and ZARCH et al. (2011) suggest the quarter scale (3-month) as the minimum in order to overcome the zeros in the series to fit the gamma or the 2-parameter lognormal (LN2) distributions. They state that gamma is the most suitable probability distribution to apply in drought indices. Equation (18) represents the standardized RDI $\left(RDI_{st(k)}^{(i)}\right)$.

$$RDI_{st(k)}^{(i)} = \frac{\alpha_k^{(i)} - \overline{\alpha_k}}{\widehat{\sigma_{\alpha k}}} \quad (18)$$

where $\overline{\alpha_k}$ is the arithmetic mean of the α_k series and $\widehat{\sigma_{\alpha k}}$ is the respective standard deviation.

2.5.3. Standardized Precipitation Evapotranspiration Index

The Standardized Precipitation Evapotranspiration Index (SPEI) consists in the standardized difference between precipitation and potential evapotranspiration, as proposed by Equation (19) and (20). The SPEI computation occurs in different timescales, accumulating the difference of precipitation and potential evapotranspiration (VICENTE-SERRANO et al., 2010).

$$\gamma_k^{(i)} = \sum_{j=1}^{k} P_{ij} - \sum_{j=1}^{k} PET_{ij}\,, \qquad with\ i = 1, 2, 3, \dots, n \quad (19)$$

$$SPEI_{st(k)}^{(i)} = \frac{\gamma_k^{(i)} - \overline{\gamma_k}}{\widehat{\sigma_{\gamma k}}} \quad (20)$$

where $\gamma_k^{(i)}$ is the SPEI accumulated (summed) in k months; P_{ij} is the monthly precipitation of month j and year i and PET_{ij} is the monthly potential evapotranspiration of month j and year i and n is the total number of observations or simulations. $SPEI_{st(k)}^{(i)}$ is the standardized SPEI accumulated in i months; $\gamma_k^{(i)}$ is the SPEI accumulated in i months; $\overline{\gamma_k}$ is the SPEI arithmetic mean accumulated in i months and $\widehat{\sigma_{\gamma k}}$ is the SPEI standard deviation accumulated in i months.

2.6. Potential evapotranspiration

The Potential Evapotranspiration (PET) is the water amount transferred to the atmosphere by soil evaporation plus plants transpiration in a region, when the soil is saturated. This dissertation presents only the Thornthwaite method and results, since the comparison of performance among PET computation methods is beyond of this work scope.

2.6.1. Thornthwaite

The Thornthwaite method considers only the temperature data and the average daylight length in its computation. Equations (21), (22) and (23) represent the method.

$$PET = 16(L/12)(N/30)(10T_m/I)^a \quad (21)$$

$$a = 6.75 \times 10^{-7} I^3 - 7.71 \times 10^{-5} I^2 + 1.792 \times 10^{-2} I + 0.49239 \quad (22)$$

$$I = \sum_{i=1}^{12} (T_m/5)^{1.514} \quad (23)$$

where L is average day length (hours), N is the number of days in a month, T_m is the average temperature in monthly scale, PET is the potential evapotranspiration in mm/month, I is the heat index.

The authors TSAKIRIS et al. (2007) and VANGELIS et al. (2013) suggest applying the Thornthwaite and Blaney-Criddle method to compute the PET to perform drought studies. The Blaney-Criddle method requires the determination of the crop coefficient for both past and future drought series, causing difficulties in its determination in the future scenarios. The Thornthwaite considers only temperature in its computation and is ideal for regions where there are not sufficient data, like the interior of Brazil. The Hargraves, Priestley and Taylor, and Penman-Monteith methods require more data that are not available in most part of Brazil for their computation (data scarcity in Brazil).

2.7. Gamma distribution

The gamma distribution is widely applied in drought studies, according to the literature review. The gamma distribution presented the best fit in application of the RDI (PLOSZAI et al., 2019). The majority of authors point the gamma as the most used distribution for drought analysis, and the second is the LN2. TSAKIRIS & VANGELIS (2005), VANGELIS et al. (2013), HAO & SINGH (2015) and AMIN et al. (2015) point these two distributions are suitable for monthly or quarter (3-month) timescales and to overcome the “zeros issue” after

the procedure described below. The Equation (24) represents the Probability Density Function (PDF) of the gamma probability distribution.

$$g(x) = \frac{1}{\beta^a \Gamma(a)} x^{a-1} exp^{-x/\beta} \quad (24)$$

where $a(t) > 0$ is the shape factor; $\beta(t) > 0$ is the scale factor and $x > 0$ is the variable (precipitation or temperature). Equation (25) represents the gamma function. If $a(t) > 0$ is a positive integer, $\Gamma(a(t) + 1) = n!$ and $\Gamma\big(a(t)\big) = (n-1)!$. The location parameter in Python environment $loc = 1/\alpha$, means it is the inverse of the shape parameter.

$$\Gamma(a) = \int_0^\infty x^{a-1} exp^{-x} dx \quad (25)$$

Equation (26) represents the Cumulative Density Function (CDF) of the gamma distribution (KOUSARI et al., 2014).

$$G(x) = \int_0^\infty g(x)dx = \frac{1}{\beta^a \Gamma(a)} x^{a-1} exp^{-x/\beta} dx \quad (26)$$

To fit the gamma distribution to the sample, it requires the estimation of the $a(t)$ and $\beta(t)$ parameters, according to Equations (27), (28) e (29) (KOUSARI et al., 2014). The gamma distribution parameters were estimated applying the maximum likelihood estimator.

$$a = \frac{1}{4A}\left(1 + \sqrt{1 + \frac{4A}{3}}\right) \quad (27)$$

$$\beta = \frac{\bar{x}}{a} \quad (28)$$

$$\mathrm{A} = \ln(\bar{x}) - \frac{1}{n}\sum_{i=1}^{n} \ln(x_i) \quad (29)$$

Substituting the t variable by x/β, it returns the incomplete gamma function, represented by Equation (30). The gamma function is undefined for $x = 0$ and precipitation distributions may contain zeros (no rainfall), hence Equation (31) represents a modified cumulative probability distribution.

$$I(x) = \frac{1}{\Gamma(a)} \int_0^x t^{a-1} exp^{-t}\, dt \quad (30)$$

$$H(x) = q + (1 - q)G(x) \quad (31)$$

where q is the zero precipitation probability; $I(x)$ the incomplete cumulative gamma function, m is the number of zeros of the α_k series of the gamma probability distribution; n is the total number of records or simulations and $q = m/n$. Hence, the standardization of the cumulative probability $H(x)$ is the RDI_{st} (standardized RDI) (TSAKIRIS et al., 2008, KOUSARI et al., 2014). The procedure described in this paragraph allows fitting the gamma probability distribution in the presence of zeros in the RDI series.

2.8. Mann Kendall test

The Mann Kendall (MK) test is a non-parametric test widely applied to detect monotonic trends in the hydro-meteorological series, initially proposed by MANN (1945) and KENDALL & STUART (1963). Some authors state the MK is the most suitable test for climate change studies, since it can detect a long-term monotonic trend (MÜLLER et al., 1998; BACK, 2001; BARROS et al., 2011; BUCHIR, 2013).

It consists in comparing each value of the series in temporal order with another series in ascending order. Hence, it computes the number of times that the remaining terms are higher than the analysed. Equation (32) represents the S_{MK} statistics.

$$S_{MK} = \sum_{j=1}^{n} \sum_{i=j+1}^{n} sgn(R_j - R_i) \quad (32)$$

where n is the number of observations; R_i is the ith observation in chronological series; R_j is the jth observation in the ordered series (rank).

ROUGÉ et al. (2013) state the null hypothesis (H_0) that there is no change in the sequence of observations from both series. For a temporal series of n observations, the MK statistic uses the difference signal between two distinct observations (i e j), as represented by Equation (33).

$$sgn(R_j - R_i) = \begin{cases} 1, if\ R_j - R_i > 0 \\ 0, if\ R_j - R_i = 0 \\ -1, if\ R_j - R_i < 0 \end{cases} \quad (33)$$

where n is the number of observations; R_i is the ith observation in chronological series; R_j is the jth observation in the ordered series (rank), $j = 1, 2, \dots, n$ and $i = j + 1, j + 2, \dots, j + n$.

Under the null hypothesis, S_{MK} is normally distributed and Equations (34), (35) and (36) provide the MK test statistic (Z).

$$Z = \frac{S_{MK} - E(S_{MK})}{\sqrt{VAR(S_{MK})}} \backsim N(0,1) \quad (34)$$

$$E(S_{MK}) = 0 \quad (35)$$

$$VAR(S_{MK}) = \frac{1}{18}[n(n-1)(2n+5)] \quad (36)$$

To apply the test, the authors suggest 30 or more observations. The p-value is compared with the significance level ($\alpha = 5\%$). YILMAZ & PERERA (2014) point over the necessity to remove autocorrelation (pre-whitening) of hydrological data before applying the MK test. The MK test applies to all probability distributions (ZARCH et al., 2015).

2.9. Pettitt test

The Pettitt test is a non-parametric test widely used to detect changing point in the series. ROUGÉ et al. (2013) affirm that the Pettitt test shows no alteration in the mean, when split arbitrarily the series. It produces a comparison based on the rank of observations before and after the date τ through the Pettitt test statistics $k(\tau)$, as presented by Equation (37).

$$k(\tau) = \sum_{i=1}^{\tau} \sum_{j=\tau+1}^{n} sgn(x_j - x_i) \tag{37}$$

where n is the number of observations; x_i is an observation before $t = \tau$; x_j is an observation after $t = \tau$; τ is the ranking coefficient (arbitrary point of the sample split).

For a temporal series of n observations, the Pettitt statistic uses the difference signal between two distinct observations (i e j), as presented by Equation (38).

$$sgn(x_j - x_i) = \begin{cases} 1, if\ x_j - x_i > 0 \\ 0, if\ x_j - x_i = 0 \\ -1, if\ x_j - x_i < 0 \end{cases} \tag{38}$$

Equations (39) and (40) represent the changing point and the Pettitt test statistics, respectively. The variable $argmax$ represents the maximum values along an axis of the Pettitt test and the max represents the maximum value of the Pettitt test.

$$T = argmax_{1 \le \tau \le 12}(|k(\tau)|) \tag{39}$$

$$K = max_{1 \le \tau \le n}(|k(\tau)|) \tag{40}$$

Equation (41) represents the significance probability associated to the null hypothesis (H_0) rejection.

$$p \approx 2exp\left(-\frac{6K^2}{n^3 + n^2}\right) \quad (41)$$

2.10. Run Theory

The drought indices applied in this dissertation are based on the run theory. According to PAULO & PEREIRA (2006), a set of observations succeeded or preceded by other observations, is a run. In other words, drought events are characterized by a sequence of negative values of the standardized precipitation in time, considering the zero as the critic value to separate droughts and floods.

YEVJEVICH (1967) proposed a method to determine flow periods below a threshold level, as droughts. It is based on run theory, a statistical method to analyse sequential time series. The drought index distributions are based on the magnitude (M) (deficit volume or severity), intensity (Int) and drought duration (D) as presented by Equation (42). Intensity computation follows the Equation (43) and drought duration characterizes by the onset and end of a drought period in the Run Theory (NAM et al., 2015).

$$M = Int \times D \quad (42)$$

$$Int = M/D \quad (43)$$

Both drought magnitude and duration are measured in months, while drought intensity is dimensionless. Since the final step of the indices computation is their standardization, it results in the dimensionless intensity. Different indices can have different recommendations of threshold levels (e.g. -0.5 for the SPI/SPEI and -1.0 for the PDSI) (NAM et al., 2015). Figure 2 presents the run theory and the drought statistics, such duration, magnitude and severity.

Figure 2 – Run theory scheme.

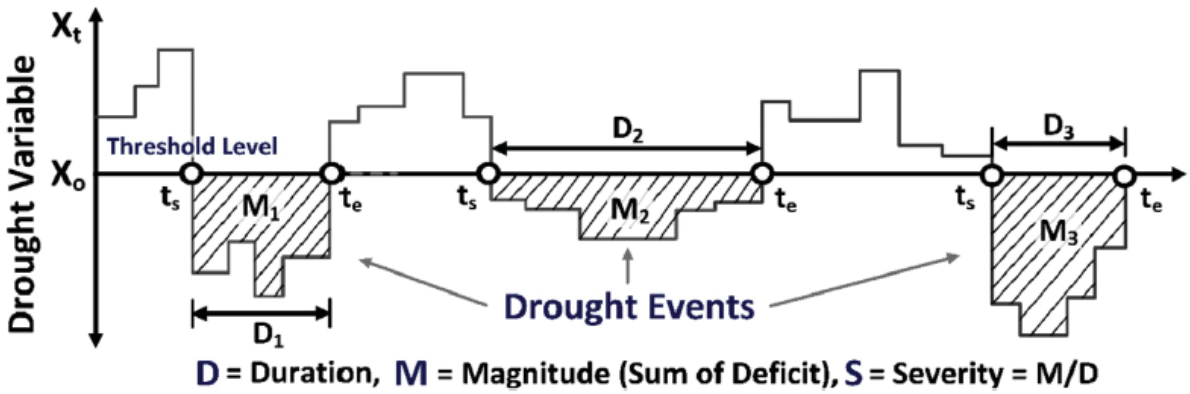

Font: YEVJEVICH (1967) *apud* NAM et al. (2015).

Drought events are characterized below 0 threshold. Moderate droughts are characterized below -1.0 threshold and severe droughts are characterized below -1.5 threshold in the Run Theory. A more robust definition of the Run Theory thresholds is in the Table 1, subchapter 2.5 Drought indices.

2.11. Chapter summary

This chapter presented all methods to develop both stationary and non-stationary drought analysis, for analysing both past and future scenarios. It introduced the flowchart and each step description, and then presented all applied methods.

It presented the Linear Regression for filling in the gaps in the historical series and the bias correction methods to apply in the RCM series. It presented the potential evapotranspiration computation and the three most applied drought indices: Standardized Precipitation Index, Reconnaissance Drought Index (RDI) and Standardized Precipitation Evapotranspiration Index (SPEI).

The application of the stationary gamma distribution in non-stationary series can generate inconsistencies in the gamma distribution fitting. For this reason, this dissertation adopts the non-stationary analysis, splitting the series in the changing point given by the Pettitt test. This chapter also presented both Mann-Kendall and Pettitt tests. The gamma probability

distribution was chosen in accordance with previous works, as highlighted in the subsection 2.2. Non-stationary Frequency Analysis.

Finally, this chapter presented the non-stationary analysis, performed by splitting the series at the changing point and using the moving-window analysis to verify the temporal parameters variation. The drought analysis of the drought indices is based on run theory and the computation of drought statistics (magnitude, intensity and duration), events occurrence frequencies, number of drought events, among others.

3. STUDY AREA AND DATA

This chapter presents the study area and data. The Parana State, Brazil, has historical records in the meteorological stations that present variations in the main statistics (e.g. mean, variance, among others), i.e., the region have a non-stationary profile. Usually, the drought indices are based on a stationary approach. In Parana State, there are few drought studies and no study considering the non-stationary approach. In this research, precipitation and temperature data were collected from 34 meteorological stations located along the Parana State to perform the non-stationary drought analysis in climate change scenarios.

3.1. Study area

The Parana State is one of the 27 Brazilian States and is located in the Southern Region. The Parana State has 399 municipalities and the most important include Foz do Iguassu, Curitiba, Sao Jose dos Pinhais, Cascavel, Londrina, Ponta Grossa, Maringa and Guarapuava (SEMA, 2015).

The Parana State locates between 48° 05′ 37″W and 54° 37′ 08″W longitude and 22° 30′ 58″S and 26° 43′ 00″S latitude. The boundaries of the Parana State include the Santa Catarina State in the South, the Mato Grosso do Sul State in the Northwest and the Sao Paulo State in the Northeast. The Atlantic Ocean is the Eastern boundary, while Paraguay is the Western boundary. The Parana State has an area of approximately 200 km² (IBGE, 2019) and the Tropic of Capricorn crosses the State in the North. It has a coast of only 98 km.

In the history of Parana State, diverse economy cycles characterized its formation, mixing both political and economic history under four distinct occupation phases. They are: (1) the discovery of gold at the seaside and in the first plateau (seventeenth century) and (2) seventeenth century also characterizes by the beginning of the mate herb cycle. The (3) coffee growing which moved from Sao Paulo to the Northern Parana territory (end of the nineteenth century), and the (4) migration coming from Santa Catarina and Rio Grande do Sul States (beginning of the twentieth century), occupying the South-West and growing corn and soy beans. The Parana population concentrated in rural areas until the 1950s and between 1970 and 2000, the Parana suffered a rural exodus due to the agriculture technological boom, characterized by mechanization mainly in the South-West region (SEMA, 2015).

The mate herb phase in the Parana State started in the eighteenth century but only in the nineteenth century; began the mate herb industrialization in the Parana State. The mate herb has its importance in the Parana State history because it is a native herb widely used among the native tribes present in Latin America. The mate herb was widely used by both Spanish and Portuguese colonizers and it was important to insert the Parana State in the international trade (BONDARIK et al., 2006).

According to SEMA (2015), the Parana State has 16 hydrographic basins: Ivai, Iguassu, Paranapanema, Ribeira, Litoranea, Cinzas, Itarare, Tibagi, Pirapo and Piquiri. All of them except the Litoranea are converging to the Parana River. The aquifer units in the Parana are the Karst, Guarani, Palaeozoic (inferior, superior and medium-superior), Pre-Cambrian, Caiua, Costeira, Guabirotuba and Serra Geral Norte and Sul.

The Iguassu River Basin is the most important basin in Parana State and its source is located in the Curitiba Metropolitan Region (CMR). It is one of the tributaries of the Parana River, contributing to the La Plata River Basin, the second major hydrographic basin of the Latin America, besides the Amazonian River Basin. According to SAURRAL & BARROS (2010), the La Plata River Basin is the fifth more important hydrographic basin in the world. The Iguassu River basin drains approximately 70,800 km² of area and 81% situates in the Parana State and the other 19% in the Santa Catarina State (MAACK, 2002). A small portion of the basin is in Argentina and has only around 1,830 km² of area. The Iguassu River basin occupies a 28% of the total area of Parana State and has a population of about 4.400.000 inhabitants (SEMA, 2015; IBGE, 2019).

Besides the Iguassu River, located in the South of Parana State, there are other important hydrographic basins located in the North (Paranapanema River), West (Parana River) and East (Ribeira River). The largest are the Paranapanema River and the Iguassu River, which cross the State from East to West. The majority of the Parana population lives in these basins. The basin exutory of the Iguassu River Basin is in the triple boundary between Brazil, Paraguay and Argentina. The Parana River is a natural boundary between Parana State and Paraguay in the West and Mato Grosso do Sul State in the Northwest.

The Parana State has four different climatic types (Figure 3) according to Köppen, as: (1) tropical wet-dry climate (Aw), (2) wet subtropical (Cwa), (3) humid subtropical climate (Cfa) and (4) marine west coast climate (Cfb). The Köppen classification is one of the climate classification systems more used all over the world (ALVARES et al., 2013). The natural

vegetation is an expression of the regional climate and each vegetation influences areas using the Köppen classification.

Figure 3 – Köppen climate classification for the Parana State.

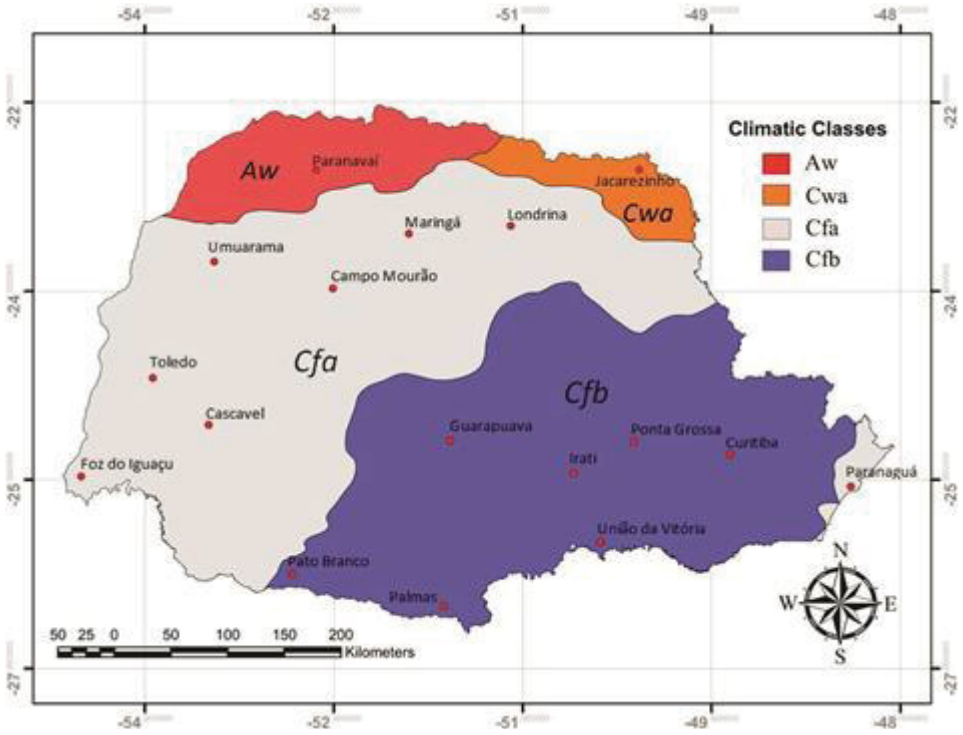

Font: APARECIDO et al. (2016). The corresponding climates: Aw is the tropical wet-dry climate, Cwa is the wet subtropical, Cfa is the humid subtropical climate, and Cfb is the marine west coast climate.

The savannah climate occurs in the Northwest, with an average annual temperature of 20°C and pluviometry around 1,300 mm/year. This region's main characteristic is a reduction of the rainfall patterns in the winter, generating drought periods, and presenting, in the summer, high temperatures. In the Central and Southeast of the Parana State, as well as in the littoral plain and the less elevated plateaus (West), the classification is the oceanic climate. This climate type presents 1,500 mm/year of pluviometry and average annual temperature around 19°C. Besides these, Parana presents the wet subtropical in the Central and West of the State and a portion in the North, presenting 1,200 mm/year of pluviometry and an average annual temperature of 17°C. This climate presents mild summers and rainfalls well distributed along the year (MAACK, 2002). Figure 3 represents the Köppen climate classification for the Parana State.

The Parana State suffered from a strong climate phenomenon called black frost in both South and North regions. The black frost was responsible for a migratory inhabitants flow from rural to urban areas in 1975, since it damaged the coffee agricultural culture. It estimates that around 13% of rural inhabitants moved from Parana State to Mato Grosso do Sul State after the black frost event. The temperature in the fields was around -9°C during the black frost, provoking permanent damage in the coffee culture (RODRIGUES & PELEGRINI, 2017). In the same year (1975), it snowed in Curitiba.

Conifers and broadleaved firstly marked the vegetation. It estimates the Mata Atlantica covered the State around 46% of Parana State before urbanization and now this forest situates only in the Serra do Mar. The typical specie of the Parana State is the Pinheiro do Parana (Araucaria Augustifolia) and other species like mate herb, cedar, and imbuia are other typical trees from the Parana State (MMA, 2016).

The Parana State has the sixth major Brazilian population (around 5.5% of the national population). It has the fifth major Gross Domestic Product (GDP); besides of Rio Grande do Sul, Minas Gerais, Rio de Janeiro and Sao Paulo States. Around 40% of the Parana GDP relates to industry, 45% to commerce and services and only 15% to agriculture. The population is 11,433,957 inhabitants and the demographic density is around 52.40 inhabitants/km² (IBGE, 2019).

The Parana State exports poultry meat, soybean, corn, wheat, sugar, coffee, tomato, manioc and tea, besides it is one of the Brazilian automotive poles, located in Sao Jose dos Pinhais city. The agroindustry, paper and cellulose industries are significant in the country and many locate in Parana State. The plant extractivism, mate herb and wood contribute significantly for the Parana State economy. The logger and food are the most important poles in the secondary sector of the Parana State (IPARDES, 2019).

The Parana State has a great hydropower potential and contributes significantly within the National Interconnected System (SIN, acronym in Portuguese). Besides other important hydropower plants, in Parana State, the Binational Itaipu Hydropower Plant, on the Parana River is the largest of the country. The Itaipu reservoir lies in the boundary between Mato Grosso do Sul and Parana and it is the international boundary between Parana State and Paraguay.

Itaipu has an installed capacity of 14,000 MW. Other important hydropower plants are Foz do Areia, Segredo, Salto Santiago, Salto Osorio and Salto Caxias, all with more than 1,000 MW of installed capacity each, besides other important hydro plants located across the State. The Iguassu hydropower plants represent around 8.5% of the installed capacity from all hydropower plants of the SIN (ANEEL, 2014).

3.2. Data

In order to perform the drought study, precipitation and temperature data were acquired from 34 meteorological stations located across the Parana State. These meteorological stations are considered representative of the region, since these stations have few gaps and extensive observation periods. Figure 4 presents the 34 meteorological stations in the Parana.

Figure 4 – Location of the meteorological stations along the Parana State.

Font: Author.

Table 2 – General information of the meteorological stations along Parana State.

#	Code	Name	City	Latitude (°)	Longitude (°)	Altitude (m)	Institute
1	83844	Paranagua	Paranagua	-25.53	-48.51	4.50	INMET
2	02548038	Morretes	Morretes	-25.30	-48.49	59.00	IAPAR
3	02548039	Guaraquecaba	Guaraquecaba	-25.16	-48.32	40.00	IAPAR
4	83842	Curitiba	Curitiba	-25.43	-49.26	923.50	INMET
5	02449013	Cerro Azul	Cerro Azul	-24.49	-49.15	360.00	IAPAR
6	02549091	Lapa	Lapa	-25.47	-49.46	910.00	IAPAR
7	02349030	Joaquim Tavora	Joaquim Tavora	-23.30	-49.57	512.00	IAPAR
8	02550024	Ponta Grossa	Ponta Grossa	-25.13	-50.01	880.00	IAPAR
9	02350017	Cambara	Cambara	-23.00	-50.02	450.00	IAPAR
10	02350018	Bandeirantes	Bandeirantes	-23.06	-50.21	440.00	IAPAR
11	83813	Castro	Castro	-24.78	-50.00	1008.80	INMET
12	02550025	Fernandes Pinheiro	Fernandes Pinheiro	-25.27	-50.35	893.00	IAPAR
13	02450011	Telemaco Borba	Telemaco Borba	-24.20	-50.37	768.00	IAPAR
14	02351011	Ibipora	Ibipora	-23.16	-51.01	484.00	IAPAR
15	02251027	Bela Vista do Paraiso	Bela Vista do Paraiso	-22.57	-51.12	600.00	IAPAR
16	02351063	Maua da Serra	Maua da Serra	-23.54	-51.13	1020.00	IAPAR
17	02551010	Guarapuava	Guarapuava	-25.21	-51.30	1058.00	IAPAR
18	02351008	Apucarana	Apucarana	-23.30	-51.32	746.00	IAPAR
19	02651043	Palmas	Palmas	-26.29	-51.59	1100.00	IAPAR
20	02652003	Clevelandia	Clevelandia	-26.25	-52.21	930.00	IAPAR
21	02552009	Laranjeiras do Sul	Laranjeiras do Sul	-25.25	-52.25	880.00	IAPAR
22	83766	Londrina	Londrina	-23.31	-51.13	566.00	INMET
23	83767	Maringa	Maringa	-23.40	-51.91	542.00	INMET
24	02352017	Paranavai	Paranavai	-23.05	-52.26	480.00	IAPAR
25	02452050	Nova Cantu	Nova Cantu	-24.40	-52.34	540.00	IAPAR
26	83783	Campo Mourao	Campo Mourao	-24.05	-52.36	616.40	INMET
27	02352019	Cianorte	Cianorte	-23.40	-52.35	530.00	IAPAR
28	02652035	Pato Branco	Pato Branco	-26.07	-52.41	700.00	IAPAR
29	02553018	Quedas do Iguaçu	Quedas do Iguaçu	-25.31	-53.01	513.00	IAPAR
30	02653012	Francisco Beltrao	Francisco Beltrao	-26.05	-53.04	650.00	IAPAR
31	02353008	Umuarama	Umuarama	-23.44	-53.17	480.00	IAPAR
32	02453023	Cascavel	Cascavel	-24.53	-53.33	660.00	IAPAR
33	02553015	Planalto	Planalto	-25.42	-53.47	400.00	IAPAR
34	02453003	Palotina	Palotina	-24.18	-53.55	310.00	IAPAR

Font: Author.

Observed historical series were collected in the Weather Database for Teaching and Research (BDMEP, acronym in Portuguese) held by the National Institute of Meteorology (INMET, acronym in Portuguese) and in the Parana Agronomic Institute (IAPAR, acronym in

Portuguese). The downloaded data in the Hidroweb platform held by the National Water Agency (ANA, acronym in Portuguese), was used for filling in the gaps of the historical series.

Table 2 presents the local information such the code used by governmental institutes (INMET and IAPAR), name and city of the 34 meteorological stations located along the Parana State used in this dissertation. It shows the geographic coordinates (latitude and longitude), altitude and the respective Brazilian operating agency. These meteorological stations provide precipitation, temperature, solar radiation, among other variables series.

The daylight length data were acquired from the TIME AND DATE (2019) website for available stations (Curitiba and Londrina), for January to December of 1961. In this website, there are only daylight length data for these two sites.

The acquisition of simulated data from the GCM HADGEM2-ES and the regionalized simulations of the RCM ETA in the PROJETA platform occurred in the website of Weather Forecast and Climatic Studies Centre (CPTEC, acronym in Portuguese) held by the National Institute for Spatial Research (INPE, acronym in Portuguese). The past RCM ETA simulations relate to the baseline (control run) period, while the future simulations relate to two distinct scenarios: RCP 4.5 and RCP 8.5. These two scenarios are available in the PROJETA website for climate change studies and are the most used in climate change studies (NAM et al., 2015; CHATTOPADHYAY et al., 2017; PARK et al., 2018; LUCENA et al., 2018).

The period from January of 1961 to December of 2005 comprises the baseline (control run) period that is similar to the observed historical series. The period from January of 2006 to December of 2099 comprises the future period with RCP 4.5 and RCP 8.5 scenarios. According to FILL et al. (2013) in the CLARIS LPB project, the most suitable models for Southern America are the RCA1, PROMES and ETA (LPB, 2012). PLOSZAI & MINE (2016) pointed that the most suitable for the study region is the RCM ETA.

In order to fill in the gaps in the meteorological series, the stations 11 (Castro) and 22 (Londrina) were also selected because both regions present a distinct climate according to the Köppen classification (Figure 3) (ALVARES et al., 2013). Londrina comprises the Cfa (humid subtropical climate) and Castro comprises the Cfb (marine west coast climate). The Londrina station has high temperature rates and a well-defined seasonal behaviour. Londrina is the second largest city of the Parana. However, the Castro station has a cold climate and non-stationary behaviour.

The meteorological series normally present gaps. In order to use both precipitation and temperature series for a posterior drought analysis, the gaps evaluation was performed in these series. Table 3 presents the gaps found in both series, where the series comprises the period between January of 1961 and December of 2005, totalizing 540 months. According to the Table 3, for temperature series the maximum gaps percentage is at the Maringa station (27%), while there are several stations with only 1% of gaps. For the precipitation series, the maximum gaps percentage is also at the Maringa station (26%), while the minimum (1%) is at several stations.

In order to perform the drought analysis (Chapter 5), the main statistics of the historical and simulated series (RCP 4.5 and RCP 8.5), were computed. Table 4, Table 5 and Table 6 present the monthly descriptive statistics of both precipitation and temperature series in the historical observed, simulated RCP 4.5 and RCP 8.5 scenarios, respectively.

In the historical series (Table 4), the monthly mean precipitation of the 34 stations covering the Parana State is 144.88 mm. The maximum monthly mean precipitation occurs in the station 3 (Guaraquecaba) (199.05 mm) and the minimum (114.88 mm) in the station 5 (Cerro Azul). The minimum values are generally the same (0 means no rainfall). The maximum monthly precipitation (840.60 mm, January of 1995) occurred in the station 1 (Paranagua). Station 3 (Guaraquecaba) presents the maximum standard deviation (131.98 mm) in precipitation.

Table 4 presents the minimum standard deviation in the precipitation historical series (70.45 mm) in the station 5 (Cerro Azul). Table 4 also presents the descriptive statistics of the temperature of the historical series. The minimum monthly mean temperature (16.30°C) occurred in the station 19 (Palmas), while the maximum (22.12°C) occurred in the station 24 (Paranavai). The minimum monthly records (8.65°C, July of 2000) are in the station 19 (Palmas) and the maximum values present oscillations along the Parana State, pointing the station 9 (Cambara) as the warmest (27.68°C, March of 1969) in the State.

In the future simulated scenario (RCP 4.5 and Table 5), the monthly mean precipitation of the 34 stations covering the Parana State is 133.20 mm. The maximum monthly mean precipitation occurs in the station 19 (Palmas) (198.46 mm) and the minimum (93.89 mm) in the station 9 (Cambara). The minimum values are generally the same (0 means no rainfall in the month). The maximum monthly precipitation (806.19 mm) occurred in the station 19 (Palmas). The station 19 (Palmas) also presents the maximum standard deviation (119.93 mm) in the precipitation data, highlighting the maximum data dispersion or high variability. The

minimum standard deviation in the precipitation simulations (68.59 mm) of the RCP 4.5 scenario occurred in the station 9 (Cambara).

Table 3 – Gaps found in the historical monthly precipitation and temperature series.

						Monthly temperature			Monthly precipitation	
#	Station	Code	Start	End	Years	Gaps	Total months	% Gaps	Gaps	Total months	% Gaps
1	Paranagua	83844	1961	2005	44	85	540	16%	44	540	8%
2	Morretes	2548038	1966	2005	39	0	480	0%	0	480	0%
3	Guaraquecaba	2548039	1977	2005	28	10	348	3%	11	348	3%
4	Curitiba	83842	1961	2005	44	16	540	3%	8	540	1%
5	Cerro Azul	2449013	1972	1998	26	11	324	3%	11	324	3%
6	Lapa	2549091	1988	2005	17	8	216	4%	8	216	4%
7	Joaquim Tavora	2349030	1971	2005	34	9	420	2%	9	420	2%
8	Ponta Grossa	2550024	1961	2002	41	6	504	1%	6	504	1%
9	Cambara	2350017	1961	2005	44	2	540	0%	2	540	0%
10	Bandeirantes	2350018	1974	2005	31	15	384	4%	15	384	4%
11	Castro	83813	1961	2005	44	93	540	17%	49	540	9%
12	Fernandes Pinheiro	2550025	1963	2005	42	0	516	0%	0	516	0%
13	Telemaco Borba	2450011	1971	2005	34	51	420	12%	15	420	4%
14	Ibipora	2351011	1973	2005	32	2	396	1%	2	396	1%
15	Bela Vista do Paraiso	2251027	1973	2005	32	2	396	1%	2	396	1%
16	Maua da Serra	2351063	1978	1992	14	7	180	4%	7	180	4%
17	Guarapuava	2551010	1972	2005	33	38	408	9%	38	408	9%
18	Apucarana	2351008	1964	2003	39	23	480	5%	23	480	5%
19	Palmas	2651043	1979	2005	26	0	324	0%	0	324	0%
20	Clevelandia	2652003	1973	2005	32	0	396	0%	0	396	0%
21	Laranjeiras do Sul	2552009	1973	2005	32	9	396	2%	9	396	2%
22	Londrina	83766	1961	2005	44	73	540	14%	49	540	9%
23	Maringa	83767	1961	2005	44	144	540	27%	138	540	26%
24	Paranavai	2352017	1974	2005	31	5	384	1%	5	384	1%
25	Nova Cantu	2452050	1976	2005	29	1	360	0%	1	360	0%
26	Campo Mourao	83783	1961	2005	44	60	540	11%	40	540	7%
27	Cianorte	2352019	1971	2002	31	19	384	5%	19	384	5%
28	Pato Branco	2652035	1979	2005	26	0	324	0%	0	324	0%
29	Quedas do Iguaçu	2553018	1972	1999	27	10	336	3%	10	336	3%
30	Francisco Beltrao	2653012	1973	2005	32	4	396	1%	4	396	1%
31	Umuarama	2353008	1971	2005	34	20	420	5%	20	420	5%
32	Cascavel	2453023	1972	1999	27	20	336	6%	20	336	6%
33	Planalto	2553015	1973	2005	32	12	396	3%	12	396	3%
34	Palotina	2453003	1972	2005	33	8	408	2%	8	408	2%

Font: Author.

Table 4 – Monthly descriptive statistics of the observed precipitation (mm) and temperature (°C) series.

P HIST	Mean	STD	Min	Max	T HIST	Mean	STD	Min	Max
1	172.38	116.34	1.10	840.60	1	21.35	3.01	15.07	27.29
2	161.42	99.46	3.60	604.80	2	20.63	3.08	14.22	26.48
3	199.05	131.98	8.10	739.60	3	20.91	3.17	14.45	26.66
4	119.61	78.22	0.10	473.80	4	17.04	2.91	10.62	23.18
5	114.88	70.45	0.10	369.00	5	20.23	3.52	12.37	26.50
6	134.09	76.24	1.10	445.40	6	16.97	3.02	10.10	22.06
7	117.20	79.70	0.00	414.30	7	20.94	3.00	14.02	26.52
8	129.53	82.78	0.00	565.00	8	17.71	2.95	10.85	23.22
9	116.36	86.76	0.00	542.70	9	21.23	3.00	13.53	27.68
10	120.22	85.45	0.00	436.70	10	21.83	2.80	15.45	26.61
11	124.18	84.02	0.00	497.20	11	16.89	3.10	9.91	22.33
12	133.04	81.97	0.00	461.10	12	17.29	3.09	10.47	22.95
13	133.93	81.56	0.00	479.30	13	18.46	3.32	10.88	23.97
14	127.14	89.39	0.00	448.50	14	21.85	2.73	15.36	27.09
15	126.95	92.25	0.00	461.90	15	21.34	2.63	14.86	26.00
16	153.57	95.51	0.10	431.90	16	18.64	2.53	12.25	23.33
17	158.51	88.17	0.60	518.00	17	16.99	3.09	9.64	22.38
18	137.52	87.80	0.00	433.10	18	20.52	2.43	14.18	25.05
19	176.85	101.36	11.60	805.30	19	16.30	3.26	8.65	21.47
20	170.31	97.01	7.20	775.40	20	17.25	3.18	9.66	22.33
21	167.40	98.54	0.20	533.80	21	18.81	2.97	11.22	23.69
22	124.27	91.90	0.00	467.90	22	21.15	2.89	13.42	26.55
23	129.35	85.01	0.00	426.00	23	21.88	2.68	14.82	26.87
24	124.94	83.07	0.00	378.30	24	22.12	2.84	14.94	27.16
25	164.76	97.94	0.80	614.60	25	21.05	2.99	13.53	25.97
26	134.08	89.66	0.00	441.10	26	20.35	3.05	12.55	25.94
27	138.31	92.53	0.00	466.40	27	21.58	2.89	14.41	26.96
28	176.67	107.76	6.80	723.40	28	18.77	3.18	11.02	23.59
29	172.06	100.75	2.20	642.10	29	20.16	3.33	12.68	25.75
30	169.83	102.47	0.50	668.20	30	19.18	3.60	10.72	24.70
31	135.24	86.12	0.00	493.50	31	21.99	2.89	14.56	27.49
32	164.07	95.45	1.10	509.30	32	19.54	3.11	11.88	25.05
33	160.66	100.87	1.30	645.00	33	21.31	3.33	12.84	27.66
34	137.46	87.45	0.10	536.70	34	21.23	3.53	12.03	26.84
Mean P	**144.88**	**91.94**	**1.37**	**537.94**	**Mean T**	**19.81**	**3.03**	**12.56**	**25.22**
Max P	**199.05**	**131.98**	**11.60**	**840.60**	**Max T**	**22.12**	**3.60**	**15.45**	**27.68**
Min P	**114.88**	**70.45**	**0.00**	**369.00**	**Min T**	**16.30**	**2.43**	**8.65**	**21.47**

Font: Author.

Table 5 – Monthly descriptive statistics of the simulated RCP 4.5 precipitation (mm) and temperature (°C) series.

P RCP 4.5	Mean	STD	Min	Max	T RCP 4.5	Mean	STD	Min	Max
1	149.48	81.08	1.10	665.16	1	23.47	2.94	16.85	30.96
2	136.84	79.44	1.36	658.51	2	23.05	2.93	15.94	30.47
3	169.57	100.32	0.65	792.16	3	23.40	3.04	16.32	31.04
4	111.28	74.52	0.13	477.93	4	19.44	2.98	12.33	26.88
5	106.89	69.66	0.05	425.11	5	23.22	3.35	14.68	31.62
6	138.36	92.65	0.16	594.21	6	19.32	2.85	12.28	26.35
7	94.47	69.81	0.01	446.68	7	23.69	2.87	16.14	31.59
8	120.81	79.05	0.01	544.72	8	20.08	2.93	12.81	27.64
9	93.89	68.59	0.00	442.44	9	23.89	2.82	15.90	31.85
10	99.78	72.13	0.00	458.55	10	24.39	2.70	16.92	32.27
11	119.83	77.64	0.01	523.12	11	19.54	3.10	11.69	27.75
12	124.24	83.01	0.00	560.47	12	19.80	3.23	12.15	28.05
13	117.14	81.27	0.00	501.50	13	21.25	3.28	13.24	29.44
14	106.78	75.03	0.00	480.34	14	24.30	2.73	16.93	32.04
15	105.27	72.61	0.00	469.36	15	23.82	2.67	16.58	31.49
16	148.61	102.74	0.00	607.72	16	20.78	2.41	14.04	27.87
17	153.35	99.72	0.00	656.82	17	19.56	3.21	11.97	28.01
18	114.04	78.84	0.00	466.33	18	22.85	2.58	16.12	30.38
19	198.46	119.93	0.07	806.19	19	18.77	3.37	10.63	27.65
20	179.65	110.60	0.00	761.04	20	19.83	3.42	11.70	29.53
21	163.29	105.45	0.00	682.52	21	21.32	3.07	13.58	30.14
22	105.55	72.97	0.00	431.61	22	23.68	2.89	16.16	31.47
23	114.63	75.72	0.00	420.81	23	24.22	2.74	17.10	31.61
24	109.78	73.43	0.00	407.94	24	24.64	2.90	17.02	32.11
25	153.40	103.07	0.00	695.70	25	23.55	3.07	15.26	31.99
26	121.25	82.09	0.00	560.50	26	22.83	3.15	14.77	31.18
27	121.52	82.01	0.00	472.50	27	24.07	3.03	16.37	31.74
28	175.99	114.20	0.00	752.54	28	21.22	3.34	12.92	30.95
29	166.16	108.81	0.00	679.57	29	22.78	3.49	13.73	32.25
30	163.04	107.79	0.00	727.60	30	21.88	3.80	12.71	32.18
31	119.41	79.01	0.00	506.09	31	24.61	3.20	16.25	32.95
32	153.87	103.14	0.00	641.47	32	21.97	3.30	13.20	30.98
33	151.83	101.31	0.00	629.72	33	23.89	3.56	14.98	33.94
34	120.25	84.10	0.00	566.74	34	23.90	3.69	14.05	32.76
Mean P	**133.20**	**87.70**	**0.10**	**573.93**	**Mean T**	**22.32**	**3.08**	**14.51**	**30.56**
Max P	**198.46**	**119.93**	**1.36**	**806.19**	**Max T**	**24.64**	**3.80**	**17.10**	**33.94**
Min P	**93.89**	**68.59**	**0.00**	**407.94**	**Min T**	**18.77**	**2.41**	**10.63**	**26.35**

Font: Author.

Table 6 – Monthly descriptive statistics of the simulated RCP 8.5 precipitation (mm) and temperature (°C) series.

P RCP 8.5	Mean	STD	Min	Max	T RCP 8.5	Mean	STD	Min	Max
1	142.83	81.76	0.02	454.12	1	24.42	2.76	16.78	30.39
2	132.15	75.94	0.13	483.01	2	24.06	2.79	15.80	30.34
3	160.86	98.78	0.27	554.96	3	24.40	2.84	16.28	30.28
4	110.15	79.01	0.21	576.95	4	20.68	3.12	11.72	28.53
5	106.16	77.49	0.09	681.68	5	24.67	3.43	14.00	33.22
6	136.95	98.23	0.26	717.33	6	20.48	2.92	11.83	27.99
7	92.07	74.87	0.00	481.93	7	25.10	3.13	15.47	34.50
8	119.50	85.32	0.02	739.54	8	21.34	3.11	12.21	29.72
9	89.45	71.64	0.00	433.97	9	25.34	3.15	15.26	34.44
10	94.98	75.29	0.00	439.03	10	25.81	3.08	16.21	34.78
11	121.54	85.26	0.03	736.83	11	20.92	3.29	11.27	29.63
12	122.11	88.97	0.03	749.64	12	21.18	3.45	11.66	30.12
13	114.31	86.64	0.00	618.87	13	22.76	3.49	12.60	32.37
14	101.90	80.10	0.00	531.52	14	25.72	3.16	16.26	34.83
15	99.46	77.11	0.00	494.37	15	25.27	3.16	15.92	34.32
16	144.73	111.73	0.00	747.17	16	22.05	2.81	13.74	30.79
17	153.34	107.63	0.01	892.39	17	20.93	3.44	11.54	29.93
18	111.06	85.73	0.00	573.34	18	24.22	3.05	15.56	33.30
19	206.97	134.11	0.04	924.34	19	20.04	3.54	10.51	28.47
20	181.05	119.47	0.00	776.22	20	21.18	3.72	11.70	30.15
21	161.51	113.34	0.00	776.99	21	22.70	3.44	13.43	32.05
22	102.79	79.35	0.00	530.65	22	25.15	3.26	15.19	34.39
23	112.88	82.75	0.00	545.57	23	25.62	3.16	16.19	34.71
24	104.87	77.52	0.00	553.59	24	26.13	3.38	16.64	35.52
25	151.22	110.95	0.11	681.75	25	24.99	3.47	15.19	34.48
26	120.47	88.66	0.00	586.33	26	24.33	3.54	14.52	33.71
27	116.24	87.39	0.00	651.23	27	25.57	3.50	15.82	35.15
28	168.28	116.23	0.00	718.66	28	22.58	3.66	12.99	31.79
29	161.22	115.80	0.00	738.21	29	24.24	3.82	14.01	34.11
30	155.87	109.85	0.00	691.55	30	23.34	4.07	13.12	33.30
31	114.14	83.22	0.00	594.18	31	26.17	3.72	16.50	35.98
32	150.83	107.98	0.00	680.05	32	23.41	3.71	13.52	32.82
33	145.68	106.34	0.00	710.19	33	25.29	3.92	15.54	35.70
34	113.38	85.61	0.00	573.79	34	25.46	4.07	14.70	35.56
Mean P	**130.03**	**92.94**	**0.04**	**636.47**	**Mean T**	**23.69**	**3.36**	**14.23**	**32.57**
Max P	**206.97**	**134.11**	**0.27**	**924.34**	**Max T**	**26.17**	**4.07**	**16.78**	**35.98**
Min P	**89.45**	**71.64**	**0.00**	**433.97**	**Min T**	**20.04**	**2.76**	**10.51**	**27.99**

Font: Author.

Table 5 also presents the descriptive statistics of the temperature in the RCP 4.5 scenarios. The minimum monthly mean temperature (18.77°C) occurred in the station 19

(Palmas), while the maximum (24.64°C) occurred in the station 24 (Paranavai). The minimum monthly records (10.63°C) are in the station 19 (Palmas) and the maximum values present oscillations along the Parana State, pointing the station 33 (Planalto) as the warmest location (33.94°C).

In the future simulated scenario (RCP 8.5 and Table 6), the monthly mean precipitation of the 34 stations covering the Parana State is 130.03 mm. The maximum monthly mean precipitation occurred in the station 19 (Palmas) (206.97 mm) and the minimum (89.45 mm) occurred in the station 9 (Cambara). The minimum values are generally the same (0 means no rainfall in the month). The maximum monthly precipitation (924.34 mm) occurred in the station 19 (Palmas). The station 19 (Palmas) also presents the maximum standard deviation (134.11 mm) in the precipitation data, highlighting the maximum data dispersion or high variability. The minimum standard deviation occurred in the precipitation simulations (71.64 mm) of the RCP 8.5 scenario in the station 9 (Cambara).

Table 6 also presents the descriptive statistics of the temperature in the RCP 8.5 scenarios. The minimum monthly mean temperature (20.04°C) occurred in the station 19 (Palmas), while the maximum (26.17°C) occurred in the station 31 (Umuarama). The minimum monthly records (10.51°C) are in the station 19 (Palmas) and the maximum values present oscillations along the Parana State, pointing the station 31 (Umuarama) as the warmest location (35.98°C).

Figure 5 presents the number of months with lower than 5 mm precipitation accumulated in a month in the historical (HIST) and simulated (RCP 4.5 and RCP 8.5) series. According to these maps, in the historical series the predominant drought events are in the Northwest, Centre-North and Northeast regions, characterized by the highest amount of precipitation events lower than 5 mm. The highest amounts are in blue, while the lowest events are in red. The highest values occurred in the stations 7 (Joaquim Tavora), 9 (Cambara), 10 (Bandeirantes), 14 (Ibipora), 15 (Bela Vista do Paraiso), 18 (Apucarana), 22 (Londrina), and 26 (Campo Mourao) with more than 16 events between January of 1961 and December of 2005 (some stations start after 1961 and/or end before 2005).

In both RCP 4.5 and RCP 8.5 scenarios, the main difference when comparing to the historical scenario, is the Northwest does not comprise the highest number of precipitation events lower than 5 mm. The North and Northeast regions concentrate the highest amounts of low precipitations and this means that both North and Northeast are susceptible to have more

droughts in the future (up to 2100). The highest values occur in the stations 7 (Joaquim Tavora), 9 (Cambara) and 10 (Bandeirantes) for both scenarios (RCP 4.5 and RCP 8.5), with more than 25 events in both regions.

Figure 5 – Number of months with precipitation lower than 5 mm in the historical (HIST) and simulated (RCP 4.5 and RCP 8.5) series.

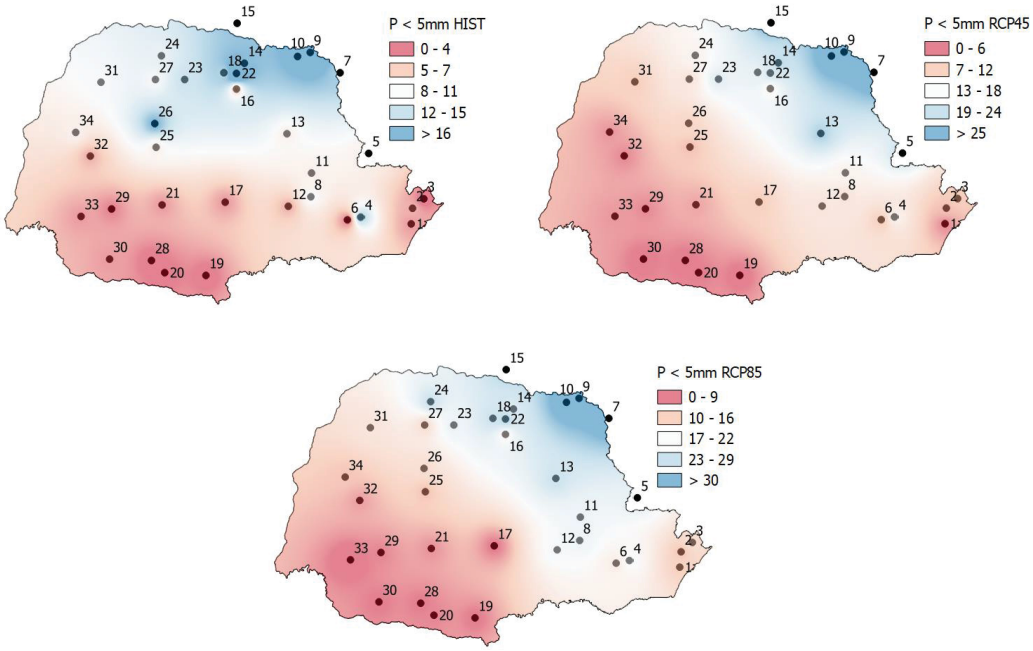

Font: Author.

3.3. Chapter summary

This chapter presented the study area and its characteristics related to general information, geography, hydrography, climate, economy and hydropower generation, highlighting the importance of the Parana State in the Brazilian economy. For the drought study, 34 meteorological stations were selected in the BDMEP and IAPAR websites, containing both precipitation and temperature data.

This chapter also presented some characteristics of the historical and future series (RCP 4.5 and RCP 8.5 scenarios), such as gaps and length of the series, main statistics (mean, standard deviation, minimum and maximum values) of the series, and maps containing the number of months with precipitation amounts below 5 mm.

4. RESULTS AND DISCUSSION

This chapter presents the dissertation results. All applications performed occurred to analyse the drought series in both stationary and non-stationary approaches, using the methods described in chapter 2.

The linear regression was used for filling in the gaps in the historical series along with the bias correction methods applied to correct the RCM ETA simulations. The Thornthwaite method was used to compute the potential evapotranspiration using the daylight hours combined with the monthly temperature series. Then, the Reconnaissance Drought Index (RDI) was computed.

It occurred the application of both trend and changing point tests to verify which historical series present non-stationary pattern, and the non-stationary series were split in the changing point. Then, the differences between the traditional stationary and the non-stationary approaches were computed. This computation analysed the main drought statistics (frequency, severity, duration and magnitude) to perform the drought analysis.

4.1. Filling in the gaps

The Simple Linear Regression (SLR) model filled the gaps in both historical precipitation and temperature monthly series. The dependent variable is the "y – Code" and the independent variable is the "x – Code". Table 7 and Table 8 show the equations of the SLR method, as well as the determination coefficient (R^2), distance between both stations and the climate according to the Köppen classification (ALVARES et al., 2013).

In both tables, the five digits code refers to the INMET meteorological stations while the eight digits code refers to the ANA hydrological stations. There are some meteorological stations with the same name in the "x – Code" and "y – Code" columns, held by different institutions. In general, the SLR presented significant correlations evidenced by the determination coefficient (R^2). In the Table 7, 0.649 was the minimum R^2 in both SLR 5 and 10, and the maximum length between a pair of stations in straight line was 80.35 km for the SLR 5. All pairs of precipitation series present the same Köppen classification.

Table 7 – SLR equations to fill in the gaps for historical precipitation series.

	y – Code	Name	x – Code	Name	Equation	R^2	Distance (km)	Climate (Köppen)
1	83813	Castro	02450010	Castro	y = 8.3177 + 0.9151x	0.8565	0.00	Cfb / Cfb
2	83842	Curitiba	02549006	Curitiba	y = 0.0369 + 0.9626x	0.891	0.00	Cfb / Cfb
3	83766	Londrina	02351010	Londrina	y = 5.8987 + 0.9299x	0.911	0.00	Cfa / Cfa
4	83844	Paranagua	02548021	Paranagua - SE	y = 21.6684 + 0.8993x	0.832	0.00	Cfa / Cfa
5	83767	Maringa	02351003	Londrina (Est. Agroclimatologica)	y = 26.6716 + 0.7684x	0.649	80.35	Cfa / Cfa
6	83783	Campo Mourao	02452005	PHC Mourao 1 Barramento 2	y = 10.0876 + 0.8974x	0.8409	0.00	Cfa / Cfa
7	83767	Maringa	02351008	Apucarana (Faz. Ubatuba)	y = 14.1027 + 0.8435x	0.722	50.30	Cfa / Cfa
8	83783	Campo Mourao	02452010	Janiopolis	y = 20.7748 + 0.816x	0.6851	42.30	Cfa / Cfa
9	83766	Londrina	02351003	Londrina (Est. Agroclimatologica)	y = 6.3861 + 0.8651x	0.799	0.00	Cfa / Cfa
10	83844	Paranagua	02548038	Morretes (Est. Exp. Frutas Trop.)	y = 18.7403 + 0.9596x	0.649	31.20	Cfa / Cfa

y – Code: INMET series

x – Code: ANA series

Font: Author.

Table 8 – SLR equations to fill in the gaps for historical temperature series.

	y – Code	Name	x – Code	Name	Equation	R^2	Distance (km)	Climate (Köppen)
1	83783	Campo Mourao	83767	Maringa	y = -3.7488 + 1.1013x	0.952	82.30	Cfa / Cfa
2	83784	Campo Mourao	83766	Londrina	y = -1.5187 + 1.0346x	0.961	80.00	Cfa / Cfa
3	83813	Castro	83842	Curitiba	y = -0.8344 + 1.04x	0.951	103.40	Cfb / Cfb
4	83842	Curitiba	83844	Paranagua	y = -2.6874 + 0.9244x	0.923	75.80	Cfb / Cfa
5	83766	Londrina	83716	Presidente Prudente	y = -4.42 + 1.1143x	0.958	133.70	Cfa / Aw
6	83767	Londrina	83784	Campo Mourao	y = 2.23 + 0.9291x	0.961	80.00	Cfa / Cfa
7	83767	Maringa	83767	Londrina	y = 2.481 + 0.9175x	0.972	79.30	Cfa / Cfa
8	83767	Maringa	83784	Campo Mourao	y = 4.2942 + 0.864x	0.952	82.30	Cfa / Cfa
9	83844	Paranagua	83842	Curitiba	y = 4.3321 + 0.9986x	0.923	75.80	Cfa / Cfb

y – Code: INMET series

x – Code: INMET series

Font: Author.

Table 8 shows larger distances between pairs of stations and showed higher determination coefficients (R^2). The minimum R^2 refers to the stations Curitiba and Paranagua in the SLR 4 (0.923). Different climates occur also in the SLR 5 for the pair of stations Londrina and Presidente Prudente. Other simulations performed with closer stations were discarded because the determination coefficients resulted lower than 0.60. The SLR analysis was significant for filling in the gaps in the series due to the determination coefficient analysis, in both variables (precipitation and temperature). Different institutions in the same city were used for filling in the gaps in the precipitation series, since there is a significant distance between

them. Most of meteorological stations presented few gaps in the series. They were filled in using the four closest months mean, as described in the Chapter 2, Methods.

4.2. Bias correction

At the same time of the SLR analysis, the bias correction methods were applied in order to correct the RCM ETA series by the historical data for each meteorological station. The most applied indices are Linear Scaling (LS), Power Transformation (PT), Variance Scaling (VAR) and Empirical Quantile Mapping (EQM). These four bias correction were applied and the most suitable for the region was chosen. The Quantile-Quantile (QQ) and Delta Change (DT) methods resulted in non-significant improvements in the corrected series, and were discarded for the posterior analyses.

The four bias correction methods (LS, PT, VAR, and EQM) were computed for the 34 meteorological stations. Table 9 presents the Mean Absolute Error (MAE) of all bias correction methods for both temperature and precipitation series. The PT application refers only to the precipitation series, while the VAR refers only to the temperature series (TEUTSCHBEIN & SEIBERT, 2012).

Analysing all MAE values of the temperature series, 100% of the minimum MAE pointed the EQM the most significant bias correction method for the temperature series. A quite similar behaviour occurred in the precipitation series, but it shows the LS method as the best for the precipitation series, except at station 8.

Other statistics computed include the mean, standard deviation, minimum, maximum, kurtosis, skewness, and percentiles 5%, 10%, 25%, 50%, 75%, 90% and 95%, confirming the EQM as the best method for the temperature series and the LS for the precipitation series. Results for other statistics (mean, standard deviation, minimum, maximum, kurtosis, skewness, and percentiles at 5%, 10%, 25%, 50%, 75%, 90% and 95%) were not shown.

Table 9 – Mean Absolute Error (MAE) of all temperature and precipitation series.

Temperature				Precipitation			
Station	**MAE LS**	**MAE EQM**	**MAE VAR**	**Station**	**MAE LS**	**MAE EQM**	**MAE PT**
1	1.31	1.23	1.29	1	92.19	106.69	105.84
2	1.55	1.40	1.50	2	78.68	82.43	81.95
3	1.52	1.49	1.57	3	79.33	87.02	86.45
4	1.41	1.39	1.44	4	80.63	86.27	86.30
5	1.42	1.35	1.46	5	82.60	83.22	83.43
6	1.44	1.28	1.34	6	83.84	89.26	87.41
7	1.55	1.35	1.41	7	81.21	86.72	85.09
8	1.63	1.34	1.37	8	102.98	102.23	101.58
9	1.38	1.34	1.39	9	90.77	92.20	92.31
10	1.55	1.35	1.38	10	89.08	91.33	91.20
11	1.40	1.38	1.42	11	94.99	101.25	99.86
12	0.90	0.04	0.26	12	84.91	93.75	93.08
13	1.39	1.32	1.36	13	96.49	101.43	100.33
14	1.44	1.35	1.37	14	101.45	106.94	105.92
15	1.46	1.36	1.44	15	85.55	91.88	91.55
16	1.55	1.36	1.44	16	83.21	87.50	87.70
17	1.64	1.41	1.46	17	77.60	81.91	81.03
18	1.56	1.44	1.49	18	106.68	108.36	108.48
19	1.53	1.37	1.47	19	87.96	94.19	94.13
20	1.62	1.37	1.43	20	93.34	99.11	98.86
21	1.47	1.36	1.40	21	102.62	108.32	108.36
22	1.46	1.39	1.42	22	100.83	104.71	104.93
23	1.42	1.30	1.36	23	103.92	114.30	112.23
24	1.41	1.36	1.41	24	107.23	111.70	111.98
25	1.68	1.42	1.46	25	87.72	92.86	93.77
26	1.58	1.39	1.43	26	106.89	108.82	108.27
27	1.57	1.40	1.44	27	103.58	109.27	109.97
28	1.59	1.43	1.51	28	91.92	96.62	96.24
29	1.47	1.46	1.51	29	74.06	81.44	80.46
30	1.57	1.50	1.58	30	63.73	67.64	67.29
31	1.44	1.40	1.47	31	76.40	76.56	77.19
32	1.40	1.35	1.43	32	77.18	78.65	78.74
33	1.42	1.39	1.45	33	75.90	83.46	83.13
34	1.49	1.42	1.52	34	75.28	78.71	78.98

Font: Author.

4.3. Daylight hours and RDI preparation

The next step is the computation of the Potential Evapotranspiration (PET) and the drought indices. To compute them, it is necessary to compute PET using daylight length per each month, presented in Table 10 for all 34 meteorological stations.

Table 10 – Daylight length hours according to latitude for all meteorological stations.

#	City / Station	JAN	FEB	MAR	APR	MAY	JUN	JUL	AUG	SEP	OCT	NOV	DEC
1	Paranagua	13.52	12.95	12.23	11.48	10.87	10.57	10.72	11.24	11.94	12.69	13.36	13.70
2	Morretes	13.51	12.94	12.23	11.49	10.89	10.59	10.73	11.25	11.95	12.69	13.35	13.69
3	Guaraquecaba	13.50	12.94	12.22	11.49	10.89	10.60	10.74	11.26	11.95	12.68	13.34	13.68
4	Curitiba	13.51	12.95	12.23	11.49	10.88	10.58	10.72	11.25	11.95	12.69	13.35	13.70
5	Cerro Azul	13.45	12.91	12.22	11.51	10.93	10.64	10.78	11.28	11.95	12.67	13.30	13.63
6	Lapa	13.52	12.95	12.23	11.48	10.88	10.58	10.72	11.24	11.95	12.69	13.35	13.70
7	Joaquim Tavora	13.38	12.87	12.21	11.54	10.99	10.72	10.85	11.33	11.96	12.64	13.23	13.54
8	Ponta Grossa	13.49	12.94	12.22	11.49	10.89	10.60	10.74	11.26	11.95	12.68	13.34	13.67
9	Cambara	13.36	12.86	12.21	11.55	11.01	10.74	10.87	11.34	11.96	12.63	13.22	13.52
10	Bandeirantes	13.37	12.86	12.21	11.55	11.01	10.74	10.87	11.34	11.96	12.63	13.22	13.53
11	Castro	13.47	12.92	12.22	11.50	10.91	10.62	10.76	11.27	11.95	12.67	13.32	13.65
12	Fernandes Pinheiro	13.50	12.94	12.23	11.49	10.89	10.59	10.73	11.25	11.95	12.69	13.34	13.68
13	Telemaco Borba	13.44	12.90	12.22	11.52	10.95	10.66	10.80	11.29	11.95	12.66	13.28	13.61
14	Ibipora	13.37	12.86	12.21	11.55	11.00	10.73	10.86	11.33	11.96	12.63	13.23	13.53
15	Bela Vista do Paraiso	13.33	12.84	12.21	11.56	11.03	10.77	10.90	11.35	11.96	12.62	13.19	13.49
16	Maua da Serra	13.40	12.88	12.22	11.54	10.98	10.71	10.84	11.32	11.96	12.64	13.25	13.56
17	Guarapuava	13.50	12.94	12.22	11.49	10.89	10.59	10.74	11.25	11.95	12.69	13.34	13.68
18	Apucarana	13.38	12.87	12.21	11.54	10.99	10.72	10.85	11.33	11.96	12.64	13.23	13.54
19	Palmas	13.57	12.98	12.23	11.46	10.83	10.52	10.67	11.21	11.94	12.71	13.40	13.76
20	Clevelandia	13.56	12.98	12.23	11.46	10.83	10.52	10.67	11.21	11.94	12.71	13.40	13.75
21	Laranjeiras do Sul	13.50	12.94	12.23	11.49	10.89	10.59	10.73	11.25	11.95	12.69	13.34	13.68
22	Londrina	13.38	12.87	12.21	11.54	10.99	10.72	10.85	11.33	11.96	12.64	13.23	13.54
23	Maringa	13.39	12.87	12.21	11.54	10.99	10.72	10.85	11.32	11.96	12.64	13.24	13.55
24	Paranavai	13.36	12.86	12.21	11.55	11.01	10.74	10.87	11.34	11.96	12.63	13.22	13.53
25	Nova Cantu	13.45	12.91	12.22	11.51	10.93	10.65	10.79	11.28	11.95	12.66	13.30	13.62
26	Campo Mourao	13.43	12.89	12.22	11.52	10.95	10.67	10.81	11.30	11.95	12.66	13.28	13.60
27	Cianorte	13.39	12.87	12.21	11.54	10.99	10.72	10.85	11.32	11.96	12.64	13.24	13.55
28	Pato Branco	13.55	12.97	12.23	11.47	10.84	10.53	10.68	11.22	11.94	12.71	13.39	13.74
29	Quedas do Iguaçu	13.51	12.94	12.23	11.49	10.88	10.59	10.73	11.25	11.95	12.69	13.35	13.69
30	Francisco Beltrao	13.55	12.97	12.23	11.47	10.84	10.54	10.68	11.22	11.94	12.71	13.39	13.74
31	Umuarama	13.39	12.87	12.21	11.54	10.99	10.71	10.85	11.32	11.96	12.64	13.24	13.55
32	Cascavel	13.46	12.91	12.22	11.51	10.93	10.64	10.78	11.28	11.95	12.67	13.30	13.63
33	Planalto	13.51	12.95	12.23	11.49	10.88	10.58	10.72	11.25	11.95	12.69	13.35	13.69
34	Palotina	13.44	12.90	12.22	11.52	10.95	10.66	10.80	11.29	11.95	12.66	13.28	13.61

Font: adapted from TIME AND DATE (2019).

The PET computation requires two inputs, the daylight length (in hours) and the monthly temperature. The daylight length does not change significantly through time and depends on both Earth's axial tilt and latitude. Thus, the daylight length for each meteorological station is needed and is presented in Table 10. The daylight length (in hours) was collected in the TIME AND DATE (2019) website for the main cities (Curitiba and Londrina) from January to December of 1961. The daylight length in the other 32 meteorological stations, was derived from the Curitiba and Londrina values by linear interpolation.

Data from Table 10 were used to compute the monthly PET, using also the monthly temperature. All data were computed in the accumulation periods (3, 6, 12, 24, 36, 48, and 60 months) to obtain the ak of the RDI drought indices, according to equations in the section 2.5.2 Reconnaissance Drought Index. Several drought indices accumulated in distinct periods were generated, comparing their p-values with the p-values of both Mann Kendall and Pettitt tests for the historical monthly series (precipitation and temperature). This comparison enabled the analysis of each series to compare stationary and non-stationary patterns.

4.4. Indices versus historical series trend analysis

As explained in chapter 2, the application of both Mann Kendall (MK) and Pettitt (PT) tests occurred in both monthly precipitation and temperature series and in distinct accumulation periods to verify trend or changing point in both historical and drought indices series. Under a hypothesis of non-stationary series, it was necessary to split them and fit distinct probability distributions before and after the changing point. The MK and PT tests were computed for both precipitation and temperature series of all meteorological stations and drought indices.

If both precipitation or/and temperature series of the original and each accumulated period present p-values lower than 0.05, it turns necessary to split the RDI series in the changing point. Then, one gamma distribution is fitted from the beginning to the Changing point (CP), and another, from the changing point to the end of the series (e.g. 1961 to CP, CP to 2005). This application occurred only in the computation of the RDI series (ak). Both Standardized Precipitation Index (SPI) and Standardized Precipitation Evapotranspiration Index (SPEI) computations were not considered in the following analyses. All drought indices computation

rely in the assumption of fitting a probability distribution and gamma was adopted, according to the work of PLOSZAI et al. (2019).

The p-value is the probability threshold for the null hypothesis rejection, i.e., the smallest significance level to verify trends and/or changing points in time series, assuming the null hypothesis is true (DEVORE, 2010). The p-value of a statistical test is the probability of type I error when H_0 is rejected.

Table 11 – Trend and changing point tests results for RDI in the historical observed series.

HIST	P	T	ak							HIST	P	T	ak						
Station	1	1	3	6	12	24	36	48	60	Station	1	1	3	6	12	24	36	48	60
1										18									
2										19									
3										20									
4										21									
5										22									
6										23									
7										24									
8										25									
9										26									
10										27									
11										28									
12										29									
13										30									
14										31									
15										32									
16										33									
17										34									

P: monthly precipitation series
T: monthly temperature series
ak: RDI series accumulated in 3, 6, 12, 24, 36, 48, and 60 months

	Trend and changing point		Only changing point		Only trend		No trend, nor changing point

Font: Author.

The MK and PT tests were applied to verify the stationarity or non-stationarity in the RDI series for all accumulation periods (3, 6, 12, 24, 36, 48, and 60 months). Table 11 presents the stations that presented only trend (blue), trend and changing point (green), or only changing point (orange) in both monthly series and accumulation periods for the RDI series. Table 11

presents the comparison of monthly precipitation and temperature series with all RDI accumulation periods in the historical observed series. The blanks indicate neither trend nor change point and hence stationarity.

Analysing Table 11, few stations presented trend and changing point (coloured green) or only changing point (orange) in both monthly historical precipitation or temperature series and accumulation periods of the RDI series (ak). The station 1 (Paranagua) presented trend and changing point (green) in the monthly precipitation series and also in the 3, 6, 12 and 48 months RDI accumulation periods. The station 8 (Ponta Grossa) presented trend and changing point (green) in the monthly precipitation series and also in the 3, 6, and 12 months RDI accumulation periods.

The station 11 (Castro) presented only changing point (orange) in the monthly precipitation series as well as in the 3 month accumulation period. It presents trend and changing point (green) in the 6 and 12 months RDI accumulation periods. The station 21 (Laranjeiras do Sul) presented trend and changing point (green) in the monthly precipitation series and also in the 6 month accumulation period. Station 22 (Londrina) presented only changing point (orange) in the monthly precipitation series. However, it also presented both trend and changing point (green) in the monthly temperature series and in the 3-, 6- and 12-month accumulation periods.

Station 8 (Ponta Grossa) presented only trend (blue) in the historical series, for accumulation periods of 24, 36, 48 and 60 months. Station 22 (Londrina) also presented only trend (blue) in the 36 month accumulation periods.

Table 12 presents the comparison of monthly precipitation and temperature series and all RDI accumulation periods for RCP 4.5 scenarios. Practically all precipitation series of the Parana State presented only changing point (orange) in the simulated series, except the station 20 (Clevelandia) which presented trend and changing point (green) in the series.

The accumulation periods that presented only changing points (orange) in the 3 month RDI accumulation periods are the stations 2 (Morretes), 3 (Guaraquecaba), 7 (Joaquim Tavora), 9 (Cambara), 10 (Bandeirantes), 11 (Castro), 14 (Ibipora), 15 (Bela Vista do Paraiso), 16 (Maua da Serra), 22 (Londrina) and 23 (Maringa). The accumulation periods that presented only changing point (orange) in the 6 month RDI accumulation periods are the stations 1

(Paranagua), 2 (Morretes), 3 (Guaraquecaba), 9 (Cambara), 10 (Bandeirantes), 14 (Ibipora), 15 (Bela Vista do Paraiso) and 34 (Palotina).

Table 12 – Trend and changing point tests results for RDI in the simulated RCP 4.5 scenarios.

RCP 4.5	P	T	ak							RCP 4.5	P	T	ak						
Station	1	1	3	6	12	24	36	48	60	Station	1	1	3	6	12	24	36	48	60
1										18									
2										19									
3										20									
4										21									
5										22									
6										23									
7										24									
8										25									
9										26									
10										27									
11										28									
12										29									
13										30									
14										31									
15										32									
16										33									
17										34									

P: monthly precipitation series
T: monthly temperature series
ak: RDI series accumulated in 3, 6, 12, 24, 36, 48, and 60 months

	Trend and changing point		Only changing point		Only trend		No trend, nor changing point

Font: Author.

Table 13 presents the comparison of monthly precipitation and temperature series and all RDI accumulation periods for RCP 8.5 scenarios. All 34 monthly temperature series presented trend and changing point (green) and some stations presented only changing point in the precipitation series.

Practically all 34 stations presented trend and changing point (green) in the 3-, 6-, and 12-month RDI accumulation periods, except the stations 19 (Palmas), which presented neither trend nor changing point in the accumulation periods, and 20 (Clevelandia), which presented only changing point (orange) in the 12-month accumulation period. For larger accumulation

periods (e.g. 24, 36, 48 and 60 months), some stations present both trend and changing point (green), while others present only trend (blue).

General stations varied in the presentation of trend and changing point (green) or only trend (blue) in the higher. The only trend (blue) was unconsidered in this method as explained in previous paragraph.

Table 13 – Trend and changing point tests results for RDI in the simulated RCP 8.5 scenarios.

RCP 8.5	P	T	ak							RCP 8.5	P	T	ak						
Station	1	1	3	6	12	24	36	48	60	Station	1	1	3	6	12	24	36	48	60
1										18									
2										19									
3										20									
4										21									
5										22									
6										23									
7										24									
8										25									
9										26									
10										27									
11										28									
12										29									
13										30									
14										31									
15										32									
16										33									
17										34									

P: monthly precipitation series
T: monthly temperature series
ak: RDI series accumulated in 3, 6, 12, 24, 36, 48, and 60 months

	Trend and changing point		Only changing point		Only trend		No trend, nor changing point

Font: Author.

ZARCH et al. (2015) compared the performance of both RDI and SPI in humid areas. They also found some differences in the middle of both indices. According to them, the RDI is a better drought index to perform global warming analysis, since it considers the effects of potential evapotranspiration. In a general analysis, they found the SPI presents more increasing drought trends (becoming wet) than RDI in the humid areas, according to MK and PT tests.

Other authors defend the use of the SPI, like KHADR (2016). According to him, the main advantage of the SPI is the use of only standardized precipitation in its computation. Topography and other variables do not affect its performance.

The MK and PT tests application showed which accumulation periods presented trend and/or changing point in the meteorological stations of the RDI series. This analysis showed differences between the three RDI scenarios (historical, RCP 4.5 and RCP 8.5) as well as presented which stations, it is necessary to split the RDI series in the changing point to perform the non-stationary drought analysis.

4.5. Differences in the drought indices statistics

The previous section pointed the stations and their respective accumulation periods to apply the non-stationary analysis. From the analysis of the Table 11, Table 12 and Table 13, in a general overview the most significant non-stationary scenarios occurred in the 3, 6 and 12 month accumulation periods.

Table 14 - Non-stationary scenarios in Parana State in the 3-, 6-, and 12-month accumulation periods in the historical and both future (RCP 4.5 and RCP 8.5) scenarios.

Accum.	**Historical period stations**																	
3	1	8	11	22														
6	1	8	11	21	22													
12	1	8	11	22														
Accum.	**Future RCP 4.5 scenario stations**																	
3	2	3	7	9	10	11	14	15	16	22	23							
6	1	2	3	9	10	14	15	34										
12																		
Accum.	**Future RCP 8.5 scenario stations**																	
3	1	2	3	4	5	6	7	8	9	10	11	12	13	14	15	16	17	
	18	21	22	23	24	25	26	27	28	29	30	31	32	33	34			
6	1	2	3	4	5	6	7	8	9	10	11	12	13	14	15	16	17	
	18	21	22	23	24	25	26	27	28	29	30	31	32	33	34			
12	1	2	3	4	5	6	7	8	9	10	11	12	13	14	15	16	17	
	18	20	21	22	23	24	25	26	27	28	29	30	31	32	33	34		

Font: Author.

Table 14 presents the non-stationary stations in the Parana State for both historical period (HIST) and simulated future (RCP 4.5 and RCP 8.5) scenarios. According to the Table 14, in the historical period for the 3-month accumulation period, the stations 1 (Paranagua), 8 (Ponta Grossa), 11 (Castro), and 22 (Londrina) presented non-stationarity in the RDI series. The Changing point (CP) presented in the Pettitt test application in the RDI series will split these series. In the 6-month accumulation period, the station 21 (Laranjeiras do Sul) includes among the previous in the non-stationary stations. The 12-month accumulation period presented non-stationarity in the same stations that the 3-month accumulation period.

Following in the Table 14, the RCP 4.5 scenarios presented non-stationarity in the 3-month accumulation period in the stations 2 (Morretes), 3 (Guaraquecaba), 7 (Joaquim Tavora), 9 (Cambara), 10 (Bandeirantes), and 11 (Castro). The stations 14 (Ibipora), 15 (Bela vista do Paraiso), 16 (Maua da Serra), 22 (Londrina), and 23(Maringa) also presented non-stationarity in the RDI series. The CP presented in the Pettitt test application in the RDI series will split these series. In the 6-month accumulation period of the RCP 4.5 scenarios, the stations 1 (Paranagua), 2 (Morretes), 3 (Guaraquecaba), 9 (Cambara), 10 (Bandeirantes), 14 (Ibipora), 15 (Bela Vista do Paraiso), and 34 (Palotina) presented non-stationarity in the RDI series. The CP presented in the Pettitt test application in the RDI series will split these series. There is not any station that presented non-stationarity in the 12-month accumulation period in the RCP 4.5 scenario.

The RCP 8.5 scenarios in the 3- and 6-month accumulation periods presented non-stationarity in almost all 34 stations, except the stations 19 (Palmas) and 20 (Clevelandia) which presented stationarity. In the 12-month accumulation period, almost all 34 stations presented non-stationarity, except the station 19 (Palmas).

Table 15 – General non-stationary scenarios and the method border conditions.

For HIST 12 scenarios, stations with less than 30 periods length									
Stations	3	5	6	16	19	25	28	29	32
For HIST scenarios, stations with min length (30 periods) to fit the gamma									
Stations	1	4	8	9	11	12	18	21	22	23	30	31
ak	6	6	3	6	6	3	3	3	6	6	3	6

Font: Author.

The differences between stationary and non-stationary approaches presented in the text refer only to the 3-month accumulation periods. The other accumulation periods (6- and 12-months) are in the Appendix. A limitation of the proposed method consists in the determination of the minimum length to fit a probability distribution (30-period length) (KOUTSOYIANNIS, 2006).

For this reason, the selection of the HIST scenarios in the 12-month accumulation period with less than 30 period length, was performed. The stations 3 (Guaraquecaba), 5 (Cerro Azul), 6 (Lapa), 16 (Maua da Serra), 19 (Palmas), 25 (Nova Cantu), 28 (Pato Branco), 29 (Quedas do Iguacu), and 32 (Cascavel) presented less than 30 periods when accumulated in 12-months. These stations cannot be accumulated in 12-months and then fit a probability distribution due to a small sample after clustering (less than 30-periods) (KOUTSOYIANNIS, 2006).

In the next lines of the Table 15, only for the historical observed series analysis, the stations 1 (Paranagua), 4 (Curitiba), 9 (Cambara), 11 (Castro), 22 (Londrina), 23 (Maringa), and 31 (Umuarama), can accumulate only the 3 and 6 months in order to fit probability distributions larger than 30-periods and reduce the errors of the small sampling fitting. The stations 8 (Ponta Grossa), 12 (Fernandes Pinheiro), 18 (Apucarana), 21 (Laranjeiras do Sul), and 30 (Francisco Beltrao) can accumulate only the 3 months in order to satisfy this condition also.

Table 16 – Non-stationary scenarios in Parana State in the 3-, 6-, and 12-month accumulation periods in the historical and both future (RCP 4.5 and RCP 8.5) scenarios, after applying the border conditions correction.

Accum.	**Historical period stations**
3	1 8 11 22
6	1 11 22
Accum.	**Future RCP 4.5 scenario stations**
3	2 3 7 9 10 11 14 15 16 22 23
6	1 2 3 9 10 14 15 34
Accum.	**Future RCP 8.5 scenario stations**
3	1 2 3 4 5 6 7 8 9 10 11 12 13 14 15 16 17 18 21 22 23 24 25 26 27 28 29 30 31 32 33 34
6	1 2 3 4 5 6 7 8 9 10 11 12 13 14 15 16 17 18 21 22 23 24 25 26 27 28 29 30 31 32 33 34
12	1 2 3 4 5 6 7 8 9 10 11 12 13 14 15 16 17 18 20 21 22 23 24 25 26 27 28 29 30 31 32 33 34

Font: Author.

All these combined information resulted in the Table 16, where there are only stations suitable for the non-stationary approach. From the previous analysis, in the historical observed scenarios, the stations 1 (Paranagua), 8 (Ponta Grossa), 11 (Castro), and 22 (Londrina) presented non-stationarity in the RDI series in the 3-month accumulation period. In the 6-month accumulation period, the stations 1 (Paranagua), 11 (Castro), and 22 (Londrina) presented non-stationarity in the RDI series. The respective CP presented in the Pettitt test application in the RDI series split these stations in both accumulation periods (3- and 6-month). In this analysis the 12-month accumulation period turned into stationary due to the minimum 30-period length requirement to fit a probability distribution (KOUTSOYIANNIS, 2006). Both simulated (RCP 4.5 and RCP 8.5) scenarios remained equal, because the series are extended (January of 2006 to December of 2099, resulting in 1128 months), when compared to the historical series (540 months). The 12-month accumulation period is the minimum to satisfy the 30-period length in both future simulated scenarios.

Using the Table 16 information, the algorithm performed the drought analysis computing the main drought statistics, like duration, frequencies (thresholds 0, -1.0 and -1.5, which represent mild, moderate and severe droughts, respectively). The algorithm computed also the magnitude (mean, median and maximum), minimum value, and number of differences (between stationary and non-stationary approaches).

In order to verify the non-stationary analysis performance to evaluate droughts, the algorithm computed differences in these drought statistics and elaborated colour maps, as follow in the Figure 6, Figure 7, Figure 8, Figure 9, Figure 10, Figure 11, Figure 12, Figure 13, Figure 14, and Figure 15. It is important to highlight that these maps generation in the QGIS free software used the Inverse Distance Weighting (IDW) interpolation technique. Its name attributes to a weighted average, resulting in the proximity of each point, in terms of the distance's inverse. The IDW consists in a multivariate deterministic interpolation method using known set points. The other values were obtained from the set points using this weighting average of the known points (ACHILLEOS, 2011). In all maps (Figure 6, Figure 7, Figure 8, Figure 9, Figure 10, Figure 11, Figure 12, Figure 13, Figure 14, and Figure 15) there are only the non-stationary stations. These maps show the percentage difference between the stationary and non-stationary approaches.

Figure 6 presents the percentage difference between stationary and non-stationary approaches in the maximum drought duration of both historical (HIST) and simulated (RCP 4.5 and RCP 8.5) series. According to it, in the historical RDI series, most of Parana area presented differences of around 10.64% in drought duration, between stationary and non-stationary approaches. Exceptions occurred in the stations 8 (Ponta Grossa) and 11 (Castro), presenting lower values (1.14%). However, the station 22 (Londrina with 29.64%) and station 1 (Paranagua with 39.14%) presented higher values.

The simulated (RCP 4.5) series presented more non-stationary stations and the difference in drought duration is between 2.00% and -13.23%. Positive difference values indicate the stationary approach generates a larger value when compared to the non-stationary approach, while negative difference values indicate the non-stationary approach generates a larger value when compared to the stationary approach. It means that **positive differences** result in drought duration **overestimation** whether adopting the **stationary approach**, while the **negative differences** result in drought duration **underestimation** whether adopting the **stationary approach**. In a general scenario, there is a general drought duration underestimation, except for the Northeast and East (coast side) of the Parana State.

Figure 6 – Difference (%) between stationary and non-stationary approaches in the maximum drought duration of the historical (HIST), and simulated (RCP 4.5 and RCP 8.5) series.

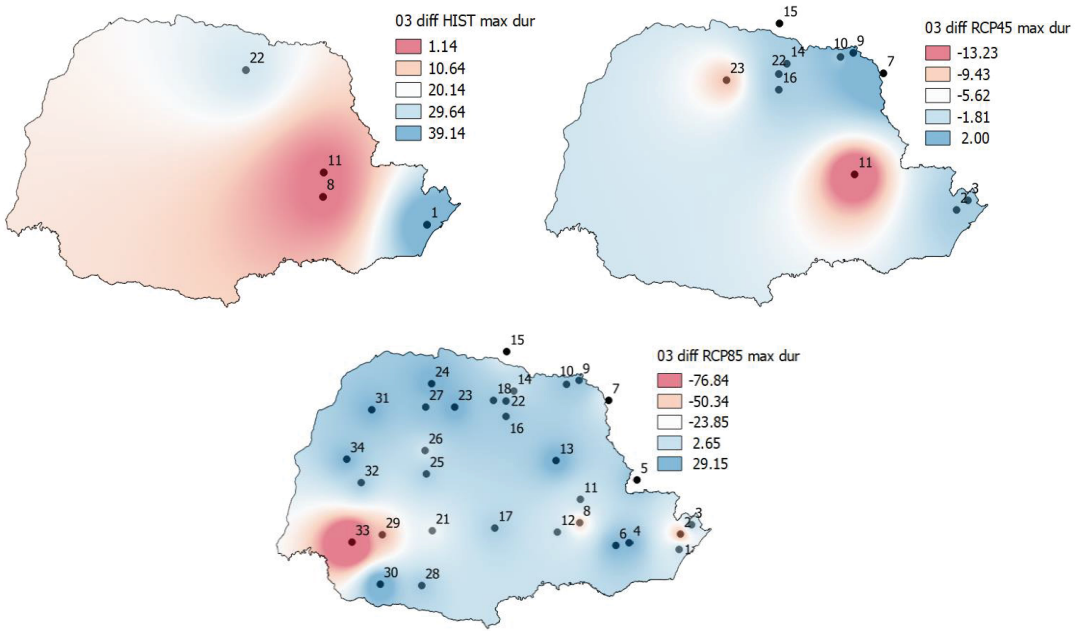

Font: Author.

In the RCP 8.5 scenario, there is a general drought duration overestimation in terms of area, with few stations located in the Southwest presenting great underestimation (highest underestimation in the station 33 – Planalto, with -76.84%). Some areas between stations across the Parana State presented a slight drought duration underestimation, when adopting the non-stationary scenario. It means the non-stationary approach indicates a drought with larger duration than the traditional stationary approaches do, highlighting the importance of considering the non-stationarity in drought analysis. The stations 29 (Quedas do Iguassu), followed by the stations 8 (Ponta Grossa) and 2 (Morretes) presented significant drought duration underestimation up to -50.34%.

Figure 7 presents the percentage difference between stationary and non-stationary approaches in the zero threshold frequency of droughts of the historical (HIST) and simulated (RCP 4.5 and RCP 8.5) series. The statistic drought frequency of zero threshold means the occurrence of droughts, where all RDI values below zero are considered droughts, according to the Run Theory (see subchapter 2.10 Run Theory). According to it, in the historical observed RDI series, the general Parana State presented differences of around 0.64% in the frequency of droughts under a zero threshold, when comparing the stationary and non-stationary scenarios. The stations 11 (Castro) and 22 (Londrina) presented 2.63% variation. In the littoral area, the station 1 (Paranagua) presented -5.32% variation.

The simulated (RCP 4.5) series presented less percentage variation than the historical series. However, the RCP 4.5 has more stations with a non-stationary approach, resulting in a different behaviour. The highest differences (red) in the zero threshold frequency of droughts are in the stations 3 (Guaraquecaba), 10 (Bandeirantes), 11 (Castro), 14 (Ibipora) and 22 (Londrina), while the lowest differences are in the stations 7 (Joaquim Tavora), 9 (Cambara), 15 (Bela Vista do Paraiso) and 23 (Maringa). Even in this scenario occurred only underestimation in the frequency of droughts (zero threshold) and it occurred few variations in absolute value. This means that using the traditional stationary models, occurs an underestimation in the frequency of droughts. This fact highlights the importance of adopting non-stationary models for drought analysis.

The RCP 8.5 scenario presented differences in the variation of drought frequencies in the entire Parana State. There is an overestimation of drought frequency in the Central-North, North, Northwest and West, except for the station 34 (Palotina with -2.46%), which presented

an underestimation of the drought frequency of zero threshold. This means that half of the Parana State, when adopting the stationary models, has a variation between -1.11% and 1.59%, meaning underestimation and overestimation, respectively. In the Centre-South, Southeast and East, the map showed a general underestimation from Centre-South to East of around -2.47%, and few stations in these subareas presented -1.11% variation (e.g. station 12 – Fernandes Pinheiro). The historical scenario presented more drought frequency differences when compared to both future scenarios.

Figure 7 – Difference (%) between stationary and non-stationary approaches in the zero threshold frequency of the historical (HIST), and simulated (RCP 4.5 and RCP 8.5) series.

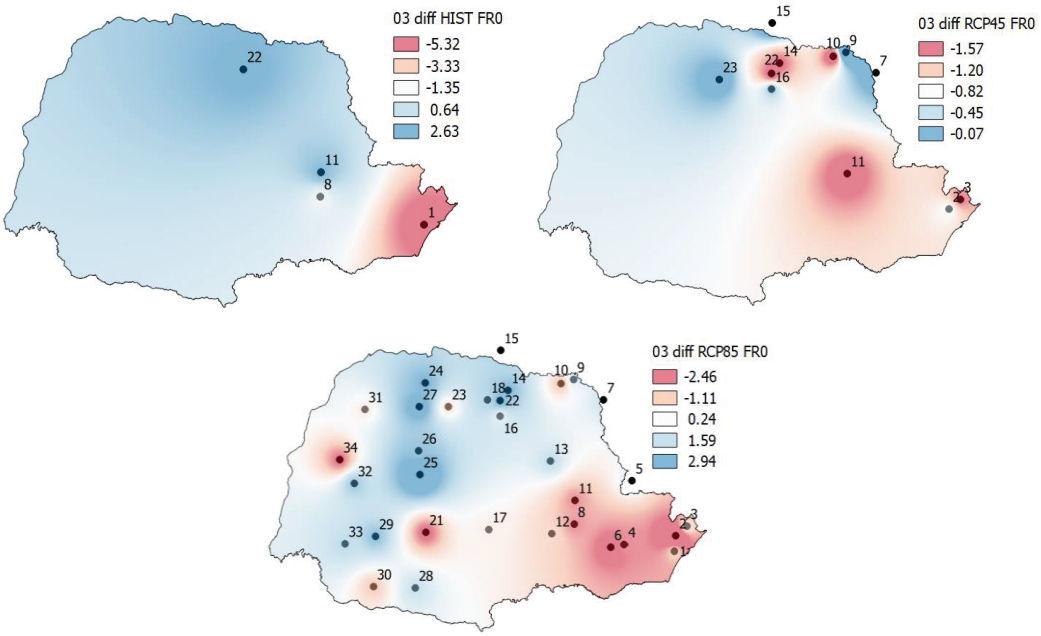

Font: Author.

Figure 8 presents the percentage difference between stationary and non-stationary approaches in the -1.0 threshold frequency of droughts of the historical (HIST) and simulated (RCP 4.5 and RCP 8.5) series. According to it, in the historical observed RDI series, Parana State presented generally differences of around -2.35% in the frequency of droughts under a -1.0 threshold, comparing the stationary and non-stationary scenarios. The station 11 (Castro) presented -8.40% variation, while the neighbour station (8 – Ponta Grossa) presented 3.71% variation. The station 8 presented overestimation, while the station 22 presented underestimation between non-stationary and stationary approaches. At the coast occurred a

different behaviour since the station 1 (Paranagua) presented 15.82% positive variation. This means that close to the coast-side, there is drought overestimation when using the stationary approach.

The simulated (RCP 4.5) series presented less percentage variation than the historical series (percentage differences range from -2.08% to 2.43%). The stations 7 (Joaquim Tavora), 9 (Cambara) and 16 (Maua da Serra) presented the highest positive percentage (overestimation), while the stations 3 (Guaraquecaba), 11(Castro) and 22 (Londrina) presented the lowest percentage (underestimation). Negative values mean that in these areas occurred underestimation of the drought frequencies when using the traditional stationary models. In other areas of the country (light blue and blue), there is a slight overestimation of drought frequencies between 0.17% and 1.30%. In the light red areas, there is a mild underestimation of moderate drought occurrence of about -0.96% difference.

Figure 8 – Difference (%) between stationary and non-stationary approaches in the -1.0 threshold frequency of the historical (HIST), and simulated (RCP 4.5 and RCP 8.5) series.

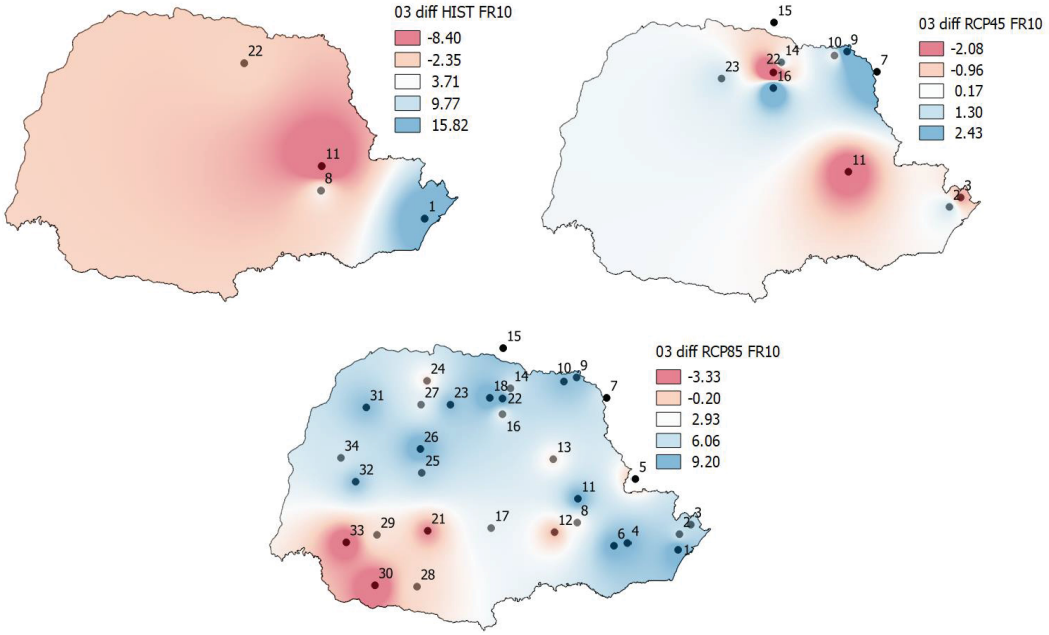

Font: Author.

The RCP 8.5 scenario presented more variation in the drought frequencies than the RCP 4.5 scenario. The RCP 8.5 presented a general overestimation of the drought frequencies when adopting the stationary models, evidenced by the range of positive values (between 2.93% and

9.20%) in almost the entire Parana State. In the light red areas, represented by stations 5 (Cerro Azul), 12 (Fernandes Pinheiro), 28 (Pato Branco) and 29 (Quedas do Iguassu), and in the Southwest (mild variation in the moderate drought occurrence frequency) occurred -0.20% variation. The stations 21 (Laranjeiras do Sul), 30 (Francisco Beltrao) and 33 (Planalto) presented the highest negative variations (-3.33%), meaning in both red and light red areas occur a slight underestimation of the drought frequencies. This happens when the stationary model is adopted and highlights the importance of considering the non-stationary models in drought analysis. The -1.0 threshold relates to the occurrence of moderate droughts, according to the droughts classification presented in the subsection 2.5 Drought indices.

Figure 9 presents the percentage difference between stationary and non-stationary approaches in the -1.5 threshold frequency of droughts of the historical (HIST) and simulated (RCP 4.5 and RCP 8.5) series. According to it, in the historical scenario occurred underestimation of the severe droughts, pointed by the negative differences between stationary and non-stationary approaches. The -1.5 threshold (severe droughts) is an important statistic to evaluate the drought phenomena, since it reveals a severe drought.

Figure 9 – Difference (%) between stationary and non-stationary approaches in the -1.5 threshold frequency of the historical (HIST), and simulated (RCP 4.5 and RCP 8.5) series.

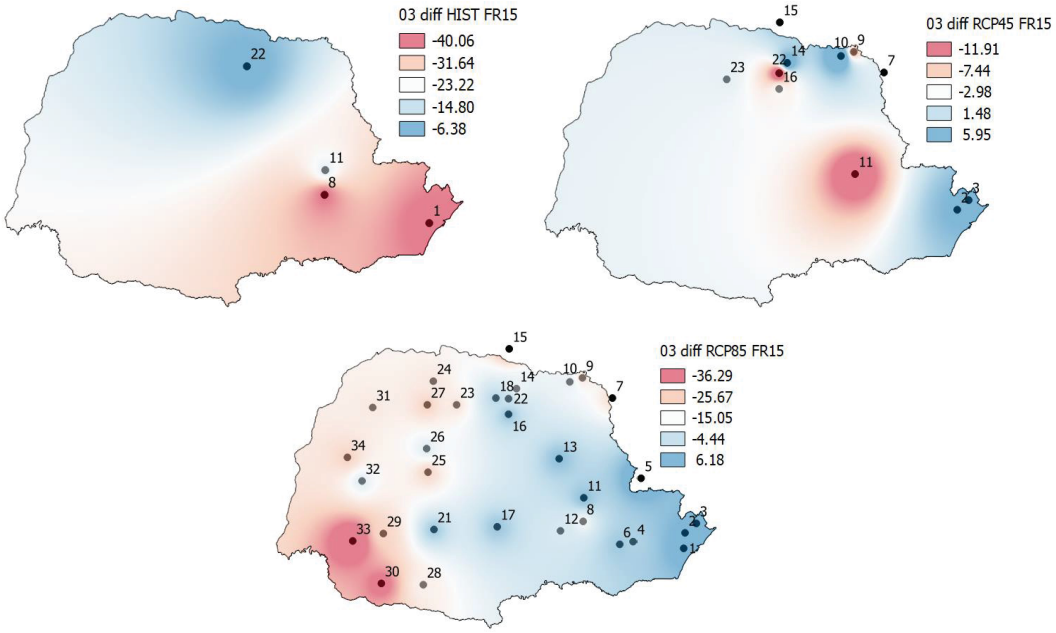

Font: Author.

In the historical scenario, the highest variations occurred in the seaside (East), South and Southeast, in a range between -23.22% and -40.06%, represented by white and red. In the North, Northwest and West, occurred the milder differences (between -6.38% and -14.80%) represented by light blue and blue, respectively. The lowest severe drought occurrence differences occurred in the station 22 (Londrina) with -6.38% difference between stationary and non-stationary approaches, meaning the stationary approach underestimates the non-stationary approach.

The simulated (RCP 4.5) series presented more variation in both stations 11 (Castro) and 22 (Londrina) with -11.91% variation. The second highest variation occurred at the station 16 (Maua da Serra) with -7.44% variation. In other Parana areas, occurred differences between -2.98% and 5.95%, represented by blue to white gradual transition. There is a general overestimation in the differences of severe drought occurrence frequencies, represented by light blue and blue in the map (positive signal).

The RCP 8.5 presented a clear pattern in the differences between stationary and non-stationary approaches. There is a white line splitting the Parana State in two areas. The red to light red areas represent the higher differences (between -25.67% and -36.29%) and the light blue (-4.44%) to blue (6.18%) represent the lower differences. In the RCP 8.5 scenario, there was a slight drought overestimation (6.18% variation represented by blue circles) in the stations 5 (Cerro Azul), 13 (Telemaco Borba), 17 (Guarapuava), and 21 (Laranjeiras do Sul), among others. There is an increase in the frequency of severe droughts, when compared to the RCP 4.5 scenario and a mild decrease, when compared to the historical scenario.

Figure 10 presents the percentage difference between stationary and non-stationary approaches in the maximum drought magnitude of both historical (HIST) and simulated (RCP 4.5 and RCP 8.5) series. In the historical series occurred a general overestimation of the maximum drought magnitude, meaning the stationary approach results in a larger maximum magnitude, when compared to the non-stationary analysis. This means more severe droughts than actually are. Lower variations occur in the North, where the station 22 (Londrina) presented 1.02% difference (red). Higher variations occur close to the seaside and the station 1 (Paranagua) resulted in the maximum drought magnitude difference in the entire State (21.34% in blue).

A different behaviour happens in the simulated future series (RCP 4.5 and RCP 8.5). In the RCP 4.5 scenario, there is a general overestimation of the maximum drought magnitudes in

almost the entire State, mainly in the North region. Exceptions are the red areas regarding the stations 11 (Castro) with -16.90% difference and 2 (Morretes) between -10.80% and -16.90%, both indicating underestimation of maximum drought magnitude. In the light red area between station 2 and 11 occurred a -10.80% difference, meaning an underestimation of the maximum drought magnitude, when adopting the stationary approach.

Figure 10 – Difference (%) between stationary and non-stationary approaches in the maximum drought magnitude of the historical (HIST), and simulated (RCP 4.5 and RCP 8.5) series.

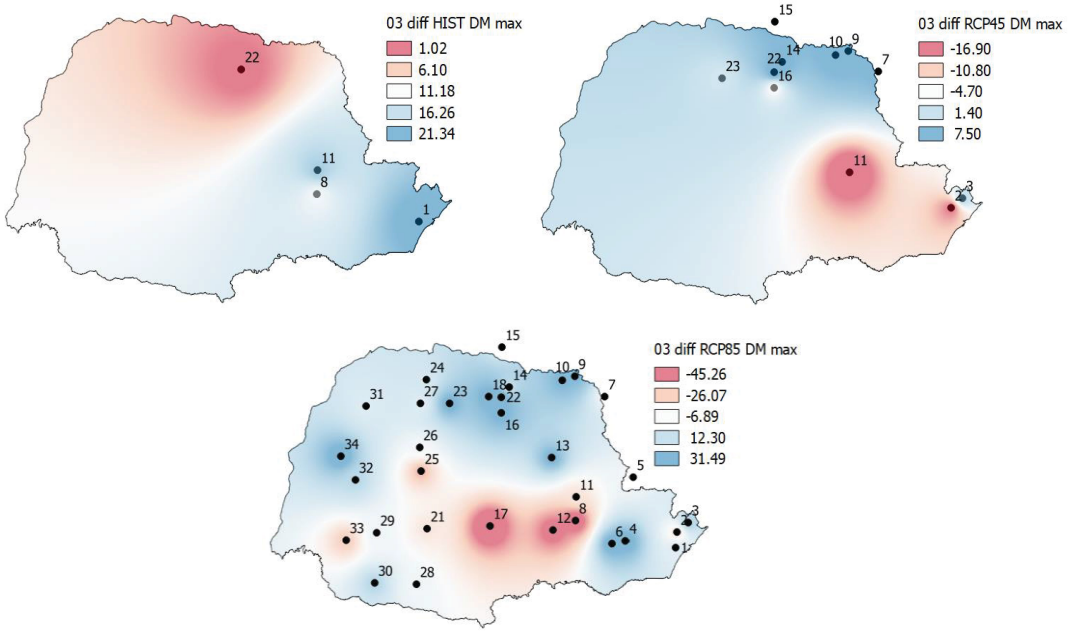

Font: Author.

In the RCP 8.5 scenario, more stations presented non-stationary behaviour and Parana State presented an overestimation of the maximum drought magnitudes, being the maximum value 31.49% in various localities. An exception in this scenario occurred in the Central region, where occurred underestimation of the maximum drought magnitudes reaching -45.26% in the locations 8 (Ponta Grossa), 12 (Fernandes Pinheiro), and 17 (Guarapuava). Analysing all scenarios simultaneously (historical and future), there is a general overestimation of the maximum drought severities in a great part of the Parana State.

Figure 11 presents the percentage difference between stationary and non-stationary approaches in the mean drought magnitude of both historical (HIST) and simulated (RCP 4.5 and RCP 8.5) series. In the historical series occurred an overestimation of the mean drought

magnitudes in the Parana area. The less significant difference in the mean drought magnitude occurred at the station 1 (Paranagua) with 5.04% variation, while the most significant occurred at the station 22 (Londrina) with 12.50% variation, both positive, indicating overestimation in the mean drought magnitudes. This means that by the traditional stationary analysis there is an overestimation of the mean drought magnitudes, evidencing more intense droughts than actually they are.

Figure 11 – Difference (%) between stationary and non-stationary approaches in the mean drought magnitude of the historical (HIST), and simulated (RCP 4.5 and RCP 8.5) series.

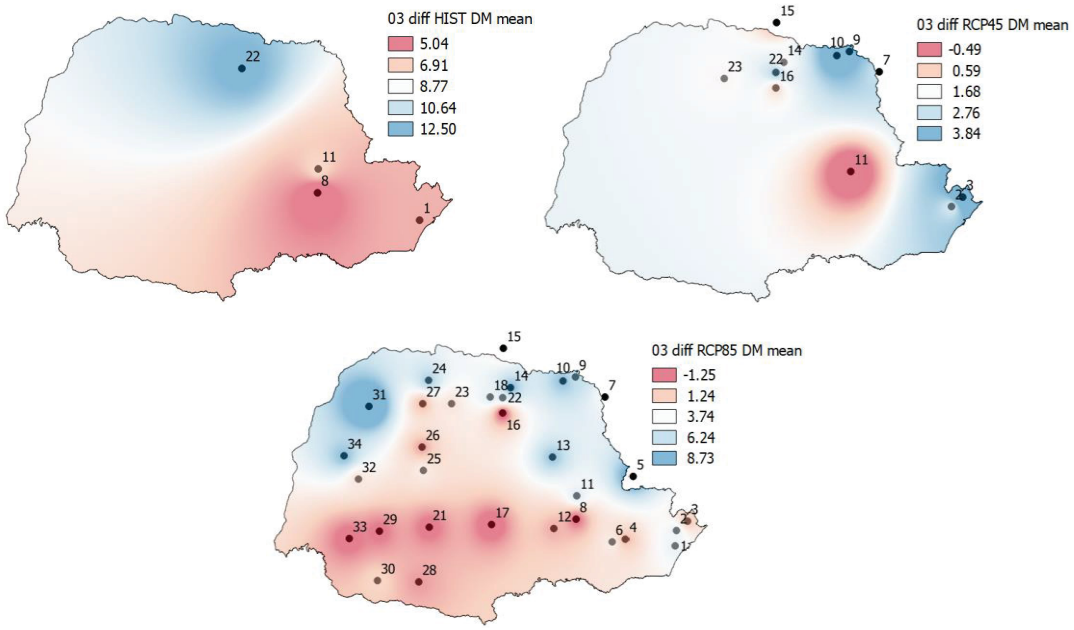

Font: Author.

In the RCP 4.5 scenario occurred a similar behaviour in the mean values than that observed in the historical series. The higher variations occurred in the North (reaching 3.84% difference in blue) and the lower variations in the Centre as presented by station 11 (Castro with -0.49%). In the RCP 8.5 scenario, a general overestimation occurred from Northwest to Northeast, represented by blue (8.73%) and light blue (6.24%). The underestimation occurred in the Central-South region, represented by red (-1.25%). The light red (-0.47%) present in the majority of Parana State represent a slight overestimation of the mean drought magnitude. Except the red regions, there is a general overestimation of the mean drought magnitude,

meaning the current drought analysis shows more intense droughts than actually they are. A white line clearly separates both regions (underestimation and overestimation).

Figure 12 presents the percentage difference between stationary and non-stationary approaches in the median drought magnitude of both historical (HIST) and simulated (RCP 4.5 and RCP 8.5) series. In the historical series occurred overestimation of the median drought magnitudes in the Central, North, and West Parana (in blue). A different behaviour (underestimation) occurred in the coastal region (East), reaching a -9.66% difference (in red) between stationary and non-stationary approaches. In the Southwest occurred a milder underestimation reaching -1.18% difference between both approaches.

Figure 12 – Difference (%) between stationary and non-stationary approaches in the median drought magnitude of the historical (HIST), and simulated (RCP 4.5 and RCP 8.5) series.

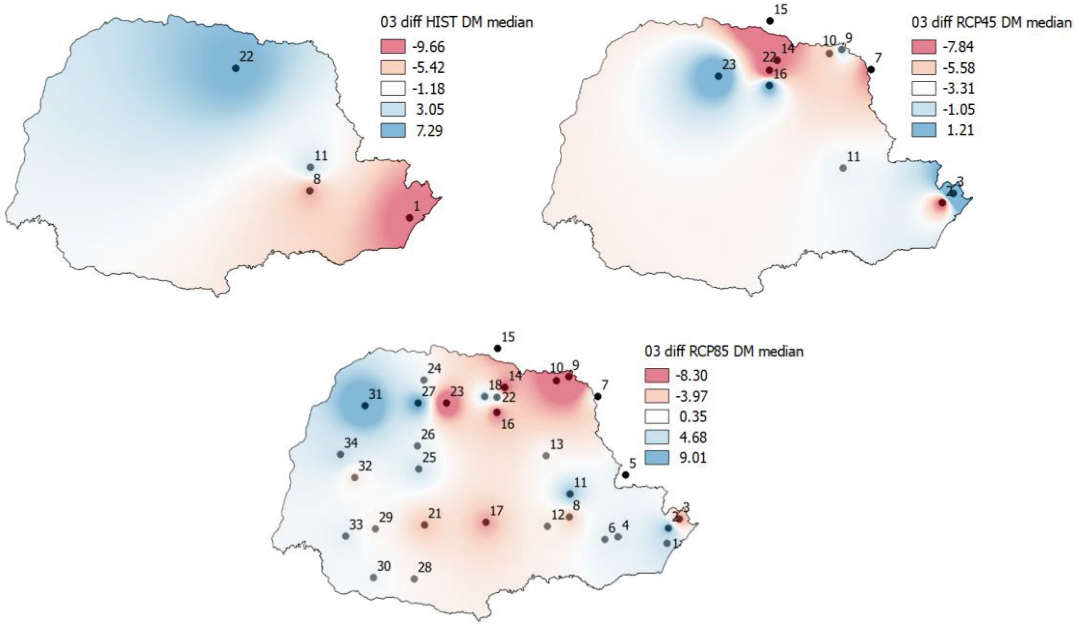

Font: Author.

In the RCP 4.5 scenario, stations 3 (Guaraquecaba), 16 (Maua da Serra) and 23 (Maringa) presented a slight overestimation in the median drought magnitudes. From light blue to red areas, there is underestimation of the mean drought magnitudes, reaching -7.84% difference at stations 14 (Ibipora), 15 (Bela Vista do Paraiso) and 22 (Londrina). Most part of Parana State presented underestimation of mean drought magnitudes.

In the RCP 8.5 scenario occurred underestimation of the median drought magnitude in most part of the Parana State, except for the Northwest, West and East, which presented overestimation. Some stations in the North reached -8.30% difference, while others in the Northwest reached 9.01%. The most significant differences in the median drought magnitudes are in the positive values (overestimation) at the stations 27 (Cianorte) and 31 (Umuarama). At the same time, important negative values (underestimation), were found in the stations 9 (Cambara), 10 (Bandeirantes), 14 (Ibipora), 16 (Maua da Serra), and 23 (Maringa).

Figure 13 – Difference (%) between stationary and non-stationary approaches in the minimum values of the historical (HIST), and simulated (RCP 4.5 and RCP 8.5) series.

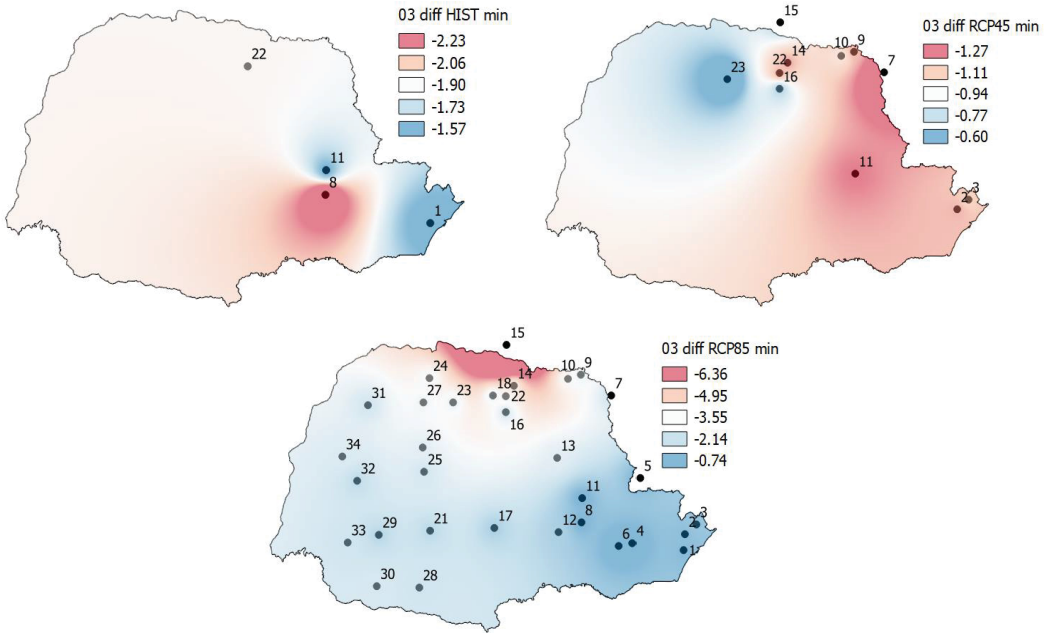

Font: Author.

Figure 13 presents the percentage difference between stationary and non-stationary approaches in the minimum values of both historical (HIST) and simulated (RCP 4.5 and RCP 8.5) series. According to it, in all scenarios (HIST, RCP 4.5 and RCP 8.5) occurred underestimation of the minimum values. This implies that applying the traditional stationary analysis shows drought intensities less severe, when compared to the non-stationary analysis. This fact also highlights the importance of considering the non-stationary analysis in regions where weather scientists affirm they are non-stationary. A drought analysis considering less

intense droughts when actually they are more intense, can fail in forecasting studies and a worse phenomenon can happen.

Figure 14 – Total number of drought events difference (%) between stationary and non-stationary approaches of the historical (HIST), and simulated (RCP 4.5 and RCP 8.5) series.

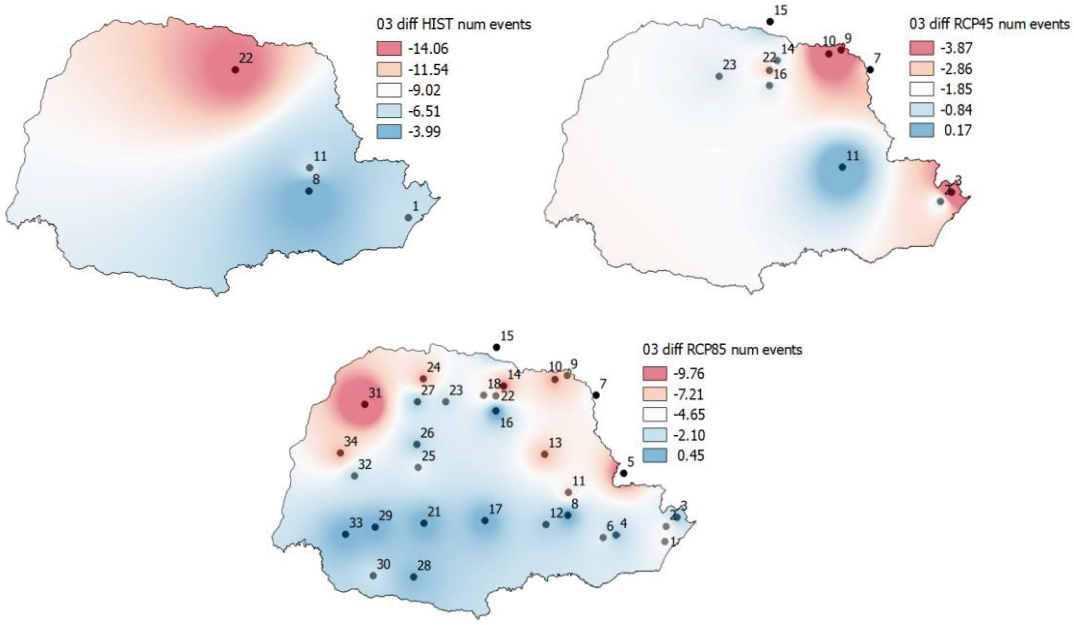

Font: Author.

In the historical scenario, the higher differences occurred around the station 8 (Ponta Grossa) with -2.23% difference in the minimum values. Smaller differences occurred at stations 1 (Paranagua) and 11 (Castro), with both reaching up to -1.57% difference. In the remaining Parana area occurred differences between -1.73% and -2.06%, coloured light blue to light red, respectively. The difference is concentrated in the white strip covering a transition area of the Parana and reaching -1.90% difference in the minimum values.

In the RCP 4.5 scenario, the difference in the minimum values are lower, when compared to the historical scenario. It varies from -0.60% to -1.27%, coloured in blue and red, respectively. The higher differences situate in the Northeast region, represented by stations 7 (Joaquim Tavora) and 11 (Castro), both in red. Lower variations occurred in the station 23 (Maringa) with -0.60%.

In the RCP 8.5 scenario, differences situate between -0.74% and -4.95% in almost the entire Parana area. An exception occurs in the North region, where the highest difference relates to station 15 (Bela Vista do Paraiso with -6.36% difference) and the neighbouring stations situate in the range between -3.55% (white) and -4.95% (light red).

Figure 14 presents the percentage difference of the total number of drought events between stationary and non-stationary approaches. Sometimes an event considered drought in the stationary analysis is flood in the non-stationary analysis and vice-versa. These differences highlight the importance in performing the non-stationary drought analysis, in regions, which present non-stationary behaviour.

In the historical series, the major differences (in absolute value) occurred in the station 22 (Londrina with -14.06% difference), while the lower in absolute value occurred in the station 8 (Ponta Grossa with 3.99% difference). The historical series presents higher differences in drought events in the Northwest, North and Northeast regions, when compared to the Centre, South and East regions. These differences show that the stationary analysis underestimates drought events, turning important to perform the non-stationary drought analysis. In the historical scenarios, there are only drought events underestimation.

In the RCP 4.5 scenario occurred the same pattern as observed in the historical scenario. Generally, negative differences were found in the RCP 4.5 scenario, meaning an underestimation of drought events when using the stationary approach. The maximum absolute differences were found in the Northeast and East regions (-3.87%), while the minimum differences were found at station 11 (Castro).

In the RCP 8.5 scenario, there is an underestimation in almost all Parana area, except in some stations in the South and Centre-South, which presented a slight overestimation of droughts (positive percentage difference, 0.45%). The underestimation/overestimation in drought events compares the percentage difference between stationary and non-stationary analyses. The negative signal represents the underestimation, while the positive signal the overestimation in the number of drought events, when compared the non-stationary to the stationary analysis. In the Northwest and Northeast regions, there are some sites, which presented higher underestimation of drought events (-9.76%). In almost all Parana area, differences in drought events are between -7.71% and -2.10%.

Figure 15 presents the percentage difference between stationary and non-stationary approaches in the number of times there are difference in droughts of both historical (HIST), and simulated (RCP 4.5 and RCP 8.5) series. In the historical scenario, higher differences relate to the stations 8 (Ponta Grossa) and 11 (Castro) with 57.14% and lower differences in the station 22 (Londrina) with 55.64%. It means that in Parana State, at least 50% difference occurred when adopting the stationary model.

Figure 15 – Difference (%) between stationary and non-stationary approaches in the number of times there are difference in droughts in the stationary and non-stationary approaches of the historical (HIST), and simulated (RCP 4.5 and RCP 8.5) series.

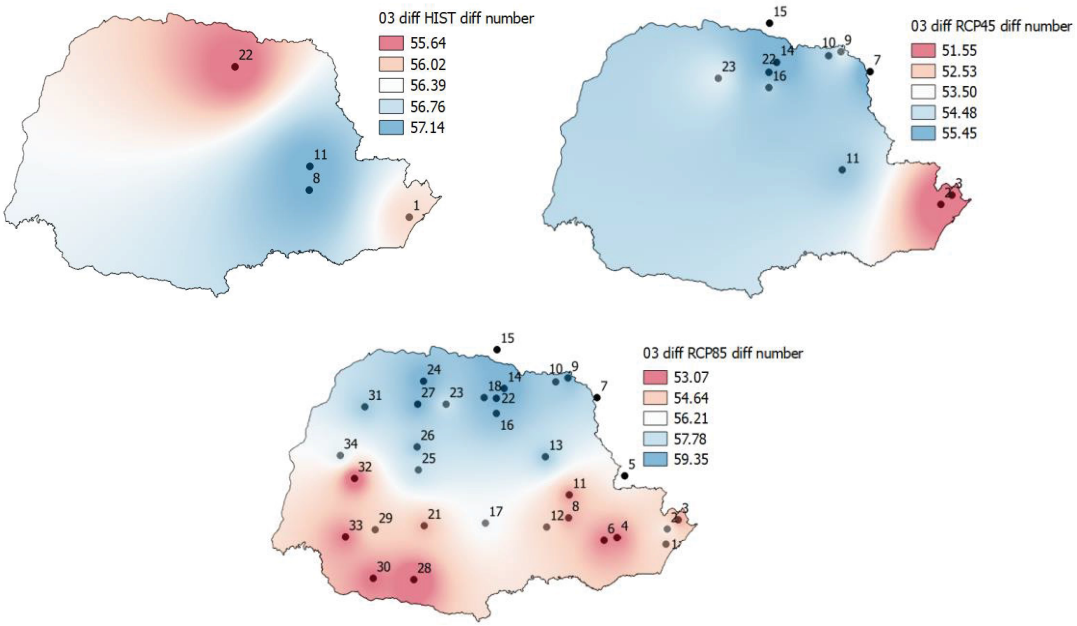

Font: Author.

In the RCP 4.5 scenario occurs a similar behaviour in the simulated series in terms of the minimum differences found between the two approaches. The lower differences occur at the coast (East) (red), increasing gradually to the West and North, where there are higher differences, as presented by stations 14 (Ibipora), 15 (Bela Vista do Paraiso) and 22 (Londrina) in blue.

In the RCP 8.5 scenario, the lower differences (red) occur in the Southwest, South and Southeast and they gradually increase toward the North (blue). There is a white strip splitting the Parana and showing that higher differences occur in the South, while smaller differences

occur in the North. Together the three scenarios (historical and both future) show an agreement between the drought characterization in both stationary and non-stationary approaches.

Figure 16 – Stationary versus non-stationary (split) RDI for the meteorological station 1 (Paranagua) and 12-month accumulation period.

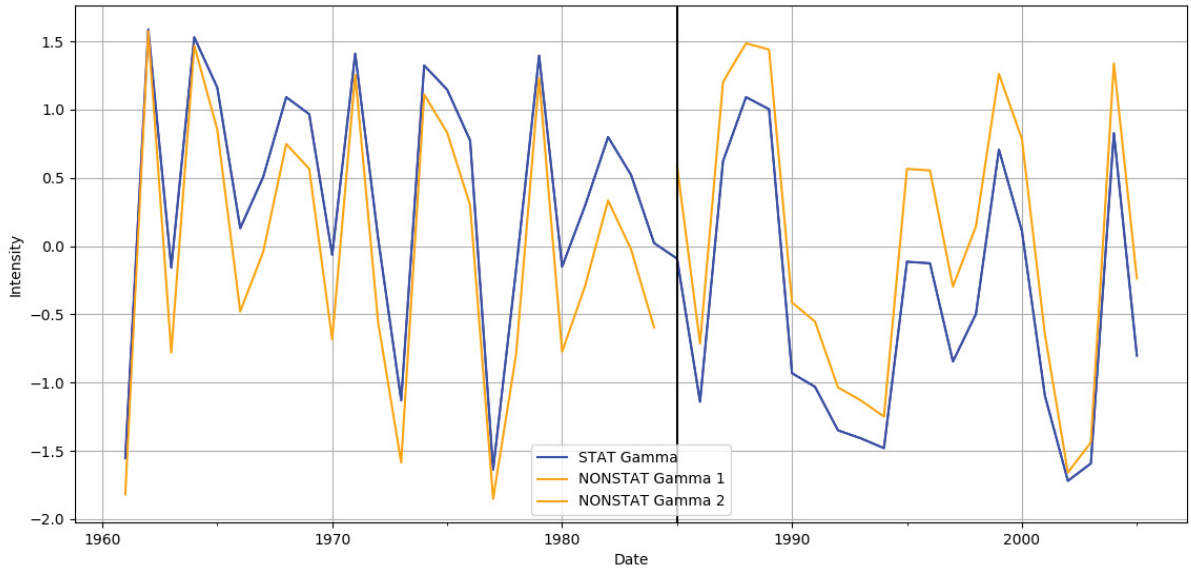

Font: Author.

Figure 17 – Stationary versus non-stationary (split) RDI for the meteorological station 8 (Ponta Grossa) and 12-month accumulation period.

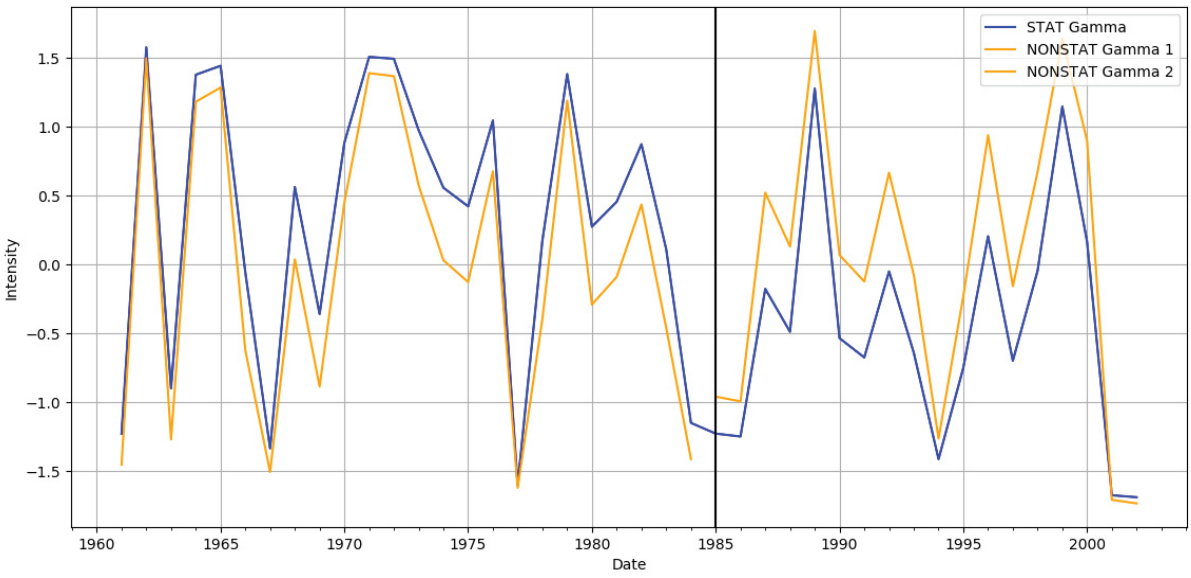

Font: Author.

Figure 18 – Stationary versus non-stationary (split) RDI for the meteorological station 11 (Castro) and 12-month accumulation period.

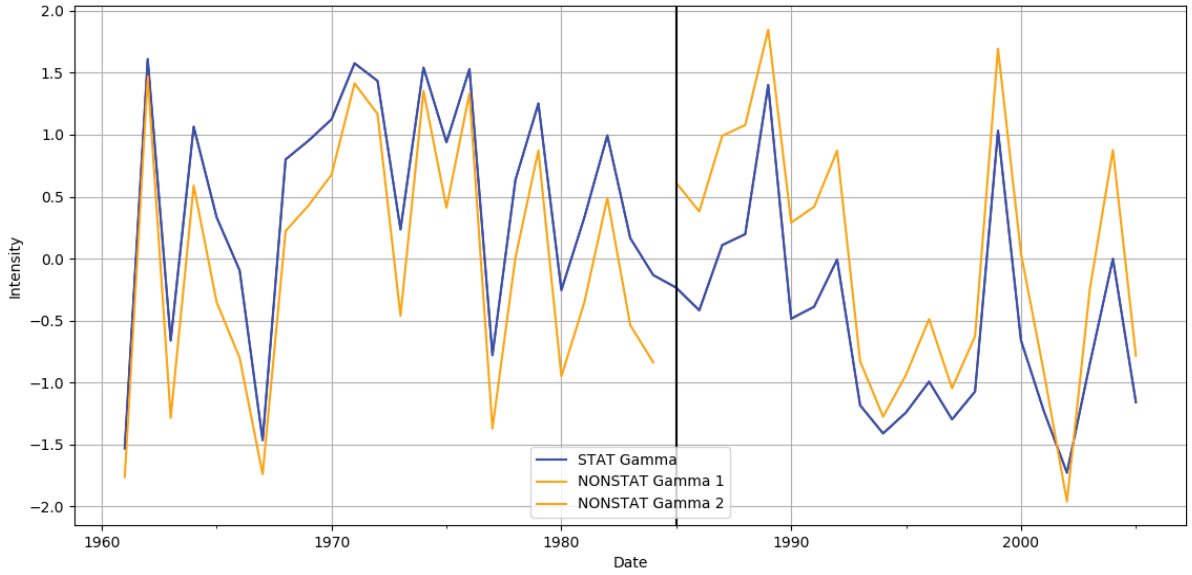

Font: Author.

Figure 19 – Stationary versus non-stationary (split) RDI for the meteorological station 22 (Londrina) and 12-month accumulation period.

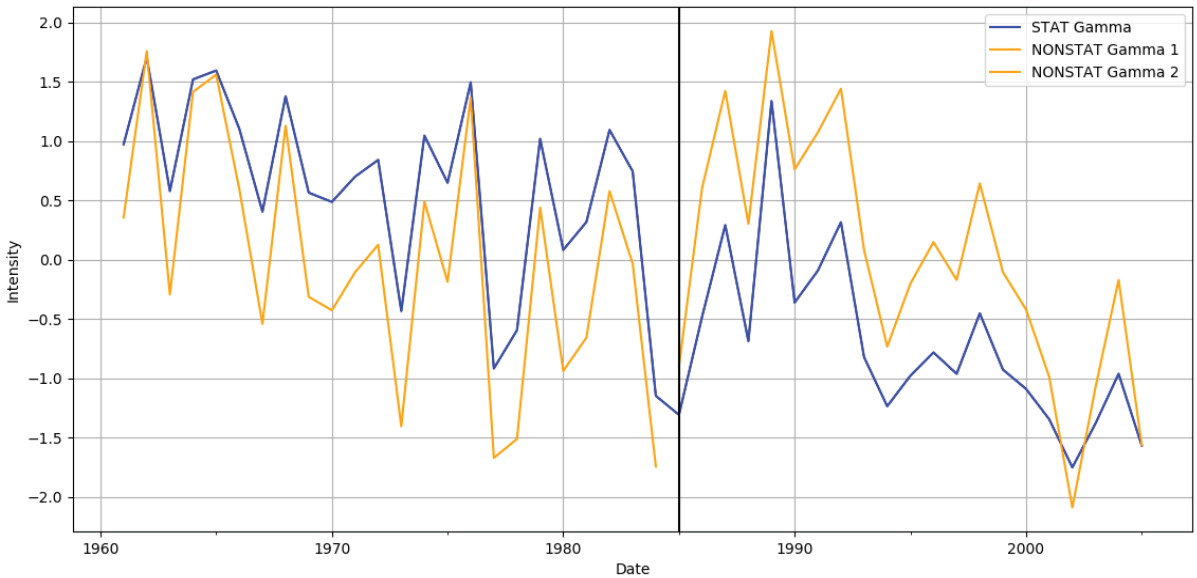

Font: Author.

ZARCH et al. (2015) recommend the RDI for application in climate change studies since the RDI incorporates the potential evapotranspiration and consequently, the temperature in its computation, returning a more realistic drought evaluation. There were performed RDI graphs showing the visual differences between stationary and non-stationary analyses.

Figure 16 represents the station 1 (Paranagua) RDI graph for the 12-month accumulation period. STAT Gamma means stationary approach and NONSTAT Gamma 1 and 2 mean non-stationary approach. According to Figure 16, there is a general underestimation of the non-stationary analysis for the first split. However, in the non-stationary analysis of the second split, there is a slight overestimation in comparison with the stationary analysis.

Figure 17 represents the station 8 (Ponta Grossa) RDI graph for the 12-month accumulation period. STAT Gamma means stationary approach and NONSTAT Gamma 1 and 2 mean non-stationary approach. According to Figure 17, there is a general underestimation of the non-stationary analysis for the first split. However, in the non-stationary analysis for the second split, there is a slight overestimation in comparison with the stationary analysis.

Figure 18 represents the station 11 (Castro) RDI graph for the 12-month accumulation period. There is a general underestimation of the non-stationary analysis for the first split. However, the non-stationary analysis in the second split presented a slight overestimation in comparison with the stationary analysis.

Figure 19 represents the station 22 (Londrina) RDI graph for the 12-month accumulation period. There is a general underestimation of the non-stationary analysis for the first split, but for the second split, there is a slight overestimation in comparison with the stationary analysis.

At the four stations presented in the graphs, it occurs the same behaviour when comparing the stationary and the non-stationary analyses, a general underestimation in the first split, while in the second split there is an overestimation of the non-stationary analysis.

4.6. Positive and negative times

Some differences between the stationary and non-stationary approaches resulted in positive, while others resulted in negative number of elements (NEL), i.e. number of times that indices presented positive or negative differences between the stationary and non-stationary

analysis in the 3-, 6- and 12-month accumulation periods. For this reason, these occurrences were computed in order to see a decreasing and/or increasing trend in most part of the statistics.

Table 17, Table 18 and Table 19 present the number of times that indices presented positive or negative differences, between stationary and non-stationary analyses in the 3-, 6- and 12-month accumulation period, respectively.

In the 3-month accumulation period (Table 17), there are 4 non-stationary stations (NEL) in the historical series and some differences in statistics resulted in positive NEL, i.e., they increased when using the non-stationary analysis, meaning the traditional stationary approach overestimates the drought statistics. The predominance in negative NEL indicates the underestimation of these statistics when the stationary approach is used.

Table 17 shows the stations that presented only positive NEL in the statistics. They are mean drought magnitude (diff mean), maximum drought magnitude (diff max), and maximum drought duration (diff max dur). They indicate the overestimation pattern if the stationary analysis is used. The entire negative (NEL equal 4) occurred in the minimum (diff min), severe drought occurrence frequency (diff FR15) and number of drought events (diff nev). The remained statistics presented both underestimation and overestimation pattern, when adopted the stationary approach.

Table 17 – Number of times (NEL) that indices presented positive or negative differences between the stationary and non-stationary analysis in the 3-month accumulation period.

	NEL	**4**		**NEL**	**11**		**NEL**	**32**
03 HIST	**(-)**	**(+)**	**03 RCP45**	**(-)**	**(+)**	**03 RCP85**	**(-)**	**(+)**
Diff mean	0	4	Diff mean	1	10	Diff mean	7	25
Diff med	2	2	Diff med	8	3	Diff med	14	18
Diff max	0	4	Diff max	3	8	Diff max	13	19
Diff FR0	2	2	Diff FR0	7	4	Diff FR0	15	17
Diff min	4	0	Diff min	11	0	Diff min	32	0
Diff FR10	2	2	Diff FR10	4	7	Diff FR10	5	27
Diff FR15	4	0	Diff FR15	6	5	Diff FR15	22	10
Diff max dur	0	4	Diff max dur	2	9	Diff max dur	7	25
Diff n. ev.	4	0	Diff n. ev.	9	2	Diff n. ev.	24	8

Font: Author.

In the future RCP 4.5 scenario, there are 11 stations under a non-stationary approach (NEL equal 11) and the most significant positive differences are in the mean drought magnitude (diff mean with 10), maximum drought duration (diff max dur with 9) and maximum drought magnitude (diff max with 8). The negative significant differences occurred in the minimum NEL (diff mean with 11) and number of drought events (diff nev with 9). Remaining differences presented both increase in some stations and decrease in others.

In the RCP 8.5 scenario, 32 stations presented non-stationary approach (NEL 32) and the most significant positive pattern occurred in the moderate drought occurrence frequency (diff FR10 with 27), mean drought magnitude (diff mean) and maximum drought duration (diff max dur), both with 25 events presenting positive differences. However, significant negative pattern was observed in the minimum NEL (diff min) where 32 of the 32 events presented lower minimum NEL. It means that adopting the stationary analysis, droughts can be less severe than actually are (minimum underestimation).

Table 18 presents the number of times that indices presented positive or negative differences between the stationary and non-stationary analysis in the 6-month accumulation period. In the historical period, there are more positive NEL (overestimation in relation to the stationary approach), in the maximum drought magnitude (diff max). However, more negative NEL occurred in the mild and moderate drought occurrence frequency (diff FR0 and diff FR10), respectively. There are only 3 stations in the historical series that presented non-stationarity in the RDI series (diff nev 3).

Table 18 – Number of times (NEL) that indices presented positive or negative differences between the stationary and non-stationary analysis in the 6-month accumulation period.

	NEL	**3**		**NEL**	**8**		**NEL**	**32**
06 HIST	**(-)**	**(+)**	**06 RCP45**	**(-)**	**(+)**	**06 RCP85**	**(-)**	**(+)**
Diff mean	2	1	Diff mean	1	7	Diff mean	7	25
Diff med	2	1	Diff med	3	5	Diff med	9	23
Diff max	0	3	Diff max	8	0	Diff max	25	7
Diff FR0	3	0	Diff FR0	6	2	Diff FR0	22	10
Diff min	1	2	Diff min	8	0	Diff min	32	0
Diff FR10	3	0	Diff FR10	1	7	Diff FR10	6	26
Diff FR15	1	2	Diff FR15	6	2	Diff FR15	13	19
Diff max dur	2	1	Diff max dur	1	7	Diff max dur	26	6
Diff n. ev.	1	2	Diff n. ev.	5	3	Diff n. ev.	24	8

Font: Author.

In the RCP 4.5 scenario, there are 8 stations that presented non-stationarity (NEL 8) and the most significant positive differences occurred in the mean drought magnitude (diff mean), moderate drought occurrence frequency (diff FR10) and maximum drought duration (diff max dur), with 7 stations presenting positive difference (overestimation increase in comparison to the stationary approach). However, the most significant negative differences were found in the maximum drought magnitude (diff max) and in the minimum NEL (diff min), both with 8 stations presenting negative differences.

In the RCP 8.5 scenario, the line (NEL 32) shows the number of stations who presented non-stationarity in the RDI series. The most significant positive differences occurred in the moderate drought occurrence frequency (diff FR10 with 26 times), mean drought magnitude (diff mean with 25 times) and median drought magnitude (diff med with 23 times). However, the most significant negative differences occurred in the RCP 8.5 scenario in the minimum NEL (diff min with 32 events), maximum drought duration (diff max dur with 26 events), and maximum drought magnitude (diff max with 25 events). Other statistics showed both positive and negative differences.

Table 19 – Number of times (NEL) that indices presented positive or negative differences between the stationary and non-stationary analysis in the 12-month accumulation period.

	NEL	**33**
12 RCP85	**(-)**	**(+)**
Diff mean	7	26
Diff med	7	26
Diff max	24	9
Diff FR0	12	21
Diff min	9	24
Diff FR10	25	8
Diff FR15	21	12
Diff max dur	4	29
Diff n. ev.	25	8

Font: Author.

Table 19 present the number of times that indices presented positive or negative differences between the stationary and non-stationary analysis in the 12-month accumulation period. Only the RCP 8.5 scenario presented 33 stations (NEL 33) with non-stationary pattern

in the 12-month accumulation period. In both historical and RCP 4.5 scenarios, all 34 stations presented stationarity in the 12-month accumulation period. The most significant positive statistics are the maximum drought duration (diff max dur with 29 events), mean and median drought magnitudes (diff mean and diff med, both with 26 events). However, the most significant negative statistics are moderate drought occurrence frequency (diff FR10 with 25 events), number of drought events (diff nev also with 25 events) and maximum drought magnitude (diff max with 24 events). Positive NEL indicate statistics increase when adopting the stationary approach, while negative NEL indicate decrease. In other words, overestimation and underestimation, respectively. Other statistics remained both positive and negative in all stations.

4.7. Moving window

The previous sections highlighted the non-stationary stations and then, the comparison of the non-stationary approach with the stationary approach, was performed. In order to verify the parameters temporal evolution, the next drought evaluation is the moving window analysis.

Figure 20 – Shape parameter $(\alpha(t))$ in the 30-period moving window analysis of the RDI station 11 (Castro) and 6-month accumulation period.

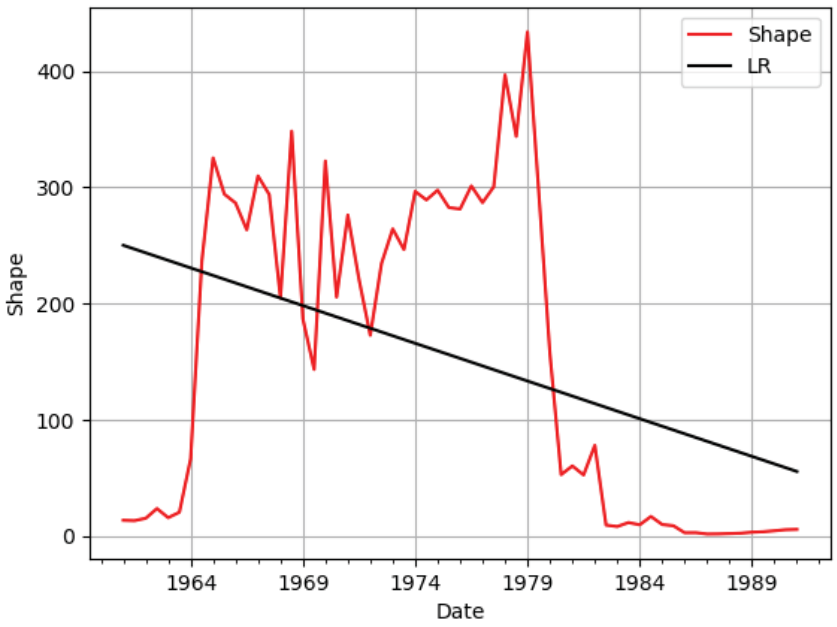

Font: Author.

LI et al. (2019) applied the 30-year moving window in the series of both maximum annual rainfall intensity and rainfall volume and fitted the time-dependent marginal distribution Generalized Extreme Value (GEV) for both variables. CHENG & AGHAKOUCHAK (2014) suggest the application of non-stationary frequency analysis in hydrological data (rainfall), varying in time and maintaining the other parameters stationary. Meanwhile, other authors YILMAZ & PERERA (2014) applied statistical and graphical tests to verify whether these trends correspond to the series non-stationarity.

Figure 21 – Location parameter (loc) in the 30-period moving window analysis of the RDI station 11 (Castro) and 6-month accumulation period.

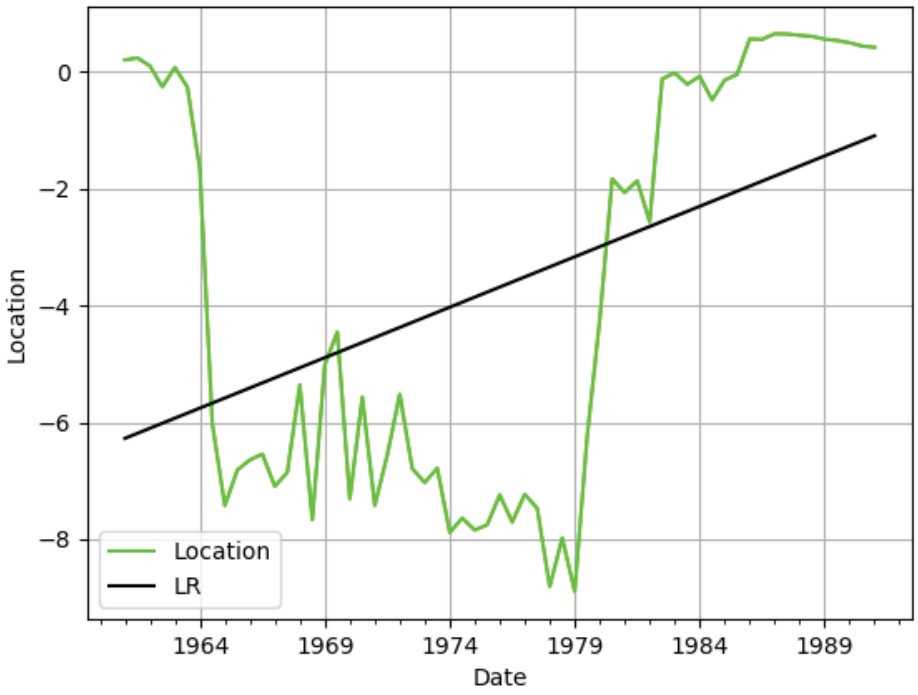

Font: Author.

According to KHADR (2016), it is necessary to fill in the gaps before applying the SPI and use a 30-year series as the minimum length for drought studies. The authors MCKEE et al. (1993) suggested the maximum likelihood method to estimate the parameters of the gamma distribution. This dissertation follows the same method that LI et al. (2019) applied, using the gamma distribution instead of the GEV for the drought series in order to verify the temporal

parameters evolution. Hence, the computation of the 30-period moving window analysis occurred in the non-stationary scenarios, pointed by results of the Mann-Kendall and/or Pettitt tests, in the subsection 4.4.

Among the 26 stations/accumulation periods analysed, the parameters evolution of the RDI at the station 11 (Castro) in the 6-month accumulation period was selected. The RDI presented well the drought phenomenon in the region in the previous analyses, as shown in the Figure 16, Figure 17, Figure 18 and Figure 19.

Figure 22 – Scale parameter $(\beta(t))$ in the 30-period moving window analysis of the RDI station 11 (Castro) and 6-month accumulation period.

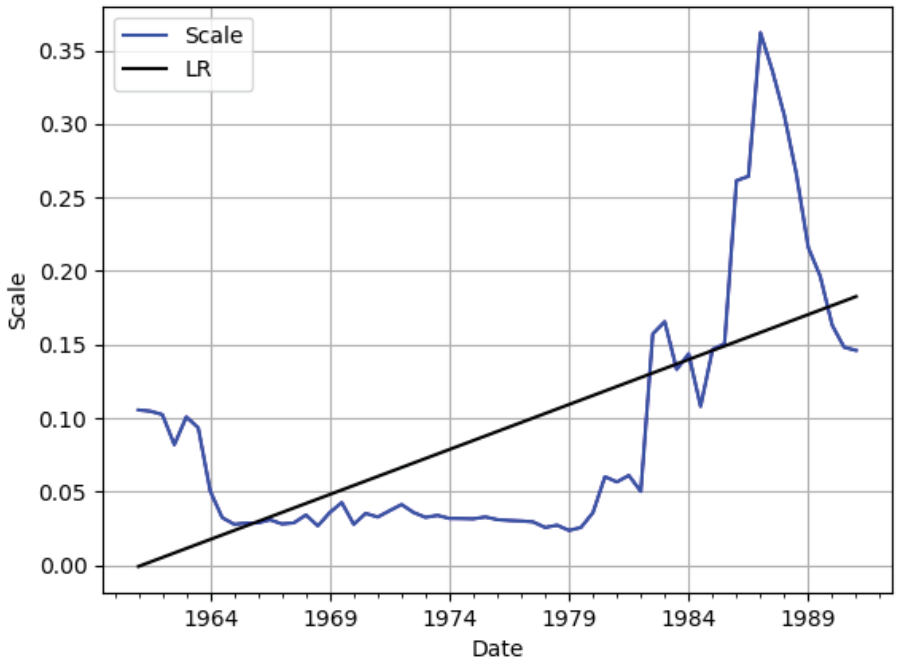

Font: Author.

Figure 20 illustrates the shape parameter $(\alpha(t))$ evolution in the 30-period moving window analysis of the RDI station 11 (Castro) in the 6-month accumulation period. Results show an abrupt increase of the shape parameter in 1964, maintaining oscillations until 1979 and an abrupt decrease until the end of the series. In 1969, there is an abrupt decrease followed by an abrupt increase in the shape parameter. This also may be a random variation of the parameter. Results also show in the mean a decrease in the shape parameter along time (SLR line analysis).

Figure 21 illustrates the location parameter (loc) evolution in the 30-period moving window analysis of the RDI at station 11 (Castro) and 6-month accumulation period. Results showed an abrupt decrease of the location parameter in 1964, followed by oscillations until 1979. In this year, the location parameter suffered an abrupt increase and followed increasing until 1979. In the year 1969, it happened a more pronounced variation in the location parameter. After the peak of 1987, it decreases again until the end of the series (1992). Results also showed on average an increase in the location parameter along time (SLR line analysis).

Figure 22 illustrates the scale parameter ($\beta(t)$) evolution in the 30-period moving window analysis of the RDI at station 11 (Castro) in the 6-month accumulation period. Results showed small oscillations of the scale parameter from 1964 to 1979, where it started to increase abruptly until 1987 and then decreased until the end of the series. Results also show an average increase in the location parameter along time (SLR line analysis).

Figure 23 – Minimum values in the 30-period moving window analysis of the RDI station 11 (Castro) and 6-month accumulation period.

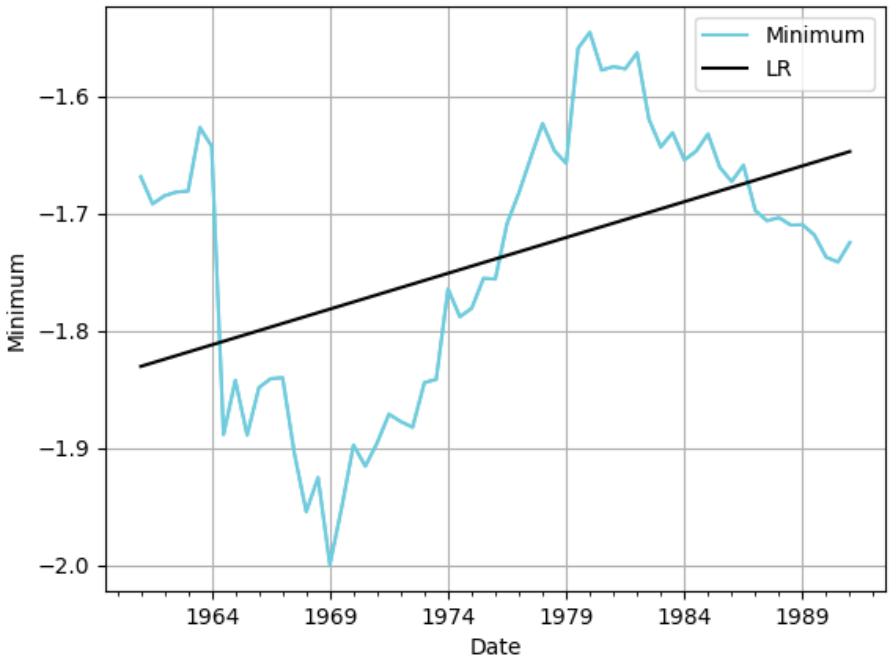

Font: Author.

Figure 23 illustrates the minimum values evolution in the 30-period moving window analysis of the RDI at station 11 (Castro) and 6-month accumulation period. Results showed an

abrupt decrease of the minimum values in 1964, followed by oscillations until 1973. After this year, the minimum values suffered a gradual increase until 1980, followed by an also gradual decrease until the end of the series. All the period 1964-1971 presents smooth decreasing oscillations probably of random nature. Results also showed an average increase in the minimum values along time (SLR line analysis), meaning that drought severities tend to intensify in the end of the historical series.

In the 30-period moving window analysis, the parameter temporal variation presented a decrease in the shape parameter only. Both location and scale parameters, including also the minimum values suffered an increase along most of the time. This increase is concentrated over relatively short period. The increasing trend in the minimum values highlighted the importance of performing the non-stationary drought analysis using the climate change scenarios, projected by the RCM ETA. It is important to highlight that in this section, the linear regression computation occurred just to show the parameters temporal evolution in the historical series.

4.8. Chapter summary

In this chapter, all results obtained in the applied methods were presented. The linear regression methods used for filling in the gaps in the meteorological series, performed well with a determination coefficient higher than 0.64 in both precipitation and temperature series.

At the same time, the algorithm applied the bias correction methods: Linear Scaling (LS), Power Transformation (PT), Variance Scaling (VARI) and Empirical Quantile Mapping (EQM). The best method to correct the RCM ETA simulations, for the temperature series is the Empirical Quantile Mapping (EQM), while the best method for the historical precipitation series is the Linear Scaling (LS).

Hence, the algorithm computed the Reconnaissance Drought Index (RDI), using the Thornthwaite method to compute the potential evapotranspiration (PET). The RDI computation occurred in the 3-, 6-, 12-, 24-, 36-, 48-, and 60-month accumulation periods.

It was necessary to test the original precipitation and temperature series for trend and/or changing point to verify the stationarity/non-stationarity in the series and for the accumulated series of the drought indices. When the historical monthly series presented trend and/or changing point in the accumulation period, the algorithm split the series in the given changing

point. Then, it computed the drought indices again fitting two gamma probability distributions: one from the beginning until the changing point and other from the changing point until the end of the drought series.

Therefore, an analysis was necessary to perform the drought indices statistics due to the minimum values of the drought indices. This analysis led to a better evaluation of the minimum values and showed a different behaviour before and after the split. Overestimation or underestimation of the minimum values, depending on each case, was observed.

Some statistics presented droughts overestimation and/or underestimation along the future in both future scenarios. The most significant statistics differences occurred in the maximum drought magnitude, drought duration and number of drought events.

The algorithm computed the number of differences between the stationary and the non-stationary approaches, as well as differences between the occurrence frequencies for the given thresholds. The computation or the main statistics of the drought analysis (duration, severity and magnitude), was performed. The mean, median and maximum drought magnitude, were computed. Results pointed a general underestimation of the maximum drought magnitude in the stations 1 (Paranagua), 11 (Castro) and 22 (Londrina). It means that the stationary approach underestimates the magnitude of droughts. The same behaviour (drought underestimation) occurred in the minimum values, meaning that the traditional stationary approach underestimates droughts.

Finally, the 30-period moving window analysis evaluated the parameter temporal variation. Results of the shape parameter showed a decreasing trend, while both scale and location parameters presented a slight increasing trend, according to a linear regression line fitted to the data. The minimum values presented an increasing trend, leading to the conclusion that droughts tend to intensify in the end of the series, evidencing the importance in performing drought analysis in climate change scenarios.

5. DROUGHT ANALYSIS

This chapter presents the drought analysis applying the methods of this dissertation. Part of the drought analysis is the evaluation of the drought indices statistics, mixing the stationary approach for stationary stations and the non-stationary approach for non-stationary stations. There are 34 stations and three scenarios (historical, RCP 4.5 and RCP 8.5), returning a large amount of data.

5.1. Analysing stations separately

In a first analysis, the stations were analysed separately. The stations that presented non-stationarity in the historical series, are the stations 1 (Paranagua), 8 (Ponta Grossa), 11 (Castro) and 22 (Londrina). WU et al. (2018) propose a drought classification related to the accumulation periods. The 3-month refers to a short-term drought, while the 6-month refers to a mid-term drought. The most common drought analysis occurs in the 12-month accumulation period and it relates to a long-term drought. Thus, the 3-, 6-, and 12-month accumulation periods are analysed in this subchapter to evaluate short-, mid- and long-term droughts.

5.1.1. Station 1 (Paranagua)

Figure 24 presents both historical (HIST) and future simulated (RCP 4.5 and RCP 8.5) RDI series of the station 1 accumulated in 3, 6, and 12 months, respectively. In the 3-month accumulation period (first graph named severity 3), there are several periods of moderate to severe droughts (from -1.0 to -2.0) in both historical series (blue line) and future series (RCP 4.5 and RCP 8.5).

The major droughts seem to have their peaks around 1973, 1977, 1982, 1994 in the historical scenario. The major droughts in the future series (2024 and 2084) occur in the same period in both RCP 4.5 and RCP 8.5 scenarios. These drought events were confirmed analysing both scenarios severity 6 and severity 12, corresponding to the 6- and 12-month accumulation periods (second and third graphs, respectively).

Figure 24 – Historical (HIST) and future simulated (RCP 4.5 and RCP 8.5) RDI series of the station 1 accumulated in 3, 6, and 12 months, respectively.

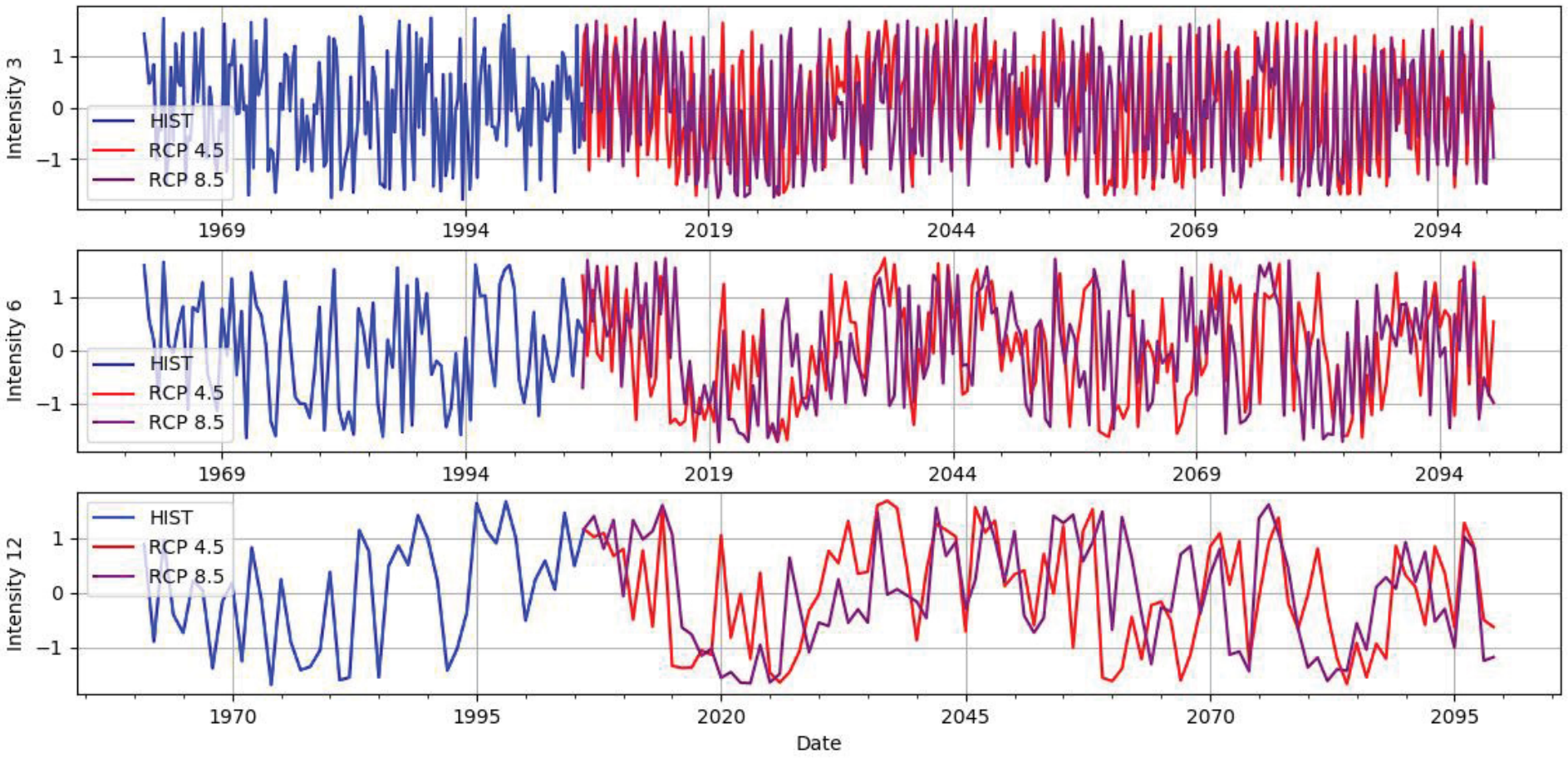

Font: Author.

Differences in moderate to severe droughts occur analysing the RCP 4.5 and the RCP 8.5 separately. Looking at the 12-month accumulation period (third graph), the RCP 4.5 scenario (red line) presented lower than -1.0 values in 2059 and 2067, while the RCP 8.5 scenario (purple line) presented drought in 2072. There is a delay in the red line when compared to the purple line between 2080 and 2085, meaning that moderate to severe droughts start before in the RCP 8.5 scenario, when compared to the RCP 4.5 scenario. Both future scenarios presented a general cycle of droughts and wet periods (positive values).

Table 20, Table 21 and Table 22 present the main drought statistics of both historical (HIST) and future simulated (RCP 4.5 and RCP 8.5) series of the station 1 accumulated in 3-, 6- and 12-months, respectively. Table 20 (3-month) presents the differences (%) between historical and RCP 4.5 scenarios (diff % 1/2) and the highest difference occurred in drought duration (duration with 100.00%), maximum drought magnitude (max DM with 76.09%) and severe drought occurrence frequency (FR15 with -55.07%). The positive signal indicates the drought statistics are lower in the historical period, when compared to the future scenario. General differences situate lower/equal 25% (positive), as mean drought magnitude (mean DM); meaning in the future scenario it may occur more severe droughts when compared to the historical period. The relative number of drought events difference (rel num D with -16.96%) means that in the future RCP 4.5 scenario may have a decrease in quantity of drought events, when compared to the historical scenario.

Table 20 – Drought statistics of the historical (HIST) and future simulated (RCP 4.5 and RCP 8.5) series of the station 1 accumulated in 3 months.

3	**1**	**2**	**3**		
Station 1	**HIST**	**RCP45**	**RCP85**	**diff % 1/2**	**diff % 1/3**
mean DM	-4.69	-5.82	-5.31	24.15	13.29
med DM	-4.58	-5.15	-4.43	12.50	-3.40
max DM	-16.54	-29.13	-25.69	76.09	55.31
FR0	51.97	48.77	49.26	-6.17	-5.23
min	-1.78	-1.71	-1.75	-3.99	-1.80
FR10	19.29	20.67	19.84	7.18	2.89
FR15	8.55	3.84	6.93	-55.07	-18.95
duration	5.00	10.00	7.00	100.00	40.00
rel num D %	0.27	0.23	0.24	-16.96	-11.09

Font: Author.

Still in the Table 20, the major difference between historical and RCP 8.5 scenarios (diff % 1/3) are lower than (55.31%) in the maximum drought magnitude (max DM); meaning that in the RCP 8.5 scenario may occur more severe droughts, when compared to the historical scenario. Five statistics resulted in a negative difference, meaning that the future simulated RCP 8.5 scenario produced milder droughts, when compared to the historical scenario. According to these statistics (med DM, FR0, min, FR15, and rel num D), droughts may turn milder along the twenty-first century.

In the Table 21 (6-month), there are similarities in the percentages among differences between historical and RCP 4.5 scenario (diff % 1/2) and between historical and RCP 8.5 scenario (diff % 1/3), i.e. they slightly differ from each other. Exceptions were found in the FR15, duration and max DM, where there are significant differences between them.

Table 21 – Drought statistics of the historical (HIST) and future simulated (RCP 4.5 and RCP 8.5) series of the station 1 accumulated in 6 months.

6	**1**	**2**	**3**		
Station 1	**HIST**	**RCP45**	**RCP85**	**diff % 1/2**	**diff % 1/3**
mean DM	-10.13	-10.92	-10.29	7.80	1.60
med DM	-7.87	-6.00	-6.67	-23.82	-15.31
max DM	-32.04	-72.25	-57.15	125.53	78.38
FR0	49.85	51.08	49.22	2.47	-1.28
min	-1.65	-1.72	-1.72	4.54	4.74
FR10	24.36	21.69	21.88	-10.96	-10.19
FR15	7.88	6.06	6.72	-23.09	-14.74
duration	7.00	10.00	9.00	42.86	28.57
rel num D %	0.26	0.24	0.25	-6.34	-2.17

Font: Author.

The highest differences found between historical and RCP 4.5 scenario are maximum drought magnitude (max DM equal to 125.53%) and drought events duration (duration with 42.86%). These two statistics reveal that in the future simulated RCP 4.5 scenario, droughts may become more severe when compared to the historical period in terms of magnitude (severity) and duration (more extended).

Comparing the differences between both historical and RCP 8.5 series (diff % 1/3), the major differences occurred in maximum drought magnitude (max DM with 78.38%) and drought duration (duration with 28.57%). This means that droughts may become more severe

along the twenty-first century, analysing the 6-month accumulation period and the RCP 8.5 scenario. It may also have more extended droughts in months.

In the Table 22 (12-month), the highest differences between the historical and RCP 4.5 scenario (diff % 1/2) are in drought duration (duration with 175%) and maximum drought magnitude (max DM with 115.82%). These two statistics (duration and max DM) mean that droughts may become more severe and extended in the future (up to 2100). Other statistics indicate a slight drought increase or decrease in the future scenario.

Table 22 – Drought statistics of the historical (HIST) and future simulated (RCP 4.5 and RCP 8.5) series of the station 1 accumulated in 12 months.

12	1	2	3		
Station 1	**HIST**	**RCP45**	**RCP85**	**diff % 1/2**	**diff % 1/3**
mean DM	-23.32	-29.18	-32.95	25.10	41.27
med DM	-18.59	-10.70	-19.37	-42.44	4.17
max DM	-56.74	-122.45	-168.23	115.82	196.51
FR0	42.93	50.64	51.94	17.95	20.98
min	-1.69	-1.68	-1.66	-0.74	-1.56
FR10	23.09	19.50	23.25	-15.54	0.68
FR15	8.37	6.54	6.16	-21.79	-26.34
duration	4.00	11.00	11.00	175.00	175.00
rel num D %	0.22	0.18	0.16	-18.62	-28.19

Font: Author.

Meanwhile, analysing the differences between historical and RCP 8.5 scenario (diff % 1/3), the highest differences occurred in maximum drought magnitude (max DM with 196.51%), drought duration (175%) and mean drought magnitude (mean DM with 41.27%). These three statistics (max DM, duration and mean DM) presented an increase of drought severity along the future (up to 2100). They may become more severe and extended in damages to population. The relative number of drought events (rel num D with -28.19%) presented a significant decrease in the future RCP 8.5 scenario, when compared to the historical scenario, meaning less quantity of drought events.

5.1.2. Station 8 (Ponta Grossa)

Figure 25 presents both historical (HIST) and future simulated (RCP 4.5 and RCP 8.5) RDI series of the station 8 accumulated in 3, 6, and 12 months, respectively. There is a lack between the end of the historical series and the beginning of both simulated series. It happened because there is no data between January 2003 and December 2005.

Analysing all images simultaneously (3-, 6- and 12-month), there is a significant drought peak between 1966 and 1968 and other valleys in 1977, 1982 and 1985. The station 8 did not present so much severe droughts, except for these valleys. The images represent droughts evolution along time.

Both simulated series presented a similar cycle pattern mainly until 2045 and the most significant drought occurred between 2020 and 2025 in the RCP 8.5 scenario and between 2015 to 2020 and 2025 to 2029 in the RCP 4.5 scenario. Around 2058 and 2070, there are droughts pointed by both scenarios, and the most severe for the RCP 4.5 scenario occurred in 1968, 1971, and 2067. The RCP 8.5 presented a severe drought in the period 2080 and 2083, and the RCP 4.5 a slight delay in 2084, when compared to the RCP 8.5 scenario.

Table 23, Table 24 and Table 25 present the drought statistics of both historical (HIST) and future simulated (RCP 4.5 and RCP 8.5) series of station 8 accumulated in 3-, 6- and 12-months, respectively.

Table 23 presents differences between historical and simulated scenarios in the two last columns. The highest differences are maximum drought magnitude (max DM with 68.34%) and drought duration (62.50%). The positive signal indicates an overestimation of these statistics in the future scenario, when compared to the historical series. However, the relative number of drought events (rel num D with -11.68%) presented a decrease in the RCP 4.5 future scenario, when compared to the historical series, meaning in the future may have less quantity of drought events. The other statistics differed less than 11% (moderate drought occurrence frequency, FR10).

Figure 25 – Historical (HIST) and future simulated (RCP 4.5 and RCP 8.5) RDI series of the station 8 accumulated in 3, 6, and 12 months, respectively.

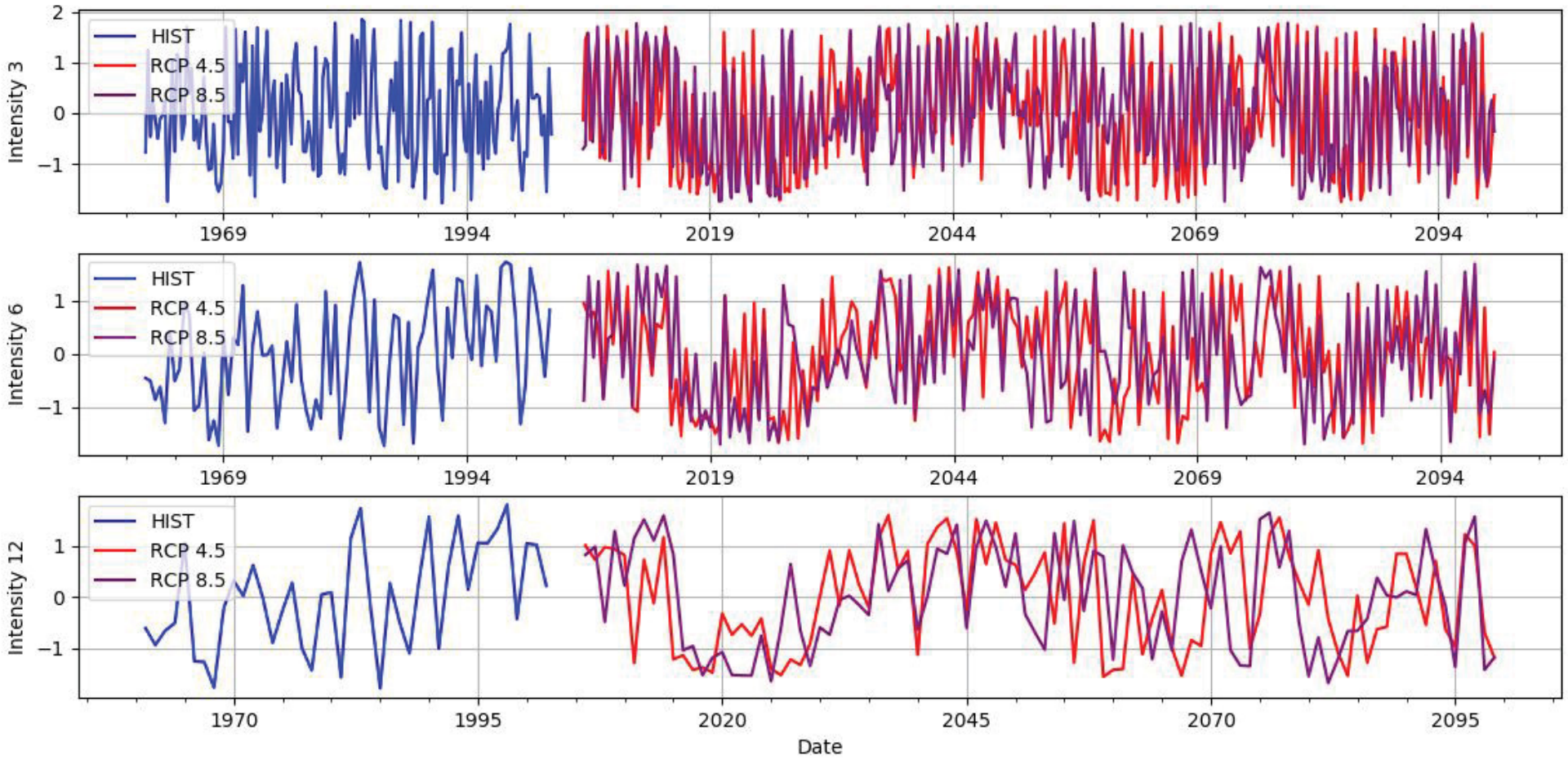

Font: Author.

The last column comprises the differences between historical and RCP 8.5 series (diff % 1/3), and the highest differences are median drought magnitude (med DM with 16.02%) and moderate drought occurrence frequency (FR10, droughts lower than -1.5 threshold with 13.16%). General differences are below 12.50% in absolute value, as occurred in drought duration (duration with -12.50%), meaning in the RCP 8.5 scenario may have milder droughts in terms of duration, when compared to the historical scenario. The RCP 8.5 presented milder variations in relation to the historical scenario, analysing the remaining statistics difference.

Table 23 – Drought statistics of the historical (HIST) and future simulated (RCP 4.5 and RCP 8.5) series of the station 8 accumulated in 3 months.

3	1	2	3		
Station 8	**HIST**	**RCP45**	**RCP85**	**diff % 1/2**	**diff % 1/3**
mean DM	-5.00	-5.57	-5.61	11.30	12.14
med DM	-3.99	-3.95	-4.63	-0.98	16.02
max DM	-24.15	-40.66	-24.99	68.34	3.48
FR0	54.04	50.32	51.12	-6.89	-5.42
min	-1.78	-1.76	-1.75	-1.24	-1.45
FR10	18.03	19.98	20.41	10.78	13.16
FR15	5.78	5.88	6.51	1.61	12.47
duration	8.00	13.00	7.00	62.50	-12.50
rel num D %	0.26	0.23	0.23	-11.68	-10.64

Font: Author.

Table 24 presents the drought statistics of both historical (HIST) and future simulated (RCP 4.5 and RCP 8.5) series of the station 8 accumulated in 6 months. The two last columns present the main drought statistics differences: (1) diff % ½ comprises the difference between historical and RCP 4.5 series and (2) diff % 1/3 comprises the difference between historical and RCP 8.5 series. The highest differences found in (1) are maximum drought magnitude (max DM with 75.48%) and drought duration (duration with 40.00%). Higher differences in these statistics (positive signal) indicate there are more severe droughts in the future series (RCP 4.5), when compared to the historical series. Other statistics indicate lower than 33.66% variation in absolute value (median drought magnitude, med DM). Negative signal variations indicate there is a decrease in the statistics from the past period, to the future period, indicating less severe drought scenario in the future.

In the RCP 8.5 scenario (last column, diff % 1/3), the highest differences are drought duration (duration with 80.00%) and maximum drought magnitude (max DM with 67.89%), meaning that magnitude and duration of droughts may become more severe in the future. Other statistics are lower than 24% in absolute value.

Table 24 – Drought statistics of the historical (HIST) and future simulated (RCP 4.5 and RCP 8.5) series of the station 8 accumulated in 6 months.

6 Station 8	1 HIST	2 RCP45	3 RCP85	diff % 1/2	diff % 1/3
mean DM	-9.45	-8.84	-9.34	-6.45	-1.21
med DM	-8.01	-5.32	-6.13	-33.66	-23.57
max DM	-30.44	-53.42	-51.11	75.48	67.89
FR0	49.90	49.16	51.99	-1.48	4.19
min	-1.73	-1.69	-1.71	-2.53	-1.37
FR10	20.45	22.26	19.85	8.88	-2.92
FR15	6.81	7.84	5.53	15.16	-18.82
duration	5.00	7.00	9.00	40.00	80.00
rel num D %	0.27	0.29	0.28	6.85	1.02

Font: Author.

Table 25 presents the drought statistics of both historical (HIST) and future simulated (RCP 4.5 and RCP 8.5) series of the station 8 accumulated in 12 months (annual scale and long-term drought) (WU et al., 2018). The main drought statistics differences computed between the historical scenario and both future scenarios are in the last columns (diff % 1/2, comprising differences between historical and RCP 4.5 scenario, and diff % 1/3 comprising differences between historical and RCP 8.5 scenario).

There are higher differences in the main statistics in this accumulation period, when compared to the previous (3-month in Table 23 and 6-month in Table 24). All statistics presented more variations in this accumulation period. In the annual scale (Table 25), the higher differences are drought duration (duration with 275%) and maximum drought magnitude (max DM with 250.02%). This means an intensification of the main drought statistics in the future series (RCP 4.5 scenario) and an intensification in the annual scale, when compared to the quarter and semester accumulation periods (Table 23 and Table 24, respectively). The severe drought occurrence frequency (FR15 with -63.76%) also presented significant variation between historical and RCP 4.5 scenarios. This statistic analysis means a decrease in the severe

drought occurrence frequency in the RCP 4.5 future scenario, when compared to the historical scenario.

Table 25 – Drought statistics of the historical (HIST) and future simulated (RCP 4.5 and RCP 8.5) series of the station 8 accumulated in 12 months.

12 Station 8	1 HIST	2 RCP45	3 RCP85	diff % 1/2	diff % 1/3
mean DM	-23.29	-26.72	-28.88	14.71	23.99
med DM	-19.29	-15.56	-14.75	-19.30	-23.50
max DM	-54.38	-190.34	-161.52	250.02	197.03
FR0	47.45	49.34	49.85	3.98	5.05
min	-1.79	-1.57	-1.69	-12.59	-5.85
FR10	19.24	24.15	23.66	25.51	22.96
FR15	12.29	4.45	7.69	-63.76	-37.42
duration	4.00	15.00	11.00	275.00	175.00
rel num D %	0.21	0.20	0.18	-5.67	-15.60

Font: Author.

Analysing the last column (diff % 1/3), the highest differences between the historical and the RCP 8.5 scenario are maximum drought magnitude (max DM with 197.03%) and drought duration (duration with 175.00%). These two main statistics presented an intensification of the drought events along the future. Other statistics presented absolute values lower than 37.42% (FR15, occurrence frequency of severe droughts).

5.1.3. Station 11 (Castro)

Figure 26 presents both historical (HIST) and future simulated (RCP 4.5 and RCP 8.5) RDI series of the station 11 accumulated in 3, 6, and 12 months, respectively. From the 3-month to the 12-month accumulation period analysis, there are significant historical droughts between 1978 and 1982, in 1985 and around 1992.

Both future series presented a similar pattern (cycle) analysing the lines continuity, when one goes up, the other follows the same pattern. It means that both scenarios have the same statistical oscillations in the same period, with some delays between each other. In the RCP 4.5 scenario (red line), the most significant droughts occurred between 2015 and 2020, 2025 to 2030, 2058 to 2062, 2066 to 2068, and 2084 and 2085. In the RCP 8.5 scenario, the

major droughts occurred between 2015 and 2025 with a small increase around 2027. Others happened between 2079 and 2084 with an abrupt valley in 2095. As highlighted, there are similarities between both time-series; despite the purple line (RCP 8.5) presented less significant drought events, when compared to the red line (RCP 4.5).

Table 26, Table 27 and Table 28 present the drought statistics of both historical (HIST) and future simulated (RCP 4.5 and RCP 8.5) series of the station 11 accumulated in 3-, 6- and 12-months, respectively.

Table 26 presents the differences between historical and simulated series of the 3-month accumulation period. Comparing the differences between the historical and the RCP 4.5 scenario (diff % ½ column), the higher differences are maximum drought magnitude (max DM and 76.23%) and drought duration (duration with 30.00%). This means droughts may become more severe in the future and last more (become longer). The other statistics differences are lower than 20% in absolute value, meaning lower increase/reduction of drought statistics along the future. The relative number of drought events (rel num D with -18.52%) presented a decrease in quantity of drought events in the future RCP 4.5 scenario, when compared to the historical scenario.

Comparing the differences between the historical and the RCP 8.5 scenario (diff % 1/3), the higher differences occurred in drought duration (duration with -30%) and median drought magnitude (med DM with 24.44%). Except for drought duration, which presented a decrease in the future scenario when compared to the historical, the median drought magnitude (med DM) presented drought severity increase along the future. It is important to highlight that the RCP 4.5 scenario presented a more hazardous scenario than the RCP 8.5 and shows inconsistencies with the GHG emission rates premises, since the RCP 4.5 is a more optimistic scenario (CO2 levels reduction along the twenty-first century). The RCP 8.5 is a more pessimistic (or realistic), because it assumes constant CO2 emission rates until 2100.

Figure 26 – Historical (HIST) and future simulated (RCP 4.5 and RCP 8.5) RDI series of the station 11 accumulated in 3, 6, and 12 months, respectively.

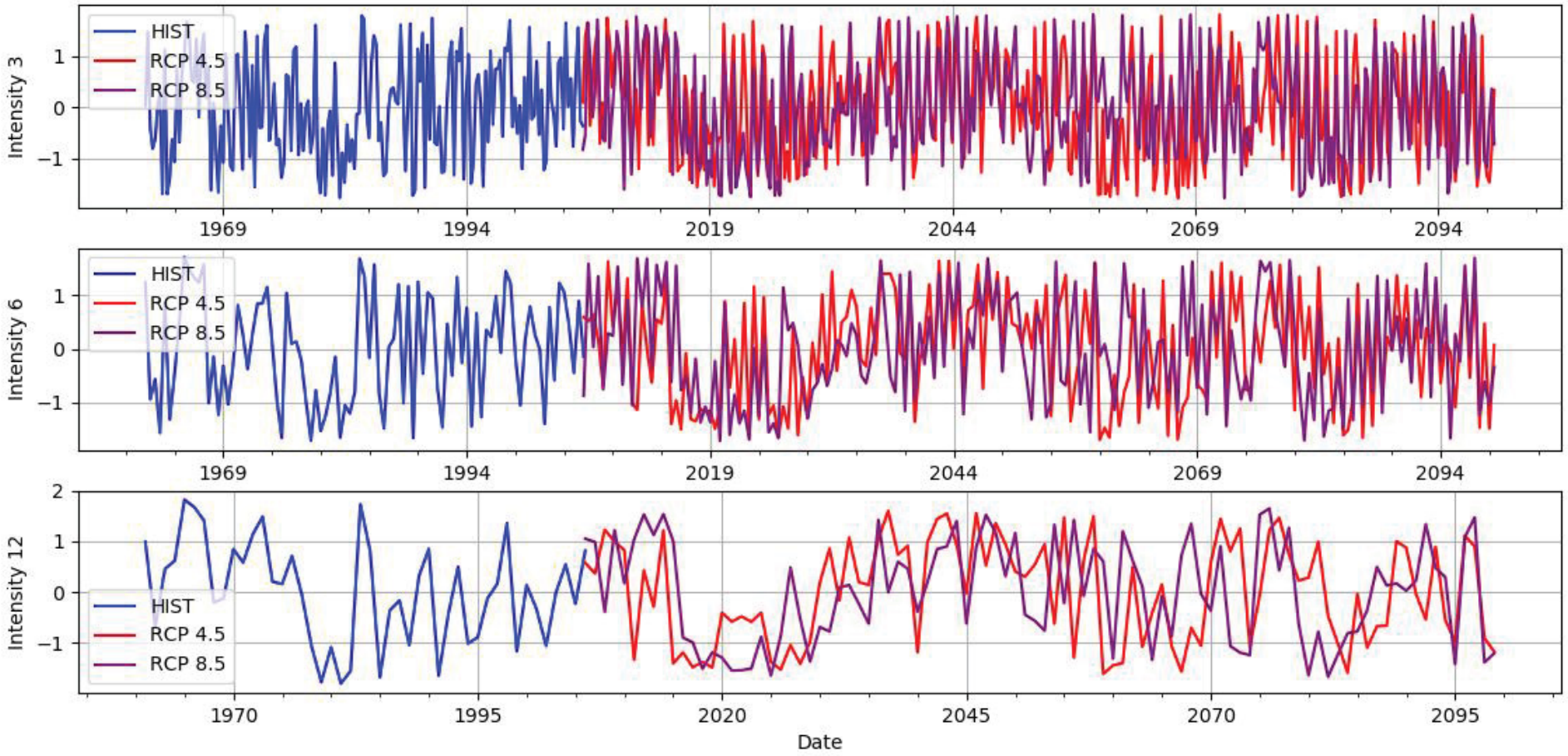

Font: Author.

Table 26 – Drought statistics of the historical (HIST) and future simulated (RCP 4.5 and RCP 8.5) series of the station 11 accumulated in 3 months.

3 Station 11	1 HIST	2 RCP45	3 RCP85	diff % 1/2	diff % 1/3
mean DM	-5.02	-5.93	-5.48	18.15	9.07
med DM	-3.62	-4.03	-4.51	11.34	24.44
max DM	-24.47	-43.12	-25.99	76.23	6.21
FR0	51.22	51.03	51.06	-0.36	-0.30
min	-1.76	-1.77	-1.77	0.60	0.37
FR10	20.75	20.93	18.47	0.86	-10.99
FR15	7.03	6.38	6.48	-9.18	-7.81
duration	10.00	13.00	7.00	30.00	-30.00
rel num D %	0.26	0.21	0.23	-18.52	-10.37

Font: Author.

Table 27 presents differences between historical and simulated series of the 6-month accumulation period. The last columns comprise the differences between (1) historical and RCP 4.5 scenario (diff % ½), and (2) historical and RCP 8.5 scenario (diff % 1/3). The highest differences found in the column diff % ½ are median drought magnitude (med DM with -29.39%) and severe drought occurrence frequency (FR15 with -18.20%). In relation to these statistics, droughts may become less severe and frequent in the future. General statistics differed less than 18% in absolute value.

Table 27 – Drought statistics of the historical (HIST) and future simulated (RCP 4.5 and RCP 8.5) series of the station 11 accumulated in 6 months.

6 Station 11	1 HIST	2 RCP45	3 RCP85	diff % 1/2	diff % 1/3
mean DM	-11.17	-9.18	-9.52	-17.84	-14.74
med DM	-7.63	-5.39	-6.59	-29.39	-13.66
max DM	-72.95	-75.99	-50.57	4.17	-30.68
FR0	49.74	48.57	51.42	-2.35	3.39
min	-1.71	-1.70	-1.72	-0.78	0.44
FR10	22.64	23.08	20.93	1.90	-7.55
FR15	7.33	5.99	5.39	-18.20	-26.43
duration	12.00	11.00	9.00	-8.33	-25.00
rel num D %	0.24	0.28	0.27	15.33	10.98

Font: Author.

In the column diff % 1/3, the highest differences are maximum drought magnitude (max DM with -30.68%) and severe drought occurrence frequency (FR15 with -26.43%). Negative differences between historical and RCP 8.5 scenarios indicate decrease, as occurred in both max DM and FR15. General differences are below -25% (drought duration). It is important to highlight that in the station 11 (Castro) accumulated in 6-months occurred differences between both RCP 4.5 and RCP 8.5 scenarios, as well as between the 3- and 6-month accumulation periods, whose presented differences in other statistics.

Table 28 – Drought statistics of the historical (HIST) and future simulated (RCP 4.5 and RCP 8.5) series of the station 11 accumulated in 12 months.

12	1	2	3		
Station 11	**HIST**	**RCP45**	**RCP85**	**diff % 1/2**	**diff % 1/3**
mean DM	-24.72	-31.47	-28.96	27.30	17.14
med DM	-16.82	-15.79	-15.76	-6.08	-6.29
max DM	-88.13	-189.35	-166.72	114.85	89.17
FR0	50.17	48.57	48.56	-3.20	-3.21
min	-1.81	-1.62	-1.67	-10.54	-7.39
FR10	24.45	23.24	20.95	-4.93	-14.30
FR15	9.59	6.96	7.47	-27.42	-22.09
duration	6.00	15.00	11.00	150.00	83.33
rel num D %	0.20	0.17	0.18	-14.89	-9.57

Font: Author.

Table 28 presents differences between both historical and simulated series of the 12-month accumulation period. There are differences between historical and RCP 4.5 scenario (diff % ½) and between historical and RCP 8.5 scenario (diff % 1/3). The diff % ½ column presented the major differences in drought duration (duration with 150.00%) and maximum drought magnitude (max DM with 114.85%). The two statistics presented an increase (intensification) in the drought characteristics along the future, whose may become more extended and more severe. Other absolute value statistics presented lower than 28% reduction or increase in the statistics, when compared to the historical series.

The diff % 1/3 column (differences between historical and RCP 8.5 scenario) presented the highest percentage variation in maximum drought magnitude (max DM with 89.17%) and drought duration (duration with 83.33%), all increasing in the future

when compared to the historical series. The other statistics remained below 23% in absolute value.

5.1.4. Station 22 (Londrina)

Figure 27 presents both historical (HIST) and future simulated (RCP 4.5 and RCP 8.5) RDI series of the station 22 accumulated in 3-, 6-, and 12-months, respectively. Looking at the droughts evolution and observing the 3-, 6-, and 12-month graphs simultaneously, there is a mild drought in 1967, a severe valley in 1989 and other drought from 1990 to 1993. Other droughts below -1.0 threshold found in both 3- and 6-month graphs do not present evolution along time and are not much severe. A same pattern was observed in the previous analyses of the stations 1 (Paranagua), 8 (Ponta Grossa) and 11 (Castro) in the Figure 24, Figure 25 and Figure 26, respectively.

Both future series (RCP 4.5 and RCP 8.5) reproduced the same behaviour (cycles) and upward and downward RDI movement along time. Moderate to severe droughts pointed in the RCP 4.5 series (red line) occur between 2015 and 2019, 2025 and 2027, 2059 and 2062, 2066 and 2069, and from 2082 to 2084. In the RCP 8.5 series (purple line), moderate to severe droughts (below -1.0 threshold in the RDI series), occur between 2020 and 2026 and from 2079 to 2084 with an abrupt peak of wet period in the middle (around 2081). Analysing both series, it indicates the RCP 4.5 is the worst scenario in terms of droughts, when compared to the RCP 8.5. Despite both scenarios (red and purple lines) presented a similar behaviour in terms of cycles and movement along time, the RCP 8.5 scenario presented more variables above the -1.0 threshold, indicating milder droughts when compared to the RCP 4.5 scenario.

MARCOS-GARCIA et al. (2017) applied the Standardized Precipitation Index (SPI) and evaluated future (RCP 8.5) droughts in the 12-month accumulation period. The authors found severe droughts between the periods 2051 and 2052, 2062 and 2063, and in 2068 in the Jucar River Basin, East Spain. Despite the Parana State and the East Spain, have different climates, both regions present drought indices increase in 2062 in the RCP 8.5 scenario, suggesting a global drought increase in the twenty-first century.

In Southern India, GUPTA & JAIN (2018) applied both SPI and SPEI in the historical series and both future scenarios (RCP 4.5 and RCP 8.5). In the RCP 4.5

scenario, the authors found moderate to severe droughts from 2060 to 2061 in both indices; and the SPI produced milder droughts when compared to the SPEI. The SPEI produced also more intense droughts between 2082 and 2084. In the RCP 8.5 scenario, the authors found moderate to severe droughts from 2078 to 2100 in the SPEI. These results show both Parana State and Southern India present increasing drought severities in similar periods. The SPEI has the contribution of the potential evapotranspiration, as does the RDI. This indicates the importance of considering the potential evapotranspiration in drought indices computation, even for wet/rainy regions (Parana State and Southern India).

Table 29, Table 30 and Table 31 present the drought statistics of both historical (HIST) and future simulated (RCP 4.5 and RCP 8.5) series of the station 22 accumulated in 3-, 6- and 12-months, respectively.

Table 29 presents the main drought statistics and comparisons with the historical series and the RCP 4.5 scenario (diff % ½) and with the historical series and the RCP 8.5 scenario (diff % 1/3). The higher differences in the column diff % ½ are maximum drought magnitude (max DM with 99.23%) and drought duration (duration with 62.50%). These two statistics indicate that droughts may become more severe in the future series; despite the severe drought frequency presented a negative variation (FR15 with -51.88%, meaning a decrease in the future). Other differences are lower than 37% (mean DM) in absolute values.

The higher differences in the column diff % 1/3 are severe drought occurrence frequency (FR15 with -39.82%), mean drought magnitude (mean DM with 22.11%) and maximum drought magnitude (max DM with 21.59%). Comparing the historical and the RCP 8.5 scenario, there is an increase in both median and maximum drought magnitude in the future, while there is a decrease in the severe drought occurrence frequency. Other statistics are below 18% difference in absolute value. The relative number of drought events (rel num D with -17.50%) indicate a decrease in the RCP 8.5 future scenario, when compared to the historical scenario.

Figure 27 – Historical (HIST) and future simulated (RCP 4.5 and RCP 8.5) RDI series of the station 22 accumulated in 3, 6, and 12 months, respectively.

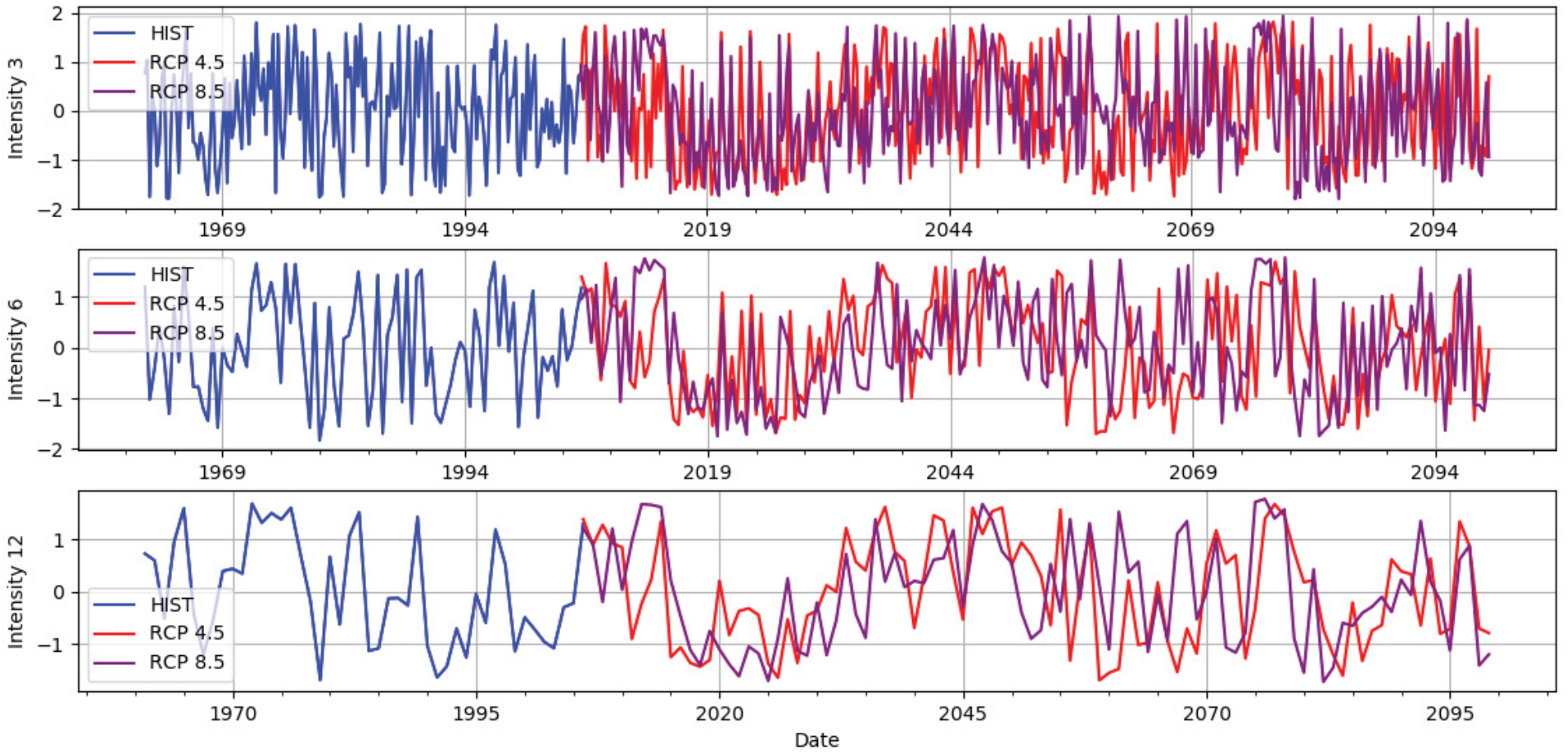

Font: Author.

Table 29 – Drought statistics of the historical (HIST) and future simulated (RCP 4.5 and RCP 8.5) series of the station 22 accumulated in 3 months.

3 Station 22	1 HIST	2 RCP45	3 RCP85	diff % 1/2	diff % 1/3
mean DM	-4.85	-6.63	-5.93	36.54	22.11
med DM	-3.83	-4.54	-4.35	18.50	13.55
max DM	-21.49	-42.81	-26.12	99.23	21.59
FR0	48.15	53.01	52.19	10.10	8.40
min	-1.78	-1.74	-1.80	-2.41	0.93
FR10	19.87	21.83	17.74	9.87	-10.71
FR15	9.22	4.43	5.55	-51.88	-39.82
duration	8.00	13.00	9.00	62.50	12.50
rel num D %	0.26	0.19	0.22	-25.65	-17.50

Font: Author.

Table 30 presents the main drought statistics and comparisons with the historical series and the RCP 4.5 scenario (diff % ½) and with the historical series and the RCP 8.5 scenario (diff % 1/3). The higher differences in the column diff % ½ are maximum drought magnitude (max DM with 103.50%) and drought duration (duration with 57.14%). These positive signals indicate more intense (severe) droughts in the RCP 4.5 scenario, when compared to the historical series in terms of magnitude and duration. Other differences are below 23% in absolute value.

Table 30 – Drought statistics of the historical (HIST) and future simulated (RCP 4.5 and RCP 8.5) series of the station 22 accumulated in 6 months.

6 Station 22	1 HIST	2 RCP45	3 RCP85	diff % 1/2	diff % 1/3
mean DM	-10.90	-13.40	-11.97	23.03	9.87
med DM	-9.20	-6.67	-6.11	-27.46	-33.60
max DM	-33.81	-68.79	-51.20	103.50	51.45
FR0	50.72	50.79	52.06	0.15	2.64
min	-1.83	-1.70	-1.75	-7.04	-4.56
FR10	22.12	23.28	17.42	5.23	-21.27
FR15	8.56	6.94	6.23	-18.97	-27.25
duration	7.00	11.00	11.00	57.14	57.14
rel num D %	0.24	0.20	0.21	-19.49	-12.96

Font: Author.

In the column (diff % 1/3), the higher differences between historical and future RCP 8.5 scenario are drought duration (duration with 57.14%) and maximum drought magnitude (max DM with 51.45%). These two statistics indicate more severe droughts along the twenty-first century. The median drought magnitude (med DM with -33.60%) presented a contrary pattern, indicating a decrease up to 2100. Other statistics presented differences lower than 28% (severe drought occurrence frequency, FR15), in absolute value.

Table 31 – Drought statistics of the historical (HIST) and future simulated (RCP 4.5 and RCP 8.5) series of the station 22 accumulated in 12 months.

12	1	2	3		
Station 22	**HIST**	**RCP45**	**RCP85**	**diff % 1/2**	**diff % 1/3**
mean DM	-33.66	-31.08	-28.51	-7.66	-15.30
med DM	-26.06	-18.21	-15.88	-30.14	-39.08
max DM	-80.87	-92.82	-152.86	14.77	89.01
FR0	56.78	47.41	51.79	-16.50	-8.78
min	-1.70	-1.70	-1.73	0.22	1.99
FR10	19.80	21.62	22.61	9.20	14.19
FR15	11.22	6.97	4.83	-37.85	-56.99
duration	7.00	10.00	11.00	42.86	57.14
rel num D %	0.16	0.17	0.18	9.42	16.26

Font: Author.

Table 31 presents the main drought statistics and comparisons in the 12-month accumulation period with the historical series and the RCP 4.5 scenario (diff % ½) and with the historical series and the RCP 8.5 scenario (diff % 1/3). The higher positive differences in the column diff % ½ are drought duration (duration with 42.86%) and maximum drought magnitude (max DM with 14.77%). These two statistics presented droughts increase along the future. However, the severe drought occurrence frequency (FR15 with -37.85%) and median drought magnitude (med DM with -30.14%) presented a decrease up to 2100. Other statistics presented lower than 17% in absolute value, when compared to the historical series.

In the column (diff % 1/3), the higher differences between historical and future RCP 8.5 scenario are maximum drought magnitude (max DM with 89.01%) and drought duration (duration with 57.14%). The severe drought occurrence frequency (FR15) presented -56.99% variation between historical and RCP 8.5 scenarios. The statistics max DM and duration

presented a drought increase along the twenty-first century, while the FR15 presented a decrease in the same period.

5.2. Overall analysis

After analysing some stations separately, an overall analysis was performed of all drought statistics comprising the entire Parana State. Figure 28 presents the maximum drought duration of both historical (HIST) and simulated (RCP 4.5 and RCP 8.5) series for zero threshold. The statistic drought frequency of zero threshold means the occurrence of droughts, where all RDI values below zero are considered droughts, according to Run Theory (see subchapter 2.10 Run Theory).

In the historical series, droughts have a maximum duration (blue) of 8.44 months and minimum (red) of 5.20 months. These values (maximum and minimum) occur in some stations and the intermediate drought duration values occur in almost entire Parana State (colour transitions from red to blue). In the future simulated RCP 4.5 scenario, the maximum drought duration (blue) is 12.85 months and the minimum (red) 6.95 months. These figures have higher drought duration when compared to the historical series. The minimum values occur in the South and West of the Parana, while the maximum values occur in the Centre, North and East. There is a clear division (white line) in the drought duration values in the maps from the South-Centre to the Northwest.

In the future simulated RCP 8.5 scenario, values occurred between historical and RCP 4.5 scenarios. This is unusual, since the RCP 8.5 produces worst scenarios (more pessimistic) in terms of highest increase in GHG emissions, when compared to the RCP 4.5 scenario. The maximum drought duration (blue) of 10.07 months occurs at some stations in Southwest and Northeast. Some sites presented maximum drought duration of 10.07 months, while others presented minimum drought duration of 5.41 months. Few locations presented the minimum drought duration, mainly in the Curitiba region (station 4).

In the Parana State, other droughts occurred in the historical scenario before 1961. According to CANAMBRA (1967), CANAMBRA (1969) and DETZEL et al. (2019), the dry periods found in the South Region are between 1944 and 1945 and the series used for study had the begins in the 1930.

CHATTOPADHYAY et al. (2017) evaluated the maximum drought duration in the Kentucky River basin, Centre-East US. The authors found maximum drought length in the range of 6 to 11 months in both future scenarios (RCP 4.5 and RCP 8.5). These results are in the same range as those obtained in Parana State, despite both regions present different climates. It is important to highlight that in the work of CHATTOPADHYAY et al. (2017), the authors found that the RCP 4.5 scenario is more severe in maximum drought length, when compared to the RCP 8.5 scenario.

SPINONI et al. (2014b) performed a global drought evaluation using the SPI and found total drought durations from 24 to more than 72 months in Parana for the period 1971 to 2010. Their results show significant differences with this work, which presented drought durations from 5 to 8 months in the historical scenario. This significant difference may relate to details in the computation, where SPINONI et al. (2014b) applied reanalysis data and did not consider the non-stationary approach.

Figure 28 – Maximum drought duration of the historical (HIST), and simulated (RCP 4.5 and RCP 8.5) series.

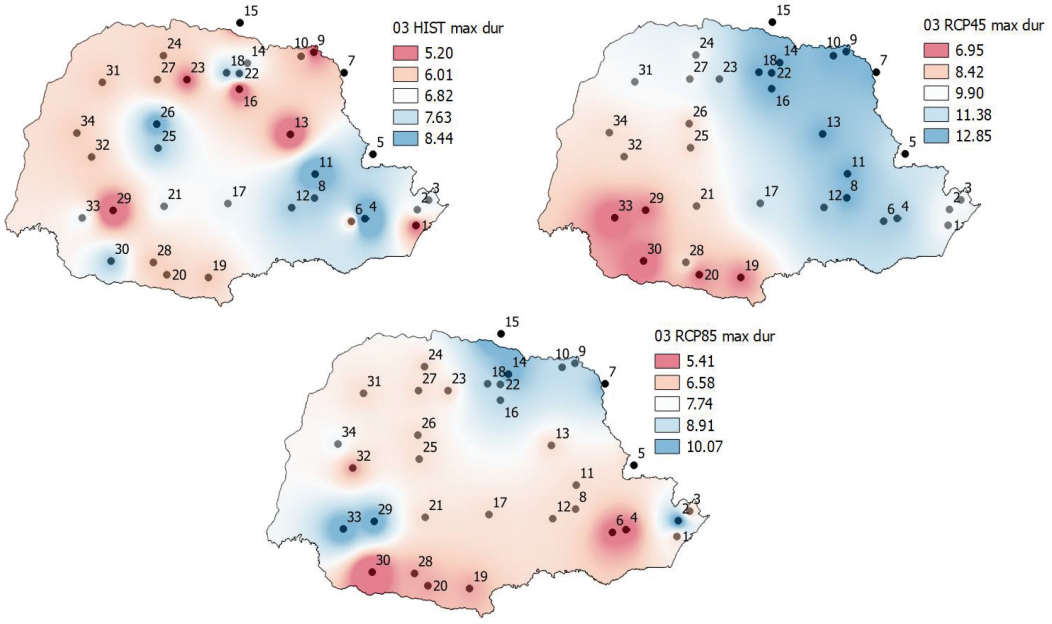

Font: Author.

AWANGE et al. (2016) evaluated the maximum drought duration in the entire Brazilian country using the SPI in the 3-month accumulation period. The authors found 5 to 15 month droughts in Parana State for the historical period. AWANGE et al. (2016) results show the SPI values are in accordance with what was presented in Figure 4 (from 5 to 8 months). However,

the South presented higher drought duration in the work of AWANGE et al. (2016) (up to 15 months), when compared to this work (around 6 months).

Some studies evaluate the mean drought duration, as performed by LLOYD-HUGHES & SAUNDERS (2002) in European continent. They found in Germany 10 to 30 month drought duration and in France 20 to 50 months, using the SPI accumulated in 12-months. Both countries present non-stationarity in the meteorological data, as happen in the Parana State. They used gridded temperature and precipitation data.

TOUMA et al. (2015) performed a drought analysis worldwide and found 2-month drought duration using the SPI in the period 2010 to 2099, at the same time the SPEI presented 8-month drought duration, both in Parana State. These results indicate the importance of considering the potential evapotranspiration effects. Both SPEI and RDI considers the potential evapotranspiration effects in their computation. Results using SPEI in TOUMA et al. (2015) (up to 8 months) are in accordance with the maximum drought duration presented in Figure 28 (from 5 to 8 months).

Figure 29 – Zero threshold frequency of the historical (HIST), and simulated (RCP 4.5 and RCP 8.5) series.

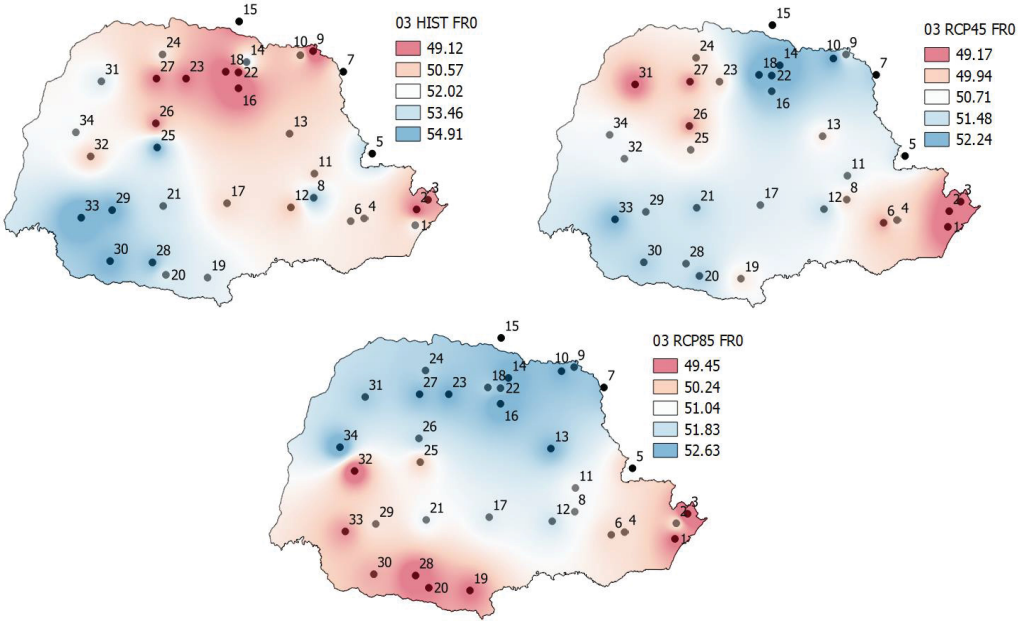

Font: Author.

Figure 29 presents the zero threshold frequency of both historical (HIST) and simulated (RCP 4.5 and RCP 8.5) series. The historical period presented the higher drought occurrence

frequencies in the Southwest region and the lower occurred in the North. The stations 25 (Nova Cantu), 28 (Pato Branco), 29 (Quedas do Iguacu), 30 (Francisco Beltrao) and 33 (Planalto) presented the highest occurrence frequency (54.91%), while some stations located in the North (e.g. 16 (Maua da Serra), 18 (Apucarana), 22 (Londrina), and others) presented the lowest occurrence frequency (49.12%).

The range (49.12% to 54.91%) means that in the entire Parana State, the drought occurrence (lower than 0 threshold) exceed 49% minimum, showing the importance in studying droughts in the Parana State, even it is a rainy region.

Figure 30 – The -1.0 threshold frequency of the historical (HIST) and simulated (RCP 4.5 and RCP 8.5) series.

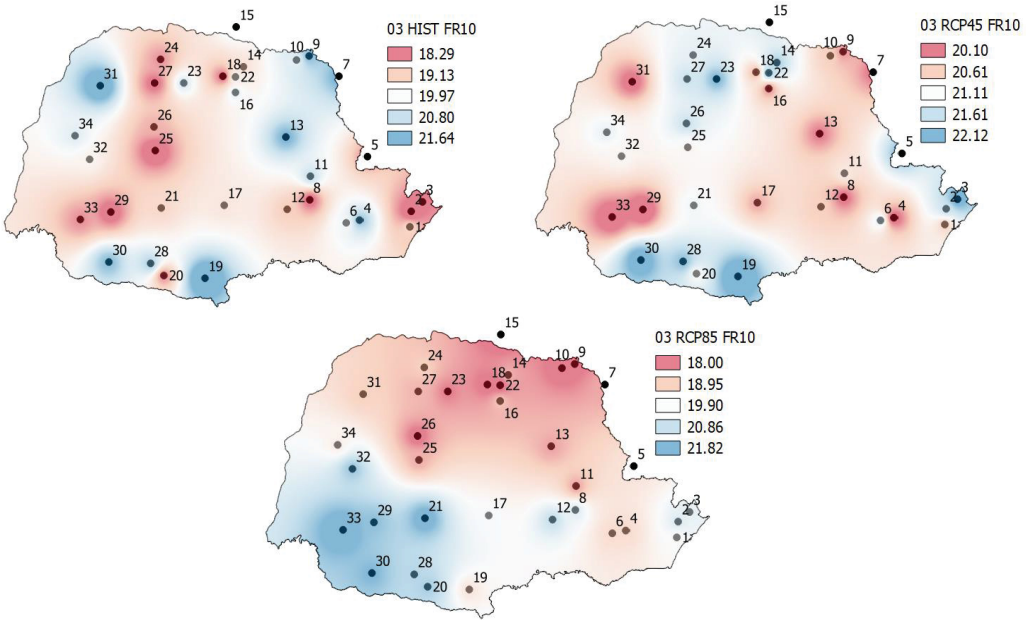

Font: Author.

In the future series (RCP 4.5 and RCP 8.5), there are few differences in terms of drought occurrences (frequency). Small increases in drought frequencies occurred in both North and Centre regions. In the RCP 4.5, the lower frequencies occurred in Northwest and East, while the higher occurred in the blue area starting in Southwest to Northeast. In the RCP 8.5 scenario, the blue areas show the higher frequency regions (Centre to North), while the red areas show the lower frequency regions (West, East and South). There is an agreement in the moderate to severe drought frequencies between the historical and both future scenarios, when compared the frequencies range among them.

SPINONI et al. (2014b) performed a global drought evaluation using the SPI and found drought frequency from 3% to more than 6% in Parana in the period 1971 to 1990. They also found in the period 1991 to 2010, drought occurrence frequency from 2% to 6%. Results are in accordance with this work, which presented for the historical scenario, moderate to severe drought occurrence frequency from 4% to 8%.

Figure 30 presents the -1.0 threshold drought frequencies of both historical (HIST) and simulated (RCP 4.5 and RCP 8.5) series. The historical period presented lower drought frequencies in almost the entire Parana State, except locally in the blue regions (high frequencies). The same pattern occurred in the simulated (RCP 4.5 and RCP 8.5) scenarios, with few variations in drought frequencies. The higher frequency found in the three scenarios is 22.12% (RCP 4.5 in blue) and the lower, 18.00% (RCP 8.5 in red).

Figure 31 presents the -1.5 threshold drought frequencies of both historical (HIST) and simulated (RCP 4.5 and RCP 8.5) series. The historical period presented a heterogeneous distribution in drought frequencies looking at the colours map. The lowest value corresponds to 4.31% (red), while the highest corresponds to 8.01% (blue). The light red, white and light blue colours cover practically the entire map. A general synthesis of the Parana State in severe drought frequency (lower than -1.50 threshold), means that almost the entire Parana State presented a mean 6.16% (white) severe drought frequency.

The RCP 4.5 scenario presented a different distribution of both lowest and highest values, when compared to the historical scenario, despite it presented low frequency variations (comparing absolute values in the range of the colour legend). The highest frequency is 6.31% (blue), while the lowest is 3.90% (red). The lower frequencies are predominant in Parana State, except in the Southwest region and some random localities, represented by stations 2 (Morretes), 3 (Guaraquecaba), 8 (Ponta Grossa), 11 (Castro), 12 (Fernandes Pinheiro) and 31 (Umuarama).

The RCP 8.5 scenario presented similar drought frequencies when compared to the historical scenario, differing in spatial distribution of these values, which is similar to the RCP 4.5 scenario. The RCP 8.5 scenario considers no reduction in GHG emission rates, i.e., it means the emission will continue increasing until the end of the century (2100). Considering this, the drought frequency statistics remain the same in the future period for the Parana State and is coherent with the historical period representation. However, the maps represent a different frequency distribution. The lowest values (4.86% in red) prevail in the West, North and Centre

of the Parana, while the highest (6.91% in blue) in east. The lowest frequency occurred in the station 19 (Palmas).

AWANGE et al. (2016) performed a drought analysis in the entire Brazilian country using the SPI accumulated in 3-, 6- and 12-month. They found from 20% to 24% drought frequency and from 2% to 6% severe drought frequency (FR15), in the 3-month accumulation period for the historical series of the Parana State. Results show similarities between the FR15 values obtained in this research (from 4% to 8%), when compared to AWANGE et al. (2016).

Figure 31 – The -1.5 threshold frequency of the historical (HIST), and simulated (RCP 4.5 and RCP 8.5) series.

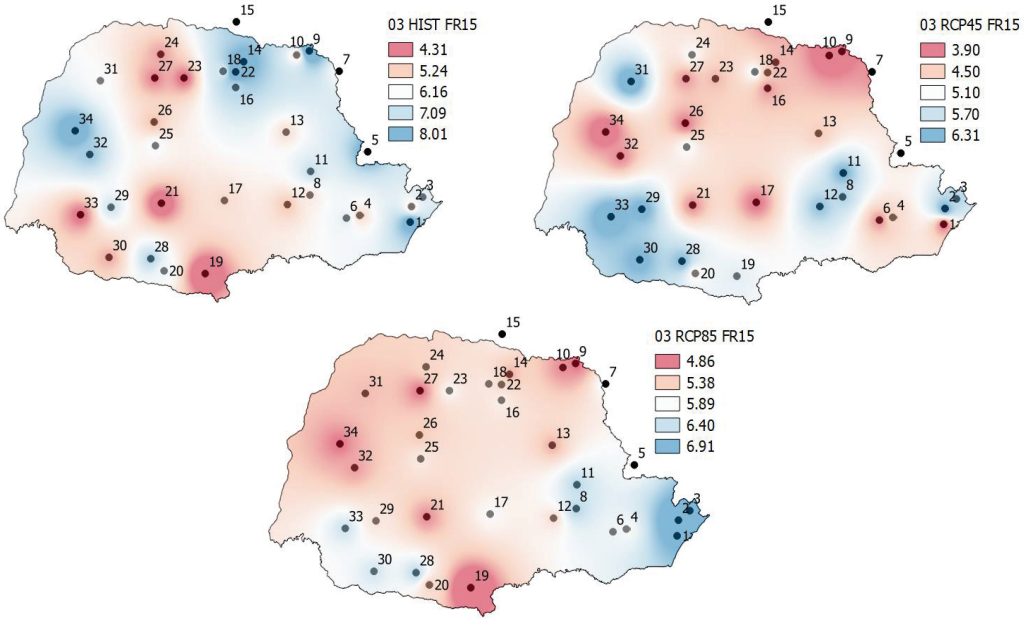

Font: Author.

Figure 32 presents the maximum drought magnitude of both historical (HIST) and simulated (RCP 4.5 and RCP 8.5) series. There is a different pattern of maximum drought magnitude among the three scenarios. The RCP 4.5 presented the worst maximum drought magnitude (-45.25) and the RCP 8.5 presented an increase in the maximum drought magnitude, when compared to the historical period (historical with -24.45 and RCP 8.5 with -30.12). The negative signal in all drought magnitude maps (Figure 32, Figure 33 and Figure 34) means the computation of the drought intensity (minimum values or RDI in negative scale) by drought duration, according to the Run Theory (see subsection 2.10 Run Theory). Since the drought intensity is negative, the multiplication results in a negative also. The module of drought magnitude (DM) comparison occurs with other studies performed worldwide.

In all analysis neglecting the drought magnitude signal, the historical scenario presented the worst maximum drought magnitude (in module) in the Centre-East region and in stations 4 (Curitiba), 8 (Ponta Grossa) and 11 (Castro). The station 26 (Campo Mourao) also presented worse maximum drought magnitude (-24.45 in red). General stations (from light red to blue) cover the Parana State area with lower maximum drought magnitude. The general area presented from -14.31 to -16.85 maximum drought magnitude.

A different spatial behaviour occurred in the RCP 4.5 scenario. The highest maximum drought magnitudes (-45.25) occurred in Centre-Northeast, represented by stations 11 (Castro) and 13 (Telemaco Borba) and in both North and Northeast, represented by stations 7 (Joaquim Tavora), 9 (Cambara), 10 (Bandeirantes), 14 (Ibipora), 15 (Bela Vista do Paraiso), 16 (Maua da Serra), 18 (Apucarana) and 22 (Londrina). Lower maximum drought magnitude are observed in the East (seaside), Southwest, Centre and South (light red to blue). The lowest maximum drought magnitudes occurred in the Southwest region, represented by stations 19 (Palmas), 20 (Clevelandia), 28 (Pato Branco) and 30 (Francisco Beltrao).

Figure 32 – Maximum drought magnitude of the historical (HIST), and simulated (RCP 4.5 and RCP 8.5) series.

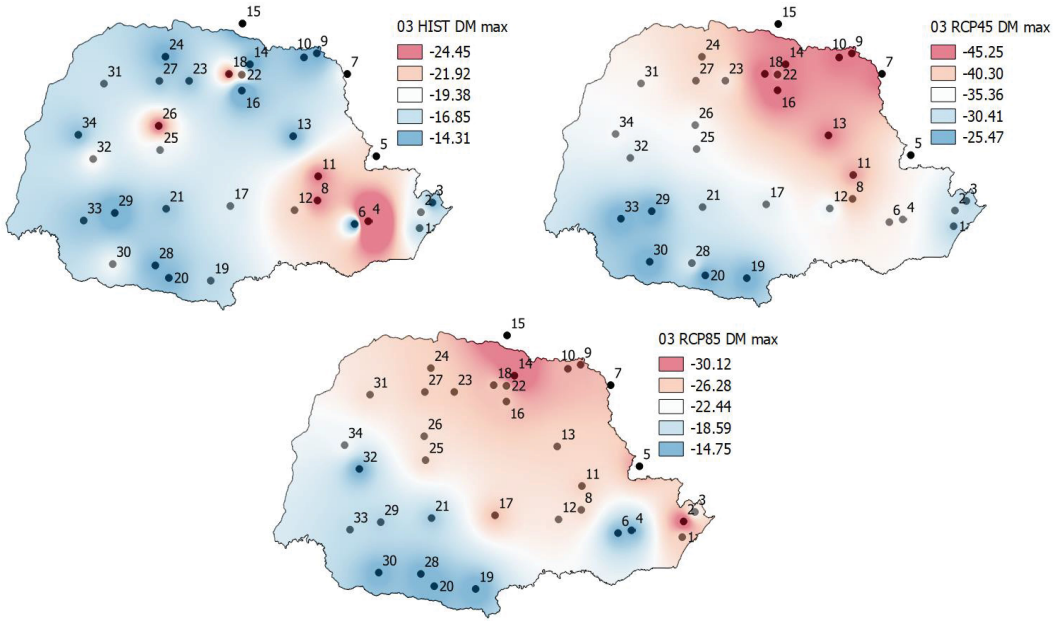

Font: Author.

The RCP 8.5 scenario presented the highest maximum drought magnitudes only at stations 14 (Ibipora) and 15 (Bela Vista do Paraiso) located in the North and in the station 2 (Morretes) in the East, each reaching -30.12 maximum drought magnitude. Other stations

(coloured light red to blue) present lower maximum drought magnitude. The minimum values were at the same sites as in the RCP 4.5 scenario, namely stations 19 (Palmas), 20 (Clevelandia), 28 (Pato Branco) and 30 (Francisco Beltrao). The lower maximum drought magnitude values are up to -14.75.

SPINONI et al. (2014b) performed a global drought evaluation using the SPI and found total drought severity from 25 to around 100 in the Parana region in the period 1971 to 2010. Results are superior of this work, which presented maximum drought magnitude (max DM) in module between 14 and 24 in the historical period. This can happen due to the use of reanalysis data and the non-consideration of the non-stationary drought analysis approach.

Figure 33 presents the mean drought magnitude of both historical (HIST) and simulated (RCP 4.5 and RCP 8.5) series. In the historical period, the mean drought magnitudes situate between the range -4.43 (blue) and -5.32 (red), indicating a slight variation. The same pattern occurred in both future simulated scenarios (RCP 4.5 and RCP 8.5), where the ranges situate between -5.49 (blue) and -6.63 (red) in the RCP 4.5, and -5.37 (blue) and -6.02 (red) in the RCP 8.5.

Figure 33 – Mean drought magnitude of the historical (HIST), and simulated (RCP 4.5 and RCP 8.5) series.

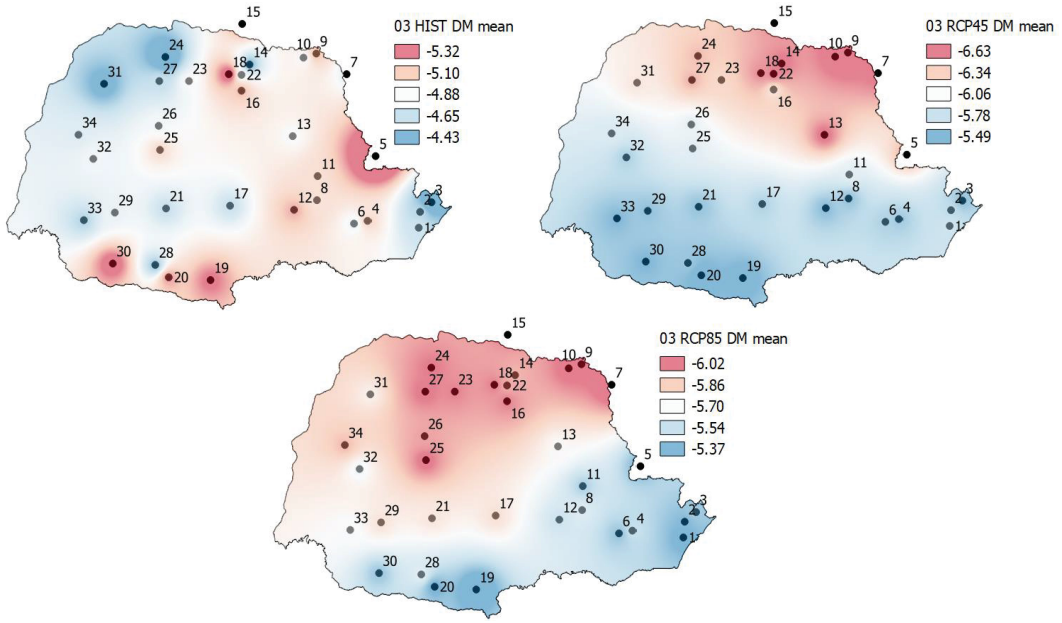

Font: Author.

The historical scenario presented few stations with highest drought magnitude means, as occurred in stations 5 (Cerro Azul), 18 (Apucarana), 19 (Palmas), 20 (Clevelandia) and 30 (Francisco Beltrao). The lowest mean drought magnitudes occurred in stations 3 (Guaraquecaba), 24 (Paranavai) and 31 (Umuarama). Differences in Parana State situate around -4.88 mean drought magnitude (in white).

In the RCP 4.5 scenario, despite of the small difference between the minimum (-5.49) and the maximum (-6.63) values, there is an evident separation between the highest (red) and the lowest (blue) values. The highest occurred in North and Northeast, while the lowest occurred in South, Centre-South and East. This analysis highlights that both North and Northeast (red) have more severe droughts, when compared to the other regions.

Figure 34 – Median drought magnitude of the historical (HIST), and simulated (RCP 4.5 and RCP 8.5) series.

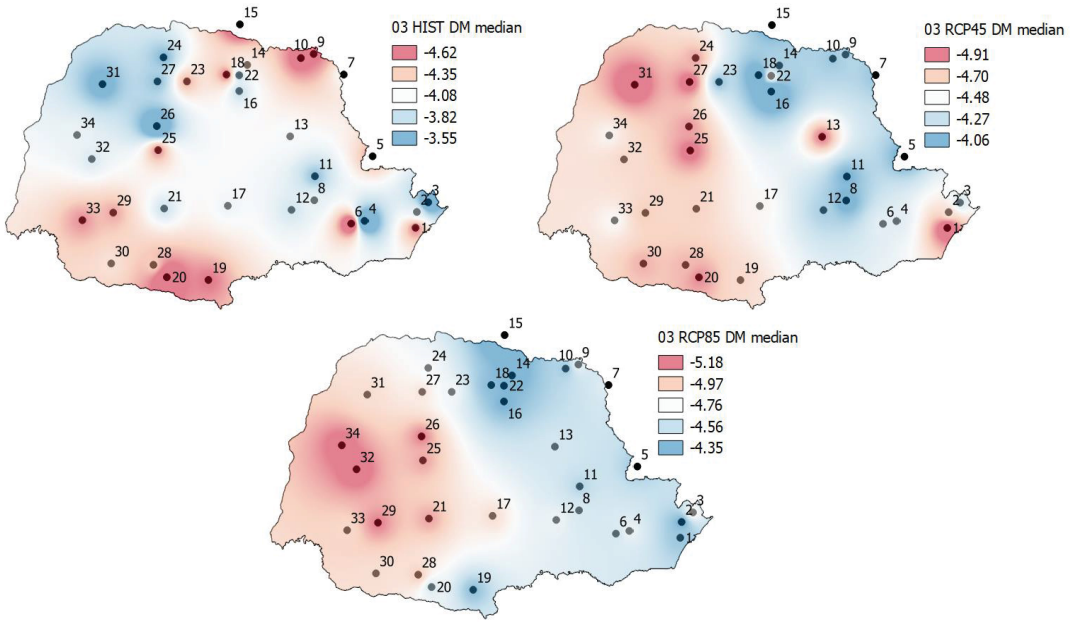

Font: Author.

In the RCP 8.5 scenario, the mean drought magnitudes show a similar behaviour, when compared to the RCP 4.5 scenario. Practically the entire Parana State presented the highest values (red) in North and Northeast. The lowest values (blue) occurred in East and South. The highest mean drought magnitude occurred in the red areas with up to -6.02 and the minimum occurred with -5.37. Both West and North of Parana State characterize by agriculture and pasture and these areas tend to become drier due to deforestation and posterior substitution by

monoculture. It means the mean drought magnitude scenario in the RCP 8.5 projection is coherent with the climate change impacts due to the anthropogenic interferences.

Figure 34 presents the median drought magnitude of both historical (HIST) and simulated (RCP 4.5 and RCP 8.5) series. The three scenarios present no significant variations in both the lowest and the highest median drought magnitudes. The historical period presented the highest values in some stations in Northeast and East. The RCP 4.5 presented a blue belt from the North to the South. The Parana State presents the highest values in Northwest, West, Centre-west, South and East (only at the seaside). The RCP 8.5 presented the highest median drought magnitudes in stations 32 (Cascavel) and 34 (Palotina), reaching -5.18 median drought magnitude. The highest values occur in West and there is a slight transition to the lowest values in the East. The median drought magnitudes do not vary significantly, when compared to the maximum drought magnitude (Figure 32).

Figure 35 – Minimum values of the historical (HIST), and simulated (RCP 4.5 and RCP 8.5) series.

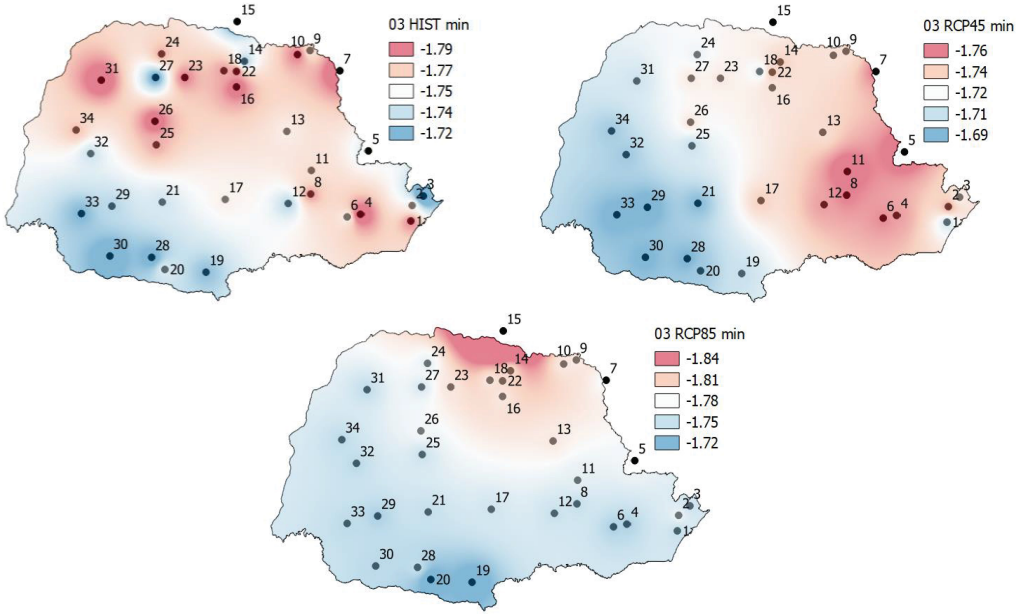

Font: Author.

Figure 35 presents the minimum values of both historical (HIST), and simulated (RCP 4.5 and RCP 8.5) series. The minimum values presented variations from one scenario to another. The historical period presented the lowest minimum value (-1.79) in most part of the Parana State and the highest minimum value (-1.72) in stations 3 (Guaraquecaba), 27

(Cianorte), and in the Southwest region. The minimum value means that there are intense droughts in the historical series in practically the entire Parana State (in red).

The RCP 4.5 presented the lowest values (-1.76 in red) in Centre-East and the highest values in West (-1.69 in blue). Comparing the RCP 4.5 scenario with the historical series, it means that until 2100, some areas with severe droughts may become less severe and others may continue to be severe. The RCP 8.5 scenario presented the lowest minimum (-1.84) value only in the North, more precisely at the station 15 (Bela Vista do Paraiso). The Parana State presented minimum values varying from -1.81 (lowest) to -1.72 (highest). It means that comparing the historical scenario with the RCP 8.5 future projection, some areas may become drier (e.g. station 15 (Bela Vista do Paraiso) from blue (-1.72 in historical) to red (-1.84 in RCP 8.5)). However, other stations maintain the minimum drought values.

ZARCH et al. (2015) evaluated droughts around the world and applied the RDI in order to identify drought patterns in both historical and future periods. They analysed the minimum values and found in Parana State, that the historical series presented normal to near normal drought severities (between 0 and -1.0 in RDI scale), while the future RCP 8.5 series presented an increase in near normal droughts (around -1.0). Results in this work also presented a slight increase in the minimum values (-1.79 in the historical series to -1.84 in the RCP 8.5 scenario). However, there may be severe droughts in both historical and RCP 8.5 scenarios, showing differences in comparison with the ZARCH et al. (2015) work. This can happen since the author used reanalysis data and did not consider the non-stationary drought analysis, as performed in this work.

AWANGE et al. (2016) evaluated the SPI minimum values in the entire Brazilian country using the SPI accumulated in 3-months. They found that most of the Parana area presented -3 in SPI scale, while the West and small portion in the North region presented up to -4.4 in the historical period. AWANGE et al. (2016) results show the SPI values are higher when compared to this work and this can happen due to each method formulation, since the RDI considers the potential evapotranspiration effects.

Figure 36 presents the total number of drought events between stationary and non-stationary approaches of both historical (HIST) and simulated (RCP 4.5 and RCP 8.5) series. The number of drought events computation occurred using the zero threshold for drought characterization. The total number of droughts in the historical series vary in the range from 29 to 44, due to differences in the historical series length. In the RCP 4.5, the range varied from

74 to 90 and in the RCP 8.5, from 80 to 91, respectively. In both simulated scenarios (RCP 4.5 and RCP 8.5), the series length is 1128 months (January 2006 to December 2099).

The historical scenario presents heterogeneity in the number of drought events across the Parana State. The lower number of events occurred in West, Southwest and in stations 5 (Cerro Azul), 6 (Lapa), 16 (Maua da Serra) and 19 (Palmas), presenting the minimum of 29 drought events (in red). The remaining Parana area presented more drought events in the historical series (regardless the series length). The blue areas presented 44 drought events in several locations all around the area.

Figure 36 – Total number of drought events between stationary and non-stationary approaches of the historical (HIST), and simulated (RCP 4.5 and RCP 8.5) series.

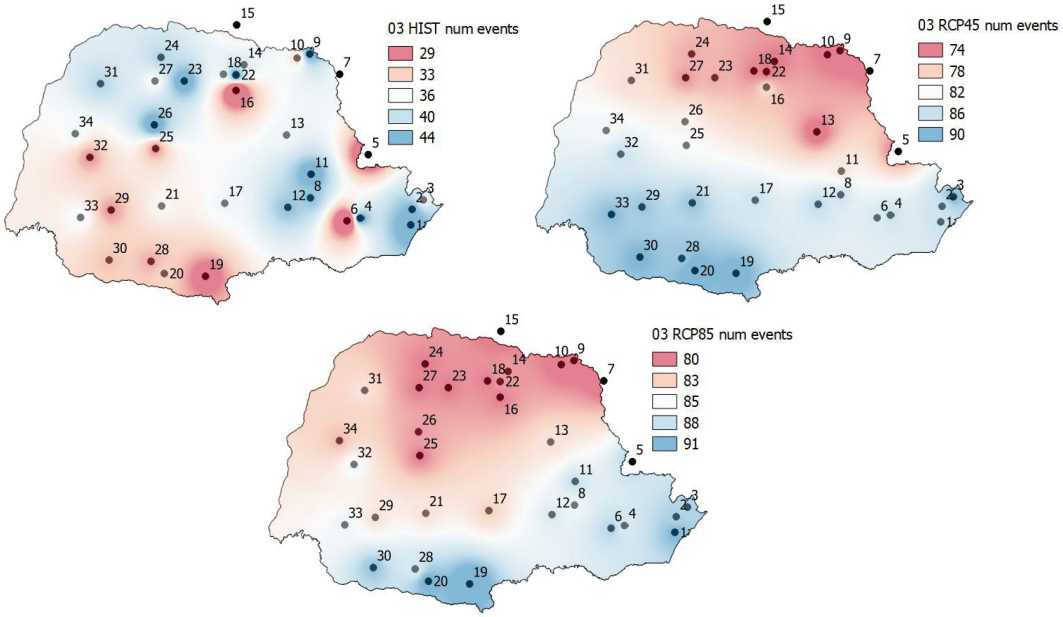

Font: Author.

In the RCP 4.5 scenario, there is a clear division between the North and the South. The North presented the lower (74 in red) number of drought events, while the South presented the higher (90 in blue). A division also occurs in the RCP 8.5 scenario, presenting both East and South regions with the higher number of drought events (91) and the remaining Parana State with the lower number of drought events (80). There is an increase in the number of drought events, when comparing the number of drought events classification (respective legends) of both RCP 4.5 and RCP 8.5 scenarios. It highlights that in the RCP 8.5 scenario occurred more droughts than in the RCP 4.5 scenario.

Figure 37 presents the boxplots of maximum drought duration (months) and mean drought magnitude (severity) of both historical (HIST) and simulated (RCP 4.5 and RCP 8.5) series. In the boxplots are the monthly maximum duration of all 34 stations of the Parana State in the left and the mean drought magnitude (severity) in the right. In the duration analysis, the median (orange line) of the historical and both future scenarios are significantly different, pointing that both future drought duration may increase. Both RCP 4.5 and RCP 8.5 scenarios presented an abrupt increase in general values (box, whiskers and outliers), when compared to the historical scenario. Despite of the increase in the maximum drought magnitude, the size of the boxes remained almost the same, meaning that there is a small data dispersion in the three scenarios. Droughts may last more in the future as evidenced by both RCP 4.5 and RCP 8.5 scenarios.

Figure 37 – Boxplots of drought duration (months) and mean drought magnitude (severity) of the historical (HIST), and simulated (RCP 4.5 and RCP 8.5) series.

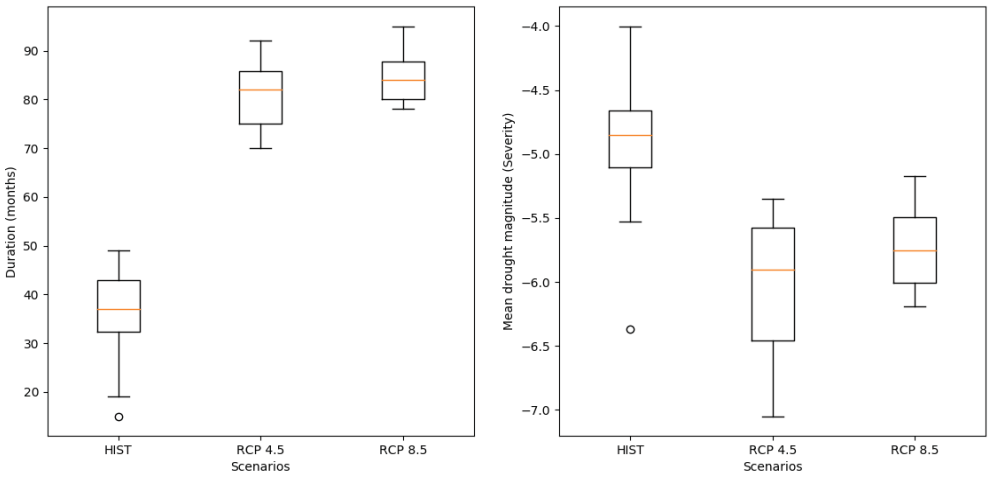

Font: Author.

In the right, there is a general decrease (increase in absolute value) in the mean values of drought severity in both future simulated scenarios (RCP 4.5 and RCP 8.5). Both scenarios presented almost the same median of all 34 stations and differed in terms of the box size (interquartile values range) and both whiskers and outliers. The RCP 4.5 presented more severe droughts (highest magnitude ranges), while the RCP 8.5 presented less severe droughts, when compared to each other. The historical scenario presented milder drought severities, when

compared to both future scenarios, meaning that droughts may become more severe in the future, according to these projections.

Figure 38 presents the median and maximum drought magnitude (severity) boxplots of both historical (HIST) and simulated (RCP 4.5 and RCP 8.5) series. In the left boxplot (median drought magnitude), the historical ensemble presented the lower absolute values. These may become more severe in the RCP 4.5 scenario and even more severe in the RCP 8.5 scenario. These results mean the RCP 4.5 scenario is a milder drought increase scenario, while the RCP 8.5 is the worst scenario, looking at the medians. The median line (orange) suffered a decrease from historical to both simulated (RCP 4.5 and RCP 8.5) scenarios, as well as the box, whiskers and outliers, shifted to a more severe scenario. In the historical scenario, there is a great dispersion of the median drought severity statistics, when compared to the RCP 8.5 scenario.

Figure 38 – Boxplots of the median and maximum drought magnitude (severity) of the historical (HIST), and simulated (RCP 4.5 and RCP 8.5) series.

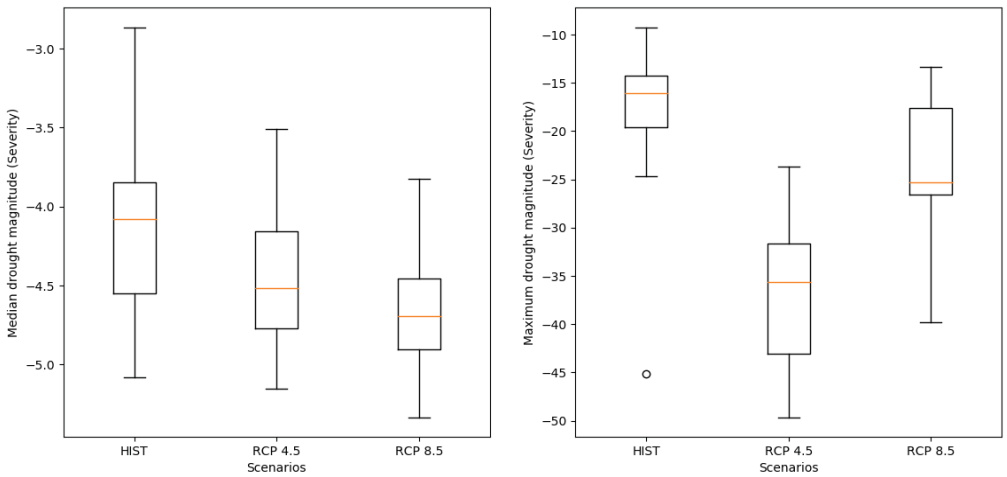

Font: Author.

In the right, the maximum drought severity boxplots presented a similar behaviour, when compared to the mean drought severity (Figure 37), where the worst scenario (more severe droughts) occurs in the RCP 4.5 series and the milder scenario in the RCP 8.5. In the maximum drought magnitude analysis, the difference is considerable when compared to the mean drought magnitude analysis. In the historical series, the box size is smaller than in both future (RCP 4.5 and RCP 8.5) scenarios, differing slightly in the size of boxes (interquartile

values range). There is a great decrease in the median values (orange line) in the RCP 4.5 scenario and the RCP 8.5 presented lower maximum drought magnitude. This analysis highlights that the RCP 4.5 scenario is the worst in terms of maximum drought severity. The RCP 4.5 scenario presented a different maximum drought severity behaviour and means that in the future (up to 2100) it may occur more severe droughts (according to the size of box), reaching up to 45 severity in some period of the future time series.

Figure 39 presents the drought frequency boxplots for both 0 (zero) and -1.0 (moderate drought) threshold of both historical (HIST) and simulated (RCP 4.5 and RCP 8.5) series. Comparing the three boxplots in the left figure, the historical scenario presented the larger range of drought frequencies in the zero threshold, i.e., for any drought occurrence. The median (orange line) remains between 50% and 52% in the three scenarios (historical, RCP 4.5 and RCP 8.5). There are differences in the size of boxes, presenting the historical scenario as the worst in terms of drought occurrences. The RCP 8.5 scenario is the worst between both future scenarios. The RCP 4.5 scenario is the less hazardous in terms of drought frequencies and presents the low data dispersion.

Figure 39 – Boxplots of the drought frequency of both 0 (zero) and -1.0 (moderate drought) threshold of the historical (HIST), and simulated (RCP 4.5 and RCP 8.5) series.

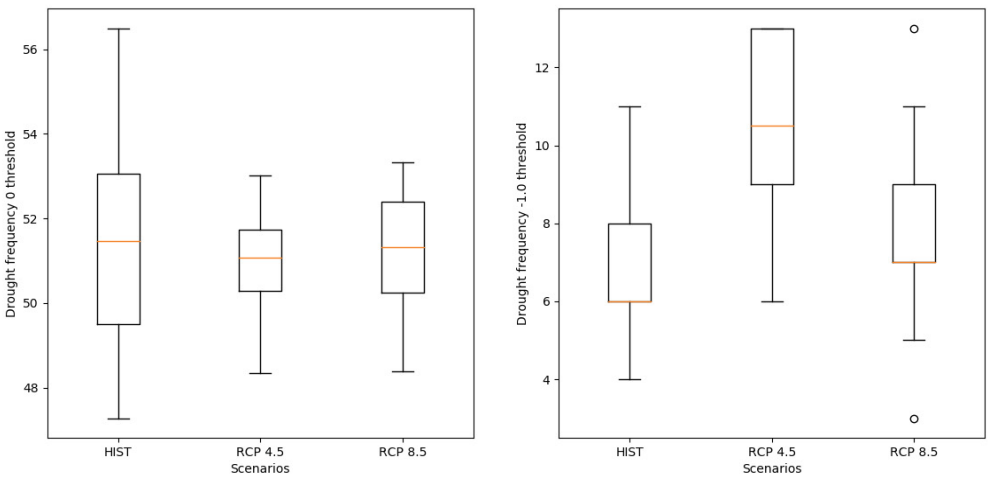

Font: Author.

The size of boxes vary from historical and future scenarios, and in both future scenarios, there is a decrease in the drought occurrence. The historical series presented the larger whiskers

meaning a wider variation of drought occurrence frequency. In the right figure are the moderate to severe drought occurrence frequencies (below -1.0 threshold). There is an increase in the moderate drought frequencies in the RCP 4.5 scenario and a slight increase in the RCP 8.5 scenario, when compared to the historical scenario. The median values (orange lines), box size and the whiskers highlight this increase. The larger whiskers are in the historical scenario. There are two outliers in the RCP 8.5 scenario and the RCP 4.5 is the worst scenario, when compared to both historical and RCP 8.5 scenarios. This means the moderate to severe drought occurrences may become more frequent in the future, considering both future projections.

Figure 40 – Boxplots of the minimum values and the number of drought events of the historical (HIST), and simulated (RCP 4.5 and RCP 8.5) series.

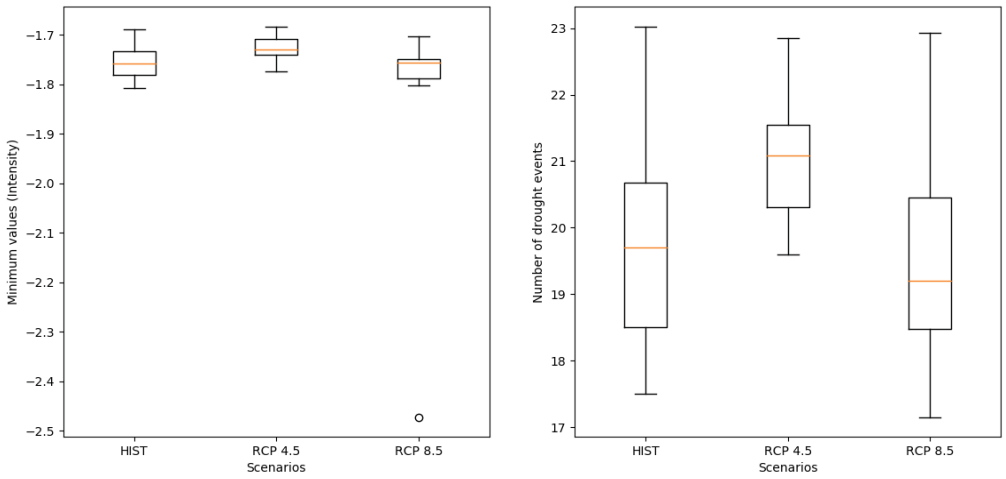

Font: Author.

Figure 40 presents the boxplots of the minimum values and the number of drought events of both historical (HIST) and simulated (RCP 4.5 and RCP 8.5) series. The minimum values (left image) situate between -1.7 and -1.8 and the RCP 8.5 scenario presented an outlier (between -2.4 and -2.5), represented by a circle. The median values (orange lines) remain in the same range (-1.7 and -1.8). Both boxes and whiskers are almost in the same range; despite there are variations in the whiskers length and the size of boxes among the three scenarios. This means the minimum values remain practically in the same range in the three scenarios, i.e., minimum values may remain constant along both future scenarios.

In the right image there is the representation of the number of drought events and according to it, there is an increase in the number of drought events in the RCP 4.5 scenario. Considering that both future series length are approximately the double size of the historical series, there are variations in the number of drought events. The simulated RCP 8.5 series presented a slight box size variation, meaning a lower interquartile values variation (between 25% and 75%). However, the RCP 4.5 presented an increase in the number of drought events, when compared to both historical and RCP 8.5 scenarios.

The superior whisker limits remained up to 23 drought events in all scenarios and the inferior whiskers differed between both future scenarios. Both median values (orange lines) are between 19 and 21 drought events in all scenarios and the median in the historical scenario is around 20 drought events. There is an increase in the number of drought events in the RCP 4.5 scenario, which presented 21 events. The RCP 8.5 presented a slight decrease in the median values (orange line), when compared to the historical scenario. If adopted the RCP 4.5 scenario, there may have more drought events along the twenty-first century.

Figure 41 – Boxplots of the drought frequency of -1.5 threshold (severe droughts) of the historical (HIST), and simulated (RCP 4.5 and RCP 8.5) series.

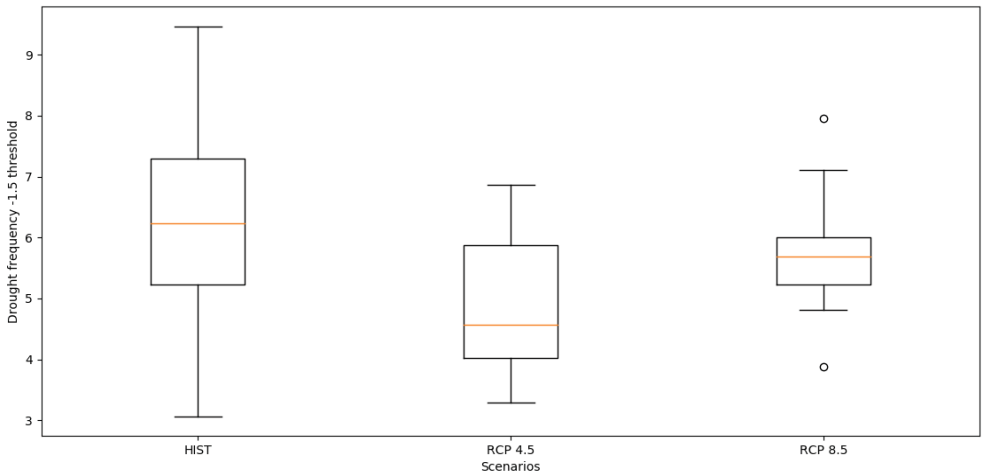

Font: Author.

Figure 41 represents the boxplots of drought frequency for -1.5 threshold (severe droughts) of both historical (HIST) and simulated (RCP 4.5 and RCP 8.5) series. The historical period presented a similar box size, when compared to the RCP 4.5 scenario. The RCP 8.5

presented a decrease, when compared to both historical and RCP 4.5 scenarios. The severe drought occurrence frequency is higher in the historical scenario than in both future scenarios, perhaps because of the length of the record. The occurrence median reduced in both future (RCP 4.5 and RCP 8.5) scenarios, dropping from around 6.2% to around 4.7% in the RCP 4.5 scenario. This means a reduction in the frequency of severe or extreme droughts in the future. In the RCP 8.5 scenario, there is a small reduction in the medians (orange lines), from 6.2% to 5.7%, approximately. There are two outliers in the RCP 8.5 scenario and in the historical series; the whiskers are larger when compared to both future scenarios, meaning the severe drought frequency is larger in the historical series.

5.3. Chapter summary

This chapter presented the drought analysis results of this study for Parana State. The drought analysis occurred in two sections: (1) single meteorological non-stationary analysis and (2) Parana State overall analysis. In the first analysis, there were applied the drought indices evolution along time scales, i.e., the RDI accumulated in quarter, semester and annual scales in order to verify the drought temporal evolution and persistence. There were also applied the difference found between the historical period and both RCP 4.5 and RCP 8.5 future scenarios, in the main drought statistics, to verify whether there is drought increase or decrease in both future scenarios.

In the second analysis, the main statistics in the entire Parana State were computed using the Inverse Distance Weighting (IDW) interpolation technique, to perform the colours map. Also in the second analyses, all statistics were represented in boxplots for a latter comparison between the past and both future scenarios. In both analyses, there were found significant differences in the main statistics, such a general increase in both maximum and median drought magnitude and maximum drought duration in both future scenarios.

According to results presented in the first analysis, the most significant drought statistics in the stations 1 (Paranagua), 8 (Ponta Grossa), 11 (Castro) and 22 (Londrina) are number of drought events in the series, drought duration (months), maximum drought magnitude (severity), as well as occurrence frequencies and minimum values.

The RCP 4.5 series presented the worst scenario when compared to the RCP 8.5, i.e., the RCP 4.5 presented more intense drought statistics. This is a strange phenomenon because the RCP 4.5 is a moderate GHG emissions rate scenario with a decline along the twenty-first century according to the IPCC, while the RCP 8.5 is the worst scenario, where the GHG emission rates may increase until 2100.

Analyses of maps corroborate with the single station analyses, because they pointed to the same more significant drought statistics to evaluate droughts. The boxplots also highlighted that the minimum values are an important statistic for droughts evaluation in Parana State. Results showed that maximum drought duration, maximum drought magnitude and number of drought events might intensify in both future scenarios.

CONCLUSIONS

Both RDI stationary and non-stationary analyses evidenced that no extreme droughts occurred in the historical observed series and there is no projection to occur extreme droughts in the future. There are mild, moderate and severe droughts in the entire Parana State at some periods of both historical and future (RCP 4.5 and RCP 8.5) scenarios.

Droughts may become more intense along the future and the RCP 4.5 scenario may be the worst future scenario, when compared to the RCP 8.5 scenario. This is contradictory with the literature and common sense, since the worst scenario should be the RCP 8.5 and the RCP 4.5 should be a milder scenario. The RCP 4.5 considers a Greenhouse Gases (GHG) reduction after 2050, while the RCP 8.5 considers a constant increase in the GHG emission rates since 2000 until 2100. This fact highlights the importance in evaluating these Regional Climate Models scenarios (RCP 4.5 and RCP 8.5), before applying them in any research.

Drought statistics pointed to worse droughts in the RCP 4.5 scenario, when compared to the historical scenario, as shown by variation in maximum drought magnitude, drought duration and moderate to severe drought occurrence frequencies. Other statistics reproduced well the drought phenomena, like the minimum values, drought occurrence frequency and both mean and median drought magnitude. The minimum values did not present large differences in the future scenarios. The overall statistics mean that droughts may become worse in terms of duration and magnitude.

Paranagua, Ponta Grossa, Castro and Londrina stations pointed to non-stationarity in the historical series, being analysed in the non-stationary drought analysis approach. These historical series presented non-stationarity only in the 3- and/or 6-month accumulation periods.

The non-stationary drought analysis pointed to significant differences mainly in the minimum values viewed in the ordinate axis of the RDI graph, when compared to the stationary traditional drought analysis. Most stations produced droughts underestimation in the first split and droughts overestimation in the second split using the proposed method. The non-stationary approach improved the drought analysis because it also presented differences in drought occurrences (e.g. in the stationary approach there was no drought, while in the non-stationary approach there was drought, and vice-versa). The proposed method also produced differences in drought duration, and consequently, in drought magnitude.

These differences highlight the importance in performing the non-stationary drought analysis since droughts may be worse or milder, if adopting the traditional stationary gamma fitting.

The future simulated RCP 4.5 scenario presented non-stationarity in some stations in the 3-month and/or 6-month accumulation periods. For these stations, in the 12-, 24-, 36-, 48- and 60-month accumulation periods, the stationarity hypothesis could not be rejected. However, the RCP 8.5 scenario presented non-stationarity in practically all 34 stations in the 3-, 6-, 12-month accumulation periods, except the stations Palmas and Clevelandia, which are stationary. The remaining 24-, 36-, 48- and 60-month accumulation periods presented either stationarity or non-stationarity in the series.

The monthly precipitation and temperature series presented non-stationarity in some stations in the historical period. However, both future RCP 4.5 and RCP 8.5 scenarios presented non-stationarity for the temperature series and for a great number of the precipitation series. Some series presented only changing point, while others presented both trend and changing point. When changing point was observed in some accumulation period, the non-stationary statistic models were split at the changing point.

In the 30-period moving window analysis, the parameter temporal variation presented a decrease in the shape parameter. However, both location and scale parameters presented a significant increase. The minimum values presented an increasing trend leading to the conclusion that droughts tend to intensify at the end of the series.

The RDI is the most suitable index to apply in the study region (Parana State) due to its performance in representing the drought phenomena and best fittings of the gamma distribution (stationary and non-stationary). Both Standardized Precipitation Index (SPI) and Standardized Precipitation Evapotranspiration Index (SPEI) were applied in this research, and due to the great data amount generated, they were discarded. For this reason, only the RDI graphs and analyses are shown in this dissertation.

Some methods applied in this research and not considered in the final version were both Quantile-Quantile (QQ) and Delta Change (DT) bias correction, Multiple Linear Regression (MLR) for filling in the gaps, and Blaney-Criddle for potential evapotranspiration computation. Both QQ and DT generated the worst Mean Absolute Error (MAE) coefficients. The MLR computation generated no significant correlation between the neighbouring stations and the

Blaney-Criddle method was discarded due to its difficulty in adequately represent the future crop coefficient. The Hargreaves method was not considered because it relies on the assumption of one more variable, radiation and the Thornthwaite requires only both temperature and daylight length, being widely applied in drought studies worldwide. There is no record of the use of the Priestley and Taylor evapotranspiration method for drought analysis.

Other potential evapotranspiration widely applied methods such Penman-Monteith require many data, which are not available for all station in Parana State, and were discarded. The application of other methods to estimate the gamma distribution parameters did not improve the results. The methods investigated were the L-Moments and the Method of Moments. The GEV distribution presented the worst fit for monthly and the seven accumulation periods (3, 6, 12, 24, 36, 48, and 60 months) and was discarded from further analysis.

There is only one outlier of the extreme drought in the Parana State (RDI lower than -2.0 in the standardized form) in the RCP 8.5 scenario (minimum values boxplot). The general results showed a minimum of about -1.85 in all stations and scenarios (past and future). A very close -2.0 value occurred in the 30-period moving window analysis.

Another important aspect is the non-stationarity may have several origins, such land use change. There is not a climate model that considers this variable in the moment for future climate projections to study climate change impacts. Due to this current restriction, it is difficult to analyse the stationarity in some historical series, since it is expected that global climate change impacts generate non-stationarity in historical series. This is a complex discussion and may be treated in a close future.

This dissertation focused in analysing droughts in a non-stationary premise and the application of this method in climate change scenarios for the future. It is important do predict and forecast the climate on Earth in order to take mitigation measures, as well as for a better planning and management of the water resources, even in the close future, all predictions and forecasts prove the contrary. The error is an inherent premise in both prediction and forecasting studies. Both prediction and forecasting model results can be affected by socioeconomic crises.

It was shown that for general drought analysis, there is a need to perform the non-stationary analysis. The right choice in drought modelling allows the knowledge and understanding the potential impacts of droughts for a better planning and management of water resources, minimizing the risk and shortcoming for economy and society from droughts.

RECOMMENDATIONS

In order to improve this study, some methods and analyses as well as more data collection recommendations for further development are described, for future studies about droughts.

Other methods to compute the Potential Evapotranspiration (PET) may be used for comparison with the Thornthwaite method, to check the effect of the solar radiation and other weather variables in the PET series. It is also recommended to perform the non-stationary drought analysis using both Standardized Precipitation Index (SPI) and Standardized Precipitation Evapotranspiration Index (SPEI), as well as the Palmer Drought Severity Index (PDSI), and other drought indices to compare with the results obtained in this study.

Another recommendation is to apply the methods of this study in the Northeast Brazilian (NEB) region, performing the non-stationary drought analysis, improving several stationary drought studies in that region. Non-stationary drought analysis focusing on developing drought indices for streamflow and runoff records, as well as for low flow indices is another recommendation for future studies.

Other possible improvements in this study are the application of other methods for filling in the gaps in the historical series, like the average pondering by inverse distance weighting. Application of the Mann-Whitney (Wilcoxon) test to both historical and simulated series, to verify stationarity is another recommendation. Also alternative estimators for the probability distributions parameters such as the Probability Weighted Moments (PWM) should be tested and confronted with the method used in this dissertation (Maximum Likelihood method), is another suggestion.

Future drought periods may be classified per decade in order to compare these scenarios with meteorological phenomena (e.g. ENSO, PDO, AMO, and others) and perform a more robust drought analysis.

Due to the significant impact related to drought events, as described in the first chapter of this dissertation, it is also important to predict and forecast droughts. To do this, forecasting/prediction models for filling in the gaps or forecasting analyses using Autoregressive Conditional Heteroscedasticity (ARCH) and Generalized Autoregressive Conditional Heteroscedasticity (GARCH), are other future application.

In the future series, it is suggested to split the simulated scenarios (RCP 4.5 and RCP 8.5) in past/present (January of 2006 to December of 2040), mid future (January of 2041 to December of 2070) and far future (January of 2071 to December of 2099). This can provide more severe drought evaluation per periods and perform a posterior comparison with the IPCC reports. Also testing different Global Climate Models (GCM) or Regional Climate Models (RCM) to forecast precipitation and/or temperature and their later comparison would be useful and may give some guess about the precision of these models.

Another suggestion for future studies is related to the simulated scenarios uncertainties, since different RCM scenarios can generate different results in the same study region. It is recommendable to apply this dissertation method with other RCM or GCM scenarios and analyse the uncertainties inherent to each model application.

This dissertation method focused in detecting the changing point using the Pettitt test in the accumulated Reconnaissance Drought Index (RDI) series to perform the non-stationary approach. The non-stationarity detection can occur using only the Mann-Kendall test. In this way, another suggestion for future studies is to perform a non-stationary analysis using the non-significant changing point of the Pettitt test application, i.e., use the changing point even when the p-value is above the 0.05 (5% probability significance to reject the null hypothesis and accept there is non-stationarity in the series).

In relation to the gamma parameter series resulted of the 30-period moving window analysis, another suggestion for future studies is the application of both trend and changing point tests in the gamma parameter series to detect abrupt changes and trends in these series. It is also recommendable to compute the statistical quality of trust intervals of these series and also in both two non-stationary gamma fits and stationary approach.

It is important to highlight that the main goal of this dissertation is performing a non-stationary drought analysis in climate change scenarios. For this reason, it was applied the Simple Linear Regression (SLR) for filling in the gaps as a parsimonious method and hence, compute the non-stationary RDI approach. It might be interesting to apply other methods for filling in the gaps, such machine learning methods in future studies.

Another future studies recommendation is the discussion of this dissertation results with the drought reports in the hydroelectricity.

Finally, a comparison of this dissertation results with a Generalized Addictive Models for Location, Scale and Shape (GAMLSS) model to verify its performance is another recommendation for future study.

REFERENCES

ABARE. **Australian Crop Production Report**. 2008.

ACHILLEOS, G. A. The Inverse Distance Weighted interpolation method and error propagation mechanism - creating a DEM from an analogue topographical map. **Journal of Spatial Science**, v. 56, n. 2, p. 283–304, 2011.

AGILAN, V.; UMAMAHESH, N. V. What are the best covariates for developing non-stationary rainfall Intensity-Duration-Frequency relationship? **Advances in Water Resources**, v. 101, p. 11–22, 2017. Elsevier Ltd.

AHMADALIPOUR, A.; MORADKHANI, H.; DEMIREL, M. C. A comparative assessment of projected meteorological and hydrological droughts: Elucidating the role of temperature. **Journal of Hydrology**, v. 553, p. 785–797, 2017. Elsevier B.V. Disponível em: <http://dx.doi.org/10.1016/j.jhydrol.2017.08.047>. .

AHMED, K.; SHAHID, S.; NAWAZ, N. Impacts of climate variability and change on seasonal drought characteristics of Pakistan. **Atmospheric Research**, v. 214, n. August, p. 364–374, 2018. Elsevier. Disponível em: <https://doi.org/10.1016/j.atmosres.2018.08.020>. .

ALLEY, W. M. The Palmer Drought Severity Index: Limitations and Assumptions. **Journal of Climate and Applied Meteorology**, v. 23, n. July, p. 1100–1109, 1984. Reston, VA.

ALVARES, C. A.; STAPE, J. L.; SENTELHAS, P. C.; DE MORAES GONÇALVES, J. L.; SPAROVEK, G. Köppen's climate classification map for Brazil. **Meteorologische Zeitschrift**, v. 22, n. 6, p. 711–728, 2013.

AMENGUAL, A.; HOMAR, V.; ROMERO, R.; ALONSO, S.; RAMIS, C. A statistical adjustment of regional climate model outputs to local scales: Application to Platja de Palma, Spain. **Journal of Climate**, v. 25, n. 3, p. 939–957, 2012.

AMIN, M.; ZARCH, A.; SIVAKUMAR, B.; SHARMA, A. Droughts in a warming climate : A global assessment of Standardized precipitation index (SPI) and Reconnaissance drought index (RDI). **Journal of Hydrology**, v. 526, p. 183–195, 2015. Elsevier B.V. Disponível em: <http://dx.doi.org/10.1016/j.jhydrol.2014.09.071>. .

ANEEL. BIGANEEL - Banco de Informações de Geração da Agência Nacional de Energia Elétrica. , 2018. Brasília: ANEEL. Disponível em: <https://www2.aneel.gov.br/aplicacoes/capacidadebrasil/capacidadebrasil.cfm>. .

APARECIDO, L. E. DE O.; ROLIM, G. DE S.; RICHETTI, J.; DE SOUZA, P. S.; JOHANN, J. A.

Köppen, Thornthwaite and Camargo climate classifications for climatic zoning in the State of Paraná, Brazil. **Ciencia e Agrotecnologia**, v. 40, n. 4, p. 405–417, 2016.

ASADI ZARCH, M. A.; SIVAKUMAR, B.; SHARMA, A. Droughts in a warming climate: A global assessment of Standardized precipitation index (SPI) and Reconnaissance drought index (RDI). **Journal of Hydrology**, v. 526, p. 183–195, 2015. Elsevier B.V. Disponível em: <http://dx.doi.org/10.1016/j.jhydrol.2014.09.071>. .

AZEVEDO, L. C. DE; NERY, J. T.; ANDRADE, A. R. DE. **Análise da precipitação pluvial da bacia do rio Iguaçu-Parana**, 2006. Universidade Estadual de Maringá.

BACK, Á. J. Aplicação de análise estatística para identificação de tendências climáticas. **Pesquisa Agropecuária Brasileira**, v. 36, n. 5, p. 717–726, 2001.

BARBOSA, H. A.; LAKSHMI KUMAR, T. V. Influence of rainfall variability on the vegetation dynamics over Northeastern Brazil. **Journal of Arid Environments**, v. 124, p. 377–387, 2016. Elsevier Ltd. Disponível em: <http://dx.doi.org/10.1016/j.jaridenv.2015.08.015>. .

BARROS, V.; CLARKE, R.; DIAS, P. S. **Climate change in the La Plata Basin**. Inter American Institute on Global Change, 2011.

BARROS, V.; GONZALEZ, M.; LIEBMANN, B.; CAMILLONI, I. Influence of the South Atlantic convergence zone and South Atlantic Sea surface temperature on interannual summer rainfall variability in Southeastern South America. **Theoretical and Applied Climatology**, v. 67, n. 3–4, p. 123–133, 2000.

BONDARIK, R.; KOVALESKI, J. L.; PILATTI, L. A. A Produção de Erva-Mate e a Iniciação Industrial do Paraná . **Congresso Internacional de Administração**, v. 19°, 2006.

BUCHIR, L. M. S. T. **Análise da influência de mudanças climáticas nas precipitações**, 2013. Universidade Federal do Paraná.

BYAKATONDA, J.; PARIDA, B. P.; MOALAFHI, D. B.; KENABATHO, P. K. Analysis of long term drought severity characteristics and trends across semiarid Botswana using two drought indices. **Atmospheric Research**, v. 213, n. July, p. 492–508, 2018. Elsevier. Disponível em: <https://doi.org/10.1016/j.atmosres.2018.07.002>. .

CANAMBRA ENGINEERING CONSULTANTS LIMITES. **Estudos Energéticos da Região Centro-Sul do Brasil – Sumário do Relatório Final**. 1967.

CANAMBRA ENGINEERING CONSULTANTS LIMITES. **Estudos Energéticos da Região Sul do Brasil – Sumário do Relatório Final**. 1969.

CEBRIÁN, A. C.; ABAURREA, J. Risk measures for events with a stochastic duration: An application

to drought analysis. **Stochastic Environmental Research and Risk Assessment**, v. 26, n. 7, p. 971–981, 2012.

CHATTOPADHYAY, S.; EDWARDS, D. R.; YU, Y.; HAMIDISEPEHR, A. An Assessment of Climate Change Impacts on Future Water Availability and Droughts in the Kentucky River Basin. **Environmental Processes**, v. 4, n. 3, p. 477–507, 2017. Environmental Processes.

CHEN, J.; BRISSETTE, F. P.; LECONTE, R.; CHEN. Uncertainty of downscaling method in quantifying the impact of climate change on hydrology. **Journal of Hydrology**, v. 401, n. 3–4, p. 190–202, 2011. Elsevier B.V. Disponível em: <http://dx.doi.org/10.1016/j.jhydrol.2011.02.020>. .

CHENG, L.; AGHAKOUCHAK, A. Nonstationary Precipitation Intensity-Duration-Frequency Curves for Infrastructure Design in a Changing. **Scientific Reports**, v. 7093, n. 4, p. 1–6, 2014.

CISLAGHI, M.; DE MICHELE, C.; GHEZZI, A.; ROSSO, R. Statistical assessment of trends and oscillations in rainfall dynamics: Analysis of long daily Italian series. **Atmospheric Research**, v. 77, n. 1-4 SPEC. ISS., p. 188–202, 2005.

CLARK, P. U.; ALLEY, R. B.; POLLARD, D. Global Climate Change. **Science's compass**, v. 286, n. November, p. 1104–1111, 1999.

COLLISCHONN, W.; MARENGO, J. A.; MARANGON LIMA, L. M. **Impacto das mudanças climáticas na geração hidrelétrica**. 1º ed. Brasília, DF, 2014.

COMEC (COMMISSION OF THE EUROPEAN COMMUNITIES). **Communication from the commission to the European parliament and the council: addressing the challenge of water scarcity and droughts in the European Union**. Brussels, 2007.

COSCARELLI, R.; CALOIERO, T. Analysis of daily and monthly rainfall concentration in Southern Italy (Calabria region). **Journal of Hydrology**, v. 416–417, p. 145–156, 2012. Elsevier B.V. Disponível em: <http://dx.doi.org/10.1016/j.jhydrol.2011.11.047>. .

DAI, A. Drought under global warming: A review. **Wiley Interdisciplinary Reviews: Climate Change**, v. 2, n. 1, p. 45–65, 2011.

DERECZYNSKI, C. P.; VINICIUS, M.; PRISTO, D. J.; et al. Anuário do Instituto de Geociências - UFRJ Avaliação das Previsões do Modelo Eta na Região da Serra do Mar (Estado de São Paulo), Brasil Evaluation of Eta Model Forecasts at Serra do Mar Region (São Paulo State), Brazil Os modelos numéricos regionais. **Anuário do Instituto de Geociências - UFRJ**, v. 33, n. 2, p. 36–51, 2010.

DETZEL, D. H. M. **Modelagem De Séries Hidrológicas : Uma Abordagem De Múltiplas Escalas Temporais**, 2015. Universidade Federal do Paraná.

DETZEL, D. H. M.; FILHO, L. R. M.; RANGEL, L. M. Á.; BESSA, M. R.; GEUS, K. DE. Acerca Do Período Crítico Das Usinas Hidrelétricas Brasileiras. XXIII SIMPÓSIO BRASILEIRO DE RECURSOS HIDRÍCOS ACERCA. **Anais...** . p.1–10, 2019. Foz do Iguaçu, PR.

DIFFENBAUGH, N. S.; ASHFAQ, M. Intensification of hot extremes in the United States. **Geophysical Research Letters**, v. 37, n. 15, 2010.

DUBROVSKY, M.; SVOBODA, M. D.; TRNKA, M.; et al. Application of relative drought indices in assessing climate-change impacts on drought conditions in Czechia. **Theoretical and Applied Climatology**, v. 96, n. 1–2, p. 155–171, 2009.

ENGSTRÖM, J.; WAYLEN, P. The changing hydroclimatology of Southeastern U.S. **Journal of Hydrology**, v. 548, p. 16–23, 2017.

FANG, G. H.; YANG, J.; CHEN, Y. N.; ZAMMIT, C. Comparing bias correction methods in downscaling meteorological variables for a hydrologic impact study in an arid area in China. **Hydrology and Earth System Sciences**, v. 19, n. 6, p. 2547–2559, 2015.

FILL, H. D.; MINE, M. R. M.; FERNANDES, C. V. S.; BESSA, M. R. Impact of climate change on hydropower production within the La Plata Basin. **International Journal of River Basin Management**, v. 11, n. 4, p. 449–462, 2013. Taylor & Francis. Disponível em: <http://dx.doi.org/10.1080/15715124.2013.865638>. .

FU, G.; YU, J.; YU, X.; et al. Temporal variation of extreme rainfall events in China, 1961-2009. **Journal of Hydrology**, v. 487, p. 48–59, 2013. Elsevier B.V. Disponível em: <http://dx.doi.org/10.1016/j.jhydrol.2013.02.021>. .

GIRALDO OSORIO, J. D.; GARCÍA GALIANO, S. G. Non-stationary analysis of dry spells in monsoon season of Senegal River Basin using data from Regional Climate Models (RCMs). **Journal of Hydrology**, v. 450–451, n. 2012, p. 82–92, 2012. Elsevier B.V. Disponível em: <http://dx.doi.org/10.1016/j.jhydrol.2012.05.029>. .

GLADSTONE RODRIGUES, A.; MÁRCIO BENEDITO, B.; MAURO, N. Estudo para Identificação de Tendências do Regime Pluvial na Região Metropolitana de Belo Horizonte a Partir de Métodos Estatísticos. **Revista Brasileira de Recursos Hídricos**, v. 15, n. 2, p. 115–126, 2010.

GOCIC, M.; TRAJKOVIC, S. Analysis of precipitation and drought data in Serbia over the period 1980-2010. **Journal of Hydrology**, v. 494, p. 32–42, 2013. Elsevier B.V. Disponível em: <http://dx.doi.org/10.1016/j.jhydrol.2013.04.044>. .

GROPPO, J. F.; MILDE, L. C. E.; GUAMERO, M. E.; MORAES, J. M. DE; MARTINELLI, L. A. Análise de Séries Temporais de Vazão e de Precipitação na Bacia do Rio Piracicaba. **Revista de Ciência**

e Tecnologia, , n. v.8, nº18, p. 109–117, 2001.

GU, L.; CHEN, J.; XU, C. Y.; et al. The contribution of internal climate variability to climate change impacts on droughts. **Science of the Total Environment**, v. 684, p. 229–246, 2019. Elsevier B.V. Disponível em: <https://doi.org/10.1016/j.scitotenv.2019.05.345>. .

GU, X.; ZHANG, Q.; SINGH, V. P.; CHEN, X.; LIU, L. Nonstationarity in the occurrence rate of floods in the Tarim River basin, China, and related impacts of climate indices. **Global and Planetary Change**, v. 142, p. 1–13, 2016. Elsevier B.V. Disponível em: <http://dx.doi.org/10.1016/j.gloplacha.2016.04.004>. .

GÜÇLÜ, Y. S. Multiple Şen-innovative trend analyses and partial Mann-Kendall test. **Journal of Hydrology**, v. 566, n. September, p. 685–704, 2018. Elsevier. Disponível em: <https://doi.org/10.1016/j.jhydrol.2018.09.034>. .

GUO, Y.; HUANG, S.; HUANG, Q.; et al. Assessing socioeconomic drought based on an improved Multivariate Standardized Reliability and Resilience Index. **Journal of Hydrology**, v. 568, n. August 2018, p. 904–918, 2019. Elsevier. Disponível em: <https://doi.org/10.1016/j.jhydrol.2018.11.055>. .

GUPTA, V.; JAIN, M. K. Investigation of multi-model spatiotemporal mesoscale drought projections over India under climate change scenario. **Journal of Hydrology**, v. 567, n. October, p. 489–509, 2018. Elsevier. Disponível em: <https://doi.org/10.1016/j.jhydrol.2018.10.012>. .

GUTTMAN, N. B. Comparing the PDSI and SPI. **Journal of the American Water Resources Association**, v. 34, n. 1, p. 113–121, 1998.

HAO, Z.; AGHAKOUCHAK, A. Multivariate Standardized Drought Index: A parametric multi-index model. **Advances in Water Resources**, v. 57, p. 12–18, 2013. Elsevier Ltd. Disponível em: <http://dx.doi.org/10.1016/j.advwatres.2013.03.009>. .

HAO, Z.; HAO, F.; SINGH, V. P.; XIA, Y.; et al. A theoretical drought classification method for the multivariate drought index based on distribution properties of standardized drought indices. **Advances in Water Resources**, v. 92, p. 240–247, 2016. Elsevier Ltd.

HAO, Z.; HAO, F.; SINGH, V. P.; et al. A multivariate approach for statistical assessments of compound extremes. **Journal of Hydrology**, v. 565, n. August, p. 87–94, 2018. Elsevier. Disponível em: <https://doi.org/10.1016/j.jhydrol.2018.08.025>. .

HAO, Z.; HAO, F.; SINGH, V. P.; SUN, A. Y.; XIA, Y. Probabilistic prediction of hydrologic drought using a conditional probability approach based on the meta-Gaussian model. **Journal of Hydrology**, v. 542, p. 772–780, 2016. Elsevier B.V. Disponível em: <http://dx.doi.org/10.1016/j.jhydrol.2016.09.048>. .

HAO, Z.; SINGH, V. P. Drought characterization from a multivariate perspective: A review. **Journal of Hydrology**, v. 527, p. 668–678, 2015. Elsevier B.V. Disponível em: <http://dx.doi.org/10.1016/j.jhydrol.2015.05.031>. .

HEIM, R. R. A review od the 21th century drought indices used in the United States. **American Metereological Society**, , n. August, p. 1149–1166, 2002.

HOERLING, M. P.; EISCHEID, J. K.; QUAN, X. W.; et al. Is a transition to semipermanent drought conditions imminent in the U.S. **Journal of Climate**, v. 25, p. 8380–8386, 2012.

HUANG, S.; LI, P.; HUANG, Q.; et al. The propagation from meteorological to hydrological drought and its potential influence factors. **Journal of Hydrology**, v. 547, p. 184–195, 2017. Elsevier B.V. Disponível em: <http://dx.doi.org/10.1016/j.jhydrol.2017.01.041>. .

IBGE. **Dados estatísticos do Paraná**. Rio de Janeiro, Rio de Janeiro, 2019.

IPARDES. Base de dados do Estado. Disponível em: <http://www.ipardes.pr.gov.br/Pagina/Parana-em-Numeros>. .

IPCC. Evaluation of Climate Models. **IPCC Climate Change**. v. 9, p.741–866, 2013.

JAY L. DEVORE. **Probability statistics for engineering and the sciences**. 4th ed. Boston, US: Brooks Cole, 2010.

JOHNSON, F.; SHARMA, A. What are the impacts of bias correction on future drought projections? **Journal of Hydrology**, v. 525, p. 472–485, 2015. Elsevier B.V.

DE JONG, P.; BARRETO, T. B.; TANAJURA, C. A. S.; et al. Estimating the impact of climate change on wind and solar energy in Brazil using a South American regional climate model. **Renewable Energy**, v. 141, p. 390–401, 2019. Elsevier Ltd. Disponível em: <https://doi.org/10.1016/j.renene.2019.03.086>. .

KANG, H.; SRIDHAR, V. Combined statistical and spatially distributed hydrological model for evaluating future drought indices in Virginia. **Journal of Hydrology: Regional Studies**, v. 12, n. January, p. 253–272, 2017. Elsevier. Disponível em: <https://doi.org/10.1016/j.ejrh.2017.06.003>. .

KENDALL, M. G.; STUART, A. **The Advanced Theory of Statistics**. 2nd ed. Glasgow: American Statistical Association, 1963.

KHADR, M. Forecasting of meteorological drought using Hidden Markov Model (case study: The upper Blue Nile river basin, Ethiopia). **Ain Shams Engineering Journal**, v. 7, n. 1, p. 47–56, 2016. Faculty of Engineering, Ain Shams University. Disponível em: <http://dx.doi.org/10.1016/j.asej.2015.11.005>. .

KIRONO, D. G. C.; KENT, D. M.; HENNESSY, K. J.; MPELASOKA, F. Characteristics of Australian droughts under enhanced greenhouse conditions: Results from 14 global climate models. **Journal of Arid Environments**, v. 75, n. 6, p. 566–575, 2011. Elsevier Ltd. Disponível em: <http://dx.doi.org/10.1016/j.jaridenv.2010.12.012>. .

KOGAN F.N. Global Drought Watch from Space. **Bulletin of the American Meteorological Society**, v. 7, n. 8, p. 621–636, 1997.

KOPSIAFTIS, G.; TIGKAS, D.; CHRISTELIS, V.; VANGELIS, H. Assessment of drought impacts on semi-arid coastal aquifers of the Mediterranean. **Journal of Arid Environments**, v. 137, p. 7–15, 2017.

KOUSARI, M. R.; DASTORANI, M. T.; NIAZI, Y.; et al. Trend Detection of Drought in Arid and Semi-Arid Regions of Iran Based on Implementation of Reconnaissance Drought Index (RDI) and Application of Non-Parametrical Statistical Method. **Water Resources Management**, v. 28, n. 7, p. 1857–1872, 2014.

KOUTSOYIANNIS, D. Nonstationarity versus scaling in hydrology. **Journal of Hydrology**, v. 324, n. 1–4, p. 239–254, 2006.

LANA, X.; SERRA, C.; BURGUEÑO, A. Patterns of monthly rainfall shortage and excess in terms of the standardized precipitation index for Catalonia (NE Spain). **International Journal of Climatology**, v. 21, n. 13, p. 1669–1691, 2001.

LENDERINK, G.; BUISHAND, A.; DEURSEN, W. VAN. Estimates of future discharges of the river Rhine using two scenario methodologies: direct versus delta approach. **Hydrology and Earth System Sciences**, v. 3, n. 11, p. 1145–1159, 2007.

LI, B.; LIANG, Z.; ZHANG, J.; WANG, G. A revised drought index based on precipitation and pan evaporation. **International Journal of Climatology**, v. 37, n. 2, p. 793–801, 2017.

LI, H.; WANG, D.; SINGH, V. P.; et al. Non-stationary frequency analysis of annual extreme rainfall volume and intensity using Archimedean copulas: A case study in eastern China. **Journal of Hydrology**, v. 571, n. May 2018, p. 114–131, 2019. Elsevier. Disponível em: <https://doi.org/10.1016/j.jhydrol.2019.01.054>. .

LI, J.; ZHOU, S.; HU, R. Hydrological drought class transition using SPI and SRI time series by loglinear regression. **Water Resources Management**, v. 30, n. 2, p. 669–684, 2016.

LIANG, L.; LI, L.; LIU, Q. Precipitation variability in Northeast China from 1961 to 2008. **Journal of Hydrology**, v. 404, n. 1–2, p. 67–76, 2011. Elsevier B.V. Disponível em: <http://dx.doi.org/10.1016/j.jhydrol.2011.04.020>. .

LIU, Y.; ZHU, Y.; REN, L.; et al. On the mechanisms of two composite methods for construction of

multivariate drought indices. **Science of the Total Environment**, v. 647, p. 981–991, 2019. Elsevier B.V. Disponível em: <https://doi.org/10.1016/j.scitotenv.2018.07.273>. .

LLOYD-HUGHES, B.; SAUNDERS, M. A. A drought climatology for Europe. **International Journal of Climatology**, v. 22, n. 13, p. 1571–1592, 2002.

VAN LOON, A. F. No Title. , 2015.

VAN LOON, A. F.; LAAHA, G. Hydrological drought severity explained by climate and catchment characteristics. **Journal of Hydrology**, v. 526, p. 3–14, 2015. Elsevier B.V. Disponível em: <http://dx.doi.org/10.1016/j.jhydrol.2014.10.059>. .

VAN LOON, A. F.; VAN LANEN, H. A. J. Making the distinction between water scarcity and drought using an observation-modeling framework. **Water Resources Research**, v. 49, n. 3, p. 1483–1502, 2013.

LPB, C. Project Final Report. , 2012. Institut de Recherche pour le Dévelopement.

LU, Y.; CAI, H.; JIANG, T.; et al. Assessment of global drought propensity and its impacts on agricultural water use in future climate scenarios. **Agricultural and Forest Meteorology**, v. 278, n. June, p. 107623, 2019. Elsevier. Disponível em: <https://linkinghub.elsevier.com/retrieve/pii/S016819231930231X>. .

LUCENA, A. F. P.; KOBER, T.; KÖBERLE, A. C.; et al. Interactions between climate change mitigation and adaptation: The case of hydropower in Brazil. **Energy**, v. 164, p. 1161–1177, 2018.

MAACK, R. **Geografia física do Estado do Paraná**. 3rd ed. ed. Curitiba: Imprensa Oficial do Paraná, 2002.

MAITY, R.; SUMAN, M.; VERMA, N. K. Drought prediction using a wavelet based approach to model the temporal consequences of different types of droughts. **Journal of Hydrology**, v. 539, p. 417–428, 2016. Elsevier B.V. Disponível em: <http://dx.doi.org/10.1016/j.jhydrol.2016.05.042>. .

MANN, H. B. Nonparametric Tests Against Trend. **Econometrica**, v. 13, n. 3, p. 245–259, 1945.

MARCOS-GARCIA, P.; LOPEZ-NICOLAS, A.; PULIDO-VELAZQUEZ, M. Combined use of relative drought indices to analyze climate change impact on meteorological and hydrological droughts in a Mediterranean basin. **Journal of Hydrology**, v. 554, p. 292–305, 2017. Elsevier B.V. Disponível em: <https://doi.org/10.1016/j.jhydrol.2017.09.028>. .

MARENGO, J. A. Mudancas climaticas globais e regionais: Avaliacion do clima atual do Brasil e projecoes de cenarios climaticos do futuro. **Revista Brasileira de Meteorologia**, v. 16, n. 1, p. 1–18, 2001.

MARENGO, J. A.; TOMASELLA, J.; UVO, C. R. Trends in streamflow and rainfall in tropical South America: Amazonia, eastern Brazil, and norwestern Peru. **Journal of Geophysical Research**, v. 103, n. D2, p. 1775–1783, 1998.

MARENGO, J. A.; TORRES, R. R.; ALVES, L. M. Drought in Northeast Brazil - past, present, and future. **Theoretical and Applied Climatology**, v. 129, n. 3–4, p. 1189–1200, 2017. Theoretical and Applied Climatology. Disponível em: <http://dx.doi.org/10.1007/s00704-016-1840-8>. .

MATALAS, N. C. Stochastic hydrology in the context of climate change. **Climatic Change**, 1997.

MCKEE, T. B.; DOESKEN, N. J.; KLEIST, J. The relationship of drought frequency and duration to time scales. In: Proceedings of the Eighth Conference on Applied Climatology, Anaheim, CA. **American Metereological Society**, , n. Boston, p. 179–184, 1993.

MCKERNAN, M. **Drought. The Red Marauder**. Crows Nest, NSW, Australia, 2005.

MEINSHAUSEN, M.; SMITH, S. J.; CALVIN, K.; et al. The RCP greenhouse gas concentrations and their extensions from 1765 to 2300. **Climatic Change**, v. 109, n. 1, p. 213–241, 2011.

MESCHIATTI, M. C.; FONTOLAN, M. R.; HELENA, D.; FERREIRA, L. Caracterização estatística de tendências em séries anuais de dados hidro-climáticos no estado de são paulo statistical characterization of trends in annual series of hydro-climatic data in the state of são paulo, brazil. **Revista de Geografia Acad^emica**, v. 6(1), p. 52–64, 2012.

MISHRA, A. K.; SINGH, V. P. Analysis of drought severity-area-frequency curves using a general circulation model and scenario uncertainty. **Journal of Geophysical Research Atmospheres**, v. 114, n. 6, p. 1–18, 2009.

MISHRA, A. K.; SINGH, V. P. A review of drought concepts. **Journal of Hydrology**, v. 391, n. 1–2, p. 202–216, 2010. Elsevier B.V. Disponível em: <http://dx.doi.org/10.1016/j.jhydrol.2010.07.012>. .

MISHRA, A. K.; SINGH, V. P. Drought modeling - A review. **Journal of Hydrology**, v. 403, n. 1–2, p. 157–175, 2011. Elsevier B.V. Disponível em: <http://dx.doi.org/10.1016/j.jhydrol.2011.03.049>. .

MMA, M. DO M. A. Cadastro nacional de unidades de conservação. , 2016. Brasília, DF: Ministério do mio ambiente.

MODARRES, R.; SARHADI, A.; BURN, D. H. Changes of extreme drought and flood events in Iran. **Global and Planetary Change**, v. 144, p. 67–81, 2016. Elsevier B.V. Disponível em: <http://dx.doi.org/10.1016/j.gloplacha.2016.07.008>. .

MOHAMMED, R.; SCHOLZ, M. Impact of Evapotranspiration Formulations at Various Elevations on the Reconnaissance Drought Index. **Water Resources Management**, v. 31, n. 1, p. 531–548, 2017a.

Water Resources Management. Disponível em: <http://dx.doi.org/10.1007/s11269-016-1546-9>. .

MOHAMMED, R.; SCHOLZ, M. The reconnaissance drought index: A method for detecting regional arid climatic variability and potential drought risk. **Journal of Arid Environments**, v. 144, p. 181–191, 2017b. Elsevier Ltd. Disponível em: <http://dx.doi.org/10.1016/j.jaridenv.2017.03.014>. .

MOHOR, G. S.; RODRIGUEZ, D. A.; TOMASELLA, J.; SIQUEIRA JÚNIOR, J. L. Exploratory analyses for the assessment of climate change impacts on the energy production in an Amazon run-of-river hydropower plant. **Journal of Hydrology: Regional Studies**, v. 4, n. PB, p. 41–59, 2015. Elsevier B.V.

MOREIRA, E. E.; MEXIA, J. T.; PEREIRA, L. S. Assessing homogeneous regions relative to drought class transitions using an ANOVA-like inference. Application to Alentejo, Portugal. **Stochastic Environmental Research and Risk Assessment**, v. 27, n. 1, p. 183–193, 2013.

MÜLLER, I. I.; KRUGER, C. M.; KAVISKI, E. Análise de estacionariedade de séries hidrológicas na bacia incremental de Itaipu. **Revista Brasileira de Recursos Hídricos**, v. 3, n. 4, p. 51–71, 1998.

NAGHETTINI, M.; PINTO, E. J. A. **Hidrologia Estatística**. Belo Horizonte: CPRM, 2007.

NAM, W. H.; CHOI, J. Y.; YOO, S. H.; JANG, M. W. A decision support system for agricultural drought management using risk assessment. **Paddy and Water Environment**, v. 10, n. 3, p. 197–207, 2012.

NAM, W. H.; HAYES, M. J.; SVOBODA, M. D.; TADESSE, T.; WILHITE, D. A. Drought hazard assessment in the context of climate change for South Korea. **Agricultural Water Management**, v. 160, p. 106–117, 2015. Elsevier B.V. Disponível em: <http://dx.doi.org/10.1016/j.agwat.2015.06.029>. .

VAN OEL, P. R.; MARTINS, E. S. P. R.; COSTA, A. C.; WANDERS, N.; VAN LANEN, H. A. J. Diagnosing drought using the downstreamness concept: the effect of reservoir networks on drought evolution. **Hydrological Sciences Journal**, v. 63, n. 7, p. 979–990, 2018. Taylor & Francis.

PALMER, W. C. **Meteorological Drought**. Washington, DC: U.S. Weather Bureau, 1965.

PAPOULIS, A. **Probability, random variables and stochastic processes**. Tokyo, 1965.

PARK, C. E.; JEONG, S. J.; JOSHI, M.; et al. Keeping global warming within 1.5 °c constrains emergence of aridification. **Nature Climate Change**, v. 8, n. 1, p. 70–74, 2018. Springer US. Disponível em: <http://dx.doi.org/10.1038/s41558-017-0034-4>. .

PAULO, A. A.; PEREIRA, L. S. Drought concepts and characterization: Comparing drought indices applied at local and regional scales. **Water International**, v. 31, n. 1, p. 37–49, 2006.

PEDRO-MONZONÍS, M.; SOLERA, A.; FERRER, J.; ESTRELA, T.; PAREDES-ARQUIOLA, J. A review of water scarcity and drought indexes in water resources planning and management. **Journal of Hydrology**, v. 527, p. 482–493, 2015.

PEDROZO, C. **IMPACTO DAS ALTERAÇÕES CLIMÁTICAS NA GERAÇÃO DE ENERGIA ELÉTRICA DA USINA HIDRELÉTRICA DE FOZ DO AREIA NO ESTADO DO PARANÁ**, 2017. Universidade Federal do Paraná.

PEEL, M. C.; BLÖSCHL, G. Hydrological modelling in a changing world. **Progress in Physical Geography**, v. 35, n. 2, p. 249–261, 2011.

PEÑA-GALLARDO, M.; VICENTE-SERRANO, S. M.; HANNAFORD, J.; et al. Complex influences of meteorological drought time-scales on hydrological droughts in natural basins of the contiguous Unites States. **Journal of Hydrology**, v. 568, n. November 2018, p. 611–625, 2019. Elsevier. Disponível em: <https://doi.org/10.1016/j.jhydrol.2018.11.026>. .

PLOSZAI, R.; MINE, M. R. M. Rainfall trend analysis in the region of Curitiba using regional climate model scenarios. **Green Energy and Technology**, p. 193–208, 2016.

PLOSZAI, R.; MINE, M. R. M.; DETZEL, D. H. M. Índices de seca no Estado do Paraná. XXIII Simpósio Brasileiro de Recursos Hídricos. **Anais...** . p.1–9, 2019. Foz do Iguaçu, PR.

PORTO DE CARVALHO, J. R.; DELGADO ASSAD, E.; MEDEIROS EVANGELISTA, S. R.; DA SILVEIRA PINTO, H. Estimation of dry spells in three Brazilian regions - Analysis of extremes. **Atmospheric Research**, v. 132–133, p. 12–21, 2013. Elsevier B.V.

RAJCZAK, J.; KOTLARSKI, S.; SCHÄR, C. Does quantile mapping of simulated precipitation correct for biases in transition probabilities and spell lengths? **Journal of Climate**, v. 29, n. 5, p. 1605–1615, 2016.

RAJSEKHAR, D.; SINGH, V. P.; MISHRA, A. K. Multivariate drought index: An information theory based approach for integrated drought assessment. **Journal of Hydrology**, v. 526, p. 164–182, 2015. Elsevier B.V. Disponível em: <http://dx.doi.org/10.1016/j.jhydrol.2014.11.031>. .

RASHID, M. M.; BEECHAM, S. Development of a non-stationary Standardized Precipitation Index and its application to a South Australian climate. **Science of the Total Environment**, v. 657, p. 882–892, 2019. Elsevier B.V. Disponível em: <https://doi.org/10.1016/j.scitotenv.2018.12.052>. .

ROCHA, M. H. P. ANÁLISE DE TENDÊNCIAS NO REGIME DE CHUVAS EM CURITIBA USANDO CENÁRIOS DE MODELOS CLIMÁTICOS REGIONAIS. **Revista Brasileira de Recursos Hidricos**, 2015.

RODRIGUES DA SILVA, V. DE P.; BELO FILHO, A. F.; RODRIGUES ALMEIDA, R. S.; DE

HOLANDA, R. M.; DA CUNHA CAMPOS, J. H. B. Shannon information entropy for assessing space-time variability of rainfall and streamflow in semiarid region. **Science of the Total Environment**, v. 544, p. 330–338, 2016. Elsevier B.V. Disponível em: <http://dx.doi.org/10.1016/j.scitotenv.2015.11.082>. .

RODRIGUES, J. P. P.; PELEGRINI, S. DE C. A. Imprensa e memória: a geada negra de 1975. **Revista Labirinto**, v. 27, n. 1, p. 210–222, 2017.

ROMANO, E.; PETRANGELI, A. B.; PREZIOSI, E. Spatial and Time Analysis of Rainfall in the Tiber River Basin (Central Italy) in relation to Discharge Measurements (1920-2010). **Procedia Environmental Sciences**, v. 7, p. 258–263, 2011.

ROUGÉ, C.; GE, Y.; CAI, X. Detecting gradual and abrupt changes in hydrological records. **Advances in Water Resources**, v. 53, p. 33–44, 2013.

SALAS, J. D.; RAJAGOPALAN, B.; SAITO, L.; BROWN, C. Special Section on Climate Change and Water Resources: Climate Nonstationarity and Water Resources Management. **Journal of Water Resources Planning and Management**, v. 138, n. 5, p. 385–388, 2012.

SANTOS. Regional droughts: a stochastic characterization. **Journal of Hydrology**, v. 66, p. 183–211, 1983.

SANTOS, M. S.; COSTA, V. A. F.; FERNANDES, W. D. S.; DE PAES, R. P. Time-space characterization of droughts in the São Francisco river catchment using the Standard Precipitation Index and continuous wavelet transform. **Revista Brasileira de Recursos Hidricos**, v. 24, p. 1–12, 2019.

SAURRAL, R.; BARROS, V. Estudio De La Climatología Y La Hidrología De La Cuenca Del Plata En Un Conjunto De Modelo Climáticos Globales. **Meteorologica**, v. 34, n. 2009, p. 5–15, 2010.

SAYEMUZZAMAN, M.; JHA, M. K. Seasonal and annual precipitation time series trend analysis in North Carolina, United States. **Atmospheric Research**, v. 137, p. 183–194, 2014. Elsevier B.V. Disponível em: <http://dx.doi.org/10.1016/j.atmosres.2013.10.012>. .

VAN DER SCHRIER, G.; BARICHIVICH, J.; BRIFFA, K. R.; JONES, P. D. A scPDSI-based global data set of dry and wet spells for 1901-2009. **Journal of Geophysical Research Atmospheres**, v. 118, n. 10, p. 4025–4048, 2013.

SEMA. Revista Bacias Hidrograficas do Paraná. **Governo do Estado do Paraná**, 2015. Curitiba: Governo do Estado do Paraná.

SHARMA, K. P.; MOORE, B.; VOROSMARTY, C. J. Anthropogenic, climatic, and hydrologic trends in the Kosi basin, Himalaya. **Climatic Change**, v. 47, p. 141–165, 2000.

SHEFFIELD, J.; WOOD, E. F. Projected changes in drought occurrence under future global warming from multi-model, multi-scenario, IPCC AR4 simulations. **Climate Dynamics**, v. 31, n. 1, p. 79–105, 2008.

SHIRU, M. S.; SHAHID, S.; CHUNG, E. S.; ALIAS, N. Changing characteristics of meteorological droughts in Nigeria during 1901–2010. **Atmospheric Research**, v. 223, n. December 2018, p. 60–73, 2019. Elsevier. Disponível em: <https://doi.org/10.1016/j.atmosres.2019.03.010>. .

SIMS, A. P.; NIYOGI, D. DUTTA S.; RAMAN, S. Adopting drought indices for estimating soil moisture: A North Carolina case study. **Geophysical Research Letters**, v. 29, n. 8, p. 24-1-24–4, 2002.

SIVAKUMAR, M. V. K.; MOTHA, R. P.; DAS, H. P. **Natural Disasters and Extreme Events in Agriculture: Impacts and Mitigation**. Springer Berlin Heidelberg, 2005.

SMITHA, P. S.; NARASIMHAN, B.; SUDHEER, K. P.; ANNAMALAI, H. An improved bias correction method of daily rainfall data using a sliding window technique for climate change impact assessment. **Journal of Hydrology**, v. 556, p. 100–118, 2018. Elsevier B.V. Disponível em: <https://doi.org/10.1016/j.jhydrol.2017.11.010>. .

SOBRAL, B. S.; DE OLIVEIRA-JÚNIOR, J. F.; DE GOIS, G.; et al. Drought characterization for the state of Rio de Janeiro based on the annual SPI index: Trends, statistical tests and its relation with ENSO. **Atmospheric Research**, v. 220, n. January, p. 141–154, 2019. Disponível em: <https://www.sciencedirect.com/science/article/pii/S016980951830872X?dgcid=rss_sd_all>. .

SORIANO, É.; LONDE, L. D. R.; GREGORIO, L. T. DI; COUTINHO, M. P.; SANTOS, L. B. L. Water Crisis in São Paulo Evaluated Under the Disaster ' S Point of View 1. **Ambiente e Sociedade**, v. XIX, n. jan-mar, p. 21–42, 2016.

SPINONI, J.; NAUMANN, G.; CARRAO, H.; BARBOSA, P.; VOGT, J. World drought frequency, duration, and severity for 1951-2010. **International Journal of Climatology**, v. 34, n. 8, p. 2792–2804, 2014.

SPINONI, J.; NAUMANN, G.; VOGT, J. V. Pan-European seasonal trends and recent changes of drought frequency and severity. **Global and Planetary Change**, v. 148, p. 113–130, 2017. The Authors. Disponível em: <http://dx.doi.org/10.1016/j.gloplacha.2016.11.013>. .

STAGGE, J. H.; KOHN, I.; TALLAKSEN, L. M.; STAHL, K. Modeling drought impact occurrence based on meteorological drought indices in Europe. **Journal of Hydrology**, v. 530, p. 37–50, 2015. Elsevier B.V. Disponível em: <http://dx.doi.org/10.1016/j.jhydrol.2015.09.039>. .

STAGGE, J. H.; TALLAKSEN, L. M.; GUDMUNDSSON, L.; VAN LOON, A. F.; STAHL, K. Candidate Distributions for Climatological Drought Indices (SPI and SPEI). **International Journal of**

Climatology, v. 35, n. 13, p. 4027–4040, 2015.

SUGAHARA, S.; ROCHA, R. P. DA; SILVEIRA, R. Climate extremes: progress and future directions. **International Journal of Climatology**, v. 29, n. 3, p. 317–319, 2009. Disponível em: <http://dx.doi.org/10.1002/joc.1861>. .

SUN, P.; WEN, Q.; ZHANG, Q.; et al. Nonstationarity-based evaluation of flood frequency and flood risk in the Huai River basin, China. **Journal of Hydrology**, v. 567, n. September, p. 393–404, 2018. Elsevier. Disponível em: <https://doi.org/10.1016/j.jhydrol.2018.10.031>. .

SVOBODA, M. D.; LECOMTE, D.; HAYES, M. The drought monitor. **Bull. Amer. Meteor. Soc.**, v. 83, n. 8, p. 1181–1190, 2002.

SZÉP, I. J.; MIKA, J.; DUNKEL, Z. Palmer drought severity index as soil moisture indicator: Physical interpretation, statistical behaviour and relation to global climate. **Physics and Chemistry of the Earth**, v. 30, n. 1-3 SPEC. ISS., p. 231–243, 2005.

TEUTSCHBEIN, C.; SEIBERT, J. Bias correction of regional climate model simulations for hydrological climate-change impact studies: Review and evaluation of different methods. **Journal of Hydrology**, v. 456–457, p. 12–29, 2012. Elsevier B.V. Disponível em: <http://dx.doi.org/10.1016/j.jhydrol.2012.05.052>. .

TIGKAS, D.; VANGELIS, H.; TSAKIRIS, G. Drought and climatic change impact on streamflow in small watersheds. **Science of the Total Environment**, v. 440, p. 33–41, 2012. Elsevier B.V. Disponível em: <http://dx.doi.org/10.1016/j.scitotenv.2012.08.035>. .

TIME AND DATE. TIME AND DATE. Disponível em: <https://www.timeanddate.com>. Acesso em: 30/7/2019.

TODD, B.; MACDONALD, N.; CHIVERRELL, R. C.; CAMINADE, C.; HOOKE, J. M. Severity, duration and frequency of drought in SE England from 1697 to 2011. **Climatic Change**, v. 121, n. 4, p. 673–687, 2013.

TONG, S.; LAI, Q.; ZHANG, J.; et al. Spatiotemporal drought variability on the Mongolian Plateau from 1980–2014 based on the SPEI-PM, intensity analysis and Hurst exponent. **Science of the Total Environment**, v. 615, p. 1557–1565, 2018. Elsevier B.V. Disponível em: <https://doi.org/10.1016/j.scitotenv.2017.09.121>. .

TOUMA, D.; ASHFAQ, M.; NAYAK, M. A.; KAO, S. C.; DIFFENBAUGH, N. S. A multi-model and multi-index evaluation of drought characteristics in the 21st century. **Journal of Hydrology**, v. 526, p. 196–207, 2015. Elsevier B.V. Disponível em: <http://dx.doi.org/10.1016/j.jhydrol.2014.12.011>. .

TRENBERTH, K. E.; SMITH, L.; QIAN, T.; DAI, A.; FASULLO, J. Estimates of the global water

budget and its annual cycle using observational and model Data. **Journal of Hydrometeorology**, v. 8, n. 4, p. 758–769, 2007.

TSAKIRIS, G.; NALBANTIS, I.; PANGALOU, D.; TIGKAS, D.; NATIONAL, H. V. Drought meteorological monitoring network design for the reconnaissance drought index (RDI). **ResearchGate: Options Méditerranéennes Series A**, v. 80, n. January, p. 57–62, 2008. Disponível em: <http://www.researchgate.net/profile/Harris_Vangelis/publication/238622031_Drought_meteorological_monitoring_network_design_for_the_Reconnaissance_Drought_Index_(RDI)/links/02e7e53039ee8aeb2a000000.pdf>. .

TSAKIRIS, G.; PANGALOU, D.; VANGELIS, H. Regional drought assessment based on the Reconnaissance Drought Index (RDI). **Water Resources Management**, v. 21, n. 5, p. 821–833, 2007.

TSAKIRIS, GEORGE; VANGELIS, H. Establishing a drought index incorporating evapotranspiration. **European Water**, v. 9, n. 10, p. 3–11, 2005. Disponível em: <http://www.ewra.net/ew/pdf/EW_2005_9-10_01.pdf>. .

TSAKIRIS, G.; VANGELIS, H. Establishing a drought index incorporating evapotranspiration. **European Water**, v. 9, n. 10, p. 3–11, 2005.

TU, X.; WU, H.; SINGH, V. P.; et al. Multivariate design of socioeconomic drought and impact of water reservoirs. **Journal of Hydrology**, v. 566, n. June, p. 192–204, 2018. Elsevier. Disponível em: <https://doi.org/10.1016/j.jhydrol.2018.09.012>. .

TUCCI, C. E. M. **Impactos da variabilidade climática e do uso do solo nos recursos hídricos**. Brasília, DF, 2002.

VANGELIS, H.; TIGKAS, D.; TSAKIRIS, G. The effect of PET method on Reconnaissance Drought Index (RDI) calculation. **Journal of Arid Environments**, v. 88, p. 130–140, 2013. Elsevier Ltd. Disponível em: <http://dx.doi.org/10.1016/j.jaridenv.2012.07.020>. .

VICENTE-SERRANO, S. M. Differences in spatial patterns of drought on different time scales: An analysis of the Iberian Peninsula. **Water Resources Management**, v. 20, n. 1, p. 37–60, 2006.

VICENTE-SERRANO, S. M.; BEGUERÍA, S.; LÓPEZ-MORENO, J. I. A multiscalar drought index sensitive to global warming: The standardized precipitation evapotranspiration index. **Journal of Climate**, v. 23, n. 7, p. 1696–1718, 2010.

VICENTE-SERRANO, S. M.; BEGUERÍA, S.; LORENZO-LACRUZ, J.; et al. Performance of drought indices for ecological, agricultural, and hydrological applications. **Earth Interactions**, v. 16, n. 10, 2012.

VICENTE-SERRANO, S. M.; CHURA, O.; LÓPEZ-MORENO, J. I.; et al. Spatio-temporal variability

of droughts in Bolivia: 1955-2012. **International Journal of Climatology**, v. 35, n. 10, p. 3024–3040, 2015.

VITART, F.; STOCKDALE, T. N.; VITART, F.; STOCKDALE, T. N. Seasonal Forecasting of Tropical Storms Using Coupled GCM Integrations. **Monthly Weather Review**, v. 129, n. 10, p. 2521–2537, 2001. Disponível em: <http://journals.ametsoc.org/doi/abs/10.1175/1520-0493%282001%29129%3C2521%3ASFOTSU%3E2.0.CO%3B2>. .

VU, T. M.; MISHRA, A. K. Nonstationary frequency analysis of the recent extreme precipitation events in the United States. **Journal of Hydrology**, v. 575, n. March, p. 999–1010, 2019. Elsevier. Disponível em: <https://doi.org/10.1016/j.jhydrol.2019.05.090>. .

WANG, L.; YU, H.; YANG, M.; et al. A drought index: The standardized precipitation evapotranspiration runoff index. **Journal of Hydrology**, v. 571, n. February, p. 651–668, 2019.

WANG, W.; CHEN, X.; SHI, P.; GELDER, P. H. A. J. M. VAN. Detecting changes in extreme precipitation and extreme streamflow in the Dongjiang River Basin in southern China. **Hydrology and Earth System Sciences**, v. 12, p. 207–221, 2008.

WANG, Y.; LIU, G.; GUO, E. Spatial distribution and temporal variation of drought in Inner Mongolia during 1901–2014 using Standardized Precipitation Evapotranspiration Index. **Science of the Total Environment**, v. 654, p. 850–862, 2019. Elsevier B.V.

WELLS, N.; GODDARD, S.; HAYES, M. J. A Self-Calibrating Palmer Drought Severity Index NATHAN. **American Meteorological Society**, p. 2335–2351, 2004.

WILHITE, D. A. Drought as a Natural Hazard. **Drought: A Global Assessment**. p.147–162, 2000. London: University of Nebraska.

WILLKOFER, F.; SCHMID, F. J.; KOMISCHKE, H.; et al. The impact of bias correcting regional climate model results on hydrological indicators for Bavarian catchments. **Journal of Hydrology: Regional Studies**, v. 19, n. June, p. 25–41, 2018. Elsevier. Disponível em: <https://doi.org/10.1016/j.ejrh.2018.06.010>. .

WU, J.; YAO, H.; ZHENG, Y.; et al. Impacts of reservoir operations on multi-scale correlations between hydrological drought and meteorological drought. **Journal of Hydrology**, v. 563, n. 135, p. 726–736, 2018. Elsevier. Disponível em: <https://doi.org/10.1016/j.jhydrol.2018.06.053>. .

YANG, J.; CHANG, J.; WANG, Y.; et al. Comprehensive drought characteristics analysis based on a nonlinear multivariate drought index. **Journal of Hydrology**, v. 557, p. 651–667, 2018. Elsevier B.V. Disponível em: <https://doi.org/10.1016/j.jhydrol.2017.12.055>. .

YEVJEVICH, V. An objective approach to definitions and investigations of continental hydrologic

droughts. **Journal of Hydrology**, v. 7, n. 3, p. 353, 1967.

YILMAZ, A. G.; PERERA, B. J. C. Extreme Rainfall Nonstationarity Investigation and Intensity – Frequency – Duration Relationship. **Journal of Hydrologic Engineering**, v. 19, n. 6, p. 1160–1172, 2014.

ZARCH, M. A. A.; MALEKINEZHAD, H.; MOBIN, M. H.; DASTORANI, M. T.; KOUSARI, M. R. Drought Monitoring by Reconnaissance Drought Index (RDI) in Iran. **Water Resources Management**, v. 25, n. 13, p. 3485–3504, 2011.

ZHANG, D.; ZHANG, Q.; QIU, J.; et al. Intensification of hydrological drought due to human activity in the middle reaches of the Yangtze River, China. **Science of the Total Environment**, v. 637–638, p. 1432–1442, 2018. Elsevier B.V. Disponível em: <https://doi.org/10.1016/j.scitotenv.2018.05.121>. .

ZHANG, X.; WANG, J.; ZWIERS, F. W.; GROISMAN, P. Y. The influence of large-scale climate variability on winter maximum daily precipitation over North America. **Journal of Climate**, v. 23, n. 11, p. 2902–2915, 2010.

ZHAO, H.; GAO, G.; AN, W.; et al. Timescale differences between SC-PDSI and SPEI for drought monitoring in China. **Physics and Chemistry of the Earth**, v. 102, p. 48–58, 2017. Elsevier Ltd.

ZSCHEISCHLER, J.; SENEVIRATNE, S. I. Dependence of drivers affects risks associated with compound events. **Science Advances**, v. 3, n. 6, p. 1–11, 2017.

APPENDIX

Differences in the drought indices statistics of 6 months

Figure 42 – Difference (%) between stationary and non-stationary approaches in maximum drought duration of the historical (HIST), and simulated (RCP 4.5 and RCP 8.5) series.

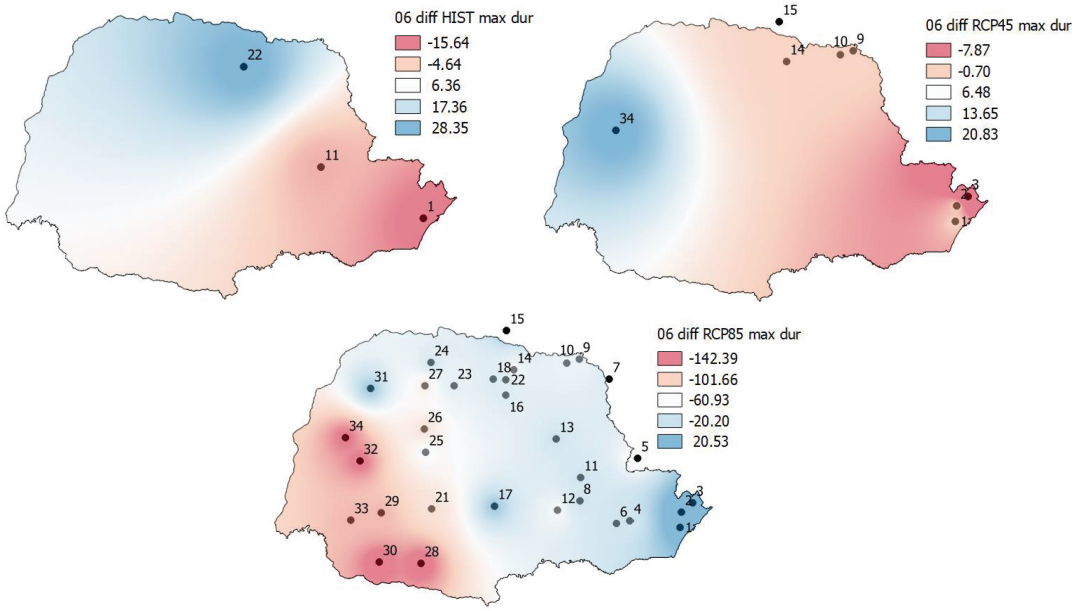

Font: Author.

Figure 43 – Difference (%) between stationary and non-stationary approaches in the zero threshold frequency of the historical (HIST), and simulated (RCP 4.5 and RCP 8.5) series.

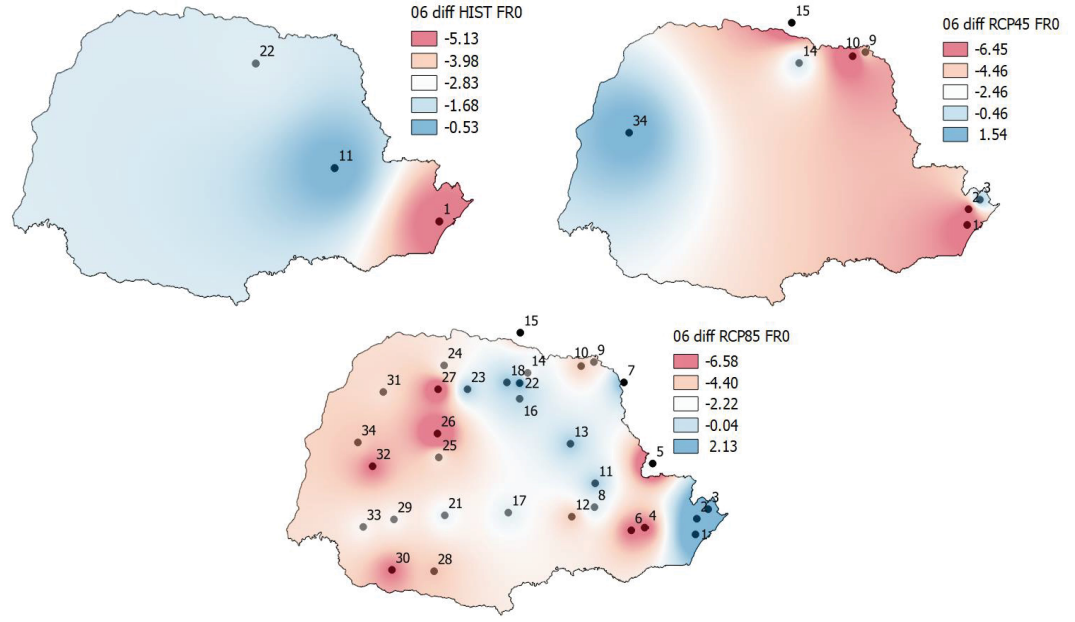

Font: Author.

Figure 44 – Difference (%) between stationary and non-stationary approaches in the -1.0 threshold frequency of the historical (HIST), and simulated (RCP 4.5 and RCP 8.5) series.

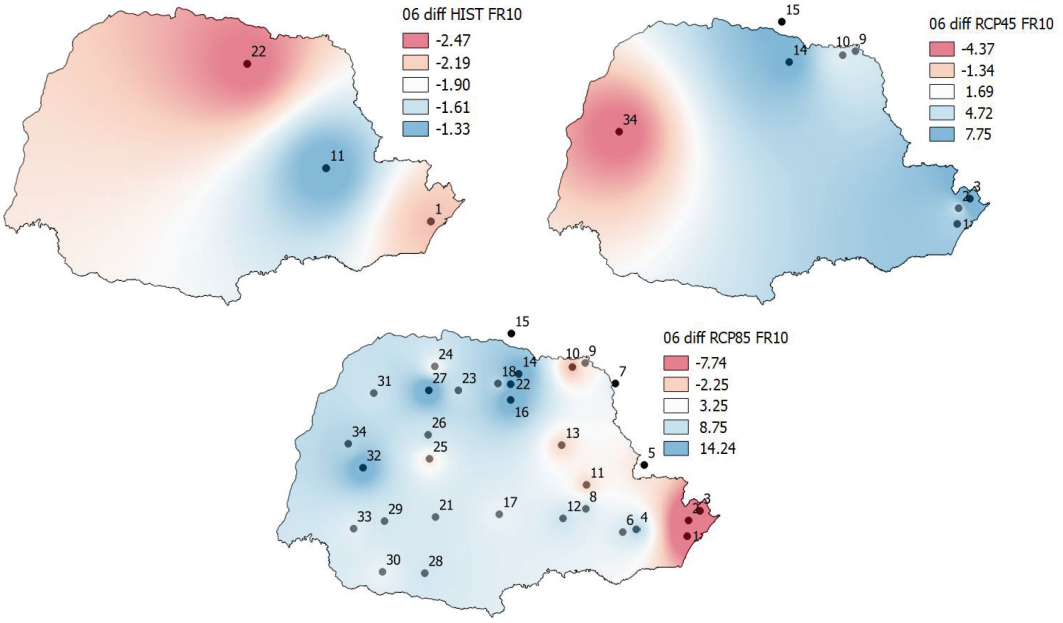

Font: Author.

Figure 45 – Difference (%) between stationary and non-stationary approaches in the -1.5 threshold frequency of the historical (HIST), and simulated (RCP 4.5 and RCP 8.5) series.

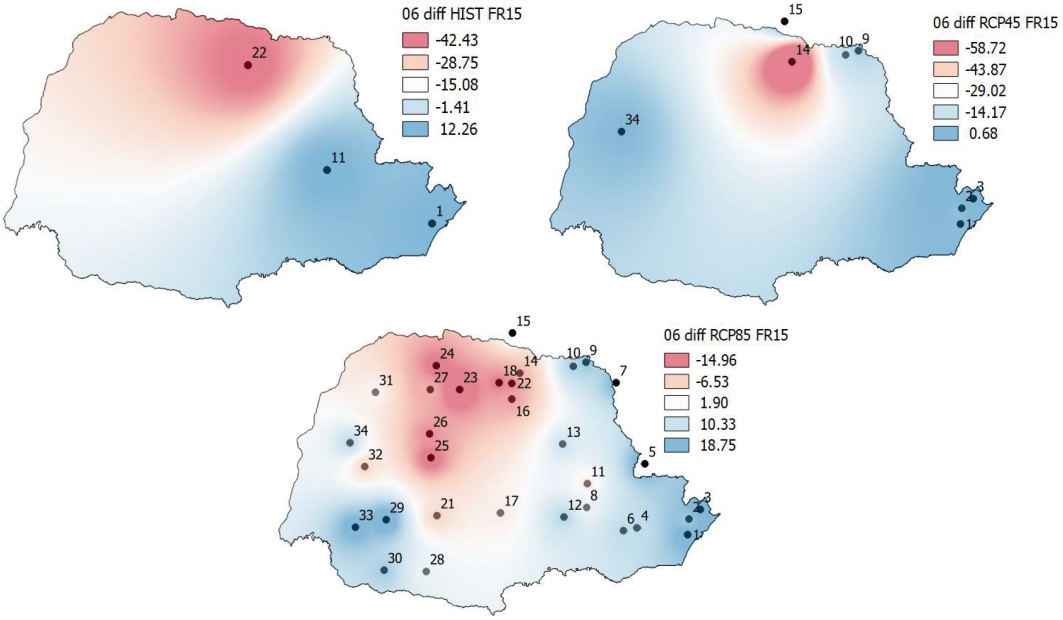

Font: Author.

Figure 46 – Difference (%) between stationary and non-stationary approaches in the maximum drought magnitude of the historical (HIST), and simulated (RCP 4.5 and RCP 8.5) series.

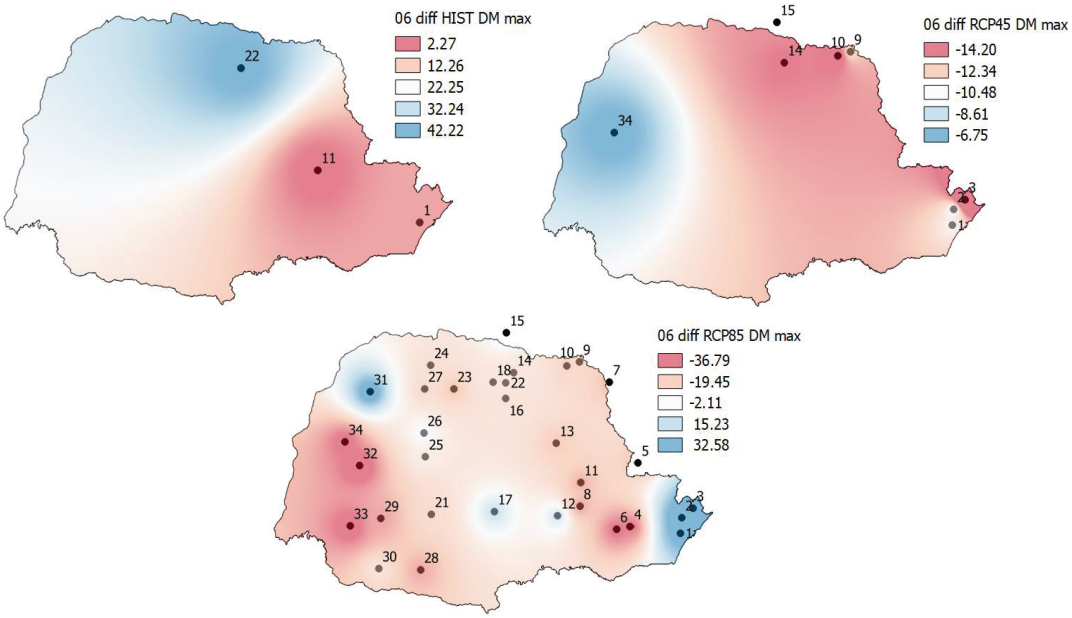

Font: Author.

Figure 47 – Difference (%) between stationary and non-stationary approaches in the mean drought magnitude of the historical (HIST), and simulated (RCP 4.5 and RCP 8.5) series.

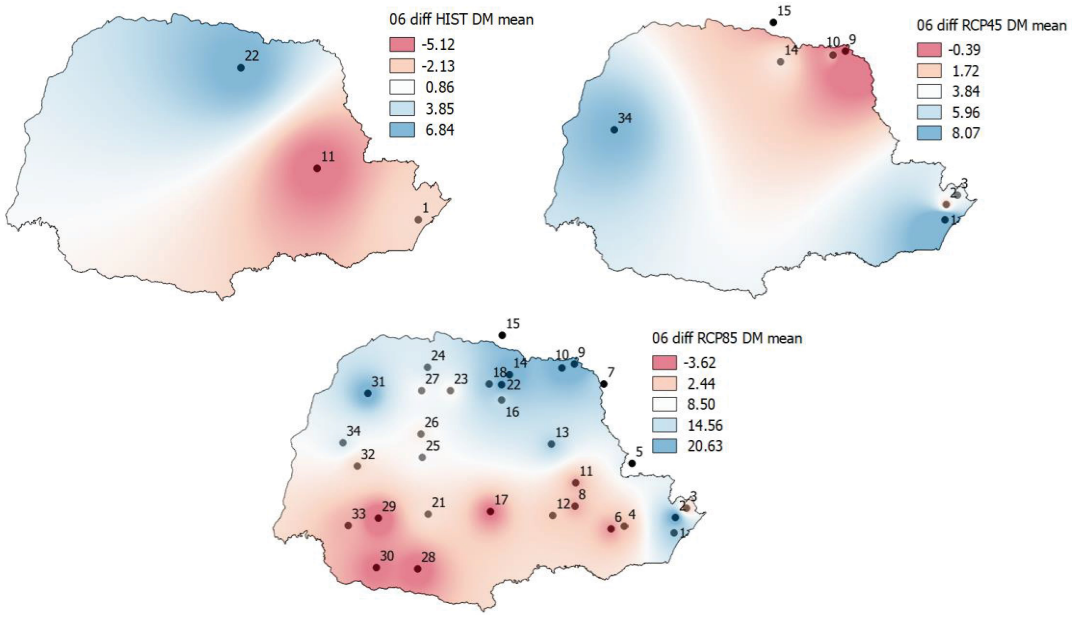

Font: Author.

Figure 48 – Difference (%) between stationary and non-stationary approaches in the median drought magnitude of the historical (HIST), and simulated (RCP 4.5 and RCP 8.5) series.

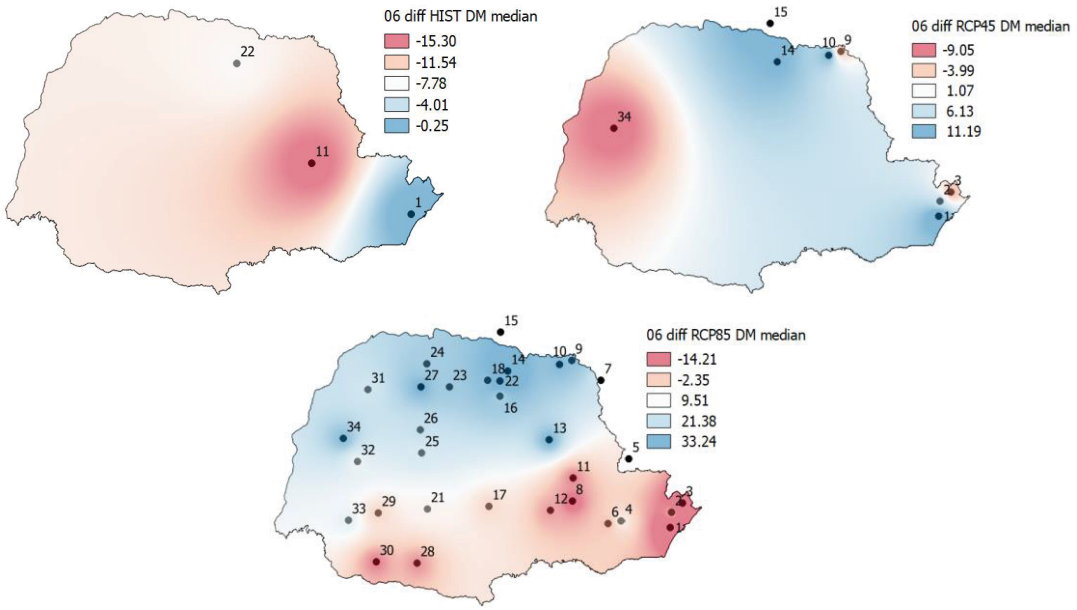

Font: Author.

Figure 49 – Difference (%) between stationary and non-stationary approaches in the minimum values of the historical (HIST), and simulated (RCP 4.5 and RCP 8.5) series.

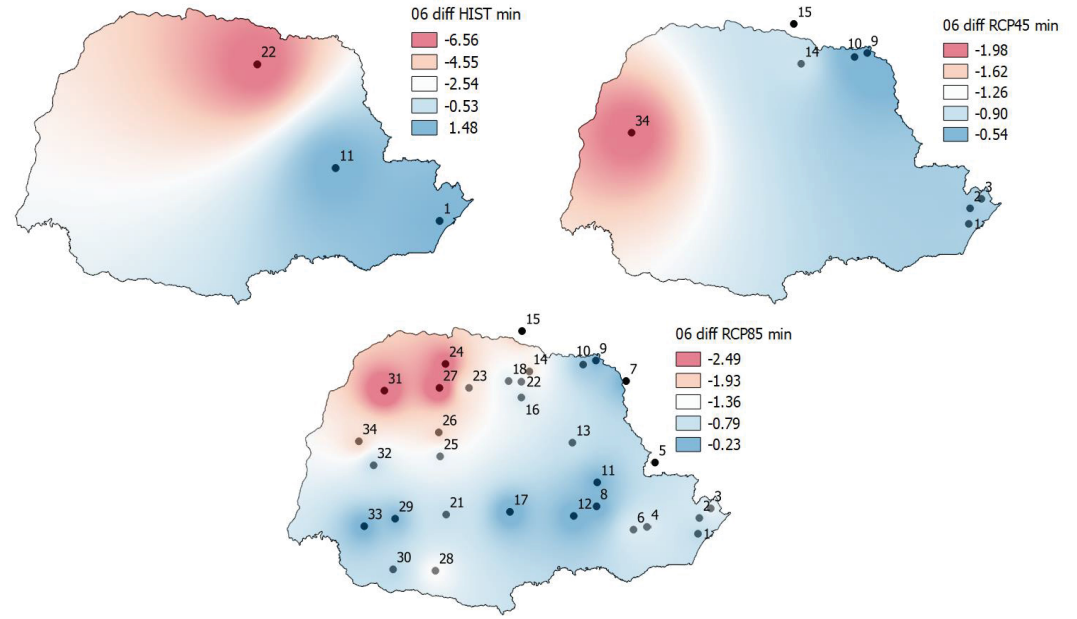

Font: Author.

Figure 50 – Number of drought events difference (%) between stationary and non-stationary approaches of the historical (HIST), and simulated (RCP 4.5 and RCP 8.5) series.

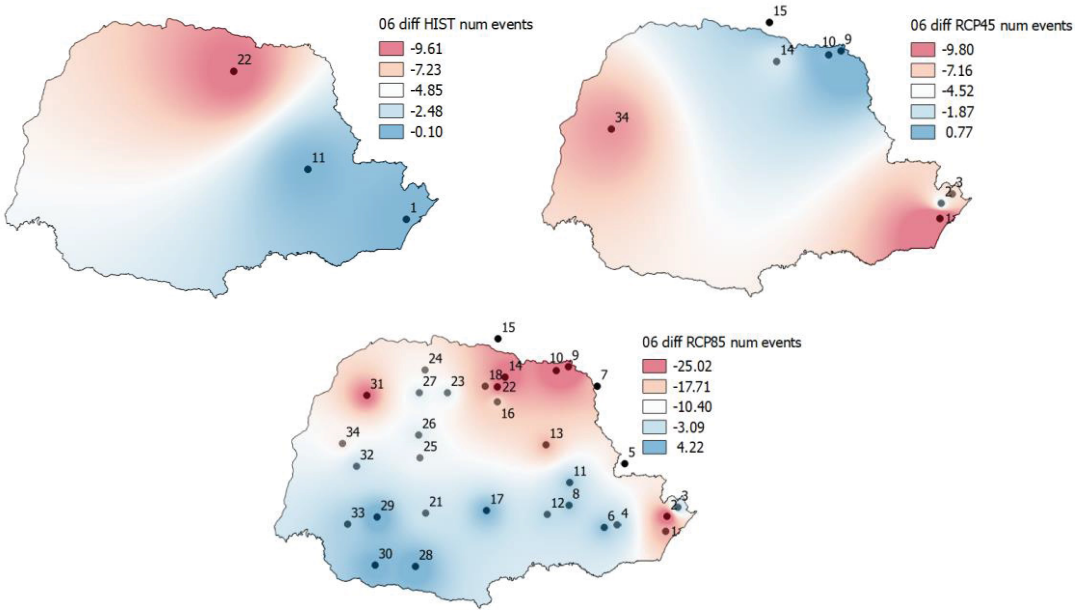

Font: Author.

Figure 51 – Difference (%) between stationary and non-stationary approaches in the drought characterization in the stationary and non-stationary approaches of the historical (HIST), and simulated (RCP 4.5 and RCP 8.5) series.

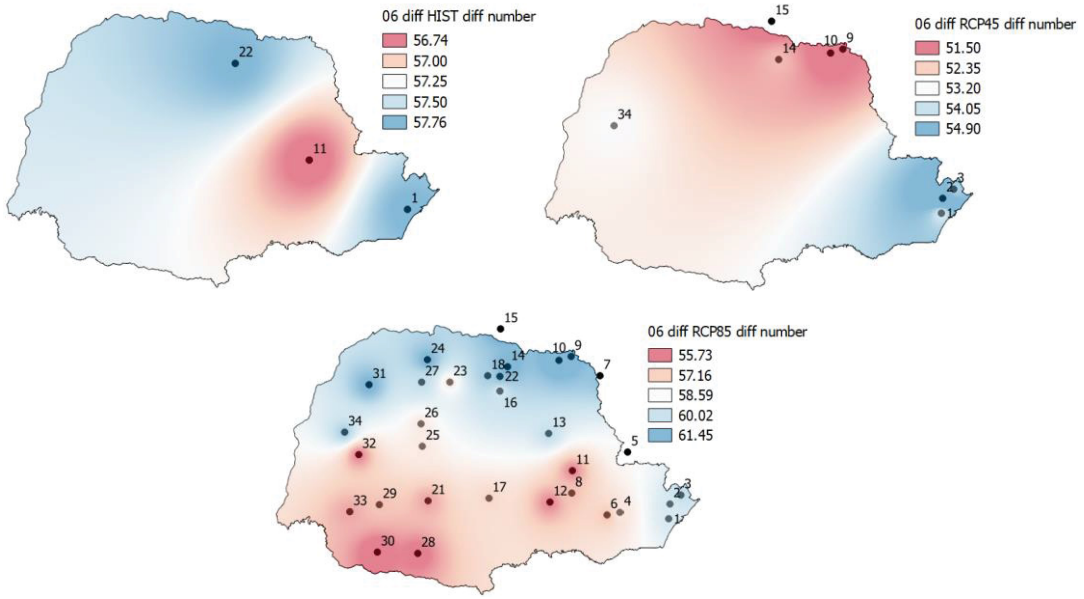

Font: Author.

Drought analysis of 6 months

Figure 52 – Maximum drought duration of the historical (HIST), and simulated (RCP 4.5 and RCP 8.5) series.

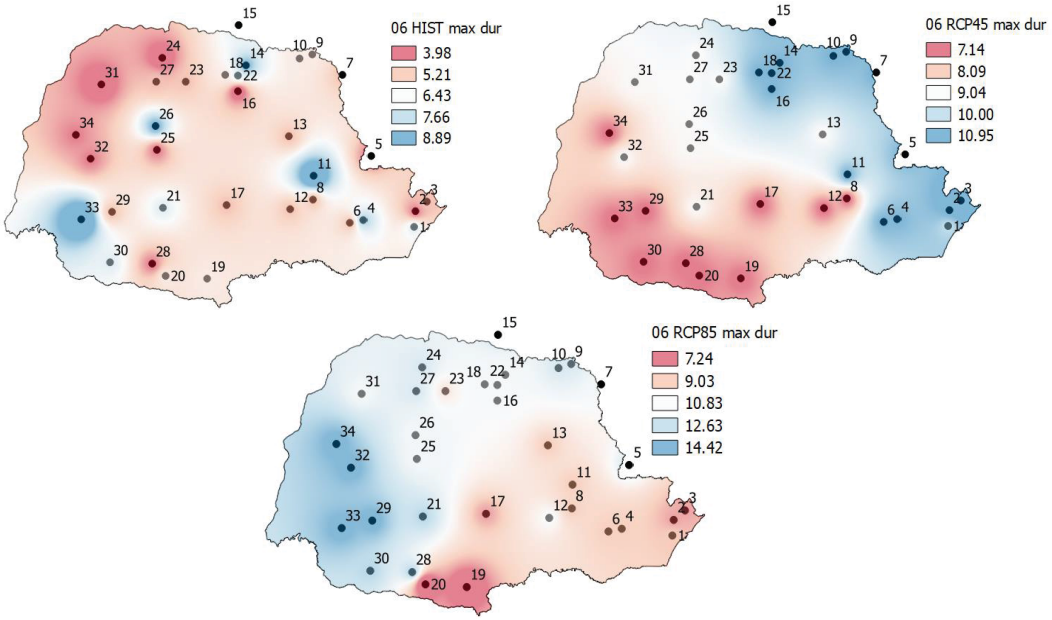

Font: Author.

Figure 53 – Zero threshold frequency of the historical (HIST), and simulated (RCP 4.5 and RCP 8.5) series.

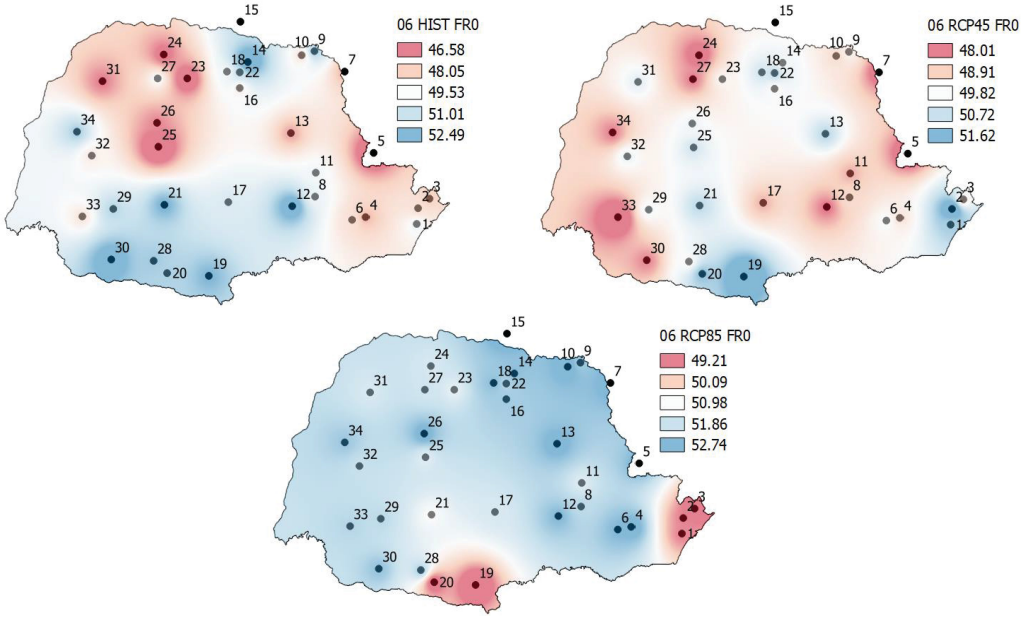

Font: Author.

Figure 54 – The -1.0 threshold frequency of the historical (HIST), and simulated (RCP 4.5 and RCP 8.5) series.

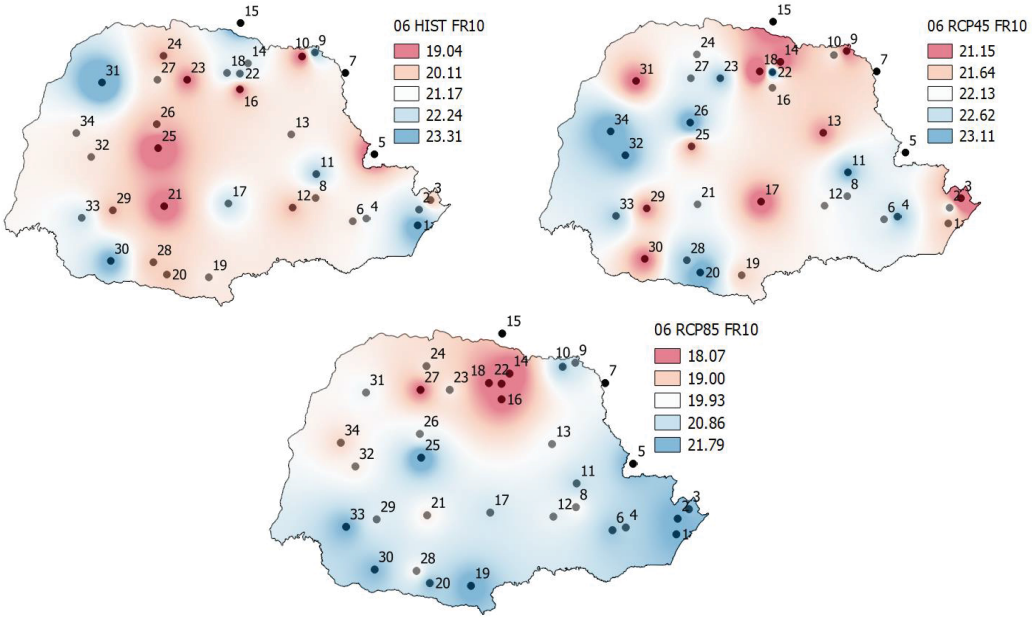

Font: Author.

Figure 55 – The -1.5 threshold frequency of the historical (HIST), and simulated (RCP 4.5 and RCP 8.5) series.

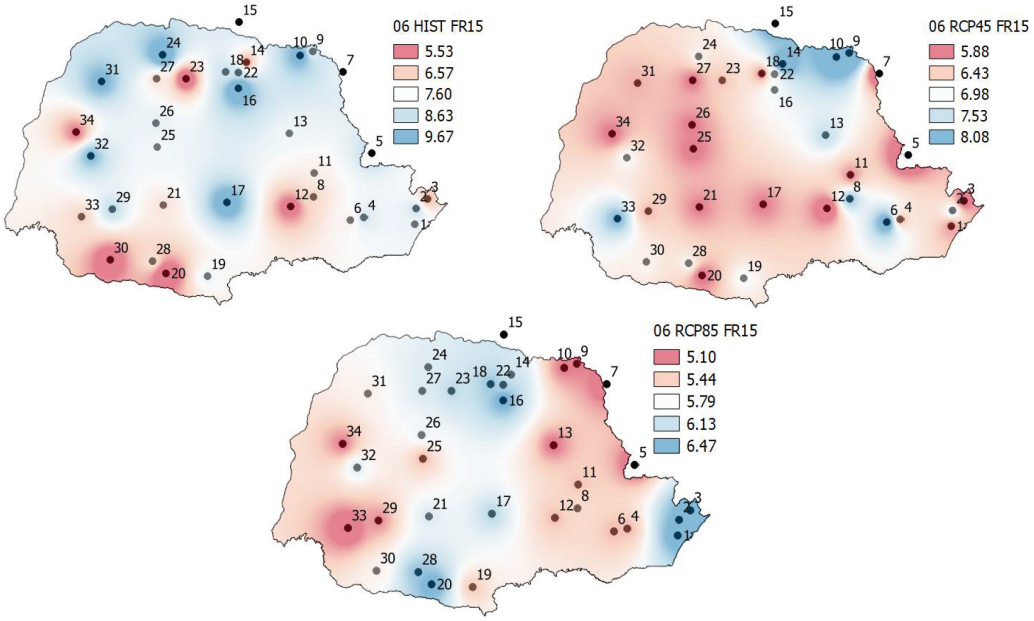

Font: Author.

Figure 56 – Maximum drought magnitude of the historical (HIST), and simulated (RCP 4.5 and RCP 8.5) series.

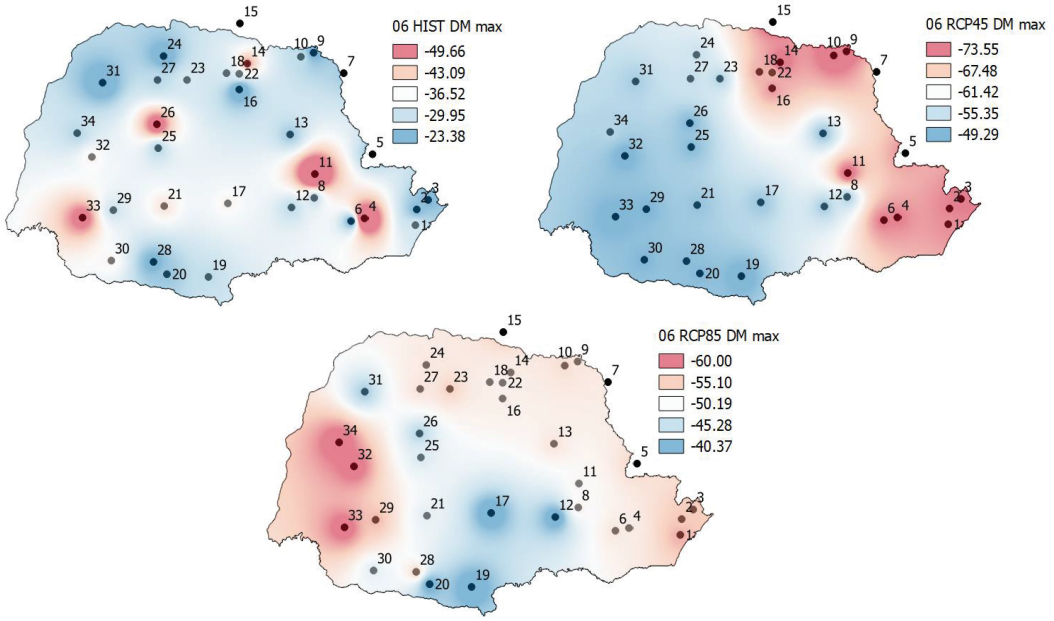

Font: Author.

Figure 57 – Mean drought magnitude of the historical (HIST), and simulated (RCP 4.5 and RCP 8.5) series.

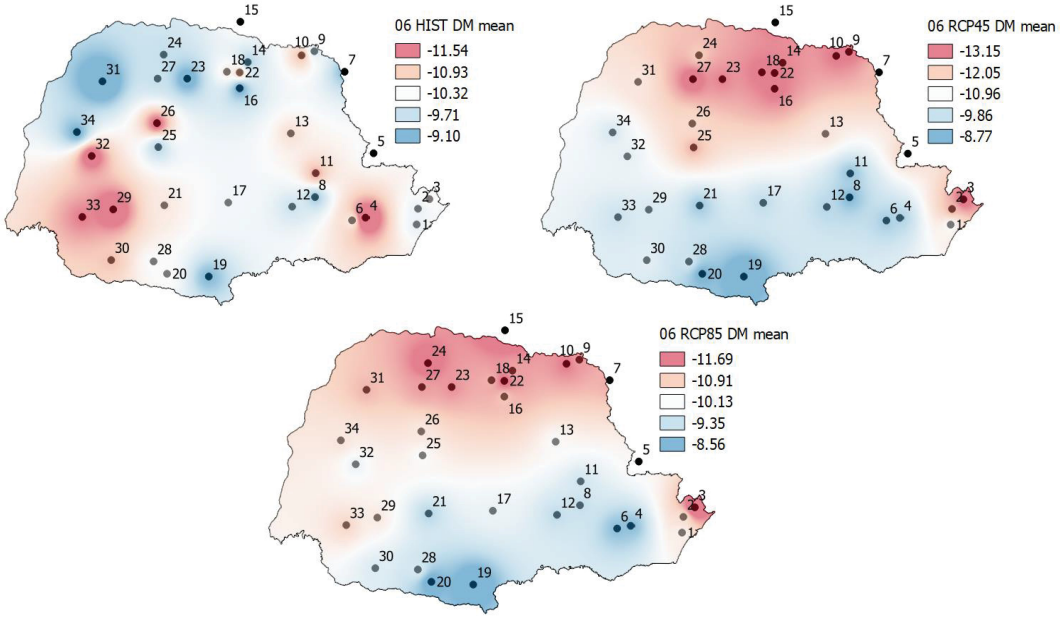

Font: Author.

Figure 58 – Median drought magnitude of the historical (HIST), and simulated (RCP 4.5 and RCP 8.5) series.

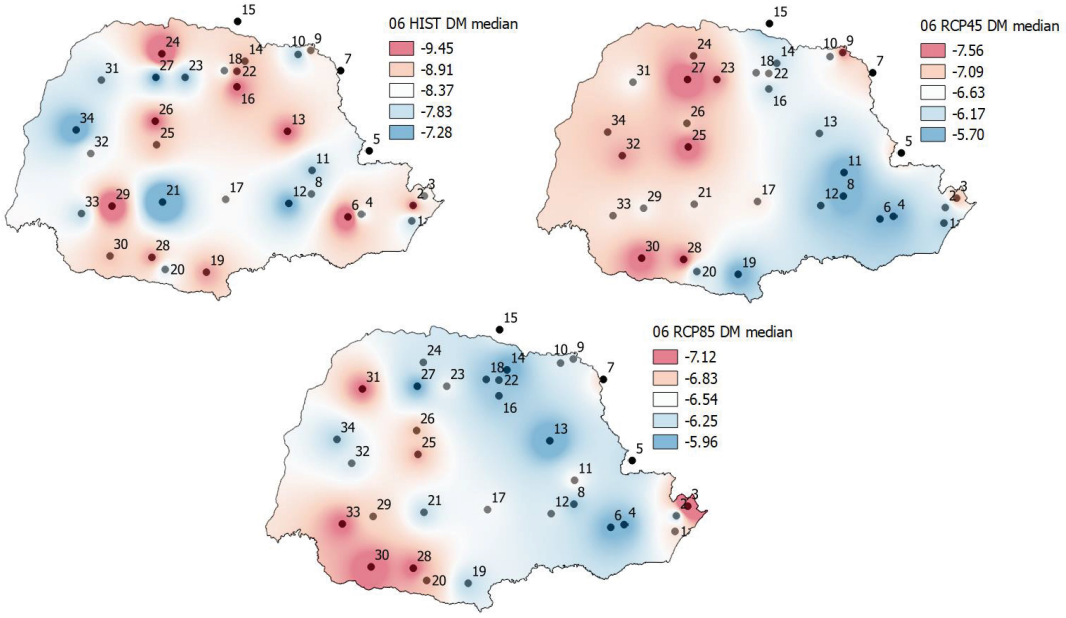

Font: Author.

Figure 59 – Minimum values of the historical (HIST), and simulated (RCP 4.5 and RCP 8.5) series.

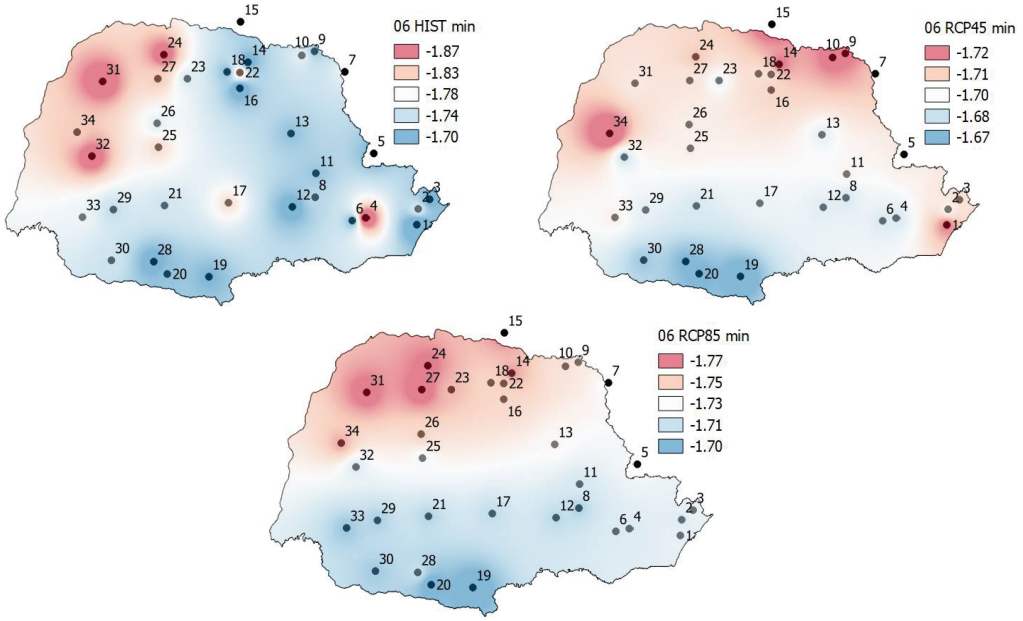

Font: Author.

Figure 60 – Total number of drought events between stationary and non-stationary approaches of the historical (HIST), and simulated (RCP 4.5 and RCP 8.5) series.

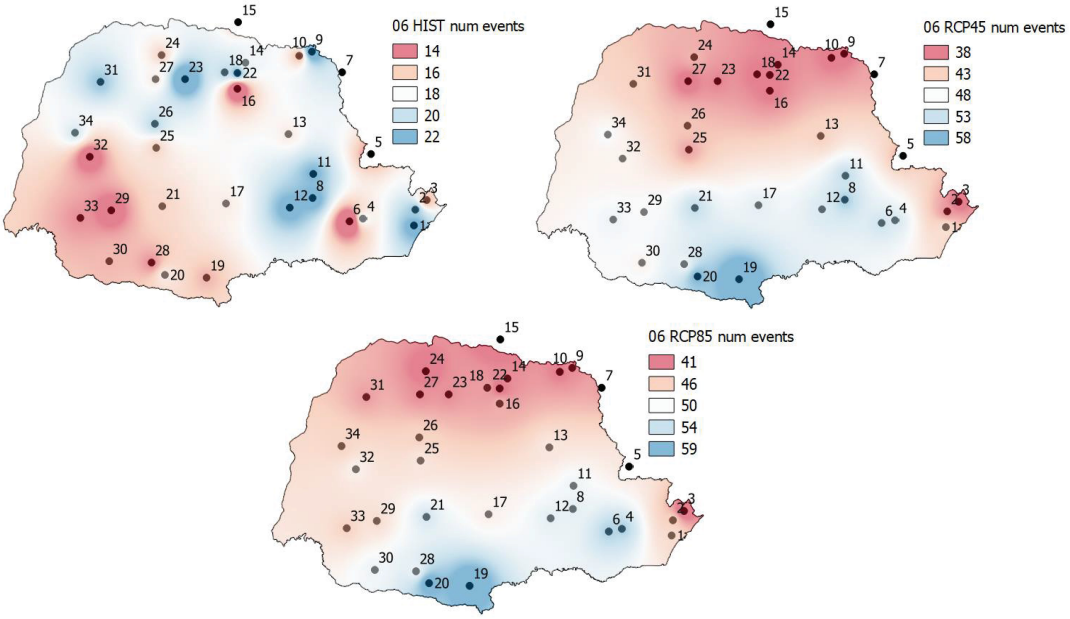

Font: Author.

Drought analysis of 12 months

Figure 61 – Maximum drought duration of the historical (HIST), and simulated (RCP 4.5 and RCP 8.5) series.

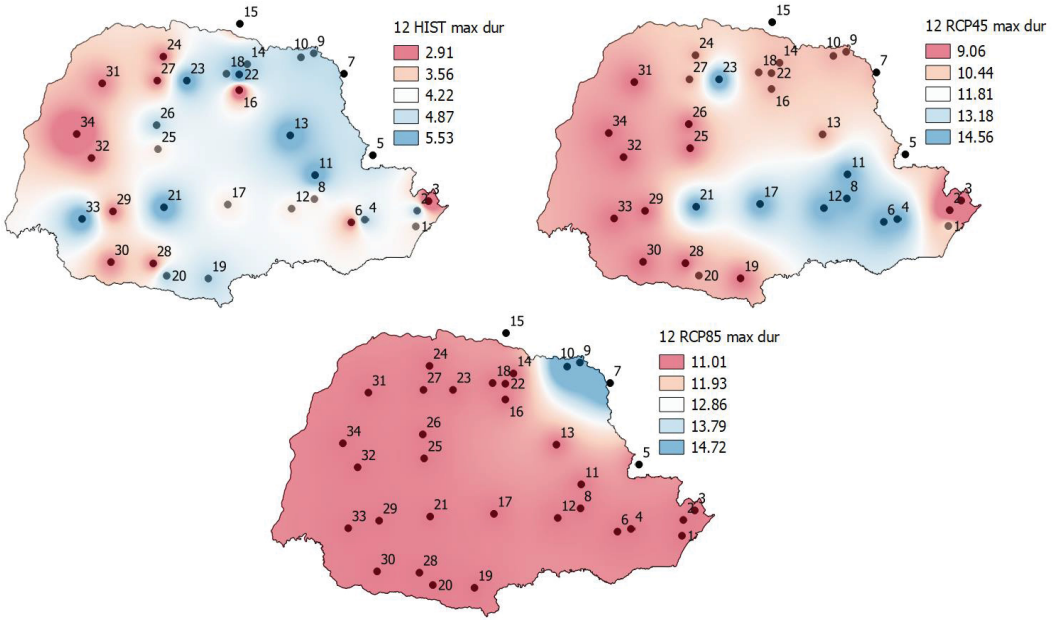

Font: Author.

Figure 62 – Zero threshold frequency of the historical (HIST), and simulated (RCP 4.5 and RCP 8.5) series.

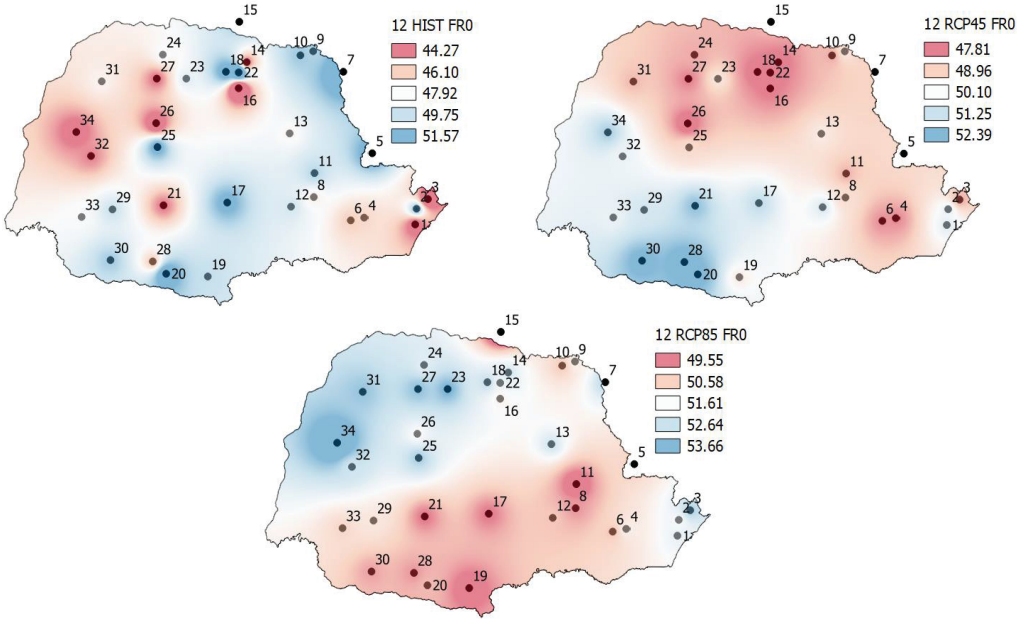

Font: Author.

Figure 63 – The -1.0 threshold frequency of the historical (HIST), and simulated (RCP 4.5 and RCP 8.5) series.

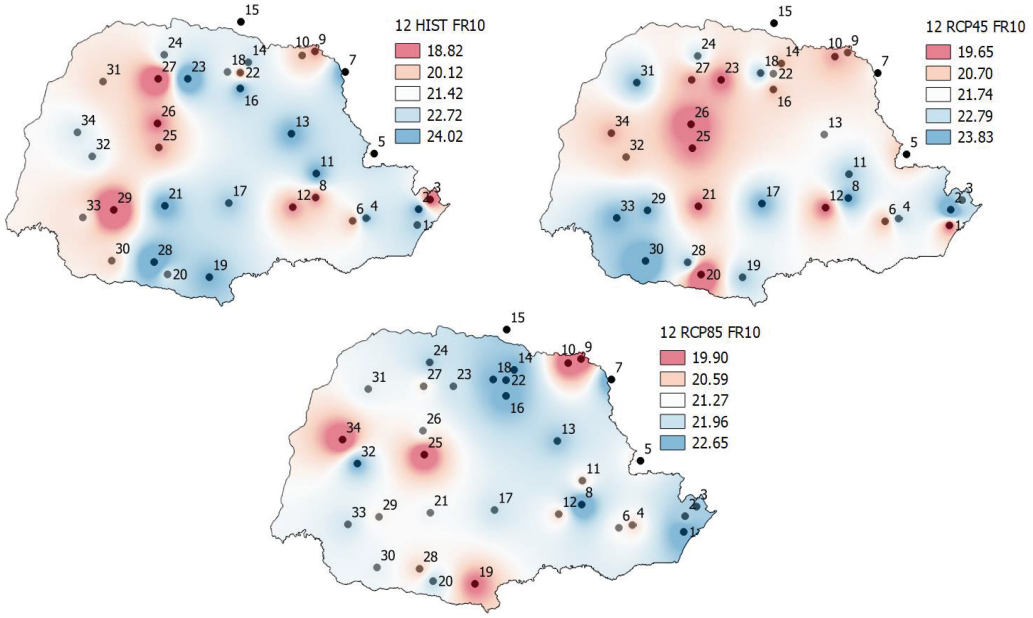

Font: Author.

Figure 64 – The -1.5 threshold frequency of the historical (HIST), and simulated (RCP 4.5 and RCP 8.5) series.

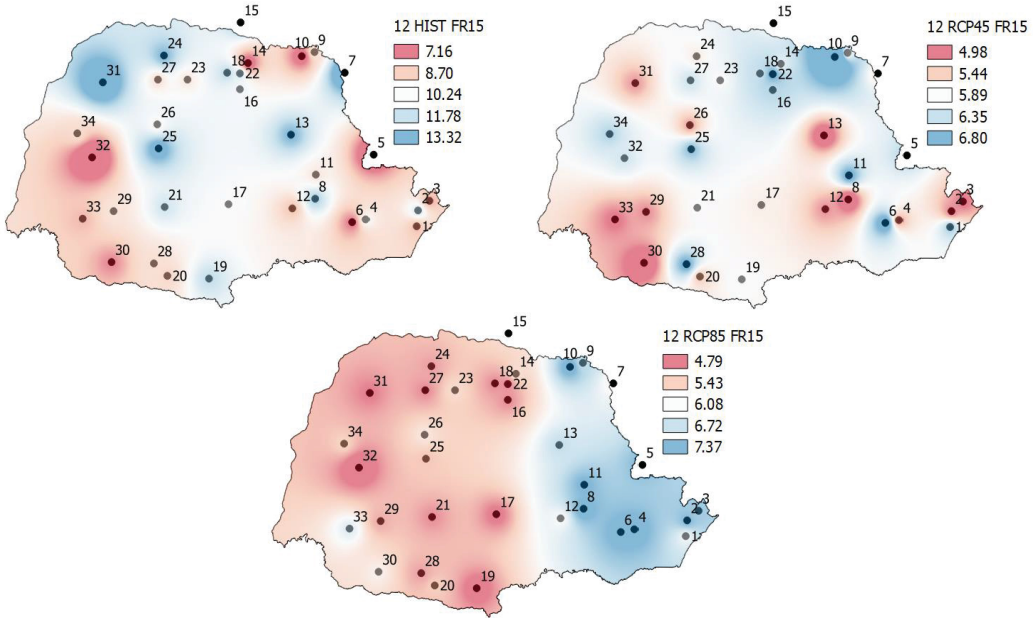

Font: Author.

Figure 65 – Maximum drought magnitude of the historical (HIST), and simulated (RCP 4.5 and RCP 8.5) series.

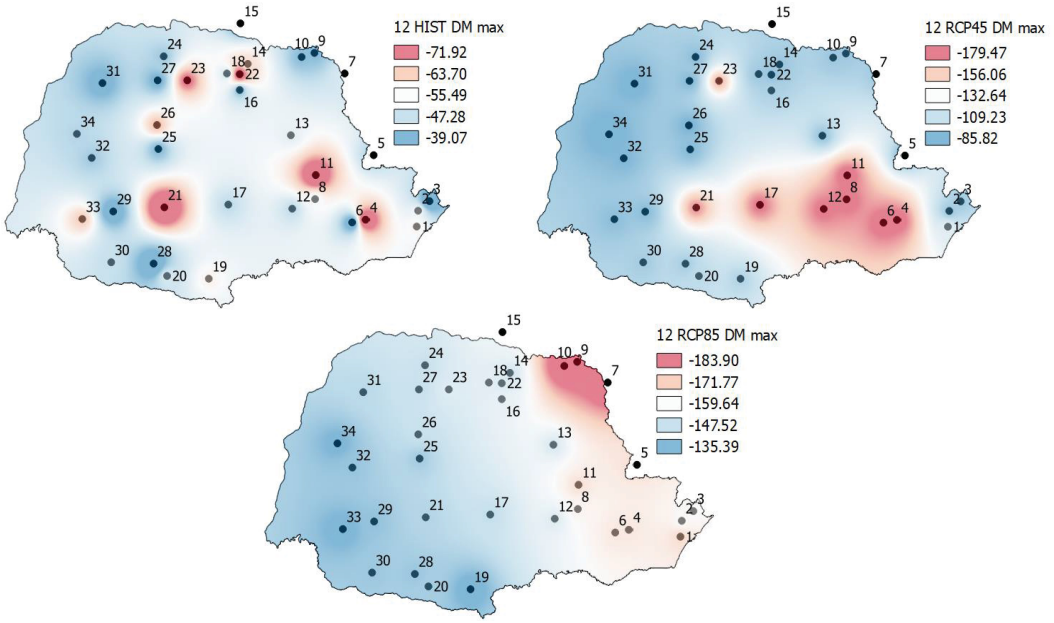

Font: Author.

Figure 66 – Mean drought magnitude of the historical (HIST), and simulated (RCP 4.5 and RCP 8.5) series.

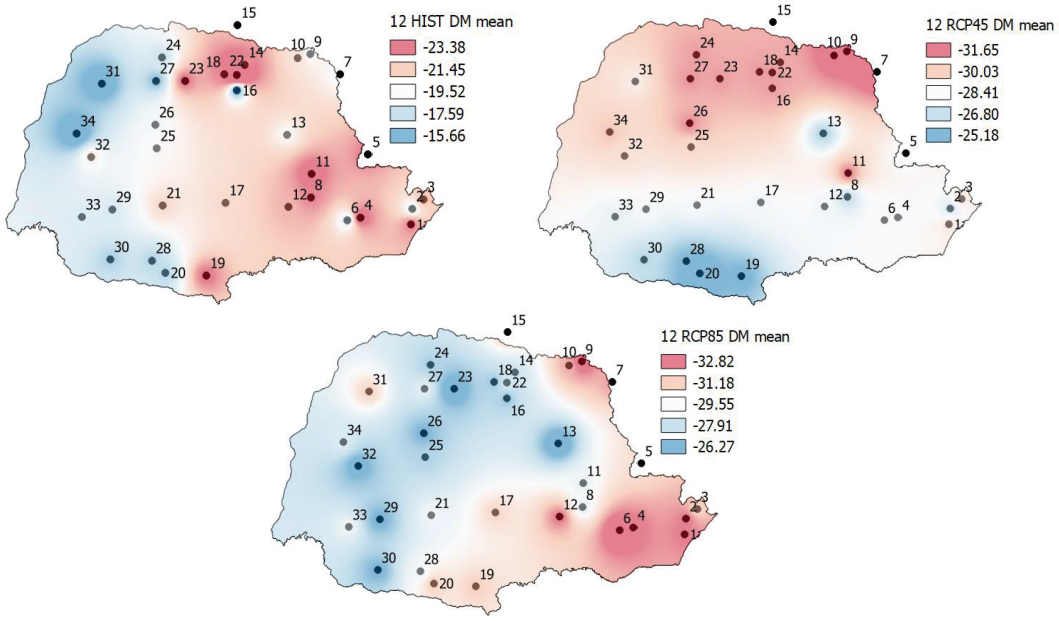

Font: Author.

Figure 67 – Median drought magnitude of the historical (HIST), and simulated (RCP 4.5 and RCP 8.5) series.

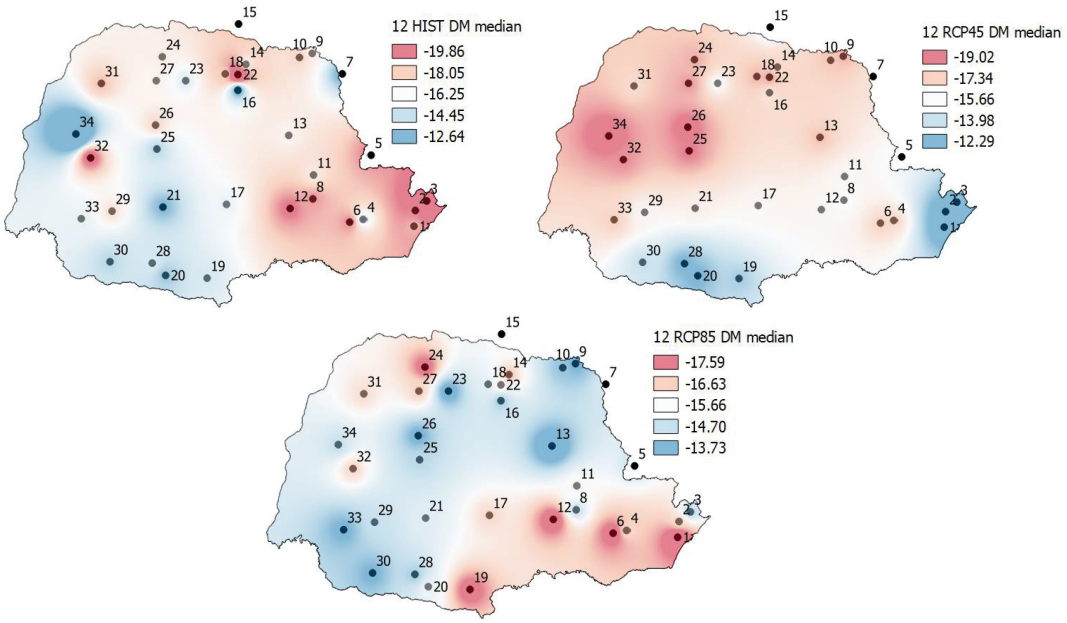

Font: Author.

Figure 68 – Minimum values of the historical (HIST), and simulated (RCP 4.5 and RCP 8.5) series.

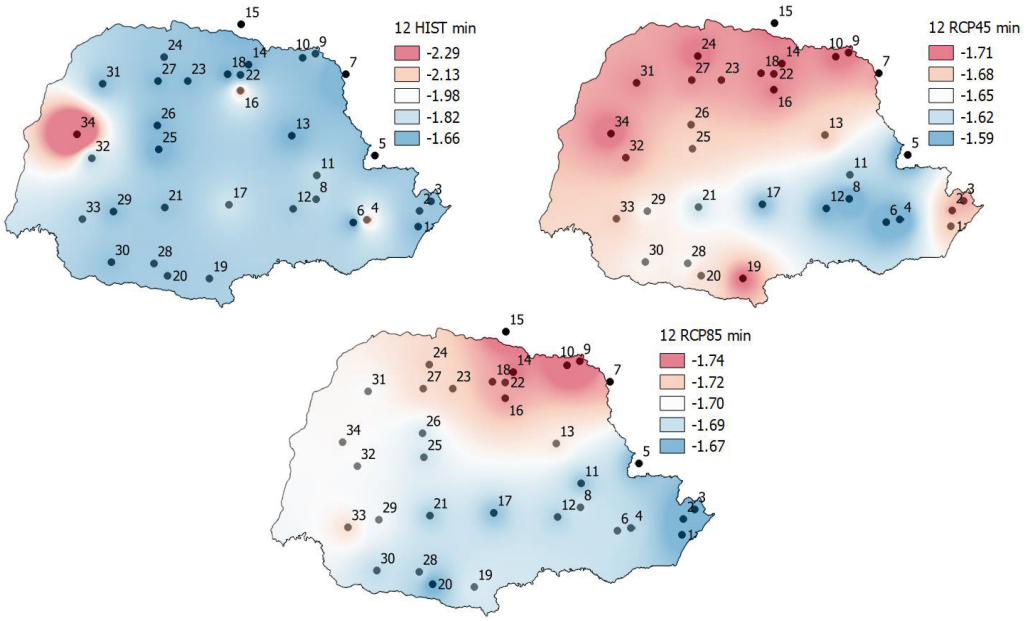

Font: Author.

Figure 69 – Total number of drought events between stationary and non-stationary approaches of the historical (HIST), and simulated (RCP 4.5 and RCP 8.5) series.

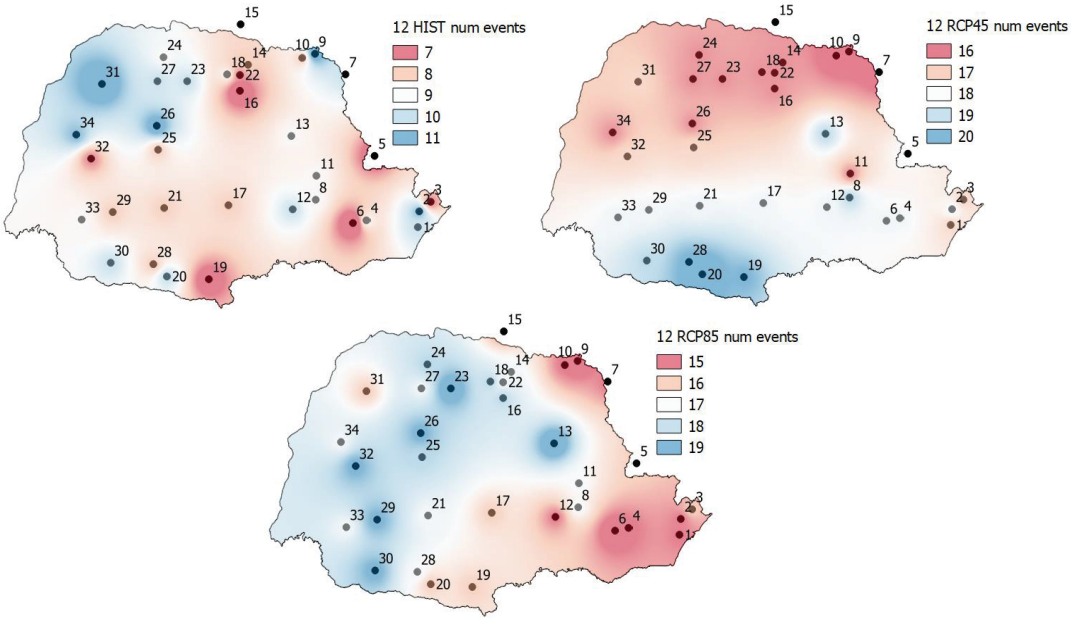

Font: Author.